GEOLOGIC STUDIES IN ALASKA BY THE
U.S. GEOLOGICAL SURVEY, 1989

Frontispiece. View northeast toward steam plume rising above Redoubt Volcano on January 22, 1990. Crater located about 2,000 feet below 10,197 foot summit. Photograph by Steven Brantley, U.S. Geological Survey, and provided courtesy of Robert G. McGimsey, U.S. Geological Survey and Alaskan Volcano Observatory.

Geologic Studies in Alaska by the U.S. Geological Survey, 1989

JAMES H. DOVER and JOHN P. GALLOWAY, Editors

U.S. GEOLOGICAL SURVEY BULLETIN 1946

U.S. DEPARTMENT OF THE INTERIOR
MANUEL LUJAN, JR., Secretary

U.S. GEOLOGICAL SURVEY
Dallas L. Peck, Director

UNITED STATES GOVERNMENT PRINTING OFFICE, WASHINGTON : 1990

For sale by the
Books and Open-File Reports Section
U.S. Geological Survey
Federal Center, Box 25425
Denver, CO 80225

CONTENTS

CONTRIBUTORS TO THIS BULLETIN

Anchorage

U.S. Geological Survey
4200 University Drive
Anchorage, Alaska 99508-4667

Bradley, Dwight C.
Dover, James H.
Karl, Susan M.
Miller, Marti L.
Miyaoka, Ronny T.

Denver

U.S. Geological Survey MS-
Box 25046 Denver Federal Center
Denver, Colorado 80225-0046

Aleinikoff, John N. MS 963
Pawlewicz, Mark J. MS 940

Menlo Park

U.S. Geological Survey MS-
345 Middlefield Road
Menlo Park, California 94025

Brew, David A. MS 904
Conrad, James E. MS 938
Ford, Arthur B. MS 904
Foster, Helen L. MS 904
Galloway, John P. MS 904
Lull, John S. MS 904
Marincovich, Louie, Jr. MS 915
McKee, Edwin H. MS 938
McLean, Hugh MS 999
Phillips, R. LawrenceMS 999
Plafker, George MS 904
Stanley, Richard G. MS 999
Turrin, Brent D. MS 938
Yeend, Warren MS 904

Reston

U.S. Geological Survey
National Center, MS-
12201 Sunrise Valley Drive
Reston, Virgina 22092

Wardlaw, Bruce R. MS 970

Outside

Bauer, Robert L.
Himmelberg, Glen R.
Department of Geology
University of Missouri
Columbia, Missouri 65211

Hooper, Robert J.
Department of Geology
University of South Florida
Tampa, Florida 33620-5200

Igarashi, Yaeko
Hokkaido University
Sapporo, Japan

Kra, Renee
International Radiocarbon Data Base
4717 E. Ft. Lowell Road
Department of Geosciences
The University of Arizona
Tucson, Arizona 85712

Kusky, Timothy M.
University of California
Institute for Crustal Studies
Santa Barbara, California 93106

Stowell, Harold H.
Department of Geology
University of Alabama
Tuscaloosa, Alabama 35487-0338

Wiggins, Virgil D.
Chevron, Inc.
San Ramon, California 94583

Geologic Studies in Alaska by the U.S. Geological Survey, 1989

By James H. Dover *and* John P. Galloway, *Editors*

INTRODUCTION

This collection of papers continues the annual series of U.S. Geological Survey (USGS) reports on geologic investigations in Alaska. From 1975 through 1988, the series was published as USGS circulars. The first of these appeared under the title "The United States Geological Survey in Alaska: Accomplishments during 1975"; the last, entitled "Geologic studies in Alaska by the U.S. Geological Survey during 1987," reflects a title change made in 1986. The change to a bulletin format began in 1988, and this volume continues that format. One change in this volume is the separation of Geologic Notes from more extensive Articles.

The eight Articles and six Geologic Notes in this bulletin represent research activities carried out in Alaska by the USGS over the past few years. The topics addressed range from mineral resource studies (including mineral fuels), stratigraphy, fabric and other structural studies, mafic-ultramafic complexes, paleotectonics, the application of new fossil and isotopic age data to regional geologic problems, geomorphic aspects of placer gold, and the compilation of a radiocarbon age file. Geographic areas represented are shown on figure 1 and span the entire State, from the North Slope, Brooks Range, interior Alaska, south-central Alaska, southeastern Alaska to southwestern Alaska; and one report covers the whole State.

Two bibliographies following the Geologic Notes list (1) reports about Alaska in USGS publications released in 1989 and (2) reports about Alaska by USGS authors in publications outside the USGS in 1989. A bibliography and index of papers in past USGS circulars that are devoted to geologic research and accomplishments in Alaska (1975 to 1986) is published as USGS Open-File Report 87-420.

Manuscript approved for publication, June 11, 1990.

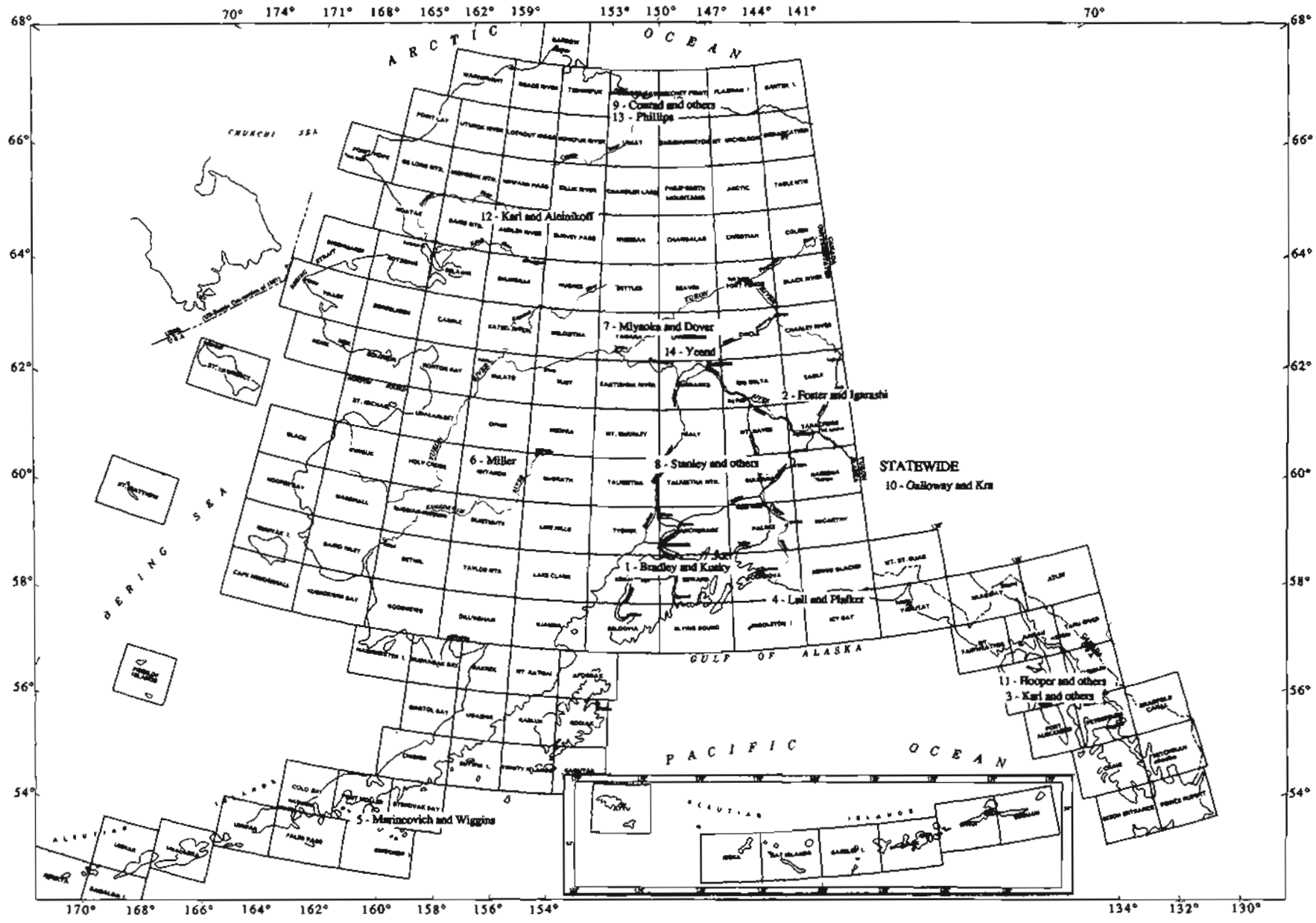

Figure 1. Index map of Alaska showing 1:250,000-scale quadrangles and general locations of study areas discussed in this bulletin. Numbers indicate order of papers in this volume; names of authors follow numbers.

ARTICLES

Kinematics of Late Faults Along Turnagain Arm, Mesozoic Accretionary Complex, South-Central Alaska

By Dwight C. Bradley *and* Timothy M. Kusky

Abstract

Mesozoic and Cenozoic rocks of the accretionary wedge of south-central Alaska are cut by abundant late brittle faults. Along Turnagain Arm near Anchorage, four sets of late faults are present: a conjugate pair of east-northeast-striking dextral and northwest-striking sinistral strike-slip faults, north-northeast-striking thrusts, and less abundant west-northwest-striking normal faults. All four fault sets are characterized by calcite-chlorite fibrous slickenside surfaces and appear to be approximately coeval. Strongly curved slickenlines on some faults of each set reveal that displacement directions changed over time and that bulk regional deformation related to brittle faulting was strongly noncoaxial. The thrust and strike-slip faults together resulted in subhorizontal shortening perpendicular to strike, consistent with an accretionary wedge setting. Motion on the normal faults resulted in strike-parallel extension of uncertain tectonic significance.

INTRODUCTION

The consensus that subduction zones are sites of mainly contractional deformation finds support in numerous studies of accretionary wedges, where thrust faults and associated folds dominate the map-scale structure (for example, Moore and Karig, 1980). Although the roles of strike-slip and extension have been less widely appreciated, these deformation regimes are also important in some convergent plate boundary zones. Extension dominates the tectonics of outer trench slopes of deep-sea trenches, where bending of the downgoing slab generates down-to-trench normal faults with displacements up to about 1 km (Jones and others, 1978). Platt (1986) showed that extension is not restricted to the downgoing plate; accretionary wedges also may undergo significant normal faulting in order to maintain a stable wedge geometry. Some oblique subduction zones are characterized by major arc-parallel wrench faults that accommodate the strike-slip component of relative plate motion (Fitch, 1972; Dewey, 1980).

The strike-slip faults emphasized in this paper cut the overriding plate and strike at a high angle to the convergent plate boundary. Such faults facilitate bulk shortening within at least one modern accretionary wedge, the inner slope of the Aleutian Trench (fig. 1; Lewis and others, 1988). Byrne (1984) identified comparable faults cutting his Paleocene Ghost Rocks Formation in a much older part of the same accretionary wedge on Kodiak Island, south-central Alaska (fig. 1, loc. 1). Here we describe a system of conjugate strike-slip faults and related thrusts in Mesozoic rocks of this accretionary wedge, near Anchorage, about 500 km along strike from Kodiak Island. Structural analysis suggests that all but a few of these brittle faults are the product of northwest-southeast convergence. However, enigmatic, curved fibrous slickenlines (striations) reveal that slip directions changed markedly during aseismic creep, suggesting that fault-related bulk strain was strongly noncoaxial and more complex than was previously recognized for faults in comparable settings in the Aleutian Trench and Kodiak Island.

The study area along Turnagain Arm (fig. 2) includes the type locality of the McHugh Complex as defined by Clark (1972). The northwestern part of the McHugh Complex's outcrop belt is a melange composed of fragments and disrupted beds of tuff, pillow basalt, and chert, in a deformed matrix of argillite. The southeastern part of the outcrop belt is mainly composed of siliciclastic rocks, including boulder and cobble conglomerate, graywacke, and argillite; bedding is laterally discontinuous in the rare places where it can be observed. Throughout the McHugh Complex, moderate to intense stratal disruption has resulted in tectonic juxtaposition of varied rock types, at all scales. The predominant mode of early deformation was layer-parallel fragmentation (Cowan, 1985; Brandon, 1989); breakup of relatively competent beds (such as chert and tuff) was accompanied by concomitant flowage of argillite matrix into gaps. The resulting fragment foliation is the most conspicuous fabric element in the McHugh Complex in the study area; it strikes north-northeast and in most places dips steeply northwest. The foliation is commonly displaced across narrow (up to a few centimeters wide), early ductile shear zones. Clark (1972) reported prehnite-pumpellyite metamorphic facies assemblages in the McHugh Complex in the study area. The fragment foliation, ductile shear zones, and contorted prehnite veinlets are cut by abundant brittle faults, described below.

The Upper Cretaceous Valdez Group (fig. 2) consists of turbidites composed of graywacke, siltstone, black argillite, and minor pebble to cobble conglomerate. Graded beds in the Valdez Group exhibit a refracted slaty cleavage that is strong in argillite and weak in graywacke; the bedding-to-cleavage angle increases with grain size within graded beds, thereby providing a younging indicator. Brittle faults like those in the McHugh Complex cut bedding and cleavage in the Valdez Group.

BRITTLE FAULTS

We studied minor faults along a 43-km transect across the strike of the accretionary complex in Turnagain Arm during eight days of fieldwork. The faults are abundant in highway and railroad cuts, and in weathered coastal exposures on both sides of Turnagain Arm. The faults juxtapose rock types assigned to a single map unit (McHugh Complex or Valdez Group); they account for some of the discontinuity of rock types that has frustrated attempts at detailed mapping along Turnagain Arm (Clark, 1972, p. D8-D9). Prominent fibrous (calcite and chlorite) slickenside surfaces mark the faults; fiber-steps clearly reveal shear sense (fig. 3). Owing to lack of markers, the magnitude of displacement is rarely evident, but we locally observed offsets of a few tens of centimeters to a few meters. In all outcrops we studied, the faults are spaced at a few meters to tens of meters. The reasonable assumption that the faults are abundant throughout the area of figure 2 suggests that they were responsible for significant regional deformation.

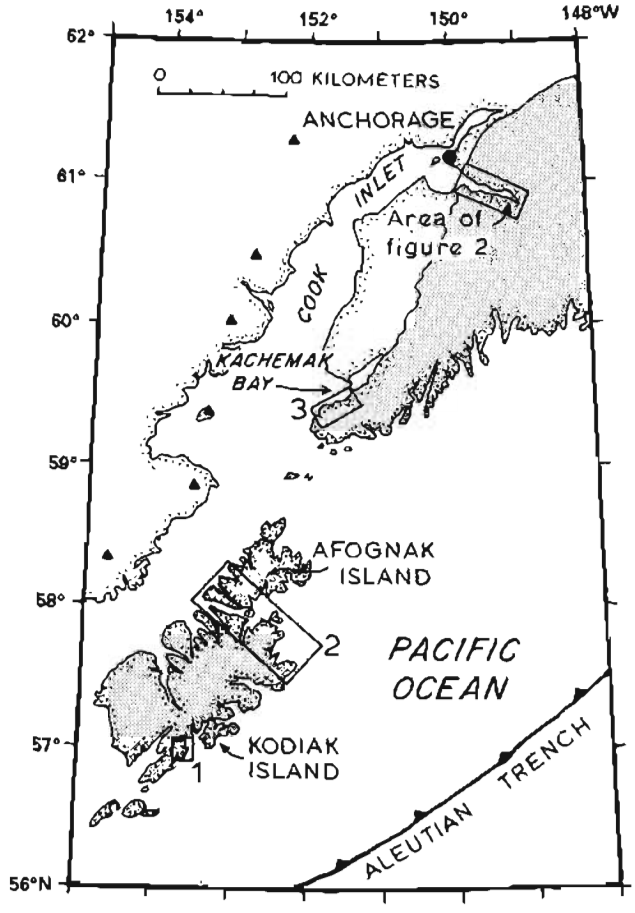

Figure 1. Locality map of south-central Alaska. Triangles, volcanoes of the Aleutian arc. Shaded area, Mesozoic-Cenozoic accretionary complex. Numbered rectangles, areas where abundant late brittle faults have been documented in the Mesozoic-Cenozoic accretionary complex. For location of map see figure 2 (inset).

We measured the attitude of 79 brittle faults and associated slickenline orientations and stepping directions at the locations shown in figure 2. Fifty of the faults cut the McHugh Complex; 29 cut the Valdez Group. We categorized the faults as contractional or extensional for slickenline rakes greater than 45°, or dextral or sinistral for rakes less than 45°. (The designations "contractional" and "extensional" here apply to faults in their present attitudes, without regard for any postfaulting rotations that might have changed the original hanging wall to the apparent footwall; see Bradley, 1989). Where appropriate, we assigned faults with two superimposed sets of slickenlines or a single set of curved slickenlines to two groups. Mean directions of lineations or poles as quoted below are visual estimates from scatter equal-area plots (fig. 4) superimposed on contour diagrams (not illustrated). The stereoplots reveal four main sets of faults on the basis of attitude and slip direction, which are summarized in figure 5.

Sets of dextral and sinistral strike-slip faults (fig. 4*E–G*) form what we interpret to be a conjugate pair. The dextral faults (30 examples) strike east-northeast (mean 070°) and dip steeply south (mean 70°); the sinistral faults (20 examples), strike southeast (mean 132°) and dip steeply southwest (mean 82°). Strike-slip faults of both sets are ubiquitous throughout the study area, in both the McHugh Complex and Valdez Group. A few of the faults that were classed on the basis of rake (less than 45°) as strike-slip faults have unusually gentle dips (fig. 6*A*).

We measured 25 contractional faults in the study area. Following Butler (1982), we use the term "thrust" for all contractional faults, regardless of dip angle. Most of the thrusts, termed synthetic thrusts below, strike south-southwest (mean 209°), and dip northwest (mean 64°)(fig. 4*A*, *B*); a few antithetic thrusts strike north-northeast and dip southeast. The mean attitude of synthetic thrusts is subparallel to fragment foliation in the McHugh Complex and bedding in the Valdez Group. The mean hanging-wall movement direction of synthetic thrusts is 102° updip. Although a few thrusts are present throughout the study area, they are abundant only directly east of the two map-scale faults: (1) at the Potter Marsh weigh station (fig. 2, loc. 1), cutting melange of the McHugh Complex immediately east of the

Knik fault (a segment of the Border Ranges fault), and (2) near Indian (fig. 2, loc. 2), cutting metasedimentary rocks of the Valdez Group in the strongly deformed footwall of the Eagle River fault. The concentration of minor thrusts in these two areas supports previous interpretations that both major faults underwent thrust displacement, at least during relatively late stages in their histories.

The study area also includes a few normal faults; we found 11 examples. Despite some scatter (fig. 4*C*), most of the faults strike east-southeast (mean 117°) and dip southwest (mean 59°). The mean hanging-wall movement direction is about 228°.

Many of the brittle faults along Turnagain Arm have slickenlines that are curved by as much as 55° within the fault plane (figs. 3, 7). Stepping directions provided a basis for determining the beginning and end of a given crystal fiber; hence we were able to class each fault as clockwise (10 examples) or counterclockwise (20 examples) on the basis of the sense of slickenline curvature when the fault plane was viewed from above (fig. 7*C*, *D*).

The curved slickenlines are intriguing but difficult to interpret. The most significant conclusion we can draw is that bulk deformation related to brittle faulting was strongly noncoaxial. All faults with curved slickenlines strike between 050° and 230° (strike directions assigned according to the right-hand rule; see fig. 7*A*, *B*), whereas only two-thirds of faults with straight slickenlines have strikes in the same range; the significance of this finding is unclear. Also inexplicable is the observation that counterclockwise slickenlines appear to converge toward a southwest-plunging zone (fig. 7*C*), whereas clockwise slickenlines appear to diverge from a southwest-dipping girdle (fig. 7*D*). On several strike-slip faults, slickenline curvature was sufficient to change the plunge direction of the instantaneous slip vector. Where this occurred on nonvertical faults, the component of dip-slip motion must have changed sense as the plunge

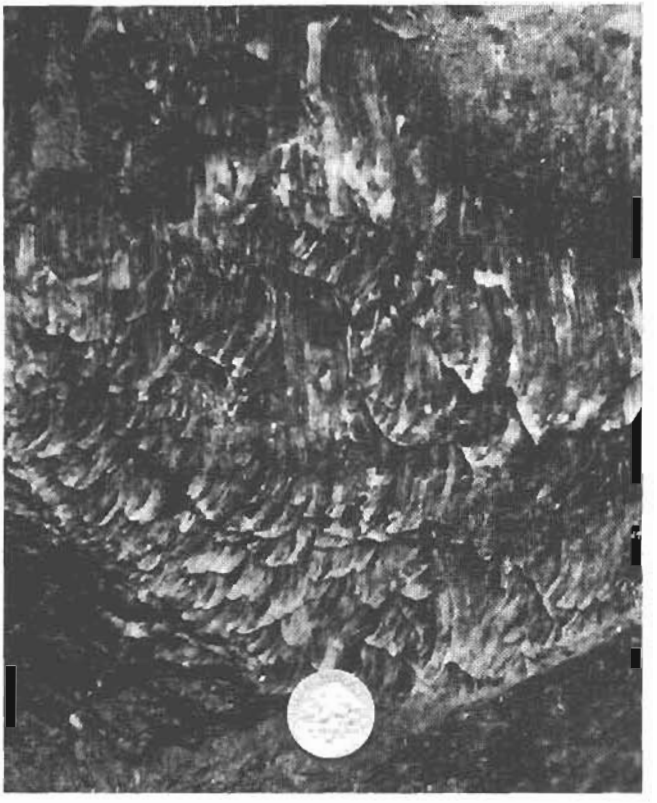

Figure 3. Slickensided high-angle fault surface with curved fibrous slickenlines. Missing block (where photographer was standing) moved down with respect to preserved block. Youngest part of a given slickenline is immediately adjacent to step where it ends. Coin is 17 mm across.

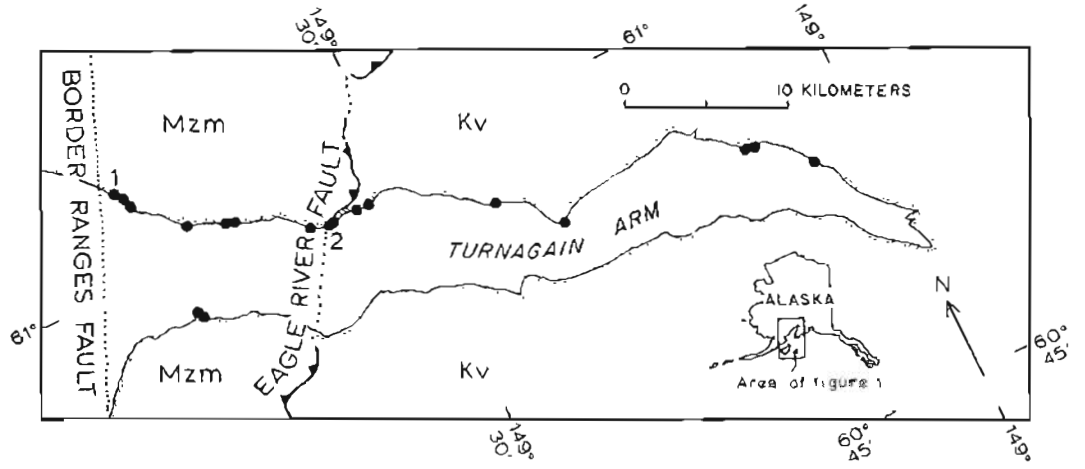

Figure 2. Generalized geologic map of Turnagain Arm. Dots, locations where minor faults were studied; numbers 1 and 2 refer to localities mentioned in text. Mzm, Mesozoic McHugh Complex; Kv, Cretaceous Valdez Group. Faults dotted where concealed; sawteeth on upper plate of Eagle River thrust fault. Modified from Magoon and others (1976).

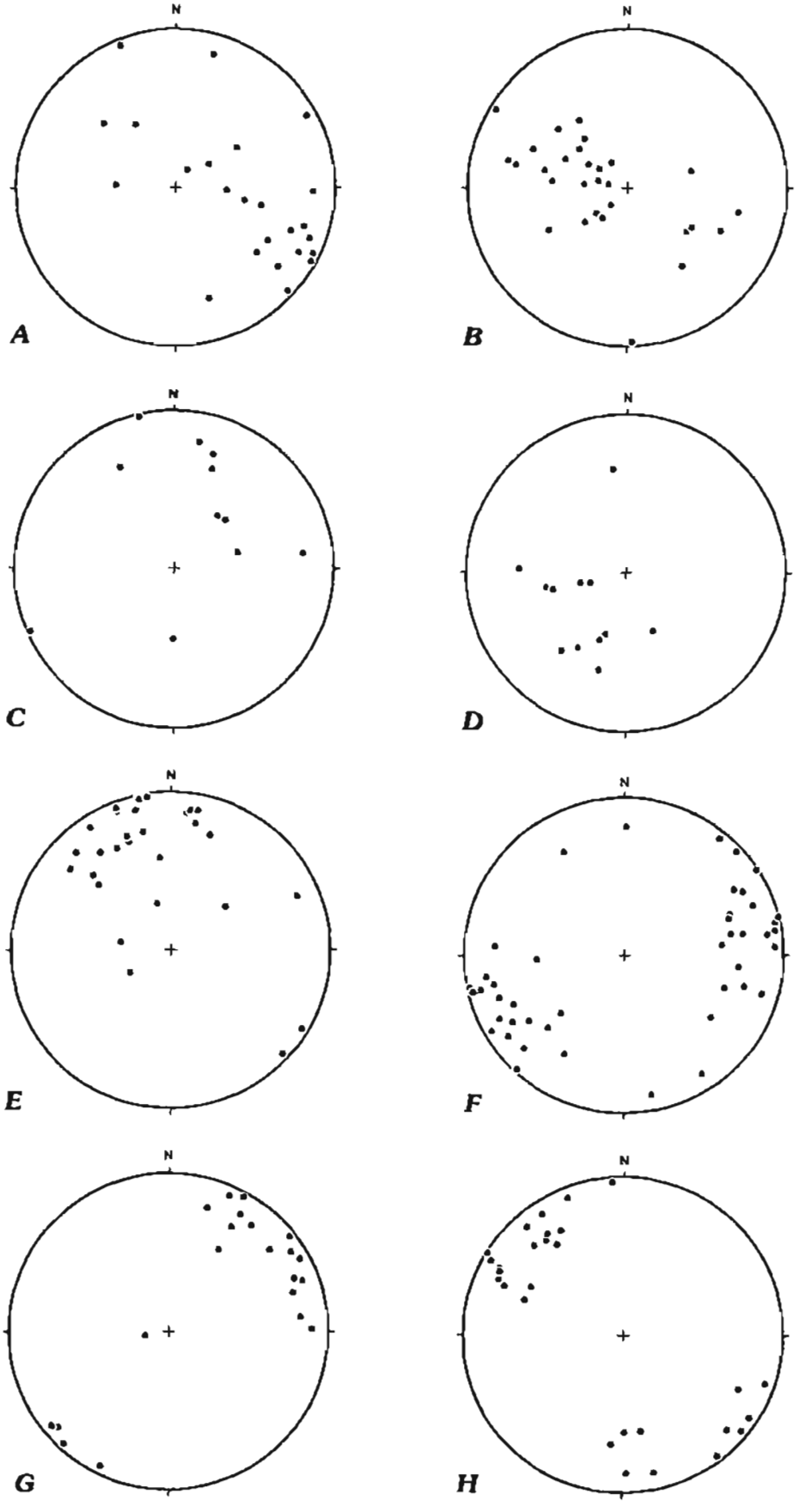
N
A
N
B
N
C
N
D
N
E
N
F
N
G
N
H

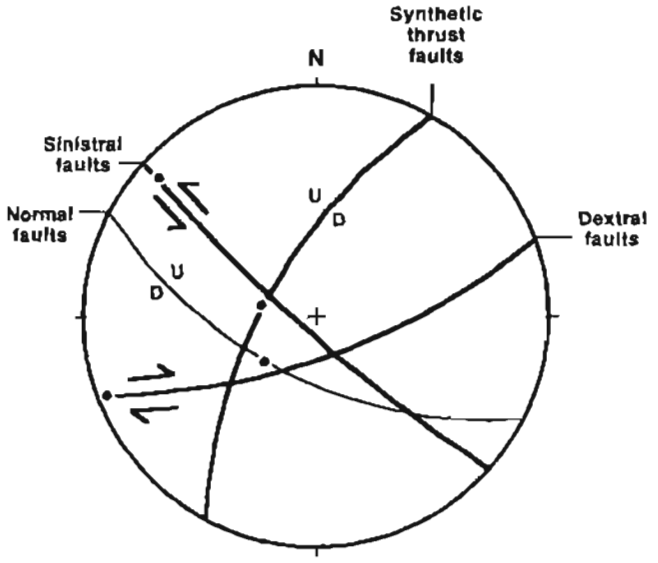

Figure 5. Lower hemisphere, equal-angle projection summarizing attitudes of major fault sets and slip directions (dots). Minor normal-fault set is not as well defined as other sets. Arrows show relative movement on sinistral and dextral faults. U, upthrown side; D, downthrown side.

direction of the slickenlines changed. Thus, judging from present attitudes, several faults in Turnagain Arm appear to have evolved from transpressional to transtensional structures (or vice versa) during fault motion.

Possible origins of curved slickenlines include (1) rotation of a fault block about an axis normal to the fault plane (rotational-translational fault motion of Mandal and Chakraborty, 1989) and (2) incremental change in translation direction (curvilinear-translational fault motion of Mandal and Chakraborty, 1989); note the exact analogy to curved fibers in dilatant veins as described by Durney and Ramsay (1973). The first mechanism is unlikely for the Turnagain slickenlines, because the radius of slickenline curvature on a given fault is constant, rather than increasing with distance from a rotation axis (fig. 8). It is fortunate that the first mechanism (fig. 8*A*) did not operate, for if it had, any paleomagnetic or paleocurrent data from Turnagain Arm probably would be spurious. We instead attribute the curvature to the second mechanism (fig. 8*B*).

Similar styles suggest that the four main fault sets—thrust, dextral, sinistral, and normal faults—are approximately coeval; any differences in age are probably minor.

All four fault sets include examples with straight and curved fibrous slickenlines that consist of calcite and chlorite (based on hand-sample identification). In only one place were we able to observe a crosscutting relation (a sinistral fault cutting an older thrust); many additional observations of this type would be necessary to establish a meaningful sequence of events. Together, the faults may represent an orthorhombic fault set (Reches, 1983; Krantz, 1989), to the extent that orthorhombic fault theory can be applied to noncoaxial deformations.

TECTONIC SIGNIFICANCE

Late brittle faults like those along Turnagain Arm appear to be widespread in the arc-trench gap of south-central Alaska. The pattern of faulting is especially similar to that described in the Paleocene Ghost Rocks Formation on southern Kodiak Island (fig. 1, loc. 1), where Byrne (1984, p. 27) reported the following sequence of late faults:

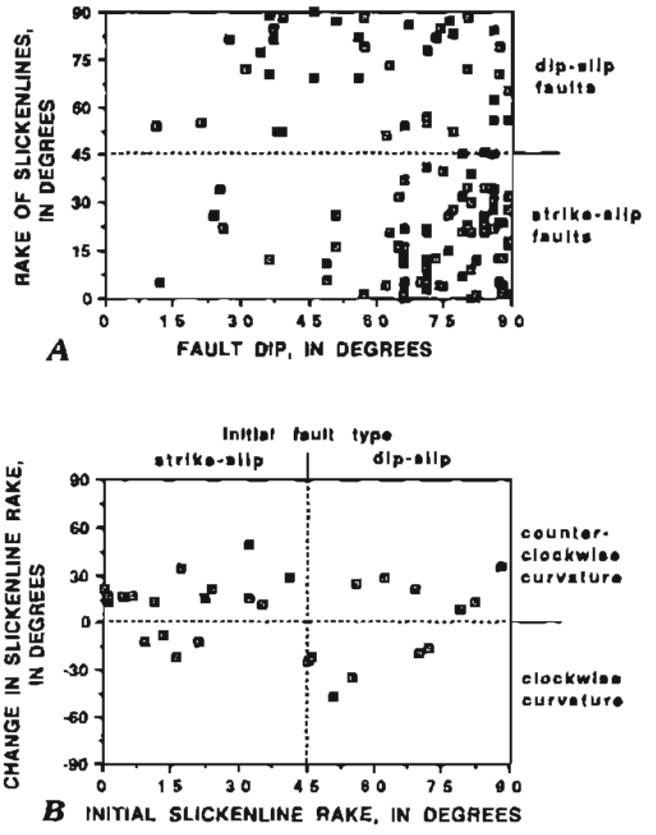

Figure 6. *A*, Plot of fault dip versus rake of slickenlines. Faults classed as strike slip on the basis of rake include several with anomalously gentle dips. Curved slickenlines are represented by both initial and final attitudes. *B*, Plot of initial rake versus change in rake on faults with curved slickenlines. Straight slickenlines would plot on horizontal dashed line. Counterclockwise curvatures (plotted as positive) predominate. Curved slickenlines occur on faults of all initial rakes.

◀ Figure 4. Lower hemisphere, equal-area projections for fault plane and slickenlines from localities shown in figure 2. *A*, Poles to thrust-fault planes. *B*, Thrust-fault slickenlines. *C*, Poles to normal-fault planes. *D*, Normal-fault slickenlines. *E*, Poles to dextral-fault planes. *F*, Dextral-fault slickenlines. *G*, Poles to sinistral-fault planes. *H*, Sinistral slickenlines. Curved slickenlines in *B*, *D*, *F*, and *H* represented by both initial and final attitudes.

(1) a conjugate pair of east-striking dextral and north-striking sinistral strike-slip faults; (2) a conjugate pair of northwest-dipping synthetic and minor southeast-dipping antithetic thrusts; and (3) a conjugate pair of east-striking normal faults. Each fault set on southern Kodiak Island appears to have its counterpart along Turnagain Arm; orientations differ slightly but the overall configurations are qualitatively alike.

On Afognak Island and northern Kodiak Island (fig. 1, loc. 2), Sample and Moore (1987) identified a comparable assemblage of late faults cutting the Upper Cretaceous Kodiak Formation (the along-strike correlative of the Valdez Group): (1) northeast-striking dextral strike-slip faults (conjugate sinistral faults were not reported); (2) northwest-dipping thrusts; and (3) normal faults with highly variable strikes. The relative age of these three fault sets is unknown, but like the Turnagain Arm faults, they postdate penetrative deformation.

Recent mapping in the Kachemak Bay region (fig. 1, loc. 3) also has revealed abundant brittle faults (D.C. Bradley and S.M. Karl, unpub. 1989 field notes): (1) northwest-striking thrusts; (2) sinistral strike-slip faults with highly variable strikes; and (3) abundant normal faults with highly variable strikes. Dextral strike-slip faults are rare. Whereas

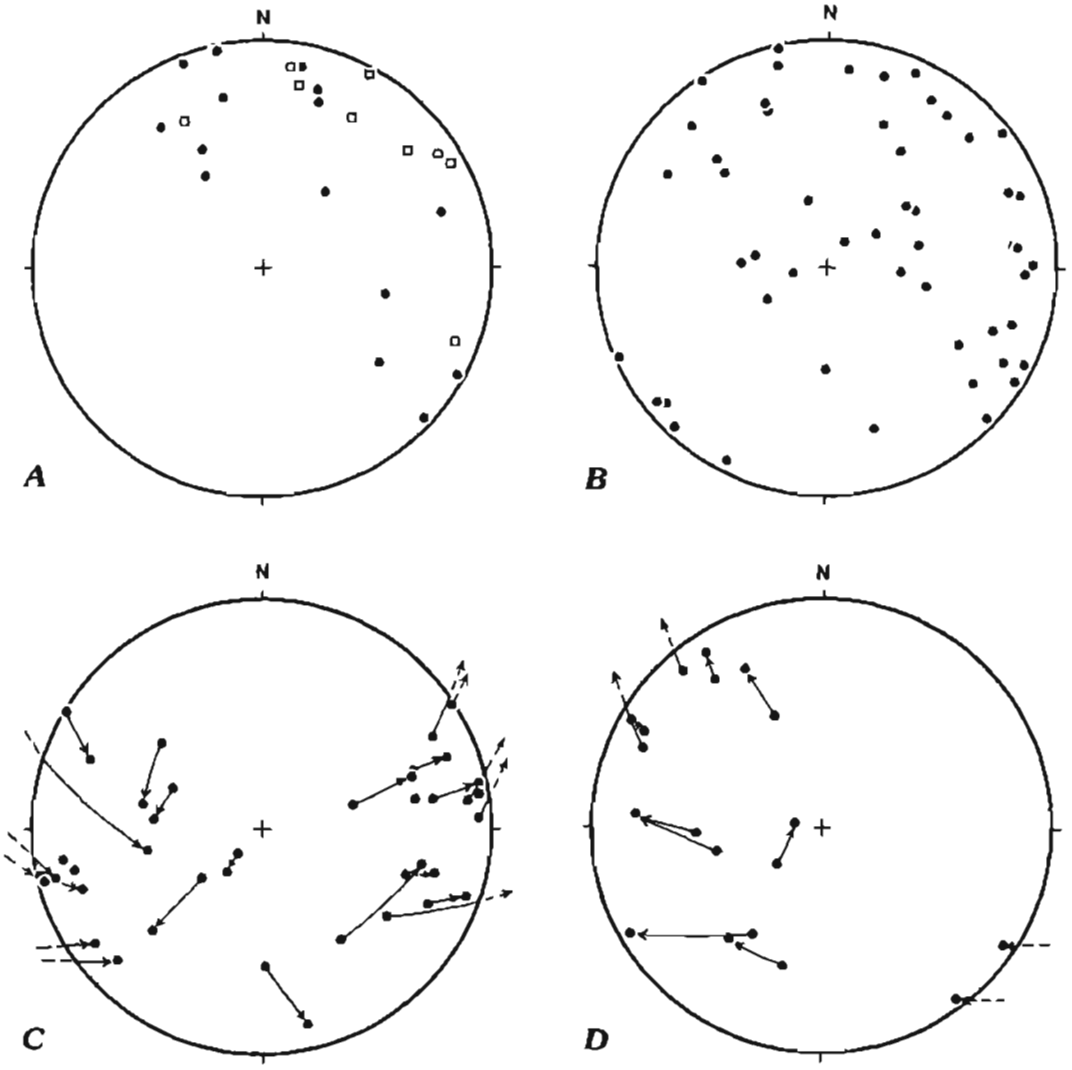

Figure 7. Lower hemisphere, equal-area projections. *A*, Poles to fault planes and associated curved slickenlines. Squares, slickenlines with clockwise curvature when viewed from above; dots, slickenlines with counterclockwise curvature when viewed from above. Note absence of faults that strike between 230° and 050°. *B*, Poles to faults with straight slickenlines. Note abundance of faults that strike between 230° and 050°. *C*, Slickenlines with counterclockwise curvature. Arrows show change in attitude through time. Some slickenline trajectories leave edge of net (dashed arrows) and reappear on opposite side. Only representative trajectories are shown where data are cluttered. *D*, Slickenlines with clockwise curvature, which are less abundant than counterclockwise lines.

more data are needed to clarify the pattern and kinematics of late faulting, the available data at least support the contention that late brittle faults are widespread, if not omnipresent, along a 500-km segment of the accretionary wedge.

In all four areas in figure 1 where late brittle faults have been studied, the attitudes of thrusts indicate subhorizontal northwest-southeast shortening. In addition, in Turnagain Arm and southern Kodiak Island, conjugate strike-slip faults indicate shortening in the same direction. Figure 9 shows how both thrust and conjugate strike-slip faults might have facilitated shortening within the southern Alaska accretionary wedge during Cretaceous and (or) Cenozoic time. Figure 9 also serves as a schematic depiction of the active tectonics of the Aleutian inner trench slope (compare with fig. 13 in Lewis and others, 1988).

One possibly significant difference between Turnagain Arm and southern Kodiak Island is that the intersection between conjugate strike-slip faults along Turnagain Arm plunges about 70° SE.; the corresponding maximum shortening direction plunges about 20° NW. (both estimates from fig. 5). In contrast, on southern Kodiak Island, the conjugate fault intersection is vertical, and the corresponding maximum shortening direction is horizontal. Byrne (1986) cited the latter fact as one line of evidence against rotation of the subduction complex toward the arc during subsequent growth of the accretionary wedge; he concluded instead that the wedge had been uplifted vertically to its present position above sea level, without rotation. If the conjugate strike-slip faults along Turnagain Arm share a common origin with those on southern Kodiak, their present attitude would indicate rotation during uplift of the wedge. Independent evidence that might provide a test for this suggestion has not yet been sought.

It is not clear how the normal faults, which strike almost perpendicular to the thrusts, might fit into the tectonic setting shown in figure 9. One possibility is that the normal faults are akin those which Platt (1986) attributed to extensional collapse of an accretionary wedge that has been oversteepened beyond its critical taper. However, a significant difference is that normal faults in Platt's (1986) model strike parallel to rather than perpendicular to the plate boundary; accordingly, a three-dimensional modification to Platt's (1986) model, involving nonplane strain, would be required to explain the Turnagain Arm normal faults. Another possibility is that the normal faults record Paleogene subduction of the Kula-Farallon spreading center. In the latter case, the normal faults might be expected to relate to igneous rocks attributed to the same event. Additional fieldwork along Turnagain Arm and in Kachemak Bay will address these and many other questions raised by the present study.

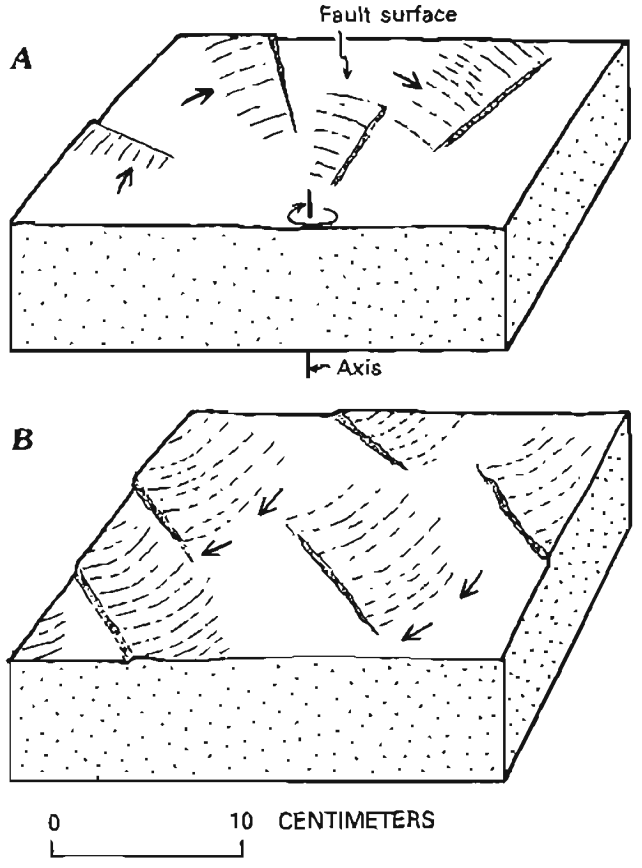

Figure 8. Two mechanisms capable of producing curved slickenlines. *A*, Rotation about an axis normal to fault plane. Slip direction (arrows), sense of displacement, and amount of curvature of slickenlines all vary systematically with position on fault surface with respect to rotation axis. *B*, Change in translation direction, without rotation. All slickenlines have similar trajectories. Second mechanism is indicated for faults with curved slickenlines along Turnagain Arm.

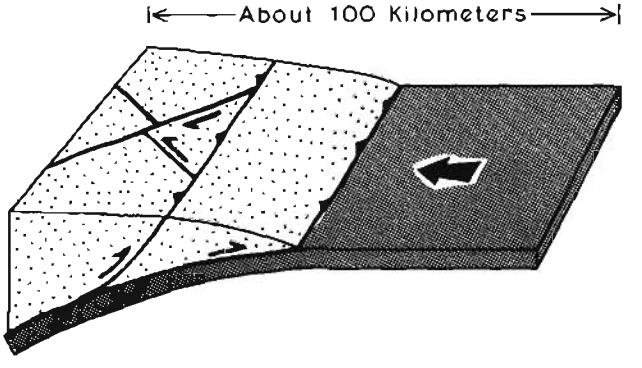

Figure 9. Schematic block diagram of frontal part of an accretionary wedge (stipple) above a subducting oceanic plate (gray), showing how conjugate strike-slip faults and thrusts (small arrows) like those along Turnagain Arm might have accommodated shortening driven by plate convergence (large arrow gives direction). By analogy with Aleutian accretionary wedge (Lewis and others, 1988), thrust faults are active at and near toe of wedge, and strike-slip faults are active closer to arc. Magmatic arc is about 100 km to left. Normal faults are not shown but would strike about perpendicular to thrust faults.

REFERENCES

Bradley, D.C., 1989, Description and analysis of early faults based on geometry of fault-bed intersections: Journal of Structural Geology, v. 11, p. 1011-1019.

Brandon, M.T., 1989, Deformational styles in a sequence of olistostromal melanges, Pacific Rim Complex, western Vancouver Island, Canada: Geological Society of America Bulletin, v. 101, p. 1520-1542.

Butler, R.W.H., 1982, The terminology of structures in thrust belts: Journal of Structural Geology, v. 4, p. 239-245.

Byrne, T., 1984, Early deformation in melange terranes of the Ghost Rocks Formation, Kodiak Islands, Alaska: Geological Society of America Bulletin Special Paper 198, p. 21-51.

——— 1986, Eocene underplating along the Kodiak shelf, Alaska: Implications and regional correlations: Tectonics, v. 5, p. 403-421.

Clark, S.H.B., 1972, The McHugh Complex of south-central Alaska: U.S. Geological Survey Bulletin 1372-D, p. D1-D11.

Cowan, D.S., 1985, Structural styles in Mesozoic and Cenozoic melanges in the western Cordillera of North America: Geological Society of America Bulletin, v. 96, p. 451-462.

Dewey, J.F., 1980, Episodicity, sequence, and style at convergent plate boundaries: Geological Association of Canada Special Paper 20, p. 553-573.

Durney, D.W., and Ramsay, J.G., 1973, Incremental strains measured by syntectonic crystal growths, *in* K.A. De Jong and R. Scholten, eds., Gravity and tectonics: New York, Wiley, p. 67-96.

Fitch, T.J., 1972, Plate convergence, transcurrent faults, and internal deformation adjacent to southeast Asia and the western Pacific: Journal of Geophysical Research, v. 77, p. 4432-4460.

Jones, G.M., Hilde, T.W.C., Sharman, G.P., and Agnew, D.C., 1978, Fault patterns in outer trench walls and their tectonic significance: Journal of the Physics of the Earth, Geodynamics of the Western Pacific, v. 26, no. 2 (supplement), p. 85-101.

Krantz, R.W., 1989, Orthorhombic fault patterns: The odd axis model and slip vector orientations: Tectonics, v. 8, p. 483-495.

Lewis, S.D., Ladd, J.W., and Bruns, T.R., 1988, Structural development of an accretionary prism by thrust and strike-slip faulting: Shumagin region, Aleutian Trench: Geological Society of America Bulletin, v. 100, p. 767-782.

Magoon, L.B., W.L. Adkison, and R.M. Egbert, 1976, Map showing geology, wildcat wells, Tertiary plant fossil localities, K-Ar age dates, and petroleum operations, Cook Inlet area, Alaska: U.S. Geological Survey Miscellaneous Investigations Series Map I-1019, scale 1:250,000.

Mandal, N., and Chakraborty, C., 1989, Fault motion and curved slickenlines: A theoretical analysis: Journal of Structural Geology, v. 11, p. 497-501.

Moore, G.A., and Karig, D.E., 1980, Structural geology of Nias Island, Indonesia: Implications for subduction zone tectonics: American Journal of Science, v. 280, p. 193-223.

Platt, J.P., 1986, Dynamics of orogenic wedges and the uplift of high-pressure metamorphic rocks: Geological Society of America Bulletin, v. 97, p. 1037-1053.

Reches, Z., 1983, Faulting of rocks in three-dimensional strain fields, II. Theoretical analysis: Tectonophysics, v. 95, p. 133-156.

Sample, J.C., and Moore, J.C., 1987, Structural style and kinematics of an underplated slate belt, Kodiak and adjacent islands, Alaska: Geological Society of America Bulletin, v. 99, p. 7-20.

Reviewers: Steve Nelson and Alison Till

Fossil Pollen from Nonmarine Sedimentary Rocks of the Eastern Yukon-Tanana Region, East-Central Alaska

By Helen L. Foster *and* Yaeko Igarashi

Abstract

New data from fossil pollen and spores confirm the occurrence of both Late Cretaceous and Tertiary nonmarine sedimentary rocks in the eastern Yukon-Tanana region. In the Tanacross quadrangle sedimentary rocks of both Late Cretaceous and Tertiary age are present, whereas in the Eagle quadrangle south of the Tintina fault zone only Tertiary sedimentary rocks have been recognized. Such genera as *Aquilapollenites* and *Taxodiapollenites* are characteristic in the Late Cretaceous rocks but are not found in the Tertiary rocks.

Part of the nonmarine sedimentary rocks probably were deposited in small depressions that resulted from local faulting, some of which may have been related to volcanic activity. Other deposits appear to be near thrust and strike-slip faults. Both the Late Cretaceous and Tertiary sedimentary rocks were deformed in Tertiary time, but it is not known whether the deformation was the result of regional or local events.

INTRODUCTION

Nonmarine, poorly indurated to well-indurated sedimentary rocks, including conglomerate, sandstone, shale, coal, and tuffaceous rocks, crop out in widely scattered areas in the eastern Yukon-Tanana region of east-central Alaska (fig. 1). Exposures are generally poor, occur in densely vegetated areas, and are rarely more than a few square meters in size. The folded and faulted sedimentary rocks lie unconformably on metamorphic rocks and in places appear to be interlayered with Cretaceous and (or) Tertiary volcanic rocks. Samples for pollen analyses were obtained during reconnaissance geologic mapping of the eastern Yukon-Tanana region from 1961 to 1970, and in limited resampling in 1984, 1985, and 1987. Many samples were barren, and some were not useful because of poor pollen preservation or possible Holocene contamination. The purpose of this paper is to present new data on fossil pollen from the nonmarine sedimentary rocks of the Eagle and Tanacross quadrangles, integrate the new data with previously published data, and discuss some implications of these data for the late Mesozoic and Cenozoic geologic history of east-central Alaska.

TANACROSS QUADRANGLE

Nonmarine sedimentary rocks crop out in several small areas in the northern, central, and southern parts of the Tanacross quadrangle (figs. 1 and 2). Generally the rocks are gray or tan, but in the southernmost area some of the rocks are orange or red brown, or have a purple cast.

West Fork Area

The northernmost area of nonmarine sedimentary rocks is a narrow strip composed of conglomerate, sandstone, minor shale and coal, and tuffaceous sandstone near the southern margin of the Taylor Mountain granitic intrusion near the West Fork of the Dennison Fork of the South Fork of the Fortymile River. The sedimentary rocks unconformably overlie amphibolite-facies metamorphic rocks, and at several localities a basal conglomerate that contains pebbles, cobbles, and boulders of the underlying metamorphic rocks is exposed. These poorly and sporadically exposed sedimentary rocks extend in an east-west direction for about 43 km and have a maximum estimated width of about 3 km. Two samples (fig. 2*B* and tables 1 and 3, no. 3) were obtained in 1961 from a borrow pit that was used when the Taylor Highway was constructed. This pit is now completely obliterated and the rocks are no longer exposed. The palynomorph flora of the two samples, identified by Robert H. Tschudy (U.S. Geological Survey, written commun., July 31, 1962), was almost identical. Tschudy reported that "many of the spores, including *Tasmanites*? and *Leiozonotriletes naumovae*? indicate an Upper Devonian assemblage, but that this assemblage is mixed with one of a more modern aspect, characterized by tricolpate, monosulcate, coniferous, and *Aquilapollenites* pollen. On the basis of the latter assemblage, an age of Late Cretaceous is suggested for these sedimentary rocks, but because of the poor preservation of the organic material, an even younger age cannot be ruled out" (Foster, 1967).

A new borrow pit, opened nearby in the 1970's, exposed 2 to 3 m of the sedimentary rock section. The exposed

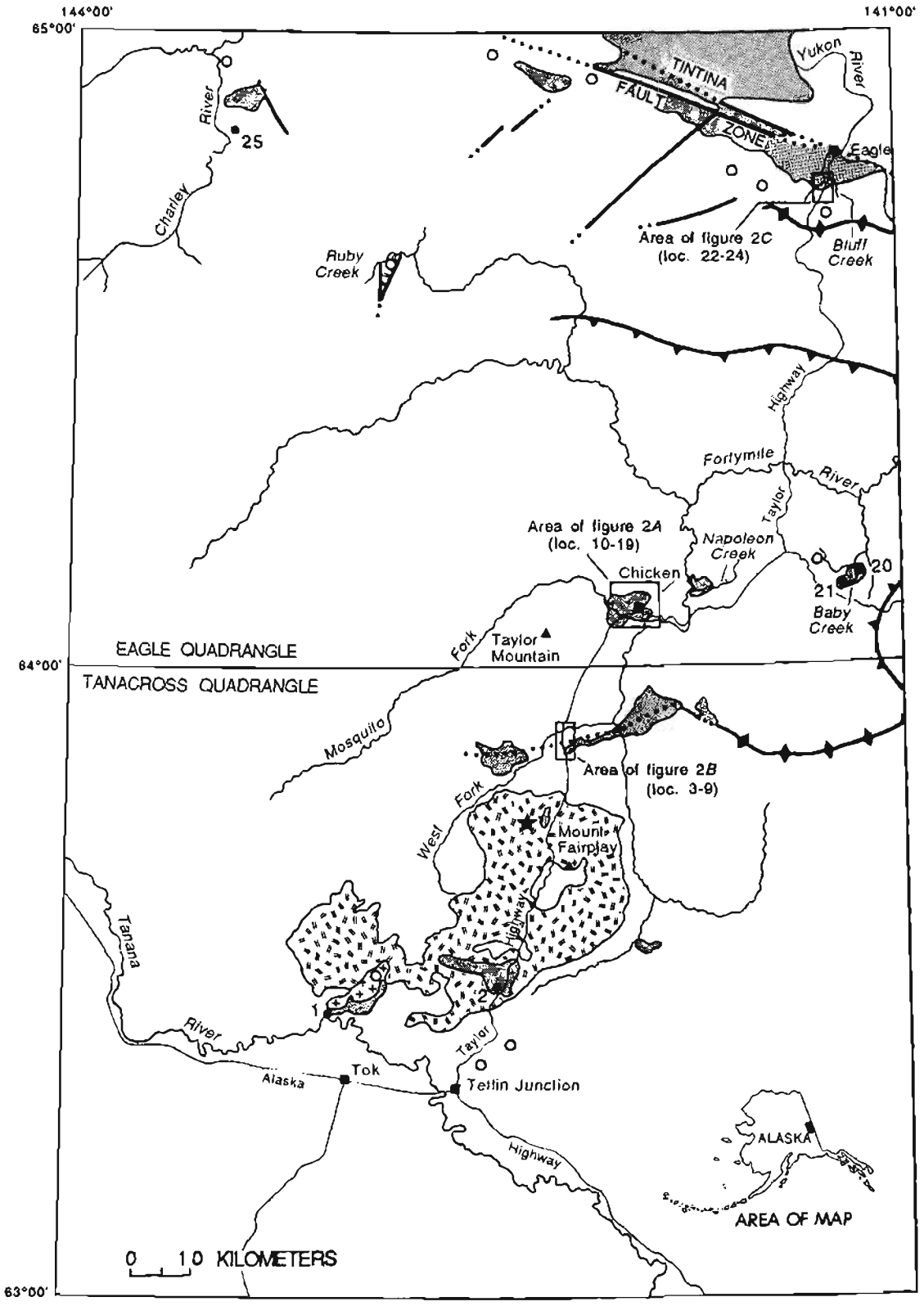

Figure 1. Geologic sketch map showing areas of Cretaceous and (or) Tertiary nonmarine sedimentary rocks and adjacent Cretaceous and (or) Tertiary volcanic rocks. Samples and localities shown are described in tables 1–3.

rocks are deformed into overturned folds and cut by small thrust faults (Foster and Cushing, 1985). A sample collected from this pit in 1983 (fig. 2*B* and table 1 and 3, no. 5) "yielded a badly degraded assemblage of nonmarine palynomorphs among which only those forms having the most distinctive outline shapes could be recognized. The assemblage includes species of *Aquilapollenites* and *Cranwellia* indicating an age of late Campanian to Maastrichtian. The species of *Aquilapollenites* compare with those described by R.H. Tschudy from the Colville Group in eastern Alaska. These results are in agreement with those previously reported by R.H. Tschudy" (D.J. Nichols and F.H. Wingate, unpublished Report on Referred Fossils, U.S. Geological Survey, April 1988).

Fossil pollen in five samples (table 1, nos. 4A through E) from the same pit discussed above but collected a few meters northeast of sample no. 5 was identified by Igarashi. Although pollen was abundant in several of these samples, *Aquilapollenites* and other Cretaceous indicators were not found. In fact, the entire flora differs from that of the 1961 and 1983 collections (table 1, no. 3 and no. 5). The presence of the exotic genera *Ulmus*, which became extinct in Alaska during the late Miocene (Wolfe and Hopkins, 1967), suggests an age older than late Miocene; and the abundance of *Picea* suggests a possible early or middle Miocene age. Because there appears to be no mixing of characteristic Cretaceous and Tertiary elements in the samples from this pit, two distinct ages of deposits are inferred to be present.

Samples of a light-brown siltstone were collected in a borrow pit on the east side of the Taylor Highway about a kilometer north of the pit just discussed (fig. 2*B* and table 1, no. 9). The siltstone contains plant impressions and poorly preserved pollen consisting of abundant *Picea* with *Betula*, *Ulmus*, *Alnus*, and monolete type fern spores, but no pollen and spores of Cretaceous types. According to the determinations of Igarashi, the assemblage appears to be Tertiary and contains some of the same elements as found in one of the collections obtained to the south (fig. 2*B* and table 1, no. 4).

Fossil pollen (fig. 2*B* and table 1, no. 7) from outcrops along a small stream 2 km east of the borrow pits just discussed was identified by Igarashi. Although the pollen is

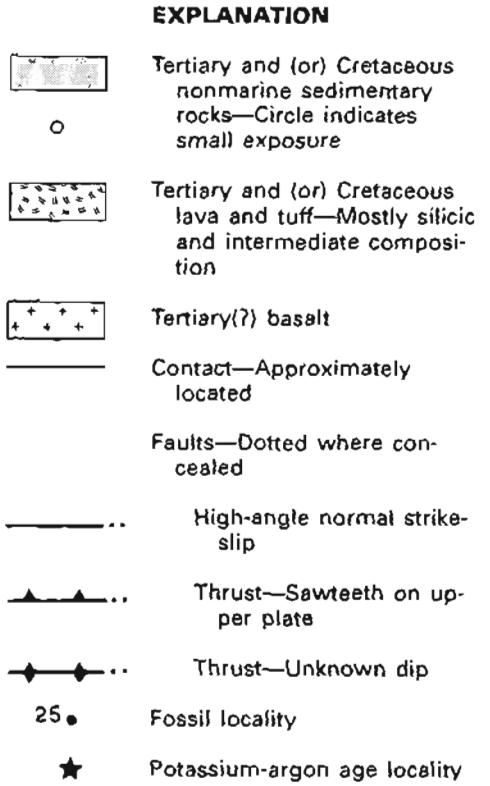

Figure 1. Continued.

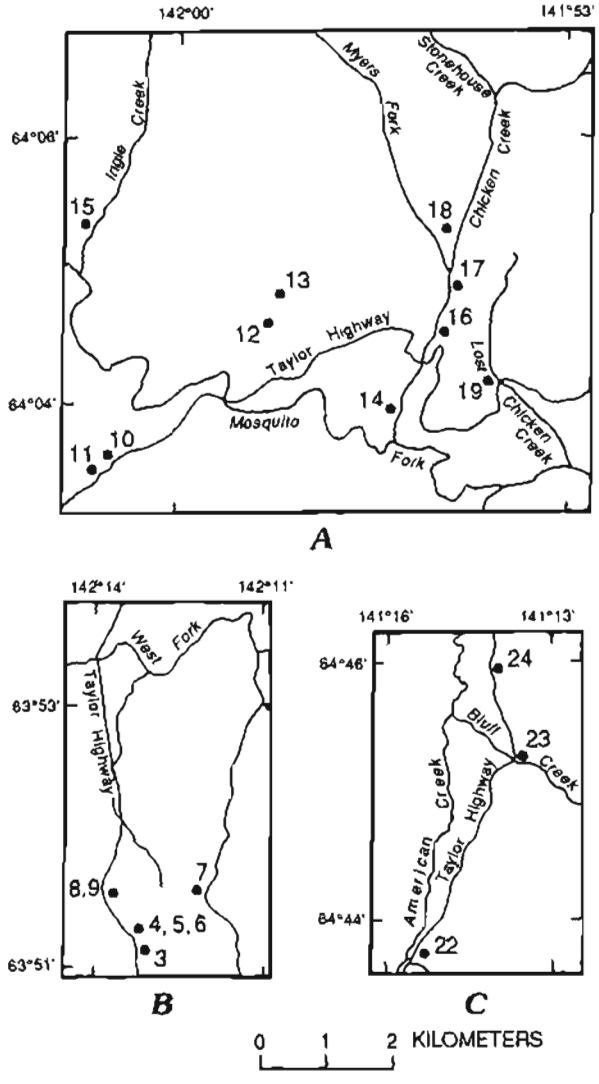

Figure 2. Sample-locality maps for three areas shown in figure 1. A, Chicken area. *B*, West Fork area. *C*, Bluff Creek area. Samples and localities are described in tables 1–3.

poorly preserved, the presence of *Aquilapollenites, Taxodiapollenites*, and *Lycopodiumsporites* suggests that these rocks are probably Cretaceous. Samples collected still farther east along strike did not contain fossil pollen.

Mount Fairplay Area

Poor exposures of moderately dipping sandstone, siltstone, and tuffaceous rocks, in places probably interlayered with lava and tuff (most fairly silicic), are on both the north and south sides of Mount Fairplay in the central part of the Tanacross quadrangle. No fossil pollen was obtained from samples collected on the north side, but a Cretaceous age for these sedimentary rocks is suggested by a K-Ar age of 93.6±2 Ma (Bacon and others, 1985) determined on a nearby tuff (sanidine; location on fig. 1). Only one sample (tables 1 and 3, no. 2) from the south side of Mount Fairplay yielded identifiable fossils and contained unusually large numbers of well-preserved plant tissues and palynomorphs. Igarashi considers this flora to be of Tertiary age, probably younger than Miocene.

As in the West Fork area, both Cretaceous and Tertiary sedimentary rocks are in the Mount Fairplay area, but exposure is so limited and preservation of fossil pollen so poor that the relative extent and ages of most of these rocks are not determinable.

Southern Area

Fossil pollen was obtained from only one locality on the north side of the Tanana River in the southernmost area of sedimentary rocks in the Tanacross quadrangle. Material collected by Arthur Fernald (U.S. Geological Survey) in 1962 and identified by Estella Leopold (fig. 1 and tables 1 and 3, no. 1) included *Aquilapollenites* and *Taxodia-ceaepollenites (Taxodiapollenites)*, suggesting that these rocks are also Cretaceous (Foster, 1970).

EAGLE QUADRANGLE

In the Eagle quadrangle samples were collected from several exposures of sedimentary rocks in the Chicken area, the Napoleon Creek area, the Baby Creek area, the Ruby Creek area, the Bluff Creek area, and at one locality along the Charley River. No pollen was found in the samples from the Napoleon Creek and Ruby Creek areas.

In the Chicken area two assemblages of sedimentary rocks contain fossil pollen and plant fragments. The more extensive assemblage consists of tan and gray sandstone, tuffaceous sandstone, and minor tuffaceous shale cut by basalt dikes and stringers. It is very poorly exposed. Gold dredge tailings believed to be derived from this assemblage include coal that contains abundant amber. Coal in vertical seams was mined and used locally in the Chicken area (Mertie, 1937). Leaves of *Metasequoia glyptostroboides* Hu and Cheng and *Alnus evidens* (Hollick) Wolfe were preserved in sandstone dredged from the lower part of Chicken Creek. *Alnus evidens* may indicate a late Oligocene or early Miocene age (J.A. Wolfe *in* Foster, 1969). Poorly preserved palynomorphs from two localities in the Chicken area (fig. 2*A* and table 2, nos. 15 and 16) near the dredge tailings are believed to indicate an early Tertiary age (Foster, 1969). Samples collected in 1984 and examined by Igarashi (fig. 2*A* and table 2, nos. 10 and 11) contain pollen that is consistent with Wolfe's suggestion of an early Miocene age.

The second assemblage of sedimentary rocks in the Chicken area consists of hard, dense, very fine grained gray and black siliceous rocks with conchoidal fracture, which are probably tuffs. Cobbles and boulders of these rocks are common in Chicken, Lost Chicken, and Stonehouse Creeks. Although searches have been made, these rocks have never been found in place. Some of the rock contains so much fragmentary plant material that it has been termed "fossilized tundra" by local people. Based on pollen and other plant fragments these rocks are believed to be younger than the sandstone, coal, and tuffaceous sandstone described above from the Chicken area, and they may be late Tertiary or early Pleistocene (Foster, 1969).

The Baby Creek locality was not recollected. Fossil pollen from the previously obtained samples (fig. 1 and table 2, nos. 20 and 21) indicate a probable late Tertiary age for these rocks (Foster, 1969).

Several samples (figs. 1 and 2*C* and table 2 and 3, nos. 22, 23, and 24) collected south of the Tintina fault zone along the Taylor Highway near Bluff Creek contain fossil pollen of Tertiary age. Also, pollen from a sample collected from an outcrop of conglomerate and sandstone along the Charley River (fig. 1 and table 2, no. 25) appears to be Tertiary.

DISCUSSION

Most of the nonmarine sedimentary rocks of the Tanacross and Eagle quadrangles were deposited unconformably on metamorphic rocks. However, in the Mount Fairplay area some of the sedimentary rocks appear to be interlayered with volcanic rocks, mostly tuff of silicic and intermediate composition. In the southern area of the Tanacross quadrangle sedimentary rocks are in contact with basalt.

Most exposures appear to represent local deposits of a restricted age. However, in the West Fork area both Late Cretaceous and Tertiary deposits are exposed in folds only a few meters apart. Rocks of the two ages appear to be in fault contact, although a sedimentary contact that has been folded and faulted cannot completely be ruled out.

The elongate pattern of distribution of the West Fork sedimentary rocks suggests accumulation in a zone of faulting, probably thrust faulting; a thrust fault is believed to be partly covered by these deposits (fig. 1). In other parts of the Tanacross quadrangle and in the Ruby Creek area, some of the sedimentary rocks may have accumulated in small depressions that resulted from volcanic activity and associated faulting. The Chicken area, Napoleon Creek, and Baby Creek deposits cannot be directly related to mapped faults, although many small normal faults and thrust faults are present in these areas. The distribution of deposits in the Chicken area suggests deposition in a small local depression that could have resulted from faulting (possibly related to volcanism). The Bluff Creek deposits appear to be related to the Tintina fault zone, a major northwest-trending zone of right-lateral strike-slip movement (fig. 1). The Bluff Creek deposits may be a small part of more extensive deposits of several ages, ranging from Cretaceous through Tertiary, that are found in and near the Tintina fault zone in both Alaska and Canada (Foster, 1976; Foster and others, 1987).

Although all of the nonmarine sedimentary rocks discussed have been deformed, the time, extent, and number of deformational events are not known. The rocks may have been involved in a regional event in late Tertiary time, or deformation may have resulted from several local events, such as high-angle faulting in the volcanic areas, thrust faulting in the West Fork area, and strike-slip movement along the Tintina fault zone. For instance, on the basis of fossil pollen the deformed beds in the Baby Creek area are considered late Tertiary in age, which suggests that at least some of the deformation in that area occurred in late Tertiary or early Quaternary time. However, Tertiary may be the most probable time of this deformation because Quaternary deposits nearby are uplifted but not folded. Thus, data on fossil pollen provide limited constraints in some areas on the time of deformation.

CONCLUSIONS

Data from fossil pollen indicate that local deposition of nonmarine sediments occurred in the eastern Yukon-Tanana region from the Late Cretaceous through much of the Tertiary. The nonmarine sedimentary rocks of the Tanacross quadrangle include rocks of both Late Cretaceous and Tertiary age whereas in the Eagle quadrangle south of the Tintina fault zone only Tertiary sedimentary rocks are known. All of the Cretaceous and Tertiary sedimentary rocks described are deformed, and in the West Fork area overturned folds and small thrust faults occur in both the Cretaceous and Tertiary sedimentary rocks, indicating that deformation was probably in the late Tertiary (post-Miocene). Deformation in the Baby Creek area (Eagle quadrangle) is believed to have occurred in the late Tertiary. Thus deformation probably occurred in late Tertiary time throughout much of the eastern Yukon-Tanana region, but it is not known whether deformation was of regional extent or from only local events. Some of the deformational events along the Tintina fault zone undoubtedly had regional extent, but there is no indication that rocks south of the Bluff Creek area were involved.

REFERENCES CITED

Bacon, C.R., Foster, H.L., and Smith, J.G., 1985, Cretaceous calderas and rhyolitic welded tuffs in the Yukon Tanana terrane, east-central Alaska: Geological Society of America Abstracts with Programs, v. 17, no. 6, p. 339.

Foster, H.L., 1967, Geology of the Mount Fairplay area Alaska: U.S. Geological Survey Bulletin 1241-B, p. B1-B18.

———1969, Reconnaissance geology of the Eagle A-1 and A-2 quadrangles, Alaska: U.S. Geological Survey Bulletin 1271-G, p. G1-G30.

———1970, Reconnaissance geologic map of the Tanacross quadrangle, Alaska: U.S. Geological Survey Miscellaneous Geologic Investigations, Map I-593.

———1976, Geologic map of the Eagle quadrangle, Alaska: U.S. Geological Survey Miscellaneous Investigations Series, Map I-922.

Foster, H.L., and Cushing, G.W., 1985, Tertiary(?) folding in the Tanacross quadrangle: *in* Bartsch-Winkler, Susan, and Reed, K.M., eds., The United States Geological Survey in Alaska: Accomplishments during 1983: U.S. Geological Survey Circular 945, p. 38-40.

Foster, H.L., Keith, T.E.C., and Menzie, W.D., 1987, Geology of east-central Alaska: U.S. Geological Survey Open-File Report 87-188, 59 p.

Mertie, J.B. Jr., 1937, The Yukon-Tanana region Alaska: U.S. Geological Survey Bulletin 872, 276 p.

Wolfe, J.A., and Hopkins, D.M., 1967, Climatic changes recorded by Tertiary land floras in northwestern North America, *in* Tertiary correlations and climatic changes in the Pacific: Pacific Science Congress, 11th, Tokyo, 1966, Symposium No. 25, p. 67-76.

Reviewers: Warren Yeend and William Patton, Jr.

Table 1. Fossil pollen and spores from Cretaceous and Tertiary sedimentary rocks of the Tanacross quadrangle

[Numbered localities are shown on figures 1 and 2. "x" indicates presence of pollen and (or) spores. Where available the amount of pollen and (or) spores is given in percent of the total sample]

Pollen and spores	1	2	3	4A	4B	4C	4D	4E	5	6	7	8	9
Sequoiapollenites	x												
Aquilapollenites	x		x						x		x		
Pinuspollenites											x		
Taxodiapollenites	x		x								x		
Baculatisporites											x		
Cicatricosisporites			x										
Cranwellia									x				
Echinatioporis											x		
Leiozonotritetes naumovae ?			x										
Lycopodiumsporites			x								x		
Osmundacidites											x		
Miscellaneous spores	x												
Tasmanites ?			x										
Inaperturopollenites											x		
Picea		80.7		x	13.3	x	x	11.6				85.5	x
Abies		0.5			0.7		x						
Conifer pollen V 2L			x										
Conifer pollen V 2S			x										
Larix (?) type					0.7			4.2					
Pinus		0.9			2.1	x						2.3	
Alnus		5.5		x	3.5			7.4					x
Betula		8.8		x	37.8	x	x	26.3					x
Acer					0.7		x						
Ericales		0.5											
Populus								1.1					
Quercus					6.3		x	1.1					
Tilia					0.7								
Ulmus					1.4								x
Corylus					0.7		x						
Araliaceae					0.7								
Carduoideae		0.5					x						
Artemisia								2.1					
Lilium					1.4								
Umbelliferae					2.1			1.1					
Epilobium							x	1.1					
Cyperaceae					2.1								
Gramineae		0.9			4.9		x	1.1					
Indeterminable				x	0.7								
Tricolpate pollen		0.5	x										
Tricolporate pollen		0.5		x	2.1			1.1					
Triporate pollen										x			
Monosulcate pollen			x										
Lycopodium					1.4		x	1.1					
Lycopodium selago													
Osmunda		0.9						2.1					
Monolete spores and monolete type				x	17.5			36.8		x			x
Equisetum												1.1	
Ceratopteris(?)												9.2	
Trilete spores, trilete type								1.1				2.3	x
Fern spores (TO)			x										
Fern spores (TY)			x										
Sphagnum		0.5											
Total number of grains		217			143			95				87	

Table 2. Fossil pollen and spores from Tertiary sedimentary rocks of the Eagle quadrangle

[Numbered localities are shown on figures 1 and 2. "x" indicates presence of pollen and (or) spores. Where available the amount of pollen and (or) spores is given in percent of the total sample]

Pollen and spores	10	11	12	13	14	15	16	17	18	19	20	21	22	23	24	25
Alnus evidens (Hollick) Wolf (leaves)					x											
Metasequoia glyptostroboides (leaves)					x											
Picea	73.0	67.2	x	x				x		x		x	x	x	x	x
Picea or *Abies*									x							
Picea cf. *engelmanii*											x					
Picea cf. *mariana*				x												
Abies				x		x	x			x					x	x
Cedrus-like, *unisaccate*										x						
cf. *Cedrus*										x						
Juniperus type												x				
Juniper or ? Sequoia									x							
Larix(?) type						x						x				
Pinus	0.5	0.4								x		x	x		x	
cf. *Pseudotsuga*										x						
Sciadopitys type												x				
Taxodiaceae				x												
Tsuga				x		x										
Alnus	3.7	2.6				x	x			x	x			x	x	
Betula	18.1	8.4		x						x	x		x	x	x	x
Acer						x										
Castanea type				x												
Carya and *Carya(?)*	0.5			x		x	x							x		
Ericales	1.9	0.7													x	
Juglans~Pterocarya						x	x								x	
Quercus		0.4														
Tilia							x									
Ulmus						x										
cf. *Artemisia*										x						
Cruciferae										x						
Onagraceae, *Epilobium* type		0.4		x												
Rhododendron type											x					
Ranunculaceae										x						
Rosaceae type									x							
Umbelliferae							x									
Cyperaceae	1.4	0.4					x									
Gramineae	0.9	0.4		x					x					x		
Tricolporate pollen								x								
Lycopodium	0.5	0.4								x				x		
Lycopodium cf. *annotium*										x						
Lycopodium selago																x
Osmunda		0.4				x	x		x	x		x				
Osmundaceae								x								
Polypodiaciae				x					x	x		x				
Monolete spores and monolete type										x						
Monolete sp., spiny										x						
Ceratopteris(?)		17.9														
Pteridium type												x				
Selaginella cf. *densa*												x				
Trilete spores, Trilete type		0.7								x						x
Monocots, undet.									x	x						
Sphagnum								x								
Total number of grains	216	274									20					

Table 3. Sample localities with fossil pollen (localities shown on figures 1 and 2 and fossil pollen identified in tables 1 and 2)

Locality (figs. 1 and 2)	Field number	Latitude	Longitude	Quadrangle	Collector	Year of collection	USGS Paleobotany location	Lithology and location	Pollen identified by	Year of study	Age
1	61F437	63°27'	143°3.8'	Tanacross B-5	Arthur Fernald	1961	D3510	Tuffaceous shale and sandstone, black and purple. Exposed along the Tanana River 12 km northwest of Tok.	Estella B. Leopold	1965	Late Cretaceous
2	8781405	63°28.6'	142°26.4'	Tanacross B-3	Yaeko Igarashi and Helen Foster	1987	_____	Sandstone, tuffaceous, and pebble conglomerate. Old borrow pit on west side of Taylor Highway 22 km north of Tetlin Junction.	Yaeko Igarashi	1988	Probably Tertiary, younger than Miocene
3	T-218a, b	63°51.2'	142°13.1'	Tanacross D-3	Helen Foster	1961	D1804-1 and D1804-2	Shale and siltstone, light-gray and tan, interlayered with sandstone. From exposure in old borrow pit on east side of Taylor Highway 4.4 km south of West Fork bridge.(Borrow pit no longer exists.)	Robert H. Tschudy	1962	Probably Late Cretaceous
4	84AFr238,A, B,C,D,E	63°51.3'	142°13.2'	Tanacross D-3	Helen Foster and Yaeko Igarashi	1984	_____	Mudstone, siltstone, sandstone, and tuff from folded and thrust-faulted sequence exposed in borrow pit on east side of Taylor Highway 4.3 km south of West Fork bridge. A. Siltstone, tan. B. Siltstone, reddish brown; interlayered with tuff and light gray clay. C. Shale, dark-gray, carbonaceous; contains abundant fragmental plant material. D. Siltstone, weathers orange-brown. E. Siltstone, dark-gray, carbonaceous.	Yaeko Igarashi	1983	Probably early Miocene
5	83AFr4177	63°51.3'	142°13.2'	Tanacross D-3	Helen Foster	1983	D6848	Shale and siltstone from folded beds of interlayered sandstone, shale, siltstone, and tuff. Plant fragments and impressions common in some layers. Exposure in borrow pit on east side of Taylor Highway 4.3 km south of West Fork bridge. Exposures have been destroyed by road-building operations.	D.J. Nichols and F.H. Wingate	1988	Late Campanian to Maastrich-tian
6	8781411	63°51.3'	142°13.2'	Tanacross D-3	Yaeko Igarashi	1987	_____	Coal from lenses of hard, black coal in a tuffaceous layer in tan, fine-grained, well-indurated sandstone. Sandstone has abundant dendrites on surface. Black carbonaceous material abundant, but palynomorphs are very poor and the assemblage of fossils is very limited. Many zones of gouge occur along slip-planes which follow gently dipping bedding. Exposure at north end of same borrow pit as localities 4 and 5.	Yaeko Igarashi	1988	Not determinable

Table 3. Continued

Locality (figs. 1 and 2)	Field number	Latitude	Longitude	Quadrangle	Collector	Year of collection	USGS Paleobotany location	Lithology and location	Pollen identified by	Year of study	Age
7	85AFr211A, B,C	63°51.6'	142°12.1'	Tanacross D-3	Helen Foster	1985	——	Shale, dark-gray, interlayered with sandstone beds up to 80 cm thick, pebble conglomerate, and lignitic beds. Abundant fragmental plant material. Crops out along bank of small stream 1.6 km east of mile 47 on the Taylor Highway and about 1.6 km east of locality 4.	Yaeko Igarashi	1988	Probably Late Cretaceous
8	84AFr239A	63°51.7'	142°13.8'	Tanacross D-3	Helen Foster	1984		Siltstone and sandstone, gray, fine-grained and carbonaceous. From old borrow pit on east side of Taylor Highway 3.1 km south of West Fork bridge.	Yaeko Igarashi	1985	Tertiary, probably younger than earlyMiocene
9	62FR219a	63°51.7'	142°13.8'	Tanacross D-3	Helen Foster	1962	——	Shale and siltstone from old borrow pit on east side of Taylor Highway 3.1 km south of West Fork bridge. Different layers of rock but same borrow pit as locality 8.	Yaeko Igarashi	1988	Possibly late Tertiary
10	84AFr245	64°3.5'	142°1.6'	Eagle A-3	Helen Foster	1984	——	Sandstone, gray, mostly fine grained; some is tuffaceous; cut by basaltic dikes and stringers. Road cut along west side of the Taylor Highway 2 km southwest of Mosquito Fork bridge.	Yaeko Igarashi	1985	Probably early Miocene
11	84AFr265	64°2.9'	142°3'	Eagle A-3	Helen Foster	1964	——	Sandstone, light tan and gray, fine to medium grained, friable and some tuffaceous; minor interlayered shale; some layers with abundant old trail cut about 2.5 km southwest of Mosquito Fork bridge.	Yaeko Igarashi	1985	Probably early Miocene
12	Eag A-2-123-64	63°4.6'	141°58.8'	Eagle A-2	Helen Foster	1964	——	Sandstone, white, medium-grained with carbonaceous fragments. Along unnamed drainage 1.25 km northeast of Mosquito Fork bridge.	Estella B. Leopold	1970	Not determinable
13	Eag A-2-124-6	64°4.8'	141°57.8'	Eagle A-2	Helen Foster	1964	D4438	Tuff, light-gray with green streaks. Appears to underlie basalt. Occurs in a ditch 1.7 km northeast of Mosquito Fork bridge.	Estella B. Leopold		Miocene or; Pliocene probably middle to late Miocene
14	59-X-64	64°3.8'	141°56.2'	Eagle A-2	Helen Foster	1964	10031	Ferruginous sandstone from top of gold dredge tailings on west side of Chicken Creek 0.8 km above the mouth of Chicken Creek.	Jack A. Wolfe (fossil leaves)	1965	Probably late Oligocene or early Miocene
15	557-63	64°5.3'	142°1.9'	Eagle A-3	Helen Foster	1963	D3346	Coal and carbonaceous shale from poor exposure along old wagon trail on west side of Ingle Creek 3.2 km northwest of Mosquito Fork bridge.	Robert H. Tschudy	1964	Early Tertiary
16	571-63	64°4.5'	141°55.4'	Eagle A-2	Helen Foster	1963	D3347	Shale from pit in terrace gravel 1.8 km north of mouth of Chicken Creek on east side of Chicken Creek.	Robert H. Tschudy	1964	Early Tertiary

Table 3. Continued

Locality (figs. 1 and 2)	Field number	Latitude	Longitude	Quadrangle	Collector	Year of collection	USGS Paleobotany location	Lithology and location	Pollen identified by	Year of study	Age
17	C-68	64°4.9'	141°55.2'	Eagle A-2	Helen Foster	1968	———	Coal with abundant amber and black, carbonaceous plant tissue from gold dredge tailings 2.5 km north of mouth of Lost Chicken Creek on east side of Chicken Creek.	Yaeko Igarashi	1988	Not determinable; possibly late Tertiary
18	55APW11	64°5.2'	141°55.5'	Eagle A-2	Troy Péwé	1955	D1161	Chert (probably siliceous tuff) cobbles containing fossil plant material from upper Chicken Creek.	Estella B. Leopold	1964	Late Cenozoic
19	Thin sections 5837A, 6001, and 5834	———	———	Eagle A-2	———	———	———	Chert (siliceous tuff?) cobbles, black, from Lost Chicken Creek. Pollen seen in 9 thin sections.	Estella B. Leopold	1964	Probably Pliocene or early Quaternary
20	713-65	64°8.1'	141°9.94'	Eagle A-1	Helen Foster	1965	D4009	Matrix from conglomerate exposed in cliffs on east side of Baby Creek. Pollen well preserved, but scant (about 20 grains found).	Estella B. Leopold	1967	Probably late Cenozoic
21	715-65	64°7.9'	141°9.98'	Eagle A-1	Helen Foster	1965	D4010	Sandstone, gray, arkosic, interbedded in conglomerate at water level on west side of Baby Creek.	Estella B. Leopold	1967	Late Tertiary
22	8782202	64°43.7'	141°15.4'	Eagle C-1	Yaeko Igarashi and Helen Foster	1987	———	Sandy layer in weathered conglomerate exposed in old borrow pit on east side of Taylor Highway about 3 km south of Bluff Creek.	Yaeko Igarashi	1988	Probably late Tertiary
23	8782203	64°45.2'	141°13.6'	Eagle D-1	Yaeko Igarashi and Helen Foster	1987	———	Sandstone, coarse, interlayered in conglomerate. Contains leaf impressions. From old borrow pit on east side of Taylor Highway on north side of Bluff Creek.	Yaeko Igarashi	1988	Possibly late Tertiary
24	8782204	64°46.1'	141°14'	Eagle D-1	Yaeko Igarashi and Helen Foster	1987	———	Sandstone, fine-grained. Pollen is poorly preserved. From east side of Taylor Highway about 1.03 km north of Bluff Creek.	Yaeko Igarashi	1988	Probably late Tertiary
25	86AFr12	64°49.8'	143°26.2'	Eagle D-5	Helen Foster	1986	———	Sandstone, light-gray, interlayered with conglomerate which is composed mostly of granitic cobbles and boulders. A few 5- to 8-cm-thick reddish-brown stained ferruginous layers. An isolated outcrop with beds dipping eastward about 23°. On east side of Charley River 5.5 km southeast of Copper Creek.	Yaeko Igarashi	1988	Probably late Tertiary

Significance of Triassic Marble from Nakwasina Sound, Southeastern Alaska

By Susan M. Karl, David A. Brew, *and* Bruce R. Wardlaw

Abstract

A Late Triassic (Karnian) conodont from marble at Nakwasina Sound, 25 km north of Sitka on Baranof Island, southeastern Alaska, provides the first age for in-place carbonate rocks of the Wrangellia or Chugach terranes on Baranof and western Chichagof Islands. Stratigraphic and structural evidence suggests that the marble is a fragment of Wrangellia that was tectonically incorporated into the Kelp Bay Group, which is part of an accretionary complex within the Chugach terrane on Baranof Island. Of the alternative models permitted by available data, field relations and vectors of oceanic plate motions best support the interpretation that the southeast Alaska segment of the Border Ranges fault formed initially by convergence between the Chugach terrane and Wrangellia, and later underwent right-lateral reactivation or was cut by other right-slip faults.

INTRODUCTION

The Border Ranges fault marks a major tectonic boundary that extends for approximately 1,700 km from south-central to southeastern Alaska (fig. 1) (MacKevett and Plafker, 1974; Plafker and others, 1976; Decker and Johnson, 1981; Decker and Plafker, 1982). The fault, which was initiated in the Middle to Late Jurassic, separates the composite Alexander/Peninsular/Wrangellia terrane of Monger and Berg (1987) from an outboard accretionary complex represented by the Chugach terrane of Berg and others (1978). This tectonic boundary has a long and complicated subsequent history of transpression and is locally the site of reactivated contractional, extensional, and translational faulting at least through the Paleogene (Little and Naeser, 1989). Some segments of the fault in south-central Alaska indicate strike-slip motion followed by low-angle thrusting (Pavlis and Crouse, 1989), whereas high-angle reverse faulting followed by normal and (or) strike-slip movement is interpreted on other segments (Little and Naeser, 1989). Interpretation of the character and relative movement history of the Border Ranges fault in southeastern Alaska has been hindered by limited exposure and the uncertainty of various geologic constraints. On western Chichagof Island (fig. 1), the Border Ranges fault was interpreted by Decker and Johnson (1981) to be a west-directed thrust fault that was later rotated more than 90 degrees to a steeply west-dipping attitude. At two localities on northern Baranof Island, the Border Ranges fault was observed to have a shallow dip (Plafker and others, 1976), although it is vertical at Peril Strait and has a linear trace for much of its mapped extent. These observations permit the interpretation that the Border Ranges fault varies considerably in orientation, character, and movement history from place to place, and raise alternative possibilities such as interactions between the Border Ranges fault and younger strike-slip faults.

Recognition of the Border Ranges fault on Chichagof Island depends on stratigraphic assignment of the Whitestripe Marble and Goon Dip Greenstone to the Wrangellia terrane (Plafker and others, 1976; Jones and others, 1977). In the absence of fossils, this assignment has been based on lithologic similarities with type-Wrangellian rocks in south-central Alaska. In this report we present the first fossil evidence for the age of large marble blocks in the Kelp Bay Group, which is separated by a structure interpreted to be the Border Ranges fault from the rocks assigned to Wrangellia on Chichagof Island. We discuss the implications of the fossil data for the question of correlations of the marble with the Whitestripe Marble or Wrangellian limestones and the implications for the identification of and local movement history on the Border Ranges fault.

GEOLOGIC SETTING

In southeastern Alaska, the rocks east, or inboard, of the Border Ranges fault (fig. 1) are interpreted to be the original "upper plate," representing the North American plate edge in the Middle to Late Jurassic (Plafker and others, 1976). On Chichagof Island these rocks consist of the Whitestripe Marble, the Goon Dip Greenstone, and various metamorphic rocks with uncertain Paleozoic or Mesozoic protoliths that are basement to the marble and greenstone (fig. 1). The rocks west, or outboard, of the Border Ranges fault are interpreted to represent the "lower plate," which was accreted to the North American margin in the Late

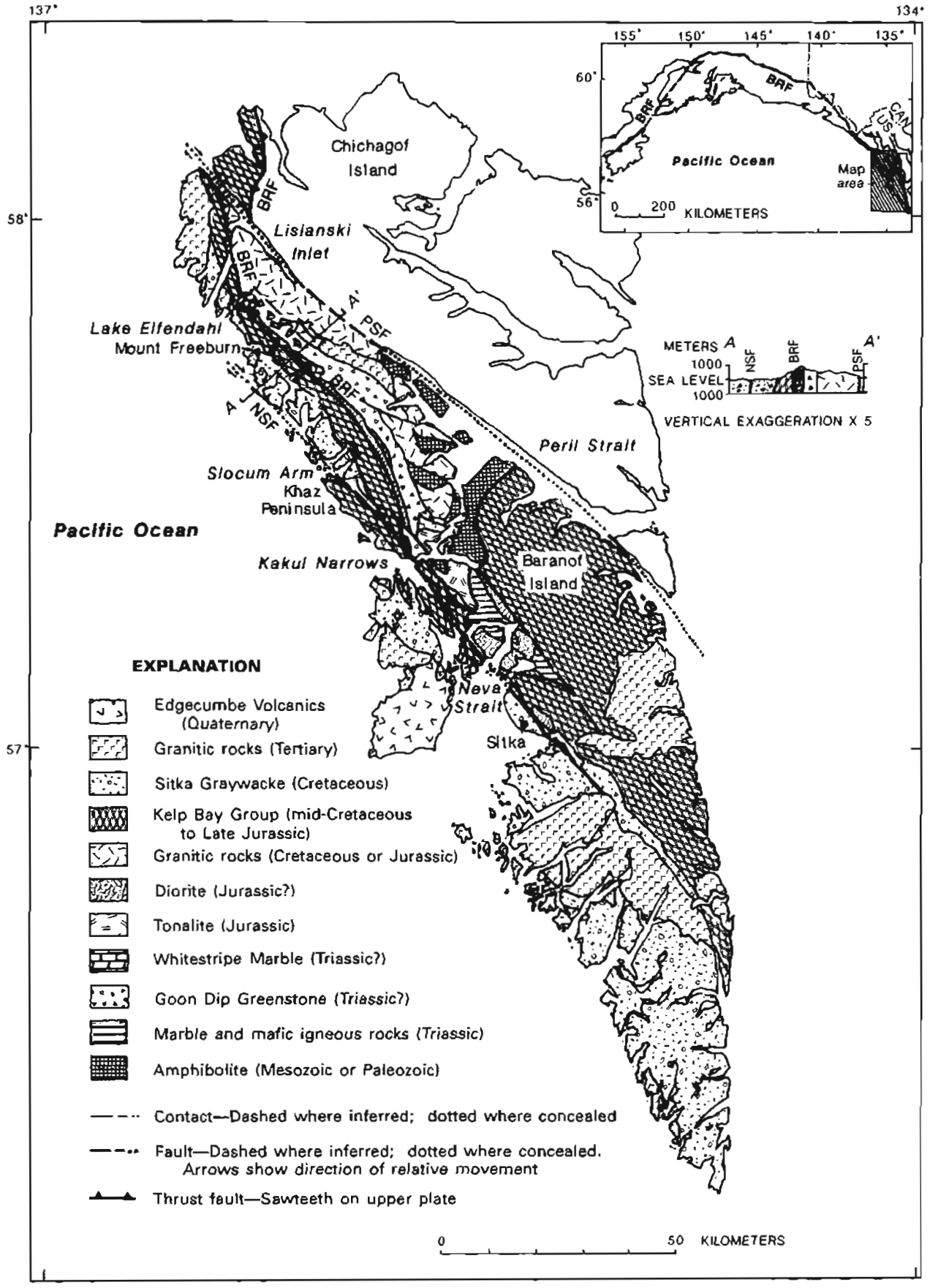
137°
134°
58°
57°
155°
150°
145°
140°
135°
60°
56°
BRF
CAN
US
Pacific Ocean
Map area
0 200 KILOMETERS
Chichagof Island
Lisianski Inlet
Lake Elfendahl
Mount Freeburn
PSF
NSF
A
A'
METERS
1000
SEA LEVEL
1000
VERTICAL EXAGGERATION X 5
Peril Strait
Slocum Arm
Khaz Peninsula
Pacific Ocean
Kakul Narrows
Baranof Island
Neva Strait
Sitka
EXPLANATION
Edgecumbe Volcanics (Quaternary)
Granitic rocks (Tertiary)
Sitka Graywacke (Cretaceous)
Kelp Bay Group (mid-Cretaceous to Late Jurassic)
Granitic rocks (Cretaceous or Jurassic)
Diorite (Jurassic?)
Tonalite (Jurassic)
Whitestripe Marble (Triassic?)
Goon Dip Greenstone (Triassic?)
Marble and mafic igneous rocks (Triassic)
Amphibolite (Mesozoic or Paleozoic)
Contact—Dashed where inferred; dotted where concealed
Fault—Dashed where inferred; dotted where concealed. Arrows show direction of relative movement
Thrust fault—Sawteeth on upper plate
0 50 KILOMETERS

Mesozoic. On Chichagof and Baranof Islands, these rocks compose an accretionary complex consisting of an inner (eastern) mélange unit, the Kelp Bay Group, and an outer (western) flysch unit, the Sitka Graywacke (fig. 1). Because the Border Ranges fault is mostly vertical in orientation in southeastern Alaska, the terms "inboard" and "outboard" are preferred for rocks on either side of this former plate boundary.

INBOARD ROCKS

On western Chichagof Island, the rocks inboard (east) of the Border Ranges fault, where it is interpreted to be a thrust fault (Plafker and others, 1976; Decker and Johnson, 1981), include the Goon Dip Greenstone and the Whitestripe Marble (fig. 1). These two units have been lithologically correlated with the Nikolai Greenstone and the Chitistone Limestone, respectively (Plafker and others, 1976), and have been assigned to the Wrangellia terrane (Jones and others, 1977).

The Whitestripe Marble forms a long, narrow, very prominent white stripe across western Chichagof Island. It is as much as 500 m wide, averages 100 m wide, and extends intermittently for more than 50 km along strike (fig. 1). The marble is massive to thick-bedded with bedding-parallel stylolitic partings and retains no sedimentary structures. It has yielded no megafossils or microfossils but is considered to be Triassic based on a coral of possible Triassic age in a boulder found in the Goon Dip River by Reed and Coats (1941). However, the boulder may have come from unnamed carbonate units or blocks in the Kelp Bay Group. The Whitestripe Marble is bounded by the Border Ranges fault on the west; its eastern contact with the Goon Dip Greenstone is conformable, sharp, and locally faulted.

The Whitestripe Marble is intruded by mafic sills and dikes and by strongly altered and cataclasized diorite that is grayish green and medium grained. The diorite has a color index of 15 to 25 and contains hornblende and biotite that is extensively altered to chlorite and epidote/clinozoisite. Owing to its extreme alteration, the diorite has not been dated, but it was assigned a Cretaceous age by Loney and others (1975) based on its similarity to other Cretaceous diorites nearby. However, some of the plutons interpreted by Loney and others (1975) as Cretaceous have been shown to be Jurassic in age (Karl and others, 1988). Petrologically similar diorite associated with massive marble similar to the Whitestripe Marble in Russell Fiord (several hundreds of kilometers to the north) yielded a 160±3 Ma K-Ar age (Hudson and others, 1977). The strongly altered and cataclasized diorite on Chichagof Island was assigned a Cretaceous(?) age by Johnson and Karl (1985), but we currently interpret the diorite as Jurassic(?) based on its similarity in composition and context to the diorites in Russell Fiord and to dated Jurassic plutons (Karl and others, 1988) on Baranof and Chichagof Islands.

The Goon Dip Greenstone is mostly massive, dark grayish to olive green, locally amygdaloidal, and locally augite porphyritic. The greenstone consists of flows, sills, and flow breccias that are 1 to 5 m thick. Minor lenses of marble indicate that some flows were subaqueous; pipe vesicles and red, oxidized flow tops indicate that other flows were subaerial. Relict labradorite and augite laths are altered to epidote, actinolite, chlorite, albite, prehnite, calcite, pyrite, and sphene. Amygdules are filled with quartz, epidote, calcite, and prehnite. There are no fossil or radiometric ages from this unit. It is assigned a Triassic age based on its spatial association with the Whitestripe Marble (fig. 1) (Loney and others, 1975; Johnson and Karl, 1985).

The Chitistone Limestone conformably overlies the Nikolai Greenstone at the Wrangellia type area. Assuming that the correlation of Jones and others (1977) is valid and that the Whitestripe Marble analogously overlies the Goon Dip Greenstone stratigraphically, then the present contact relations (fig. 1, cross section) require that the sequence must have been overturned, possibly in a fault-propagation fold along the Border Ranges fault, before the thrust fault was rotated to its present steeply west-dipping attitude. As no large folds have been identified in the marble and greenstone, a different interpretation for the orientation of the Border Ranges fault on Chichagof Island may be warranted. The thrust fault beneath the Wrangellian rocks may not be exposed, and the mapped fault may be either a slightly west-dipping strike-slip fault or a young, east-directed reverse fault that truncates the hypothetical unexposed thrust fault.

On Baranof Island, the rocks on the inboard (north) side of the Border Ranges fault include minor amounts of marble, greenstone, and amphibolite gneiss intruded by a large Jurassic tonalite body yielding K-Ar ages of 152±4 Ma for biotite and 151±5 Ma for hornblende (Loney and others, 1967). This tonalite is gray, medium grained, hypidiomorphic to seriate in texture, and well foliated. It has a color index of 20, with biotite dominating hornblende, is locally altered to chlorite and epidote/clinozoisite, and locally has a cataclastic texture (Loney and others, 1975; Johnson and Karl, 1985). Diorite is a rare phase in this pluton, but the possibility that the strongly altered and cataclasized diorite described above is related to this pluton cannot be ruled out.

OUTBOARD ROCKS

On Chichagof Island, the rocks outboard (west) of the Border Ranges fault consist of a tectonic collage of kilo-

◀ Figure 1. Generalized geologic map of western Chichagof and Baranof Islands, modified from Loney and others (1975) and Johnson and Karl (1985). BRF, Border Ranges fault; NSF Neva Strait/Slocum Arm fault; PSF, Peril Strait fault.

meter-scale blocks with no matrix, a mélange of meter- to kilometer-scale blocks within a matrix, and a thick sequence of graywacke turbidites, which together compose an accretionary complex. The blocks in the collage and the mélange consist of greenstone, greenschist, blueschist, marble, chert, graywacke, and pelitic phyllite. The matrix of the mélange is composed of argillite, tuff, and graywacke. The collage is informally named the Freeburn assemblage (Johnson and Karl, 1985), and the mélange is the Khaz Formation of Loney and others (1975); both are parts of the Kelp Bay Group of Johnson and Karl (1985). Large blocks of marble in both the collage and the mélange have been lithologically correlated with the Whitestripe Marble, and the associated blocks of greenstone with the Goon Dip Greenstone (Loney and others, 1975). The large blocks of marble and greenstone were interpreted by Plafker and others (1976) to be klippen of the Wrangellian rocks. None of the Jurassic(?) strongly altered and cataclasized diorite has been identified as blocks

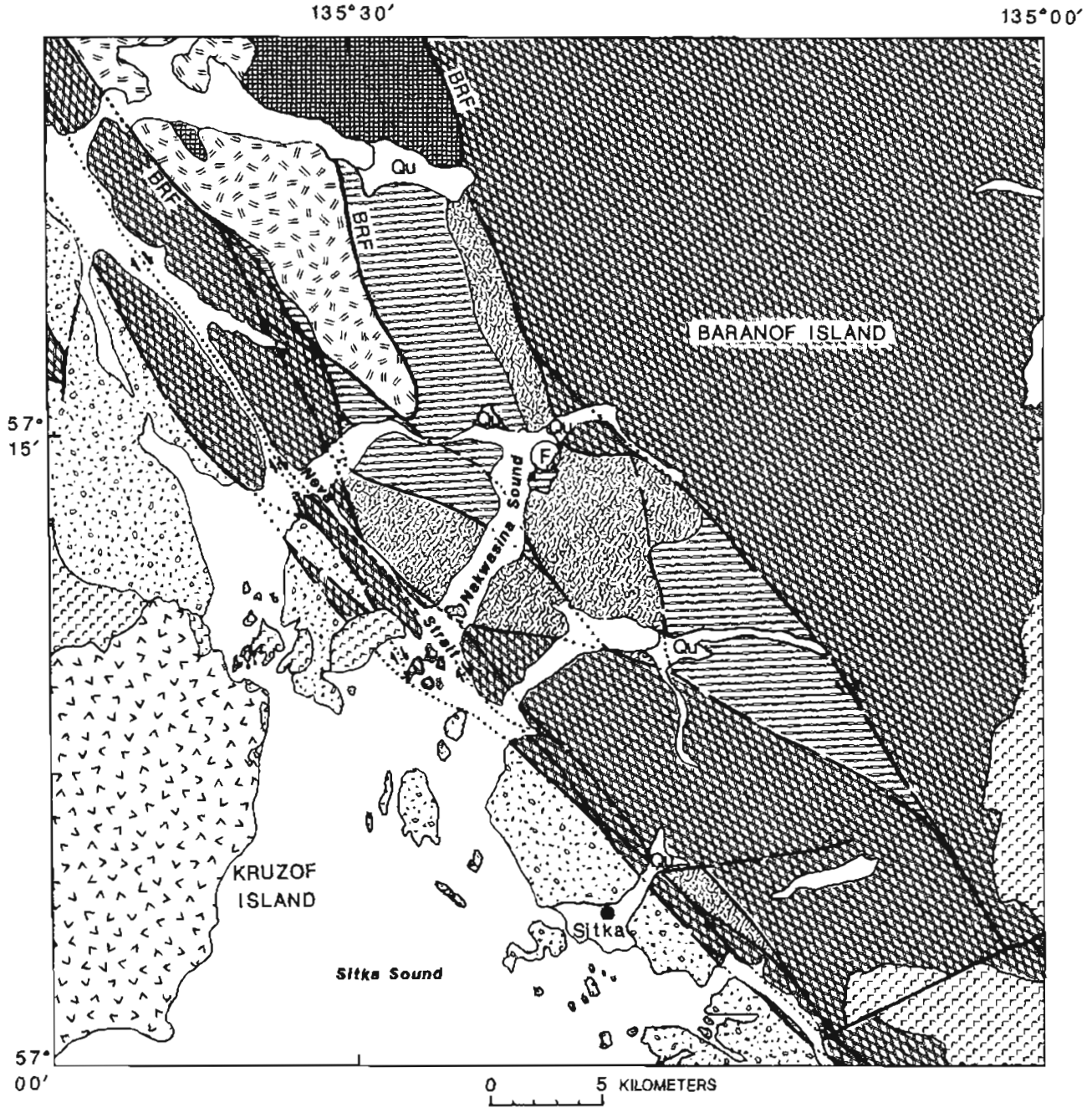

Figure 2. Geologic map of Nakwasina Sound area showing fossil location (F). BRF, Border Ranges fault. See figure 1 for explanation. Qu, Quaternary undifferentiated.

in the Freeburn assemblage or the Khaz Formation on Chichagof Island, although it forms large blocks in the correlative mélange facies of the Yakutat Group to the north in Russell Fiord, as well as forming large blocks in mélange in undivided rocks of the Kelp Bay to the south in Nakwasina Sound on northern Baranof Island.

Strongly cataclasized and altered (hornblende) diorite in the vicinity of Nakwasina Sound (fig. 2) contains inclusions of marble and greenstone ranging in scale from 1 to 100 m. This diorite occurs only as tectonic blocks in mélange. Marble, greenstone, and volcaniclastic metasedimentary rocks also occur as separate blocks in the mélange. All of these blocks are found in a mélange matrix of argillite and tuffaceous argillite in the Kelp Bay Group on northern Baranof Island. The formation of this mélange is considered to extend at least from the Jurassic (Brew and others, 1988) to the mid-Cretaceous. A mid-Cretaceous accretionary age is bracketed by the youngest (Early Cretaceous) fossil ages (Johnson and Karl, 1985) and by K-Ar isotopic ages of 91 to 106 Ma for metamorphosed rocks (Decker and others, 1980).

AGE AND DESCRIPTION OF THE FOSSIL LOCALITY AT NAKAWASINA SOUND

Marble occurs as large inclusions within altered diorite along the shores of Nakwasina Sound (fig. 2). The marble at location F (fig. 2) is well-foliated and cut by dikes of mafic rock. It contains millimeter-scale light-gray and medium-gray laminations, layers of volcanic breccia mixed with calcareous breccia, and layers of monomictic carbonate breccia with clasts less than 8 cm in diameter. Adjacent to the marble (contact unexposed) and also included in the diorite is greenstone with relict pillow structures. A poorly preserved conodont fragment, identified as Neogondolella or possibly primitive *Epigondolella* of *N. polygnathiformis* plexus, indicates a Late Triassic Karnian age for a 30-m inclusion of this marble within a diorite body on the southeast shore of Nakwasina Sound (fig. 2, location F). The conodont has a color alteration index (CAI) of 6.5, which is attributed to the intrusion by the pluton.

The marble and diorite in Nakwasina Sound have been mapped as part of the Kelp Bay Group, which is part of the accretionary complex outboard of the Border Ranges fault. The association of this marble with the greenstone and with the cataclastic altered diorite is similar to the lithologic associations of the Whitestripe Marble, and on this basis the marble is inferred to be correlative with the Whitestripe Marble, which is mapped inboard of the Border Ranges fault (fig. 1). This correlation suggests that the Whitestripe Marble may also be Late Triassic in age. The chain of evidence is tenuous, but important, because there are no other ages for the marbles in this particular geologic context on western Chichagof and northern Baranof Islands.

DISCUSSION

The Triassic age of the marble in Nakwasina Sound and its association with greenstone and diorite suggest that these tectonic blocks in the Kelp Bay Group mélange are derived from the inboard side of the Border Ranges fault and represent Wrangellian rocks. The rocks are intensely cataclasized, and geologic mapping indicates that they are not klippen because all the contacts with the mélange are vertical and that they are translated as blocks along the younger right-lateral Neva Strait/Slocum Arm fault system of Loney and others (1975). Faulted contacts between the marble/greenstone/diorite blocks and the mélange could be (1) primary fault contacts of blocks of the inboard plate tectonically kneaded into the accretionary complex (fig. 3*A*), (2) secondary faults cutting through the accretionary complex (fig. 3*B*), or (3) segments of the Border Ranges fault that have been translated into the accretionary complex by post-mid-Cretaceous strike-slip faults (fig. 3*C*).

The history of displacement on segments of the Border Ranges fault in southeastern Alaska can be inferred from geologic relations and relative plate motions between the Pacific, Kula, Farallon, and North American plates as interpreted by Wallace and Engebretson (1984). The Jurassic to Cretaceous age of the Kelp Bay Group (Brew and others, 1988) suggests that the convergent phase of the fault history began in the Jurassic. The mid-Cretaceous isotopic ages for metamorphic minerals in the Kelp Bay Group (Decker and others, 1980) may indicate the culmination of this convergent phase. The Neva Strait/Slocum Arm fault of Loney and others (1975) is a major young right-lateral system on Baranof and Chichagof Islands (fig. 1) that offsets the contact between the flysch (Sitka Graywacke) and the mélange (Kelp Bay Group) facies of the accretionary complex, and possibly segments of the Border Ranges fault as well. Right-lateral faults of uncertain age along Lisianski Inlet (such as the Peril Strait fault) (fig. 1) also offset the Border Ranges fault. At Lake Elfendahl on Chichagof Island (fig. 1), the Border Ranges fault has been intruded by an undeformed middle Tertiary granodiorite pluton, which provides a minimum age for displacement at that locality.

Vectors of Kula and Farallon plate motions as they interacted with the North American plate at the latitude of southeastern Alaska, as determined by Wallace and Engebretson (1984), are shown in figure 4. Prior to 85 Ma, the Farallon plate was obliquely underthrusting all of western North America. At about 92 Ma it was converging with southeastern Alaska in fairly dominant compression at a rate of about 100 km/m.y. (dashed arrow, fig. 4). A convergent and possibly thrusted contact would be expected between the continental margin and an accretionary complex, and the mid-Cretaceous metamorphic ages for the Kelp Bay Group (Decker and others, 1980) support this interpretation. After 85 Ma, the Kula plate was interacting more obliquely with southeastern Alaska than the Farallon plate

had done. The rate of transpression of the Kula plate reached a peak of about 200 km/m.y. between 56 and 46 Ma. After the subduction of the Kula ridge beneath southern Alaska (Byrne, 1979), at about 45 Ma, there was a pronounced shift to right-lateral transform motion between the Kula plate and southeastern Alaska at a rate of a little over 10 km/m.y. The right-lateral faulting on western Chichagof and Baranof Islands that reactivated and (or) redistributed the Border Ranges fault was probably initiated during this middle Tertiary reorientation of plate motions.

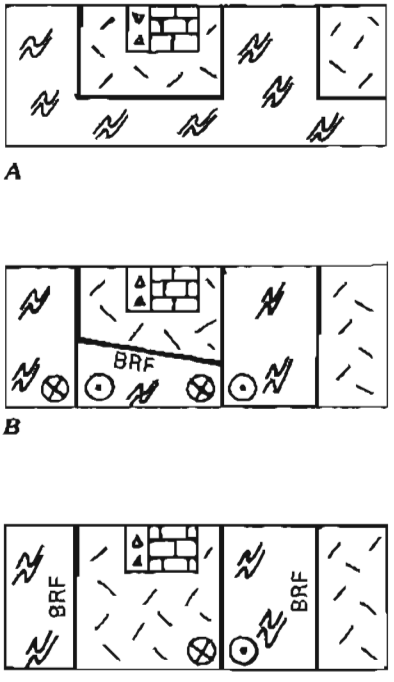

Figure 3. Hypothetical cross sections through fossil locality (F, fig. 2) on Baranof Island. *A*, Fault-bounded blocks. *B*, Truncated Border Ranges fault. *C*, Border Ranges fault rotated to vertical and repeated by young right-lateral fault.

SUMMARY AND CONCLUSION

A distinctive lithologic association of massive to thick-bedded marble, mafic flows, and cataclasized diorite forms the originally upper inboard plate to the Border Ranges fault on Chichagof and Baranof Islands. Although this suite of rocks is undated, it is lithologically correlated with Triassic greenstones and limestones of the Wrangellia terrane (Jones and others, 1977). Blocks of similar marble, greenstone, and cataclastic diorite are found in the mélange forming the originally lower outboard plate to the Border Ranges fault on Chichagof and Baranof Islands. These blocks have been variously interpreted as klippen or as tectonic inclusions derived from the inboard plate (Loney and others, 1975; Plafker and others, 1976; Johnson and Karl, 1985). A single Late Triassic conodont from a marble and greenstone inclusion in a large diorite block in the mélange of the outboard plate provides the first in-place age information for any marbles on western Chichagof and Baranof Islands. This marble block is correlated with the undated Whitestripe Marble of Chichagof Island. Although the marble dated is a block in the accretionary complex of the outboard plate, its geologic context is interpreted to represent derivation from the Wrangellian rocks of the inboard plate.

Post-Cretaceous right-slip faults of the northwest-trending Neva Strait/Slocum Arm fault system cut and offset rocks within the Kelp Bay Group mélange, its western contact with the Sitka Graywacke, and its eastern contact with the composite Wrangellia/Alexander terrane, which is represented by the Border Ranges fault. Thus, Wrangellian blocks may not have been incorporated into the Kelp Bay Group during subduction or accretion but may instead have been tectonically incorporated by post-accretion strike-slip faulting.

REFERENCES CITED

Berg, H.C., Jones, D.L., and Coney, P.J., 1978, Pre-Cenozoic tectonostratigraphic terranes of southeastern Alaska and adjacent areas: U.S. Geological Survey Open-File Report 78-1085, 2 sheets, scale 1:1,000,000.

Brew, D.A., Karl, S.M., and Miller, J.W., 1988, Megafossils (*Buchia*) indicate Late Jurassic age for part of Kelp Bay Group on Baranof Island, southeastern Alaska, *in* Galloway, J.P., and Hamilton, T.D., eds., Geologic studies in Alaska by the U.S. Geological Survey during 1987: U.S. Geological Survey Circular 1016, p. 147-149.

Byrne, T., 1979, Late Paleocene demise of the Kula-Pacific spreading center: Geology, v. 7, p. 341-344.

Decker, John, and Johnson, B.R., 1981, The nature and position of the Border Ranges fault on Chichagof Island, *in* Albert, N.R.D., and Hudson, Travis, eds., The United States Geological Survey in Alaska: Accomplishments during 1979: U.S. Geological Survey Circular 823-B, p. B102-B104.

Decker, John, and Plafker, George, 1982, Correlation of rocks in the Tarr Inlet suture zone with the Kelp Bay Group, *in*

Coonrad, W.L., ed., The United States Geological Survey in Alaska: Accomplishments during 1980: U.S. Geological Survey Circular 844, p. 119-123.

Decker, John, Wilson, F.H., and Turner, D.L., 1980, Mid-Cretaceous subduction event in southeastern Alaska [abs.]: Geological Society of America Abstracts with Programs, v. 12, no. 3, p. 103.

Hudson, Travis, Plafker, George, and Turner, D.L., 1977, Metamorphic rocks of the Yakutat-St. Elias area, south-central Alaska: U.S. Geological Survey Journal of Research, v. 5, no. 2, p. 173–184.

Johnson, B.R., and Karl, S.M., 1985, Geologic map of western Chichagof and Yakobi Islands, southeastern Alaska: U.S. Geological Survey Miscellaneous Investigations Map I-1506, scale 1:125,000, 15 p.

Jones, D.L., Silberling, N.J., and Hillhouse, J.W., 1977, Wrangellia—A displaced terrane in northwestern North America: Canadian Journal of Earth Science, v. 14, no. 11, p. 2565-2577.

Karl, S.M., Johnson, B.R., and Lanphere, M.A., 1988, New K-Ar ages for plutons on western Chichagof Island and on Yakobi Island, *in* Galloway, J.P., and Hamilton, T.D., eds., Geological Studies in Alaska by the U.S. Geological Survey during 1987: U.S. Geological Survey Circular 1016, p. 164-168.

Little, T.A., and Naeser, C.W., 1989, Tertiary tectonics of the Border Ranges fault system, Chugach Mountains, Alaska: Deformation and uplift in a forearc setting: Journal of Geophysical Research, v. 94, no. B4, p. 4333-4359.

Loney, R.A., Brew, D.A., and Lanphere, M.A., 1967, Post-Paleozoic radiometric ages and their relevance to fault movements, northern southeastern Alaska: Geological Society of America Bulletin, v. 78, no. 4, p. 511-526.

Loney, R.A., Brew, D.A., Muffler, L.J.P., and Pomeroy, J.S., 1975, Reconnaissance geology of Chichagof, Baranof, and Kruzof Islands, southeastern Alaska: U.S. Geological Survey Profes-

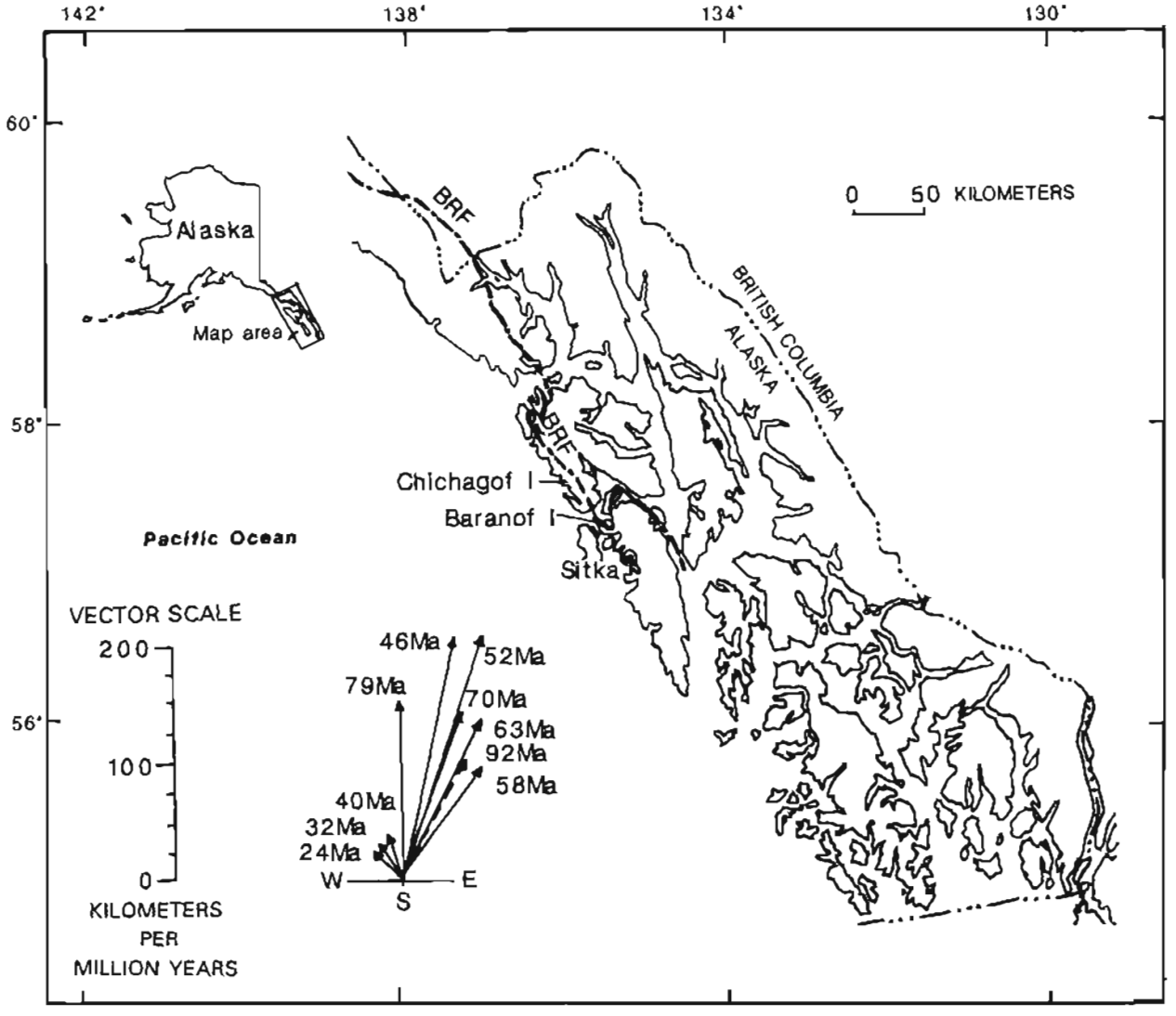

Figure 4. Oriented vectors showing direction and velocity of oceanic plate motions with respect to southeastern Alaska at various times, modified from Wallace and Engebretson (1984). Dashed vector, Farallon plate; solid vectors, Kula plate. BRF, Border Ranges fault.

sional Paper 792, 105 p.

MacKevett, E.M., Jr., and Plafker, George, 1974, The Border Ranges fault in south-central Alaska: U.S. Geological Survey Journal of Research, v. 2, no. 3, p. 323-329.

Monger, J.W.H., and Berg, H.C., 1987, Lithotectonic terranes of western Canada and southeastern Alaska: U.S. Geological Survey Miscellaneous Field Studies Map MF-1874-B, 12 p., scale 1:2,500,000.

Pavlis, T.L., and Crouse, G.W., 1989, Late Mesozoic strike slip movement on the Border Ranges fault system in the eastern Chugach Mountains, southern Alaska: Journal of Geophysical Research, v. 94, no. B4, p. 4321-4332.

Plafker, George, Jones, D.L., Hudson, Travis, and Berg, H.C., 1976, The Border Ranges fault system in the Saint Elias Mountains and Alexander Archipelago, *in* Cobb, E.H., ed., The United States Geological Survey in Alaska: Accomplishments during 1975: U.S. Geological Survey Circular 733, p. 14-16.

Reed, J.C., and Coats, R.R., 1941, Geology and ore deposits of the Chichagof mining district, Alaska: U.S. Geological Survey Bulletin 929, 148 p.

Wallace, W.K., and Engebretson, D.C., 1984, Relationships between plate motions and Late Cretaceous to Paleogene magmatism in southwestern Alaska: Tectonics, v. 3. no. 2, p. 295-315.

Reviewers: Dwight C. Bradley and Robert A. Loney

Geochemistry and Paleotectonic Implications of Metabasaltic Rocks in the Valdez Group, Southern Alaska

By John S. Lull *and* George Plafker

Abstract

A belt of metabasaltic rocks approximately 600 km long and up to 4 km in structural thickness is discontinuously exposed along the southern margin of the accretionary assemblage that composes the Upper Cretaceous Valdez Group. The metabasalt is structurally overlain to the north successively by mixed metabasaltic tuff and flysch up to 3 km in thickness and a sequence of andesitic volcaniclastic flysch up to 15 km in thickness.

The metabasaltic rocks are mostly of greenschist grade, locally amphibolite grade, and occur as pillow flows, breccias, dikes, and extensive thin tuffaceous units interbedded with flysch. They are impoverished in high-field-strength elements, depleted in light rare-earth elements relative to heavy rare-earth elements, and compatible with an island-arc tholeiite origin. Rare andesitic metatuff of the Valdez Group is calc-alkalic and probably derived from the Andean-type arc from which the Valdez sediments were eroded; it is not considered to be genetically related to the metabasalt.

We interpret the metabasalt of the Valdez Group to be the remnant of a primitive intraoceanic island arc, which formed within the Kula plate during Campanian to early Maastrichtian time and subsequently migrated toward an Andean-type continental margin. Basaltic flows and tuff from the intraoceanic arc were mixed with deep-sea fan deposits of continent-derived andesitic sediments and tuff as the island arc approached the continent. Arc-continent collision in latest Cretaceous to early Paleocene time resulted in successive offscraping and accretion to the continental margin of the flysch, mixed flysch and basaltic tuff, and basalt that make up the Valdez Group.

INTRODUCTION

Metabasaltic rocks and metadiabase occur within the Valdez Group of southern Alaska. The Valdez Group is a fault-bounded deep-sea accretionary assemblage, up to 20 km in thickness (all thicknesses quoted are structural thicknesses), of Upper Cretaceous flysch and minor oceanic basalt which makes up the main bulk of the Chugach terrane (Plafker and others, 1989). It is bounded on the north by the Border Ranges fault and on the south by the Contact fault (fig. 1). The basaltic rocks occur as metatuff interbedded with metasedimentary rocks, pillow flows and breccia, and diabasic intrusions. They are mostly restricted to the southern part of the Valdez Group and form a sequence up to 3–4 km in thickness along the southern margin of the Chugach terrane (Winkler and Plafker, 1981; fig. 1). Interbedded basaltic metatuff and flysch are present just north of the more massive metabasalt and form a zone up to 3 km thick. Layers of metatuff are sparsely distributed within the flysch north of this zone but are rare to absent in the northernmost part of the Valdez Group.

The basaltic rocks of the Valdez Group have been metamorphosed to greenschist facies and locally to amphibolite facies. They have been multiply deformed by underthrusting and accretion along the southern margin of Alaska (Nokleberg and others, 1989). This report presents petrographic and geochemical data on five samples of metabasaltic rocks collected from the Chugach Mountains for the Trans-Alaska Crustal Transect and four samples previously collected from the Yakutat area.

PETROGRAPHY

The metabasalts are fine grained with well-developed schistosity and microfolds. They are composed of (in approximate order of abundance) fibrous actinolite, chlorite, albite, and epidote ± quartz, white mica, iron oxide, and pyrite. The metadiabase is slightly foliated, fine to medium grained, and consists of actinolite, albite, chlorite, and epidote. Amphibolite (fig. 1, no. 7) is fine grained and slightly foliated. It contains hornblende and plagioclase, with minor sphene and iron oxide. The meta-andesite (fig. 1, no. 9) is very fine grained and schistose and exhibits relict volcaniclastic texture indicating a tuff or volcanogenic siltstone protolith. It is primarily composed of chlorite, albite, and epidote.

GEOCHEMISTRY

Chemical analyses are shown in table 1 for three samples of metabasalt (fig. 1, nos. 2, 3, 5) and two of metadiabase (nos. 1, 4) from the type area of the Valdez Group near Valdez and for three samples of metabasalt (nos. 6, 7,

8) and one meta-andesite (no. 9) from the Yakutat area. For the metabasalt and metadiabase, SiO_2 ranges from 48.5 to 53.7 percent (all figures given in volatile-free weight percent), K_2O from 0.04 to 0.4 percent, and TiO_2 from 0.4 to 1.2 percent. The meta-andesite has 61.5 percent SiO_2, 0.76 percent K_2O, and 0.74 percent TiO_2. The six samples with less than 52 percent SiO_2 are olivine normative, and the other three samples (including the andesite) are quartz normative. These rocks also contain from 1 to nearly 4 percent H_2O, and the meta-andesite contains 4 percent CO_2. The metabasaltic rocks show a tholeiitic trend on an AFM diagram (not shown), and the meta-andesite plots as calc-alkalic. On a discrimination plot using TiO_2, MnO, and P_2O_5, elements considered to be relatively immobile during metamorphism (Mullen, 1983), the metabasalts plot mainly in the island-arc tholeiite (IAT) field with slight overlap into the calc-alkalic basalt (CAB) field (fig. 2). On this diagram, and on discrimination plots that follow, the metabasalt of the Valdez Group differs significantly from the midocean ridge metabasalts of the McHugh Complex and schist of Liberty Creek, which form the northernmost part of the Chugach terrane.

These rocks are best characterized using relatively immobile trace elements such as the high-field-strength elements (HFSE: Ti, Zr, Hf, Nb, Ta) and the rare-earth elements (REE), due to possible mobilization of major oxides during metamorphism and alteration. The metabasalts and metadiabase of the Valdez Group are all impoverished in HFSE. Chondrite-normalized REE abundances (fig. 3) are low, with depletion of light rare-earth elements (LREE) relative to heavy rare-earth elements (HREE) (La 1–7x chondrites, Lu 9–20x chondrites, $(La/Sm)_n$ = 0.3–0.7).

Metabasalts from the type area and Yakutat area have very similar REE patterns. The two metadiabase samples (plotted separately on fig. 3) show the same REE pattern as the metabasalts but have slightly lower REE abundances. The meta-andesite is enriched in LREE relative to HREE.

On a spidergram plot (fig. 4) metabasaltic samples from the type area show a Nb-Ta trough, characteristic of island-arc rocks; the Yakutat basalts are not plotted because

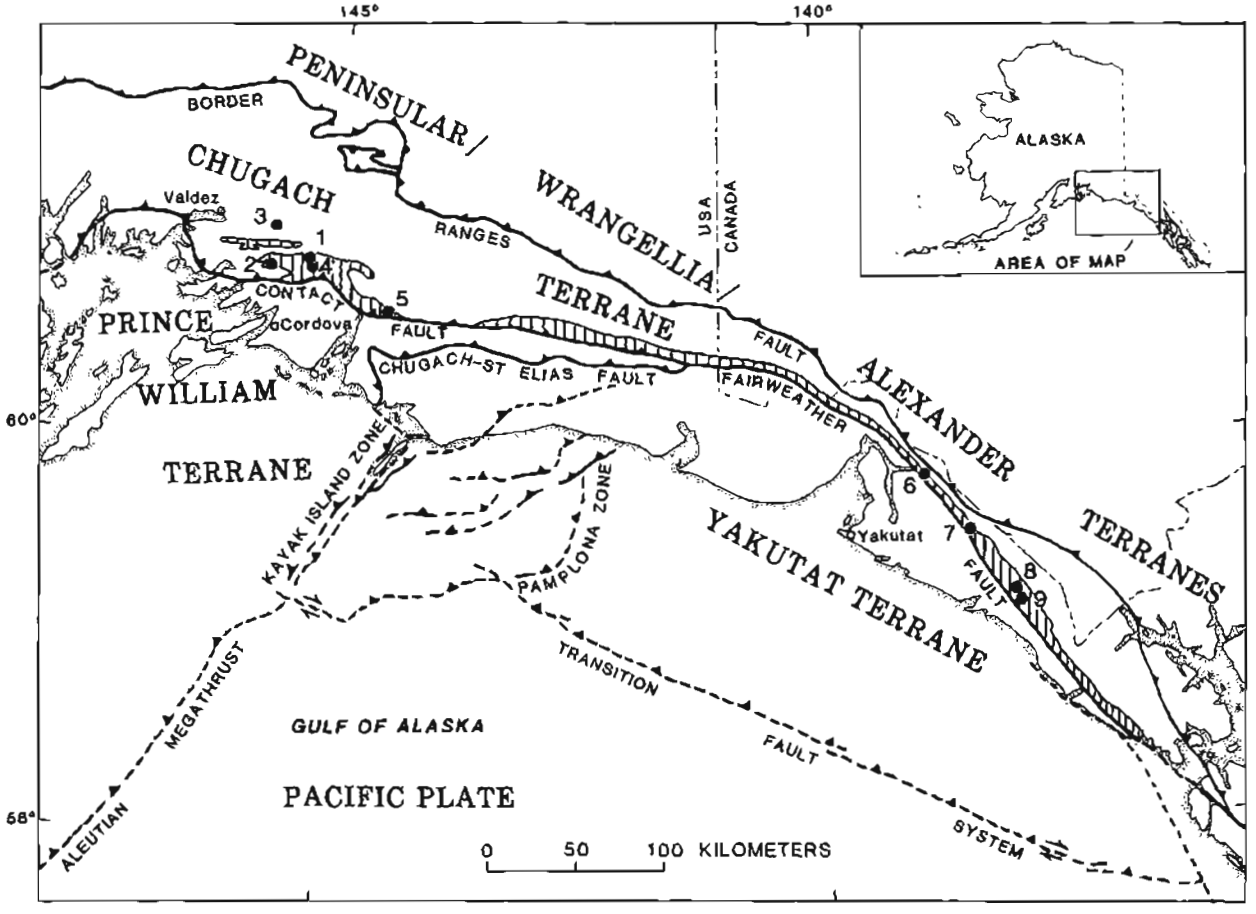

Figure 1. Index map showing regional extent of metabasaltic rocks of the Valdez Group (lined areas). Type area for the Valdez Group is northern Prince William Sound and Valdez area. Major terranes also shown. Numbered localities (dots) on map correspond to localities discussed in text and described in table 1. Samples from localities 1 and 4 are metadiabase; sample from locality 9 is meta-andesite. All others are metabasalt. Faults and thrust faults dashed where approximate; sawteeth on upper plate; arrows show direction of relative movement.

Table 1. Major oxide (normalized 100% volatile-free) and minor element composition of metabasaltic rocks of the Valdez Group from southern Alaska

[Analyses by U.S. Geological Survey. Major oxides (XRF) by A.J. Bartel, K. Stewart, J. Taggart, and R.V. Mendes (Lakewood, Colo.). Volatiles by L. Espos, P. Klock, and S. MacPherson (Menlo Park, Calif.). Cu, Ni, Sc (optical spectroscopy) by P.H. Briggs (Lakewood, Colo.) and J. Consul, R. Lerner, and R. Mays (Menlo Park, Calif.). Sr, Zr, Y, Ba (EDXRF) by T. Frost, J.R. Lindsay, and D. Vivit (Menlo Park, Calif.). Rare earth elements and remaining trace elements (INAA) by J. Budahn, R. Knight, and D.M. McKown (Lakewood, Colo.). For Yakutat area samples: XRF by V.G. Mossoti and G. Kawakita (Menlo Park, Calif.). Volatiles by P.J. Lamothe, V. McDaniel (Menlo Park, Calif.). INAA by L.J. Schwarz (Reston, Va.). For description of methods see Baedecker 1987)]

	Type area					Yakutat area			
Map no.	1	2	3	4	5	6	7	8	9
Sample No.	85APr164C	85ARh121	84APr48D	85ARh119	85APr106	80APr40A	78APr12A	78APr5	78APr7
Lithology	Metadiabase	Metabasalt	Metabasalt	Metadiabase	Metabasalt	Metabasalt	Metabasalt	Metabasalt	Meta-andesite
MAJOR OXIDE COMPOSITION (dry wt %)									
SiO_2	48.5	50.5	51.2	52.3	53.7	48.8	49.3	49.6	61.5
Al_2O_3	15.8	15.0	15.6	14.4	13.2	15.5	15.1	16.3	14.7
Fe_2O_3	1.87	2.89	1.82	2.37	5.52	2.60	3.19	1.43	1.66
FeO	8.07	7.30	8.68	7.19	7.99	8.49	9.01	10.81	5.47
MgO	12.08	8.48	8.00	8.95	6.27	8.54	8.62	11.33	3.13
CaO	10.83	12.23	9.64	13.00	7.62	12.70	11.20	6.08	9.16
Na_2O	1.77	2.93	3.42	1.14	4.58	2.30	2.30	3.19	2.61
K_2O	.15	.36	.13	.04	.04	.07	.09	.06	.76
TiO_2	.63	.72	1.17	.35	.87	.73	.98	.99	.74
P_2O_5	.05	.06	.08	.05	.08	<.05	.05	.01	.13
MnO	.18	.18	.31	.16	.19	.10	.15	.20	.15
H_2O^+	3.86	2.36	2.80	2.75	1.18	1.54	1.31	2.23	1.88
H_2O^-	.06	.07	.05	.07	.07	.02	.02	.04	.08
CO_2	.06	<.02	.08	.99	.99	<.01	.04	.05	4.13
MINOR ELEMENT COMPOSITION (ppm)									
Sc	36	48	49	45	54	53	57	57	22
Cr	685	352	373	284	69.9	320	110	170	47
Co	46.1	45.2	39.8	34.6	43.8	—	47	45	17
Ni	275	110	90	107	84	110	62	76	22
Cu	92	86	54	99	119	—	—	—	—
Zn	115	87	72	74	120	—	—	—	—
Rb	<3	13	<3	<3	—	2	2	3	26
Sr	55	48	176	20	42	71	135	77	343
Y	12	17	18	10	23	22	24	28	16
Zr	19	25	50	<10	28	41	59	48	97
Sb	.4	.3	.9	.9	—	—	—	—	—
Cs	—	.3	.4	.1	<.2	—	—	—	—
Ba	50	58	40	<20	40	18	29	28	450
La	.9	1.0	1.8	.3	.8	1.0	2.3	1.7	14
Ce	2.8	2.4	—	<1.2	3.6	2.7	6	3.7	24
Nd	3	<4	7	—	4	3	6	4	13
Sm	1.2	1.8	2.5	.6	1.6	1.4	2.0	1.8	3.3
Eu	.51	.66	.73	.27	.63	.65	.77	.77	.89
Gd	1.8	2.7	3.4	1.1	2.5	3.3	2.1	2.5	3.6
Tb	.40	.56	.62	.24	.58	—	.69	.74	.52
Yb	2.1	2.9	2.8	1.6	3.1	2.2	3.2	3.8	2.4
Lu	.3	.4	.4	.3	.5	.4	.6	.6	.4
Ta	.04	.04	.10	<.06	.03	—	<.5	<.5	.4
Th	.2	—	.2	<.1	—	—	<.9	<.9	2.9
Hf	.7	1.1	1.7	.4	1.1	—	2	1	3
U	—	<1	—	—	—	—	<.7	<.7	1.3

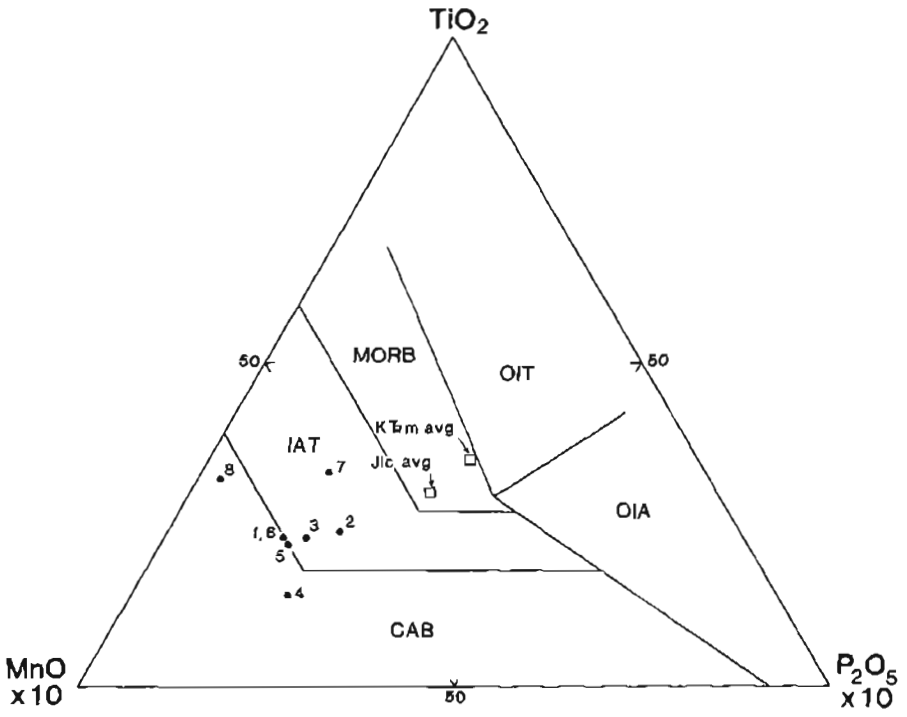

Figure 2. MnO-TiO_2-P_2O_5 ternary diagram (rocks with 45 to 54 percent SiO_2) for metabasaltic rocks of the Valdez Group. Fields from Mullen (1983). IAT, island-arc tholeiite; MORB, midocean ridge basalt; CAB, calc-alkalic basalt; OIT, ocean-island tholeiite; OIA, ocean-island alkali basalt. Squares, average values for six samples of metabasalt from Triassic to Cretaceous McHugh Complex (KTm) and three samples from Jurassic schist of Liberty Creek (Jlc). See figure 1 for sample localities.

both Nb and Ta are below detection limits. However, the trough is somewhat broader than for typical arc rocks and includes La. La/Ta ratios (20–23) are low compared to most arc basalts (Wood and others, 1979), but the ratios may not be meaningful at such low absolute abundances.

On discrimination diagrams using Ti, Zr, and Y (figs. 5 and 6*A*), the metabasalts from the type area plot in and near the field for IAT, and the samples from the Yakutat area plot mostly in the overlap field between IAT and midocean ridge basalt (MORB). Two samples (fig. 1, nos. 1 and 3) with detectable Th plot as primitive arc tholeiites on a Th-Hf-Ta diagram (fig. 6*B*). The meta-andesite plots well into the calc-alkalic field on all four diagrams.

There is some difficulty in distinguishing IAT from MORB, especially for metamorphic rocks, and we recognize that discriminant plots are only approximate indicators of paleotectonic regime because they are based on a limited set of analyses of fresh, unmetamorphosed basalts. The diagrams do indicate that the Valdez metabasaltic rocks are significantly depleted in high-field-strength cations, particularly Ti, Zr, and Ta, relative to MORB. The metabasalts could be transitional between IAT and MORB, but with a strong IAT signature. In general, metabasalts of the Valdez Group are compositionally similar to basaltic lavas of the Pleistocene to Holocene Tonga-Kermadec arc, which are

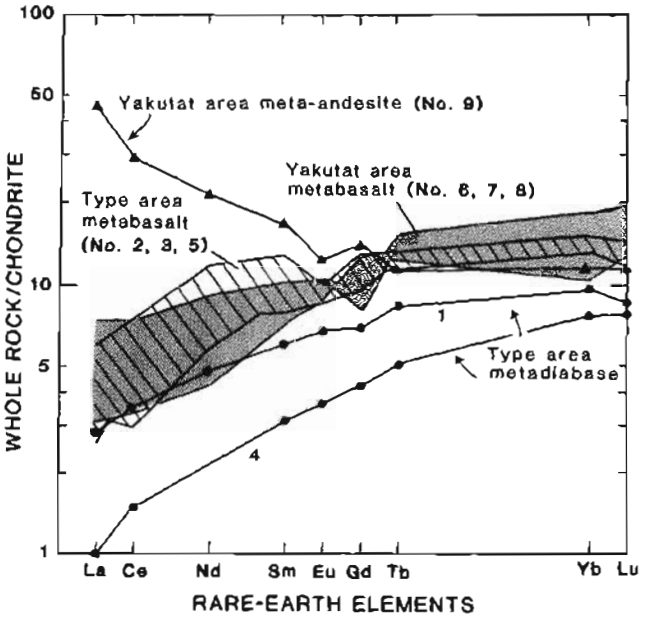

Figure 3. Chondrite-normalized rare-earth element plot for metabasaltic rocks of the Valdez Group. Chondrite values x1.31, from Anders and Ebihara (1982). See figure 1 for sample localities.

thought to have been derived through partial melting of depleted lherzolite in the mantle wedge (Ewart and Hawkesworth, 1987). In contrast, metabasalts of the McHugh Complex and the schist of Liberty Creek, which were accreted inboard of the Valdez Group and make up the northernmost part of the Chugach terrane (Plafker and others, 1989), have slightly higher REE abundances than those of the Valdez Group and plot mostly within MORB fields on various discrimination diagrams (figs. 2, 5, and 6).

The andesitic sample is calc-alkalic, clearly arc-derived, and probably unrelated to the metabasalts. We interpret it as an ash-fall deposit or an epiclastic tuff derived from the Andean-type arc that is believed to have supplied the volcaniclastic sediments that compose most of the Valdez Group (Plafker and others, 1989).

TECTONIC INTERPRETATION

In order to reconstruct the paleotectonic setting for metabasaltic rocks of the Valdez Group the following facts must be considered:

1. Based on the geochemistry, the metabasalt is compatible with a primitive island-arc origin, and the analyzed samples are compositionally similar.

2. Pillow flows, breccia, and diabase form a belt more than 600 km long and up to 4 km in structural thickness along the southern (outer) margin of the accretionary prism that makes up the Chugach terrane.

3. Just north of this belt is a zone up to 3 km in structural thickness in which metabasaltic tuffs and flows of the same composition as the more massive metabasalts are interbedded with the flysch sequence.

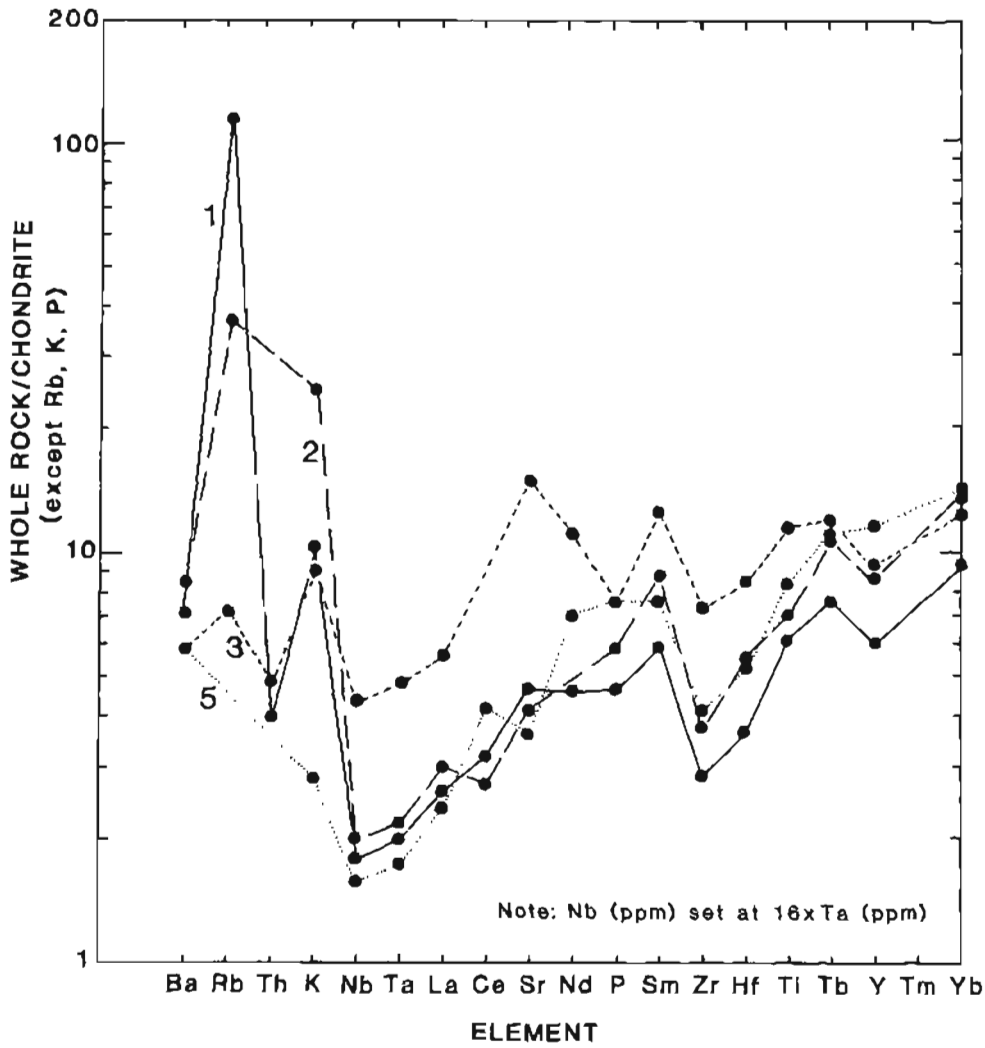

Figure 4. Chondrite-normalized, trace-element abundance plot (spider diagram) for metabasaltic rocks of the Valdez Group. Normalized using values from Thompson and others (1984). See figure 1 for sample localities.

4. The tuffaceous metabasalts occur as extensive beds from a few centimeters to 100 m thick that are intimately interbedded with the flysch.

5. Geochemistry of flysch of the Valdez Group (Plafker and others, 1989) and sedimentological studies (Zuffa and others, 1980) indicate that the flysch source was a dissected Andean-type arc.

The three most likely paleotectonic environments for the basaltic rocks of the Valdez Group are (1) midocean ridge, (2) near-trench volcanism, and (3) primitive intraoceanic island arc. For reasons discussed below, we feel that an island-arc origin best fits the data.

If the metabasalt is assumed to be oceanic crust generated at a spreading ridge, it is difficult to explain the IAT geochemical signature, why such a laterally continuous layer of basaltic rocks was accreted rather than subducted, and the presence within the flysch of extensive thin tuffaceous beds that are geochemically identical to the metabasalt. Near-trench volcanism in southern Alaska as a result of ridge-trench interaction has been postulated for the Paleocene (Marshak and Karig, 1977; Lonsdale, 1988), and lavas erupted in this setting have been shown to exhibit chemical characteristics differing from MORB (Moore and others, 1983). However, the position of the Kula-Farallon ridge or other ridges relative to the Chugach terrane during the Late Cretaceous is unknown. If ridge-trench interaction and sediment contamination of a MORB magma did take place, greater compositional diversity and more siliceous lavas would be expected than are observed for Valdez Group volcanic rocks. Furthermore, it is unlikely that ridge-trench interaction could account for the large regional extent and linearity of the basaltic sequence.

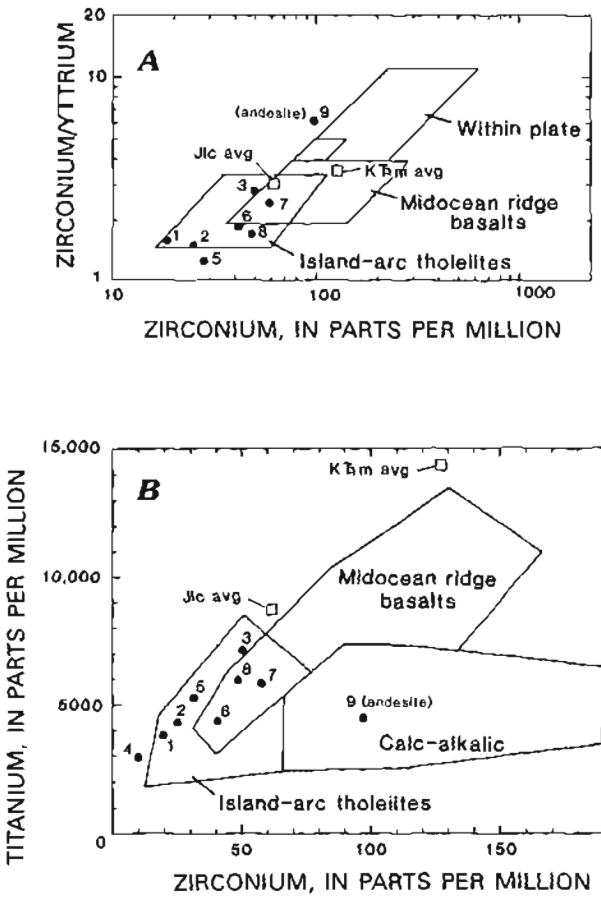

Figure 5. Discrimination diagrams for metabasaltic rocks of the Valdez Group. Squares, average values for six samples of metabasalt from Triassic to Cretaceous McHugh Complex (KTm) and three samples from Jurassic schist of Liberty Creek (Jlc). *A*, Zirconium/yittrium versus zirconium. Fields from Pearce and Norry (1979). *B*, Titanium versus zirconium. Fields from Pearce and Cann (1973). See figure 1 for sample localities.

Our preferred interpretation is that the metabasaltic rocks of the Valdez Group are the remnants of a primitive intraoceanic island arc that was accreted along the seaward margin of the dominantly clastic sequence that makes up most of the Valdez Group. The island arc is inferred to have developed during Campanian to early Maastrichtian time within the Kula plate subparallel to a coeval northwest-trending andesitic arc along the continental margin. Our model for the evolution of the Valdez Group is shown diagrammatically in plan view (fig. 7) and in cross section (fig. 8) for three time intervals in the Late Cretaceous and early Tertiary.

From the Campanian through the early Maastrichtian, sediment deposited on the ocean floor by both arcs was physically separated with probable offscraping and accretion of flysch and rare andesitic tuff on the inner wall of the continental margin arc. After the island arc migrated close enough to the continent, continent-derived deep-sea fans of dominantly volcaniclastic flysch began to mix first with island-arc-derived basaltic tuff and later with the island-arc basalt (figs. 7*A*, 8*A*). The present distribution of deep-sea fans in the northeastern Pacific Ocean indicates that such fans can extend offshore 1,000 km or more.

By the end of the Cretaceous or earliest Paleocene, continuous subduction of the Kula plate resulted in successive accretion of the flysch, mixed flysch and basaltic tuff, and island-arc basalt that compose the Valdez Group (figs. 7*B*, 8*B*).

The occurrence of a narrow flysch zone seaward of the metabasalt (fig. 8*C*) suggests that as the island arc approached the continental margin, the deep-sea fans locally were thick enough to flow across low areas in the island arc and onto the ocean floor seaward of the island arc. We speculate that it was the thickness of the island-arc sequence that prevented it from being completely subducted with the Kula plate oceanic crust upon collision with the continental margin.

During the Paleogene, the Gulf of Alaska margin was affected by counterclockwise rotation of the western limb of the Alaska orocline, about 400 km of dextral offset on the Denali fault, and continuing rapid underthrusting of the Kula plate beneath the continental margin with accretion of

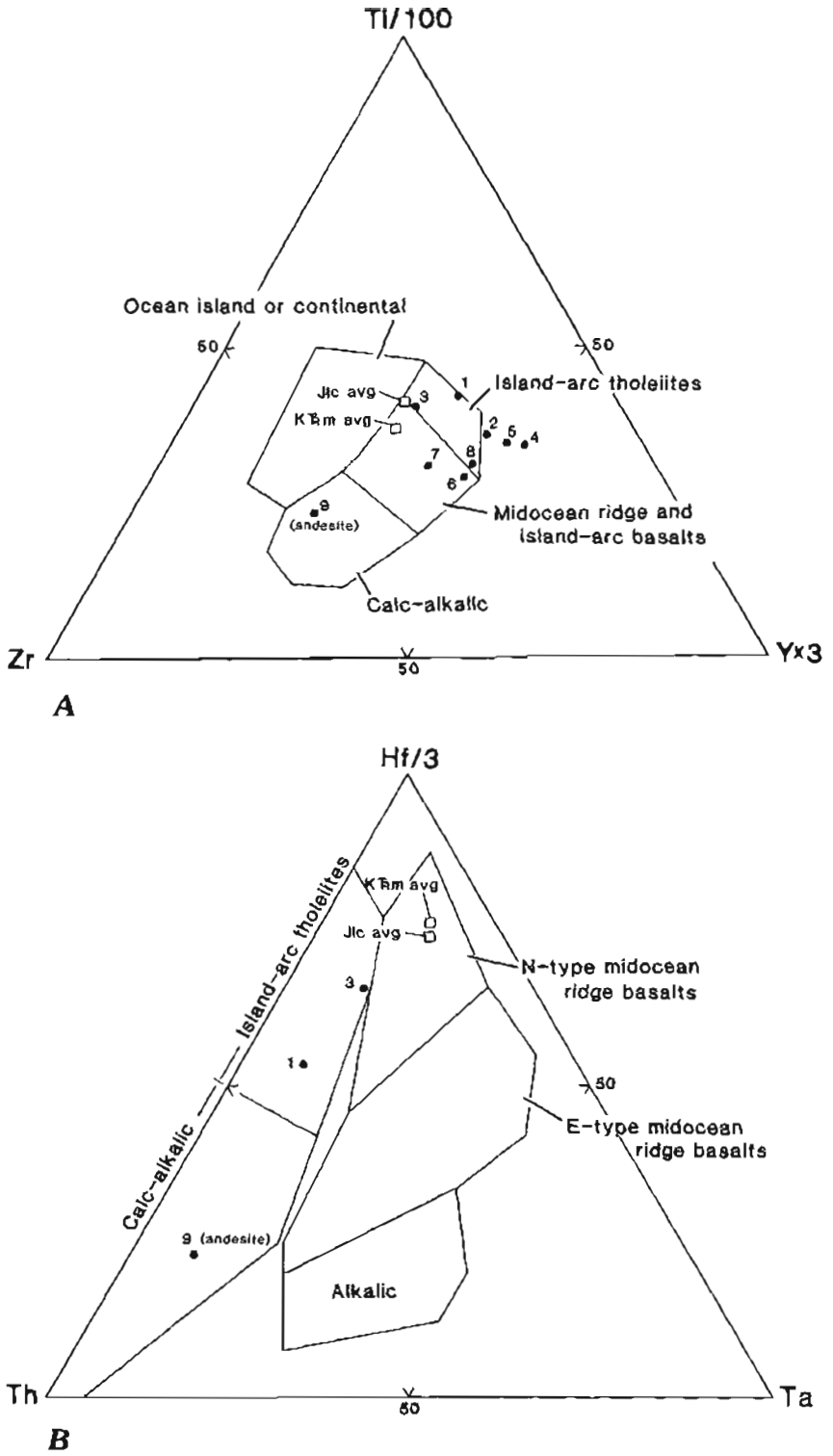

Figure 6. Ternary discrimination diagrams for metabasaltic rocks of the Valdez Group. Squares, average values for six samples of metabasalt from Triassic to Cretaceous McHugh Complex (KTm) and three samples from Jurassic schist of Liberty Creek (Jlc). A, Titanium-zirconium-yittrium. Fields from Pearce and Cann (1973). B, Thorium-hafnium-Tantalum. Fields from Wood (1980). See figure 1 for sample localities.

the Orca Group against and beneath the Valdez Group (fig. 7C). These processes were accompanied by steepening and local refolding of structures in the accretionary prism and by metamorphism and anatectic plutonism that have resulted in the present distribution and structure of the metabasaltic rocks in the Valdez Group (fig. 8C).

A major unresolved question is: Why does the metabasalt unit terminate abruptly near the Valdez area in eastern Prince William Sound? One possibility, indicated schematically in figure 7A, is that the island arc did not extend any farther west because it was bounded by an arc-trench transform in this region. An alternative is that the island arc did extend farther west, but the western part of the arc was entirely subducted. Geophysical studies of the deep crust now underway in the Prince William Sound region as part of the Trans-Alaska Crustal Transect Program may eventually provide data on which a choice between these alternatives can be made.

Acknowledgments.—We thank Fred Barker for samples collected in the Yakutat area and for helpful comments on the geochemistry, Don Richter for field mapping and collection of samples in the Cordova area, and Warren Nokleberg for field mapping in the Cordova area. We also thank Betsy Moll-Stalcup, Steve Box, and Michael Clynne for useful discussion of the geochemical data.

REFERENCES CITED

Anders, E., and Ebihara, M., 1982, Solar-system abundances of the elements: Geochemica et Cosmochemica Acta, v. 46, p. 2363-2380.

Baedecker, P.A. (ed.), 1987, Methods for geochemical analysis: U.S. Geological Survey Bulletin 1770.

Engebretson, D.C., Cox, A., and Gordon, R.G., 1985, Relative motions between oceanic and continental plates in the Pacific basin: Geological Society of America Special Paper 206, 59 p.

Ewart, A., and Hawkesworth, C. J., 1987, The Pleistocene-Recent Tonga-Kermadec arc lavas: Interpretation of new isotopic and rare earth data in terms of a depleted mantle source model: Journal of Petrology, v. 28, part 3, p. 495-530.

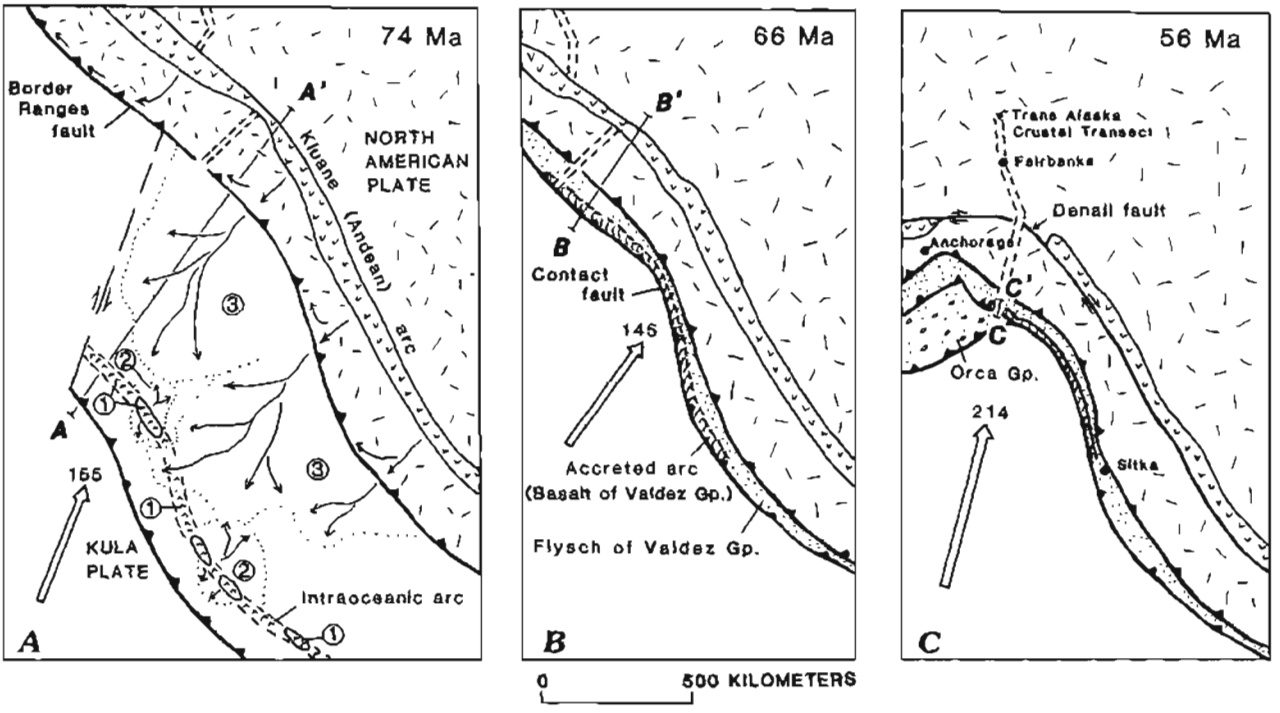

Figure 7. Schematic diagram illustrating inferred Late Cretaceous and Paleogene evolution of metabasalt of the Valdez Group and related rocks. Double arrows with numerals indicate directions and rates of relative plate motions in millimeters/year (from Engebretson and others, 1985); sawteeth on upper plate of thrust faults; arrows show direction of relative movement on strike-slip fault; single arrows (and dots) indicate sediment flow directions and deep-sea fan deposits; dots outline extent of fans. *A*, Campanian configuration of intraoceanic island arc and Kluane continental margin arc showing spatial distribution of major facies of the Valdez Group: (1) island-arc basalt (possible islands schematically outlined by solid lines); (2) mixed island-arc basaltic tuff and continent-derived sediment; and (3) dominantly continent-derived clastic sediment. *B*, Maastrichtian configuration after accretion of the Valdez Group to continental margin. *C*, Paleogene configuration of the Valdez Group and related rocks after oroclinal bending, displacement on Denali fault, and accretion of the Orca Group (Plafker 1987; Plafker and others, 1989). See figure 8 for cross sections.

Lonsdale, Peter, 1988, Paleogene history of the Kula plate: Offshore evidence and onshore implications: Geological Society of America Bulletin, v. 100, p. 733-754.

Marshak, R.S., and Karig, D.E., 1977, Triple junctions as a cause for anomalously near-trench igneous activity between the trench and volcanic arc: Geology, v. 5, no. 4, p. 233-236.

Moore, J.C., Byrne, Tim, Plumley, P.W., Reid, Mary, Gibbons, Helen, and Coe, R.S., 1983, Paleogene evolution of the Kodiak Islands, Alaska: Consequences of ridge-trench interaction in a more southerly latitude: Tectonics, v. 2, no. 3, p. 265-293.

Mullen, Ellen D., 1983, $MnO/TiO_2/P_2O_5$: A minor element discriminant for basaltic rocks of oceanic environments and its implications for petrogenesis: Earth and Planetary Science Letters, v. 62, p. 53-62.

Nokleberg, W.J., Plafker, George, Lull, J.S., Wallace, W.K., and Winkler, G.R., 1989, Structural analysis of the southern Peninsular and northern Chugach terranes along the Trans-Alaska Crustal Transect, northern Chugach Mountains, Alaska: Journal of Geophysical Research, v. 94, no. B4, p. 4297-4320.

Pearce, J.A., and Cann, J.R., 1973, Tectonic setting of basic volcanic rocks determined using trace element analyses: Earth and Planetary Science Letters, v. 19, p. 290-300.

Pearce, J.A., and Norry, M.J., 1979, Petrogenetic implications of Ti, Zr, Y, and Nb variations in volcanic rocks: Contributions to Mineralogy and Petrology, v. 69, p. 33-47.

Plafker, George, 1987, Regional geology and petroleum potential of the northern Gulf of Alaska continental margin, *in* Scholl, D.W., Grantz, Arthur, and Vedder, J.G., eds., Geology and resource potential of the continental margin of western North America and adjacent ocean basins: Houston, Texas, Circum-Pacific Council for Energy and Mineral Resources Earth

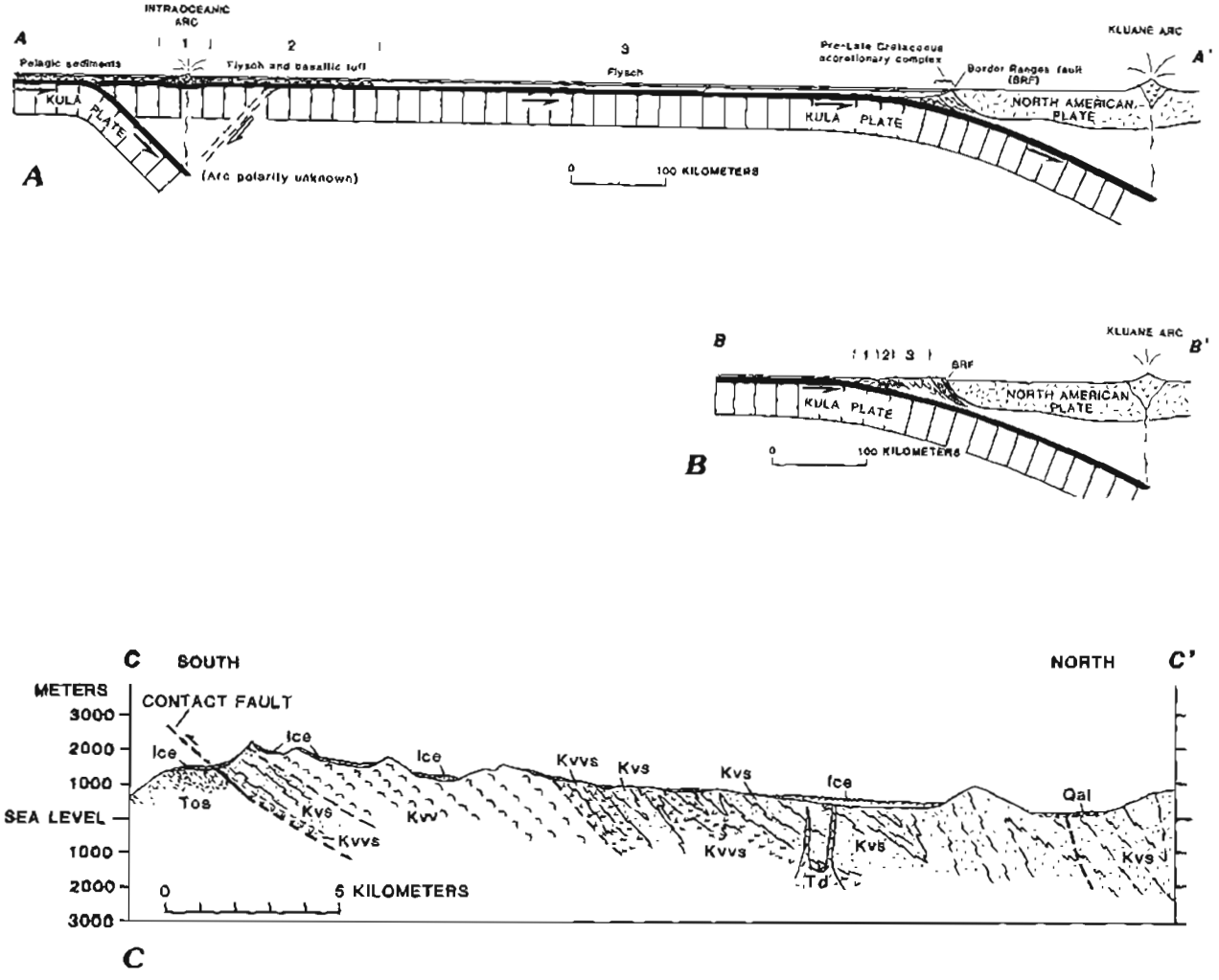

Figure 8. Diagrammatic cross sections showing structural configuration of the Valdez Group and related rocks. *A*, Campanian time. *B*, Maastrichtian time. *C*, Paleogene time. Crustal configuration in *A* and *B* is hypothetical, structure shown in *C* is from Plafker and others (1986) and unpublished data. For *C*: Qal, alluvium (Quaternary); Td, felsic dikes (Tertiary); Tos, Orca Group (Tertiary)—metasedimentary rocks; Kvs, Valdez Group (Upper Cretaceous)—metasedimentary rocks; Kvv, Valdez Group (Upper Cretaceous)—metabasalt; Kvvs, Valdez Group (Upper Cretaceous)—interbedded metasedimentary and metabasaltic rocks. Faults dashed where inferred; arrow shows direction of relative movement. See figure 7 for location of cross sections.

Science Series v. 6, p. 229-268.

Plafker, George, Nokleberg, W.J., Lull, J.S., Roeske, S.M., and Winkler, G.R., 1986, Nature and timing of deformation along the Contact fault system in the Cordova, Bering Glacier, and Valdez quadrangles, *in* Bartsch-Winkler, Susan, and Reed, Katherine, eds., Geologic studies in Alaska by the U.S. Geological Survey during 1985: U.S. Geological Survey Circular 978, p. 74-77.

Plafker, George, Nokleberg, W.J., and Lull, J.S., 1989, Bedrock geology and tectonic evolution of the Wrangellia, Peninsular, and Chugach terranes along the Trans-Alaska Crustal Transect in the northern Chugach Mountains and southern Copper River basin, Alaska: Journal of Geophysical Research, v. 94, no. B4, p. 4255-4295.

Thompson, R.N., Morrison, M.A., Hendry, G.L., and Parry, S.J., 1984, An assessment of the relative roles of crust and mantle in magma genesis: An elemental approach: Philosophical Transactions Royal Society of London, v. A310, p. 549-590.

Winkler, G.R., and Plafker, George, 1981, Geologic map and cross-sections of the Cordova and Middleton Island quadrangles, Alaska: U.S. Geological Survey Open-File Report 81-1164, scale, 1:250,000.

Wood, D.A., 1980, The application of a Th-Hf-Ta diagram to problems of tectonomagmatic classification and to establishing the nature of crustal contamination of basaltic lavas of the British Tertiary Volcanic Province: Earth and Planetary Science Letters, v. 50, p. 11-30.

Wood, D.A., Joron, J.L., and Trevil, M., 1979, A re-appraisal of the use of trace elements to classify and discriminate between magma series erupted in different tectonic settings: Earth and Planetary Science Letters, v. 45, p. 326-336.

Zuffa, G.G., Nilsen, T.H., and Winkler, G.R., 1980, Rock-fragment petrography of Upper Cretaceous Chugach terrane, southern Alaska: U.S. Geological Survey Open-File Report 80-713, 28 p.

Reviewers: Charles R. Bacon and Melvin H. Beeson

Oligocene Age of Strata on Unga Island, Shumagin Islands, Southwestern Alaska

By Louie Marincovich, Jr. *and* Virgil D. Wiggins

Abstract

Marine mollusks, dinocysts, and pollen of early Oligocene age are present in the Stepovak Formation on Unga Island, Shumagin Islands, southwestern Alaska. On the basis of pollen and marine dinocysts, these Stepovak strata, in the coastal West Head stratigraphic section of northeastern Unga Island, correlate with the lowermost part of the type section of the Unga Conglomerate Member of the Bear Lake Formation at Zachary Bay. The early Oligocene age of the lowermost part of the Unga Conglomerate Member at Zachary Bay is supported by a potassium-argon age of 31.3±0.3 Ma from biotite in a tuff bed. Stratigraphically higher beds in the Unga type section contain late Oligocene palynomorphs and megafloral remains. The marine and nonmarine Stepovak and Unga biotas correlate with faunas and floras of adjacent North Pacific and Arctic Ocean regions.

INTRODUCTION

Marine strata of Oligocene age crop out extensively on the Alaska Peninsula of southwestern Alaska (fig. 1) and have mostly been assigned to the Stepovak Formation of Burk (1965). Age assignment of these Oligocene marine strata is based principally on mollusks (Burk, 1965; Lyle and others, 1979). In many instances, precise dating of Oligocene faunas has not been possible, owing to poor knowledge of molluscan faunas in adjacent North Pacific regions. In recent years, published and unpublished studies have greatly expanded knowledge of the age and stratigraphic relations of molluscan and microfossil faunas and floras in southern Alaska and adjacent regions. Stepovak biotas containing age-diagnostic species that co-occur in adjacent North Pacific regions may now be more precisely dated. Studies of Oligocene marine dinoflagellates and nonmarine palynomorphs have helped to refine the ages of Stepovak strata and correlative stratigraphic units on Unga Island.

UNGA ISLAND OLIGOCENE STRATA

The best preserved Stepovak molluscan faunule on Unga Island is in the West Head stratigraphic section of Burk (1965) (fig. 1). Palynomorphs and marine dinoflagellates also are abundantly present. This diverse and abundant biota is the basis for the age inferences presented here. The most abundant mollusk in the West Head fauna is *Ostrea gackhensis* L. Krishtofovich, which occurs as a biostrome. Other abundant mollusks include the bivalves *Cyclocardia ezoensis* (Takeda) and *Papyridea harrimani* (Dall), as well as the gastropods *Neverita washingtonensis* (Weaver) and *Polinices lincolnensis* (Weaver). The type locality of *O. gackhensis* in the Gakhinsk Formation of western Kamchatka contains mollusks correlative with early Oligocene faunas in the Gakkha and Amana Formations of western Kamchatka and the Poronai Formation of central Hokkaido (Gladenkov and others, 1988; A.I. Kafanov, written commun., 1989). *Cyclocardia ezoensis* has been reported in numerous Oligocene formations in Sakhalin and Hokkaido (Takeda, 1953), including the Charo and Nuibetsu Formations of eastern Hokkaido and the Poronai Formation of central Hokkaido (Honda, 1986), that have been dated as early Oligocene using planktonic foraminifers (Kaiho, 1984). *Papyridea harrimani* also occurs in the lower Oligocene Nuibetsu Formation of eastern Hokkaido, as well as in lower Oligocene strata of the Machigar Formation of Sakhalin and the Mallen and Ionai Formations of the Koryak Uplands, USSR (Devyatilova and Volobueva, 1981). The two gastropods have overlapping chronostratigraphic ranges in early Oligocene faunas of Oregon and Washington (Marincovich, 1977). Based on relatively small collections, the Stepovak Formation mollusks from the West Head stratigraphic section were thought to be of "probably late middle Oligocene" age by MacNeil (in Burk, 1965). Much larger and more diverse collections made in recent years clearly indicate an early Oligocene age (following the two-fold division of the Oligocene in Palmer, 1983) based on correlations with faunas of both the northwestern and northeastern Pacific regions.

Oligocene fossils on Unga Island are present not only in the Stepovak Formation but also in the type section of the Unga Conglomerate Member of the Bear Lake Formation. The type section of the Unga is the Zachary Bay stratigraphic section of Burk (1965), which is on the west side of Zachary Bay on Unga Island (fig. 1). Burk (1965) noted that this section is 244+ meters ("800+ feet") thick, and Lyle and others (1979) (who referred to it as the White Bluff stratigraphic section) cited a thickness of up to 289

meters (948 feet) not including an "interval of unknown extent" consisting of inaccessible vertical cliffs. The Zachary Bay type section of the Unga was assigned a Miocene age by Dall (1896, 1904), due to his mistaken belief that Miocene marine mollusks had been found in this section. Assignment of a Miocene or possible Miocene age to these outcrops was repeated by later workers (Burk, 1965; Lyle and others, 1979) even though there were doubts about Dall's (1896, 1904) report of Miocene marine mollusks at this locality. All other outcrops of the Bear Lake Formation that contain marine mollusks, including those that have been assigned to the Unga Conglomerate Member (Burk, 1965), are of middle or late Miocene age (Marincovich and Kase, 1986; Marincovich, 1988; Marincovich and Powell, 1989).

The Zachary Bay strata assigned to the Unga Conglomerate Member by Burk (1965) were first studied by W.H. Dall between 1865 and 1899 (Dall, 1896, 1904). Based on the presence of sparse plant megafossils in the lower part of the Zachary Bay section, Dall (1896, p. 842) assigned most of these strata to the Kenai Group of Cook Inlet (fig. 1) that he thought to be of Oligocene age. The only marine mollusks reported by Dall (1896, 1904) from the Zachary Bay section supposedly came from a 0.3-meter ("one-foot-thick") sandstone bed that he stated to be in about the middle of the uppermost 61 meters (200 feet) of the Zachary Bay section. Dall (1896, 1904) referred to this thin sandstone bed as the "*Crepidula* bed," due to the abundance of a gastropod he identified as *Crepidula praerupta* Conrad. Dall and Harris (1892) had previously noted the presence of a *Crepidula* bed on the coasts of northeastern Unga Island and northern Popof Island, in strata now assigned to the Stepovak Formation (Burk, 1965). Dall (1896, p. 842, 846) listed 19 marine molluscan taxa from Unga Island, but did not cite exact localities, and assigned them to his Astoria Group based on their similarity to fossils from the Miocene Astoria Formation of Oregon and Washington. The mollusks listed by Dall (1896) are mostly well-known species that occur in Miocene and younger deposits of the Alaska Peninsula (Marincovich, 1983; Marincovich and Powell, 1989), including *Mytilus middendorffi* (Grewingk), *Musculus*

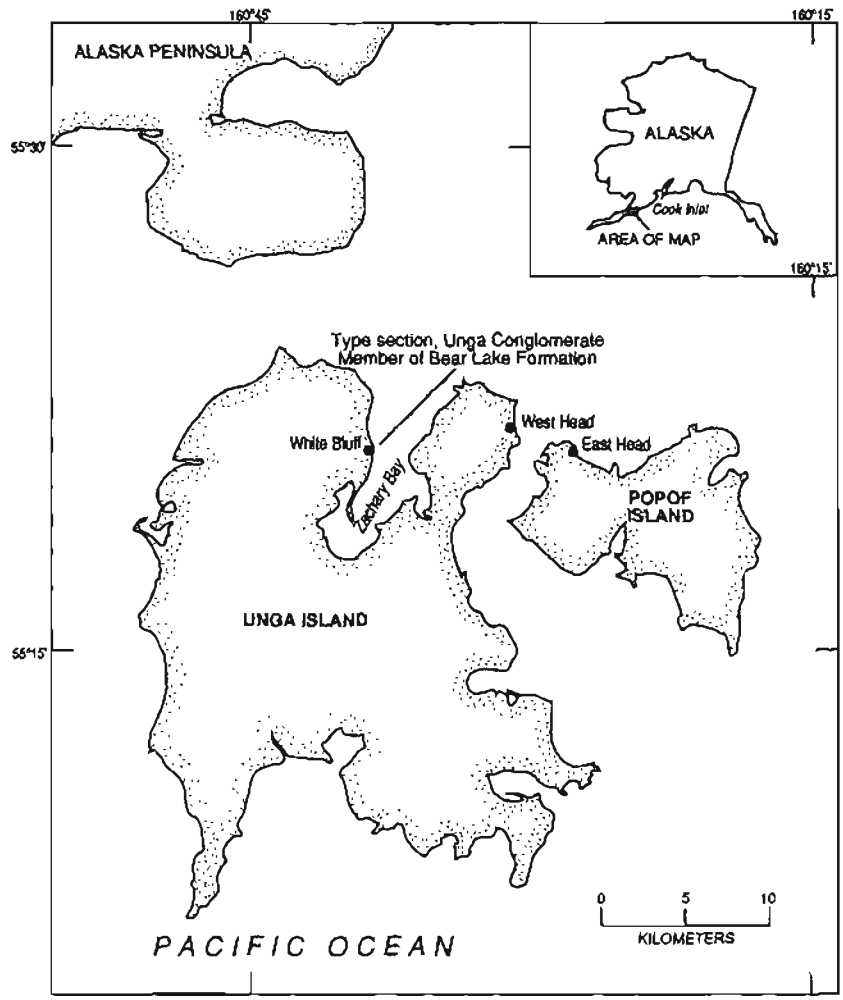

Figure 1. Index map showing location of Unga Island and nearby place names. Dots indicate fossil sample localities.

niger (Gray), *Serripes groenlandicus* (Bruguiere), and *Mya truncata* Linnaeus. However, Dall (1896) did not explicitly state that the 19 molluscan taxa came from Zachary Bay. He clearly considered the strata on northeastern Unga Island and northern Popof Island, now assigned to the Stepovak Formation (Burk, 1965) and considered to be of Oligocene age (Marincovich and Powell, 1989), to belong to his Astoria Group and to be of Miocene age (Dall, 1896). Dall (1896) stated that the *Crepidula* bed that supposedly occurred at Zachary Bay also occurred on the coasts of northeastern Unga and northern Popof Islands. F.S. MacNeil (*in* Burk, 1965) reexamined Dall's Unga Conglomerate specimens that supposedly all came from Unga Island and concluded that Dall (1896, 1904) unknowingly examined mixed Oligocene (Unga Island Stepovak Formation) and Miocene (mainland Bear Lake Formation) mollusk collections when he dealt with Unga Island strata.

Crepidula is extremely common in Stepovak outcrops on the coasts of northeastern Unga Island and northern Popof Island (the West Head and East Head stratigraphic sections, respectively, of Burk [1965]). However, no worker but Dall (1896, 1904) has cited *Crepidula* or any other marine megafossil in the Zachary Bay type section of the Unga Conglomerate. Atwood (1911) examined the Unga beds on the west side of Zachary Bay, but found no marine fossils. Burk (1965) evidently made a careful search for the *Crepidula* bed or other Miocene marine deposit along the margin of Zachary Bay, but found none. One of us (Marincovich) examined the Zachary Bay section in 1982, specifically to locate Dall's *Crepidula* bed, but found no marine fossils.

It is now clear that marine mollusks or other megafossils are not present in the type section of the Unga Conglomerate at Zachary Bay. The Miocene fossils reported from there by Dall (1896, 1904) are molluscan species well-known from the Bear Lake Formation and Tachilni Formation of the Alaska Peninsula mainland (Marincovich, 1983; Marincovich and Powell, 1989), but unknown in the Shumagin Islands. Mollusks from these mainland Miocene formations, plus Oligocene mollusks from the Stepovak outcrops at West Head and (or) East Head, were somehow mixed together by Dall and erroneously attributed to a nonexistent *Crepidula* bed at Zachary Bay.

Evidence for the age of the type section of the Unga Conglomerate Member of the Bear Lake Formation at Zachary Bay consists of pollen and dinocysts, megafloral remains, and a potassium-argon age of 31.3±0.3 Ma (Wiggins and others, 1988). The radiometric age was measured from biotite in a 2.0-m-thick tuff bed at the base of this section. This tuff bed is the stratigraphically lowest part of the basal sandstone described in the Zachary Bay section by Lyle and others (1979). The lowermost exposed 9.1 m of the Zachary Bay section contain early Oligocene pollen and Eocene to early Oligocene dinocysts in the mudstone immediately above the tuff at the section base, and early Oligocene pollen and the first occurrence of late Oligocene pollen in one sample near the top of the interval. The upper part of this 9.1-m-thick interval contains the last occurrence of *Aquilapollenites* sp. and the first occurrence of an undescribed late Oligocene species of Compositae pollen. Above this 9.1-m-thick interval, the microfloras change drastically and represent a geologically instantaneous shift from subtropical-warm temperate to temperate-cool temperate microfloras. In essence, high-diversity, predominantly deciduous taxa were replaced by a low-diversity, conifer-fern flora. This conifer-fern microflora persists throughout the overlying remainder of the Unga type section. The late Oligocene Compositae pollen occurs sporadically throughout this entire section, including the first occurrence of *Saxonipollis* and an undescribed species of freshwater dinocyst. Plant megafossils thought to be of late Oligocene? to middle Miocene age were reported by J.A. Wolfe (*in* Burk, 1965) at two localities in the Zachary Bay section, one very close to the base and the other 88 m above the base of the section. The presence of late Oligocene palynomorphs in the upper part of the Zachary Bay section essentially agrees with this megafloral age.

The high-diversity early Oligocene pollen assemblage contains many exotic taxa characteristic of this time interval, both locally and regionally throughout Alaska and western Canada. Some of the exotic pollen represents relict taxa or mophotypes from Late Cretaceous and Eocene microfloras. Such taxa are definitely not reworked, and the morphotypes similar to Late Cretaceous taxa are indigenous Tertiary species. At Zachary Bay the Late Cretaceous relicts include *Aquilapollenites* sp., "*Integricorpus*" sp., and *Cranwellia* sp., which are all very small and striately ornamented taxa. The Eocene relicts include taxa such as *Pistillipollenites mcgregorii* Rouse, *Intratriporopollenites* sp. A. of Rouse (1977), and *Corsinipollenites* sp. This exotic pollen suite also includes the last occurrences of *Momipites coryloides* Wodehouse, *Ctenosporites wolfei* Elsik and Jansonius, and "*Proteacidites*" *globosiporus* Samoilovitch, and the only known occurrence of a pollen morphotype probably related to Cactaceae.

Pollen and marine dinocysts were recovered from an intact specimen of the oyster *Ostrea gackhensis* from the West Head stratigraphic section of the Stepovak Formation. The external and internal matrix were processed separately and there was little difference between the two assemblages, except for a higher dinocyst count from the internal matrix. The internal matrix contained the following pollen taxa: *Aquilapollenites* sp., *Cranwellia* sp., *Momipites coryloides* Wodehouse, *Corsinopollenites* sp., and *Intratriporopollenites* sp. A. of Rouse (1977). An additional species is *Proteacidites* cf. *P. thalmannii* Anderson, which is probably conspecific with the *Proteacidites* sp. noted by Newman (1981) from Eocene and Oligocene floras of western Washington. The marine dinocyst assemblage from the oyster sample contains abundant specimens of a very limited number of species. *Spinidinium* spp. and *Phthanoperidinium comatum*

(Morgenroth) Eisenack and Knellström completely dominate the assemblage, and the latter taxon has a known worldwide range of middle Eocene to early late Oligocene. Minor dinocyst elements include *Paralecaniella indentata* (Deflandre and Cookson) Cookson and Eisenack, *Areosphaeridium diktyoplokus* (Klumpp) Eaton, *Areosphaeridium* sp., and *Adnatosphaeridium* sp.

Palynological assemblages comparable to those at Zachary Bay and West Head are present at the following localities: on the mainland of the Alaska Peninsula, on Sitkinak Island (south of Kodiak Island), in Cook Inlet, at Nenana in central Alaska, in the North Aleutian Basin of the Bering Sea, in the subsurface Mackenzie Delta of northwestern Canada, in the Quesnel area of British Columbia, and in western Washington. An early Oligocene to late Oligocene floristic change identical to that on Unga Island occurs on the Alaska Peninsula at McGinty Point on the west side of Beaver Bay and in the Gulf Sandy River Federal #1 well along the Bering Sea coast at a depth of approximately 3,350 to 3,660 m. Both changes occur at or near the contact of the Stepovak Formation and the Bear Lake Formation. On Sitkinak Island the late Oligocene Compositae pollen occurs throughout the nonmarine Sitkinak Formation along with an associated cool-temperate microflora. In Cook Inlet the exotic elements of the early Oligocene microflora occur throughout the subsurface part of the West Foreland Formation, including the subsurface formational type section. At Nenana the same exotic early Oligocene microflora occurs in the lower part of the Healy Creek Formation, although it is identified as of probable late Oligocene age by Wahrhaftig and others (1969) and Leopold (1979). Elements of both early and late Oligocene microflora are present in the ARCO North Aleutian COST #1 well in the Bering Sea. In the Mackenzie Delta of northwestern Canada, early Oligocene exotic elements are present in the Richards Formation (Staplin, 1976; Norris, 1982). In the Quesnel area of British Columbia, the exotic early Oligocene floral elements from Alaska are almost all represented in the microflora of the Australian Creek Formation (Piel, 1971; Rouse, 1977; Rouse and Matthews, 1979). This formation has been assigned to the lower Oligocene vertebrate Chadronian Stage based on titanothere teeth (Rouse and Matthews, 1979). Some of the Unga Island exotic pollen taxa are also present in Eocene and Oligocene floras of western Washington (Newman, 1981). Of particular interest is the restricted early Oligocene occurrence of *Gothanipollis*. The only other occurrence of this genus in Alaska is in the subsurface part of the West Foreland Formation in the southern part of Cook Inlet.

CONCLUSIONS

1. The type section of the Unga Conglomerate Member of the Bear Lake Formation contains only Oligocene palynomorphs, marine dinoflagellates, and plant megafossils.

2. The "*Crepidula* bed," said by Dall (1896, 1904) to be an interval with Miocene marine mollusks in the Unga type section, does not exist. No Miocene marine or nonmarine fossils are known from this sequence.

3. The Stepovak Formation at the West Head stratigraphic section on Unga Island contains early Oligocene mollusks, marine dinoflagellates, and palynomorphs. The same early Oligocene palynomorph taxa also occur in the lowest exposed strata of the type section of the Unga Conglomerate Member at Zachary Bay.

REFERENCES CITED

Atwood, W.W., 1911, Geology and mineral resources of parts of the Alaska Peninsula: U.S. Geological Survey Bulletin 467, 137 p.

Burk, C.A., 1965, Geology of the Alaska Peninsula — Island arc and continental margin: Geological Society of America Memoir 99, 250 p.

Dall, W.H., 1896, Report on coal and lignite of Alaska: U.S. Geological Survey 17th Annual Report, v. 4, part 1, p. 763-897.

——— 1904, Neozoic invertebrate fossils, a report on collections made by the expedition, *in* v. 4, Geology and paleontology, *of* Harriman Alaska Expedition: New York, Doubleday, Page and Co., p. 99-122 [reprinted by Smithsonian Institution, 1910].

Dall, W.H., and Harris, G.D., 1892, Correlation papers— Neocene: U.S. Geological Survey Bulletin 84, p. 232-268.

Devyatilova, A.D., and Volobueva, V.I., 1981, Atlas of Paleogene and Neogene fauna of the northeast U.S.S.R.: Moscow, Ministry of Geology of the Northeast Industrial Geological Society, 219 p.

Gladenkov, Y.B., Brattseva, G.M., Mitrofanova, L.I., and Sinelnikova, V.N. 1988. Subdivision of the Oligocene-lower Miocene sequences of eastern Kamchatka: the Korf Bay section: International Geology Review, v. 30, p. 931-944.

Honda, Y., 1986, A Paleogene molluscan fauna from Hokkaido, northern Japan: Palaeontological Society of Japan Special Paper 29, p. 3-16.

Kaiho, K., 1984, Paleogene Foraminifera from Hokkaido, Japan. Part 1. Lithostratigraphy and biostratigraphy including description of new species: Tohoku University Science Reports, Series 2 (Geology), v. 54, no. 2, 95-139.

Leopold, E.B., 1979, Late Cenozoic palynology, *in* Tschudy, R.M., and Scott, R.A., eds., Aspects of palynology: New York, Wiley-Interscience, p. 377-438.

Lyle, W.M., Morehouse, J.A., Palmer, I.F., Jr., and Bolm, J.G., 1979, Tertiary formations and associated Mesozoic rocks in the Alaska Peninsula area, Alaska, and their petroleum reservoir and source-rock potential: Fairbanks, Alaska Division of Geological and Geophysical Surveys, Geologic Report 62, 65 p.

Marincovich, Louie, Jr., 1977, Cenozoic Naticidae (Mollusca: Gastropods) of the northeastern Pacific: Bulletins of American Paleontology, v. 70, no. 294, p. 169-494.

——— 1983, Molluscan paleontology, paleoecology, and North

Pacific correlations of the Miocene Tachilni Formation, Alaska Peninsula, Alaska: Bulletins of American Paleontology, v. 84, no. 317, p. 59-155.

——— 1988, Miocene mollusks from the lower part of the Bear Lake Formation on Ukolnoi Island, Alaska Peninsula, Alaska: Natural History Museum of Los Angeles County, Contributions in Science no. 397, 20 p.

Marincovich, Louie, Jr., and Kase, T., 1986, An occurrence of *Turritella (Hataiella) sagai* in Alaska: implications for the age of the Bear Lake Formation: Bulletin of the National Science Museum [Tokyo], Series C (Geology & Paleontology), v. 12, no. 2, p. 61-66.

Marincovich, Louie, Jr., and Powell, C.L., II, 1989, Preliminary Tertiary molluscan biostratigraphy of the Alaska Peninsula, southwestern Alaska: U.S. Geological Survey Open-File Report 89-674, 2 sheets.

Newman, K.R., 1981, Palynologic biostratigraphy of some early Tertiary nonmarine formations of central and western Washington: Geological Society of America Special Paper 184, p. 49-65.

Norris, G., 1982, Spore-pollen evidence for early Oligocene high-latitude cool-climate episode in northern Canada: Nature, v. 297, p. 387-389.

Palmer, A.R., 1983, The DNAG 1983 time scale: Geology, v. 11, p. 503-504.

Piel, K.M., 1971, Palynology of Oligocene sediments from central British Columbia: Canadian Journal of Botany, v. 49, p. 1885-1920.

Rouse, G.E., 1977, Paleogene palynomorph ranges in western and northern Canada, *in* Contributions of stratigraphic palynology (with emphasis on North America), v. 1, Cenozoic palynology: American Association of Stratigraphic Palynologists Contribution no. 5A, p. 48-65.

Rouse, G.E., and Matthews, W.H., 1979, Tertiary geology and palynology of the Quesnel area, British Columbia: Bulletin of Canadian Petroleum Geology, v. 27, no. 4, p. 418-445.

Staplin, F.L., 1976, Tertiary biostratigraphy, Mackenzie Delta region, Canada: Bulletin of Canadian Petroleum Geology, v. 24, no. 1, p. 117-136.

Takeda, H., 1953, The Poronai Formation (Oligocene Tertiary) of Hokkaido and South Sakhalin and its fossil fauna: Hokkaido Association of Coal Mining, Studies in Coal Geology no. 3, 103 p.

Wahrhaftig, C., Wolfe, J.A., Leopold, E.B., and Lanphere, M.A., 1969, The coal-bearing group in the Nenana Coal Field, Alaska: U.S. Geological Survey Bulletin 1274-D, 30 p.

Wiggins, V.D., Nichols, D.J., and Obradovich, J.D., 1988, Changes in non-marine palynofloras from the Oligocene of Alaska, U.S.A.: Seventh International Palynological Congress, Brisbane, Australia, Abstracts volume, p. 181.

Reviewers: William P. Elder and William V. Sliter

Mafic and Ultramafic Rocks of the Dishna River Area, North-Central Iditarod Quadrangle, West-Central Alaska

By Marti L. Miller

Abstract

Mafic and ultramafic rocks of the Dishna River area occur as fault-bounded slivers in a 43 km by 7 km, northeast-trending belt in the north-central part of the Iditarod quadrangle. Ultramafic slivers consist of serpentinized harzburgite, minor dunite, and rare pyroxenite. Dominantly mafic slivers consist primarily of gabbronorite, pyroxene + hornblende gabbro, and hornblende gabbro and diabase, but also include pyroxenite, wehrlite, and minor dikes and pods of tonalite. Some of the mafic rocks were overprinted by low-pressure, greenschist-facies metamorphism. Based on lithology, fabric, metamorphic grade, and correlation with similar rocks outside the study area, the ultramafic and mafic slivers are probably ophiolitic in origin. If so, the ultramafic slivers represent residual mantle material, and the mafic slivers represent the overlying cumulate magmatic suite.

The age of the mafic-ultramafic rocks of the Dishna River area is uncertain. Whereas they resemble previously described Jurassic mafic-ultramafic complexes, a single K-Ar analysis on hornblende from Dishna River gabbro yields a Late Permian to Late Triassic age. However, this age may be anomalously old due to excess argon retention.

INTRODUCTION

Jurassic mafic-ultramafic complexes are widely distributed across northern and west-central Alaska and are generally thought to represent the lower part of an ophiolite sequence (for example, Patton and others, 1977; Roeder and Mull, 1978; Loney and Himmelberg, 1984, 1989). The complexes occur in close spatial relation to tectonic slices of oceanic crustal rocks consisting primarily of basalt, diabase, gabbro, and chert of Devonian to Jurassic age (Patton and others, 1977, 1989a, 1989b; Patton and Box, 1989). The mafic-ultramafic complexes and oceanic crustal rocks structurally overlie Proterozoic and Paleozoic metamorphosed continental crust and were emplaced during the latest Jurassic and Early Cretaceous (Patton and others, 1977, 1989a). Although most workers agree that these rocks are allochthonous with respect to the metamorphosed continental crust, they do not agree on the mode of emplacement. In the most widely accepted scenario, the mafic-ultramafic complexes and associated oceanic rocks form, respectively, upper and lower thrust panels of a large allochthonous sheet that was rooted in the Yukon-Koyukuk basin (Patton and others, 1977, 1989a; Patton and Box, 1989). Alternatively, Coney (1984) suggested that the allochthonous sheet was rooted in a more southerly ocean basin and thrust northward. Gemuts and others (1983) suggested that the ophiolitic rocks formed along intracontinental rifts and were emplaced over metamorphic borderlands during a later compressional event.

In this report I describe the occurrence of mafic-ultramafic rocks in the Dishna River area, in the north-central part of the Iditarod quadrangle (fig. 1). These rocks represent the farthest southwest extent of the Tozitna-Innoko belt of ophiolitic rocks described by Patton and others (1989a). Localities of samples described in the tables and text are shown in figure 2.

GEOLOGIC SETTING

Topography in the northern part of the Iditarod quadrangle is dominated by low, rounded hills that have an average relief of 150 m. A thick cover of colluvium and vegetation largely conceals the bedrock; outcrops are extremely rare, and contact and structural relations are sometimes ambiguous.

Mafic and ultramafic rocks in the Dishna River area occur as fault-bounded slivers, or blocks, exposed in a northeast-trending belt about 43 km long and up to 7 km wide (fig. 1). The mafic and ultramafic rocks generally occur as isolated blocks. Where observed, the contacts are high-angle shear zones (up to 30 m wide) that may originally have been low-angle faults prior to more recent deformation. The ultramafic rocks were first reported by Miller and Angeloni (1985). Subsequent mapping has shown the associated mafic igneous rocks to be equally extensive.

The fault-bounded blocks of mafic and ultramafic rock lie within a larger belt of fault-bounded slivers of metamorphosed continental crustal rocks and oceanic and volcanic-arc rocks; older rocks are onlapped by a basin-fill sequence

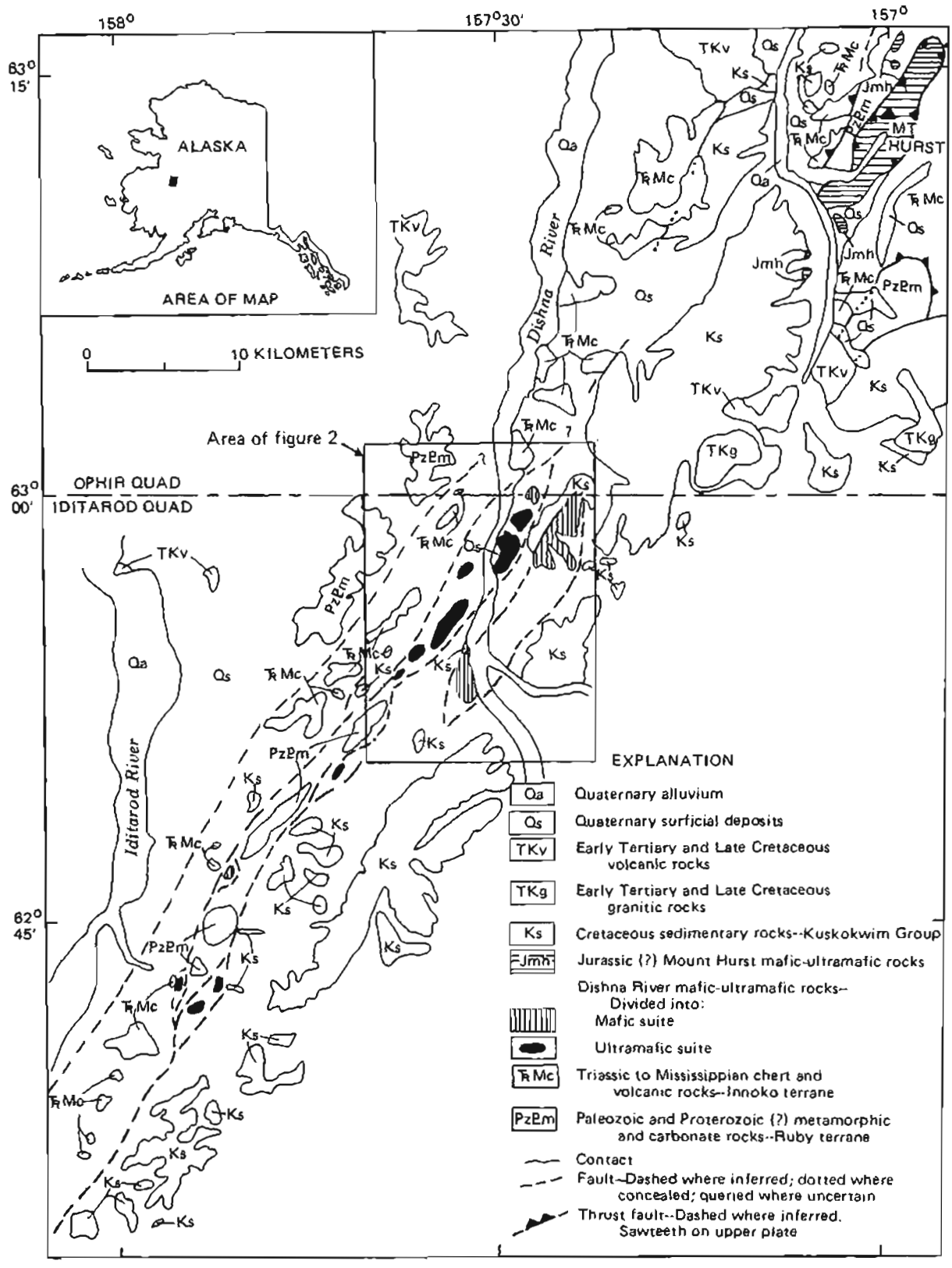

Figure 1. Geologic sketch map showing distribution of Dishna River and Mount Hurst mafic-ultramafic rocks. Geology in Ophir quadrangle summarized from Chapman and others (1985).

(fig. 1). In the Iditarod quadrangle, the metamorphosed continental crustal rocks consist of foliated greenschist-facies metaigneous and metasedimentary rocks of presumed Paleozoic age (Patton and others, 1989b), which correlate with the Ruby terrane as outlined by Jones and others (1987). The oceanic and volcanic-arc rocks consist of radiolarian chert, basalt to basaltic andesite, and metasiltstone of presumed Mississippian to Triassic (and Jurassic?) age, based on correlation outside of the study area (Chapman and others, 1985; Patton and others, 1989b). These weakly metamorphosed rocks (maximum grade, prehnite-pumpellyite facies) correlate with the Innoko terrane of Jones and others (1987). Older rocks are depositionally overlain by mid- and Upper Cretaceous sandstone of the Kuskokwim Group and Upper Cretaceous to lower Tertiary subaerial volcanic rocks.

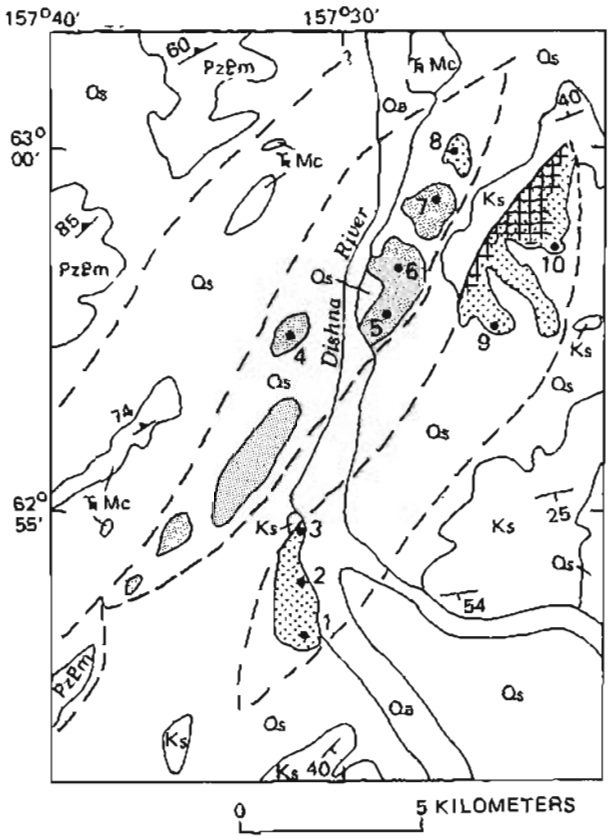

Figure 2. Geology of study area showing Dishna River mafic-ultramafic rocks, sample localities, and area of greenschist-facies metamorphic overprint.

DESCRIPTION OF MAFIC-ULTRAMAFIC ROCKS

Two mappable suites of Dishna River mafic and ultramafic rocks are recognized: (1) serpentinized ultramafic rocks not associated with other rock types and (2) mafic rocks that are locally associated with minor ultramafic and leucocratic rocks (figs. 1 and 2). The contact between the two suites is not exposed.

Ultramafic suite

The ultramafic suite is composed primarily of harzburgite, lesser lherzolite, wehrlite, and dunite, and minor orthopyroxenite. Chromian spinel, a common accessory mineral, occurs as disseminated grains that are intergranular to the primary silicates. Although all of the ultramafic rocks are now composed of at least 40 percent, and up to 95 percent, serpentine minerals, relict mineralogy is nearly always visible. Fine-grained magnetite, a by-product of serpentinization, outlines former olivine crystals in serpentinized harzburgite and dunite. Major- and trace-element analyses of two harzburgite samples from the ultramafic suite are given in table 1. Although serpentinized, these rocks retain the chemical signature of the original rock (for example, low SiO_2 and K_2O values; high MgO and Ni values). Elements of potential economic interest (Co, Cr, Pd, and Pt, table 2) are in the normal range for ultramafic rocks (for example, Levinson, 1980).

The ultramafic rocks show other alteration effects. On the barren ridge top on the east side of the Dishna River (fig. 1), rubble of gray-blue (serpentinized) harzburgite is punctuated by several bright-orange-weathered podlike exposures (6 to 15 m in diameter) of quartz + talc + magnesite + chromian spinel rock, apparently derived from dunite. The talc + magnesite assemblage is attributed to low-grade metamorphism of serpentine in the presence of H_2O and CO_2 (see for example, Winkler, 1976). Alteration by hydrothermal fluids channeled along local fracture systems has resulted in similar replacement of ultramafic rocks at Mount Hurst (Roberts, 1984), 38 km to the northeast (fig. 1).

Table 1. Major-oxide analyses (in weight percent) and trace-element data (in parts per million) for selected samples of the Dishna River mafic-ultramafic rocks

[Major oxides analyzed by Alaska Division of Geological and Geophysical Surveys, Fairbanks, Alaska using X-ray fluorescence. LOI, loss on ignition. Trace elements analyzed by R.G. McGimsey, U.S. Geological Survey, Anchorage, Alaska using Kevex. Locality numbers refer to figure 2. ND, not detected; —, not analyzed]

	Ultramafic suite		Mafic suite			
Locality	5	6	3	8	1	1
Sample No.	84AM285A	84AM284A	84AM280A	85AM87A	84AAi609B	84AAi609C
Rock type	Harzburgite	Harzburgite	Gabbronorite	Hornblende gabbro	Clinopyroxenite	Wehrlite
Percent serpentine	78.2	74.0	0	0	6.2	34.9
SiO_2	41.48	39.97	49.17	42.10	52.20	40.24
Al_2O_3	.66	.48	16.75	19.34	2.45	.34
Fe_2O_3total	7.46	7.78	8.58	13.89	4.54	12.12
MgO	39.05	39.21	11.63	7.75	18.37	37.93
CaO	.52	.54	11.93	12.69	20.97	1.79
Na_2O	ND	.07	.98	1.89	.23	.06
K_2O	ND	.01	.03	.18	.01	.01
TiO_2	.01	.01	.25	1.38	.10	.02
P_2O_5	.01	.01	.02	.12	.01	.02
MnO	.13	.13	.17	.22	.13	.16
(LOI)	10.92	11.62	.80	1.11	1.51	7.55
Total	100.24	99.83	100.31	100.67	100.52	100.24
Trace elements (ppm)						
Nb	<10	<10	<10	--	<10	<10
Rb	<10	<10	6	--	<10	<10
Sr	7	ND	337	--	22	8
Zr	11	10	16	--	11	12
Y	5	5	8	--	6	6
Ba	ND	ND	31	--	24	19
Ce	2	2	2	--	6	4
La	2	1	4	--	<5	<5
Cu	4	4	49	--	0.1	89
Ni	1,942	2,168	88	--	250	1,377
Zn	40	40	62	--	19	55

The ultramafic rocks have a tectonite fabric indicated by recrystallization and foliation. Olivine crystals in dunite display equant grain shapes and interlocking texture indicative of subsolidus recrystallization (Loney and others, 1971). In other dunite samples, foliation is defined by planar alignment of secondary, fine-grained magnetite. Postemplacement brittle fractures, containing veins of chalcedonic quartz, cut hydrothermally altered serpentine + magnesite + magnetite rock.

Mafic suite

The mafic suite consists mainly of gabbroic rocks but also contains pyroxenite, wehrlite, and minor dikes and pods of tonalite. Gabbro, diabase, and tonalite commonly have a massive, hypidiomorphic igneous texture; cumulate phase layering is locally developed in both gabbro and associated ultramafic rocks.

Three types of gabbroic rocks are represented in the mafic suite: (1) two-pyroxene gabbronorite, (2) clinopyroxene + hornblende gabbro, and (3) hornblende gabbro and diabase. The gabbronorite has crude layering of light and dark minerals and contains augitic clinopyroxene, hypersthene, plagioclase, minor opaques, and minor hornblende (after pyroxene). The plagioclase is unzoned and calcic (An_{75-85} by Carlsbad-albite twin method). The clinopyroxene + hornblende gabbro lacks layering and has hypidiomorphic-granular to subophitic textures. Clinopyroxene

Table 2. Trace-element analyses of economic interest for selected samples of the Dishna River mafic-ultramafic rocks

[Co and Cr by optical emission spectroscopy (in parts per million). Pd and Pt by ICP-Mass spectrometry (in parts per billion). Locality numbers refer to figure 2]

Locality	Sample	Rock type	Co	Cr	Pd	Pt
ULTRAMAFIC SUITE						
4	84AM276A	Serpentinite	100	1,000	2.9	4.6
5	84AM285A	Serpentinized harzburgite	100	2,000	3.0	7.8
5	84AM285B	Serpentinite	100	3,000	<0.8	2.8
6	84AM284A	Serpentinized harzburgite	100	1,500	7.6	11
6	84AM284B	Pyroxenite	100	2,000	10	9.4
7	85AM85B	Serpentinized wehrlite	100	2,000	5.7	6.8
MAFIC SUITE						
9	86AMc11A	Gabbronorite	70	200	7.5	6.4
10	86AM37A	Hornblende gabbro	70	150	15	9.6

crystallized before the hornblende, and both are partly altered to actinolite + chlorite. Plagioclase is unzoned and calcic (about An_{60-75} by Carlsbad-albite twin method). The hornblende gabbro has a variety of textures, including hypidiomorphic-granular, subophitic-microgabbroic, diabasic, and porphyritic. Hornblende is extensively altered to actinolite + chlorite, and secondary minerals (epidote + sphene) also occur in the groundmass. Plagioclase composition generally ranges from An_{45} to An_{60} in the less altered varieties but is more albitic in some samples.

Ultramafic rocks consisting of pyroxenite and layered wehrlite and olivine gabbronorite were found at one locality in association with rocks of the mafic suite (locality 1, fig. 2). The pyroxenite is clinopyroxene-rich, contains serpentinized orthopyroxene, and varies in olivine content from 0 to about 10 percent. The layered wehrlite-olivine gabbronorite rocks show light- and dark-colored bands (plagioclase-rich and plagioclase-poor, respectively) that range from 1 to 5 cm in thickness; the bands cannot be traced more than a meter due to poor exposure. Olivine shows cumulate texture in thin section, and the banding is interpreted to have formed by cumulate processes.

Minor tonalite is found within the mafic suite but is rare and occurs only locally in rubble crop mixed with gabbro. At one locality (the farthest southwest exposure of the mafic suite in fig. 1) tonalite occurs as dikes 1–6 cm wide and small pods (<0.5 m in maximum dimension) in pyroxene-hornblende gabbro; this suggests that tonalite at other locations is probably from dikes as well.

Chemical analyses of four representative samples from the mafic suite (two gabbroic and two ultramafic) are given in table 1. Both of the gabbroic rocks have very low K_2O content. The high Al_2O_3 content of the hornblende gabbro (19.34 weight percent) suggests an origin possibly involving plagioclase accumulation. Analyses of Co, Cr, Pd, and Pt in two additional gabbroic samples from the mafic suite (table 2) have values in the normal range for mafic rocks (for example, Levinson, 1980).

The hornblende gabbro and diabase are partially altered to actinolite + chlorite + epidote + albitic plagioclase + sphene + quartz, indicative of greenschist-facies metamorphism. Metamorphic crystallization was pseudomorphic and preserves original igneous textures. The lack of penetrative fabric suggests low-pressure hydrothermal rather than dynamothermal metamorphism. This metamorphic overprint is found in the northeastern part of the mafic suite (crosshatched pattern in fig. 2). Prehnite veins (1 mm to 1 cm wide) also occur locally. A higher temperature (low amphibolite facies) metamorphic assemblage of hornblende + actinolite + albitic plagioclase + biotite + epidote is developed in hornblende gabbro at several localities; this metamorphism was accompanied by static recrystallization of mafic minerals that masks the original igneous fabric. This higher grade recrystallization may represent contact metamorphism associated with later dike emplacement.

AGE RELATIONS

K-Ar age determinations were made on two gabbroic samples from the Dishna River area (table 3). Hornblende that replaces clinopyroxene in gabbro yielded a Late Permian to Late Triassic age of 225±25 Ma (sample 85AM91A). This age is older than the Middle to Late Jurassic K-Ar ages (172 to 155 Ma) obtained from mafic-ultramafic complexes in the Tozitna-Innoko ophiolitic belt (Patton and others, 1977, 1989a). Since the K_2O value is low, hornblende may have inherited excess argon from pyroxene, thus resulting in an anomalously old age. If the age is correct, then the mafic and ultramafic rocks of the Dishna River area are older than other mafic-ultramafic rocks known from this belt. Hornblende from recrystallized hornblende gabbro yielded a mid-Cretaceous age of 92±3 Ma (sample 85AM87C). This age may represent partial thermal resetting of the K-Ar isotopic system by Late Cretaceous plutonism that is pervasive in this area (Miller and Bundtzen, 1987).

DISCUSSION

The lithology, chemistry, textures, fabric, and metamorphic grade of the mafic and ultramafic rocks of the

Table 3. K-Ar ages and analytical data for gabbroic rocks from the mafic suite of the Dishna River mafic-ultramafic rocks

[Analyses by Alaska Cooperative Geochronology Laboratory, Fairbanks. Constants: $\lambda_a + \lambda_{a'} = 0.581 \times 10^{-10}yr^{-1}$, $\lambda_\beta = 4.962 \times 10^{-10}yr^{-1}$, $^{40}K/K_t = 1.167 \times 10^{-4}$mol/mol. hbld, hornblende]

Locality number	Sample	Mineral	K_2O (wt%)	$^{40}Ar_{rad}$ (10^{-11} mol/g)	$^{40}Ar_{rad}$ (%)	$^{40}Ar_{rad}/^{40}K$ (10^{-3})	Age (Ma)
2	85AM91A	hbld	0.025	0.8385	22.33	13.7209	222±23
				0.8633	23.17	14.1262	228±25
							x = 225±25
8	85AM87	hbld	0.237	3.2214	54.64	5.4938	92±3

Dishna River area are consistent with those that characterize ophiolite assemblages worldwide (for example, Coleman, 1977). Further, they are very similar to other more well exposed mafic-ultramafic complexes for which an ophiolitic origin is well established (Patton and others, 1977, 1989a). If the mafic and ultramafic rocks of the Dishna River area are ophiolitic, then the ultramafic suite represents residual mantle material, and the mafic suite represents the cumulate gabbroic sequence that commonly overlies the mantle suite in most well-exposed ophiolites (Moores, 1982). Ophiolites form in spreading ridge environments where they are subjected to the effects of high heat flow and hot circulating sea water concomitant with oceanic crust formation (Coleman, 1977). Rocks altered in this environment develop a greenschist-facies mineral assemblage without a penetrative fabric (Ernst, 1976), identical to the metamorphic effects found in the mafic suite of the Dishna River area.

Mafic and ultramafic rocks of the Dishna River area are on trend with the mafic-ultramafic complex at Mount Hurst, which lies about 38 km to the northeast (see fig. 1). The better exposed mafic-ultramafic rocks of the Mount Hurst area have been interpreted as part of a dismembered ophiolite (Loney and Himmelberg, 1984; Roberts, 1984). Rocks from both areas have similar rock compositions, mineral textures, and alteration assemblages and are adjacent to radiolarian chert, basalt to basaltic andesite, and metasiltstone of the Innoko terrane, suggesting that they share a common orogenic history.

In the Dishna River area, contact relations between the mafic-ultramafic rocks and adjacent rock types are not always clear. Where observed, the contacts are high-angle shear zones up to 30 m wide. At Mount Hurst, the mafic-ultramafic complex was interpreted by Chapman and others (1985) to be a klippe thrust over Triassic to Mississippian chert and volcanic rocks of the Innoko terrane, which in turn were thrust over Paleozoic and Proterozoic(?) metamorphic rocks of the Ruby terrane. If the same thrust relations inferred at Mount Hurst are true for the fault slivers exposed in the Dishna River area, then their original low-angle character has been obscured by subsequent high-angle faulting along a zone that can be traced from the Ophir-Iditarod quadrangle boundary, southwest for 76 km (off of figure 1). This fault zone is on trend with the Susulatna lineament (Patton, 1978), which juxtaposes mid-Cretaceous sedimentary rocks against older rocks and may have had a significant Cretaceous lateral displacement (John Decker, written commun., 1988). Postdepositional deformation of the mid- and Upper Cretaceous Kuskokwim Group and underlying basement rocks has produced a series of northeast-trending synclines and anticlines (Miller and Bundtzen, 1987). This post-Cretaceous folding may have contributed to the complicated pattern (fig. 1) of fault slivers in the Dishna River area. Hence, Kuskokwim Group rocks found between slivers of basement rocks might be remnants in the cores of synclines or grabens in normal faults.

The mafic and ultramafic rocks in both the Dishna River and Mount Hurst areas are part of a larger belt of mafic-ultramafic complexes exposed along the Ruby geanticline and called the Tozitna-Innoko ophiolite belt by Patton and others (1989a); the Dishna River mafic-ultramafic rocks represent the farthest southwest extent of this belt. No age data are available for the Mount Hurst mafic-ultramafic rocks, but other complexes of this belt yield Middle to Late Jurassic K-Ar ages (Patton and others, 1977, 1989a). The Late Permian to Late Triassic K-Ar age reported here from gabbroic rocks in the Dishna River area could suggest that these mafic-ultramafic rocks are older than others of this belt, or the K-Ar age determination may be anomalously old due to excess argon retention.

Acknowledgments.—L.M. Angeloni, T.K. Bundtzen, and R.G. McGimsey participated in mapping the mafic-ultramafic complex. E.A. Bailey provided X-ray identification of vein minerals. This paper has benefitted from discussions with S.W. Nelson and T.K. Bundtzen.

REFERENCES CITED

Chapman, R.M., Patton, W.W., Jr., and Moll, E.J., 1985, Reconnaissance geologic map of the Ophir quadrangle, Alaska: U.S. Geological Survey Open-File Report 85-203, 17 p., scale 1:250,000.

Coleman, R.G., 1977, Ophiolites: New York, Springer-Verlag, 229 p.

Coney, P.J., 1984, Structural and tectonic aspects of accretion in Alaska, *in* Howell, D.G., Jones, D.L., Cox, Allan, and Nur, Amos, eds., Proceedings of the Circum-Pacific terrane conference: Stanford University Publications in the Geological Sciences, v. 18, p. 68-70.

Ernst, W.G., 1976, Petrologic phase equilibria: San Francisco, W.H. Freeman and Co., 333 p.

Gemuts, I., Puchner, C.C., and Steffel, C.L, 1983, Regional geology and tectonic history of Western Alaska, *in* Proceedings of the 1982 Symposium on Western Alaska Geology and Resource Potential: Journal of the Alaska Geological Society, v. 3, p. 67-85.

Jones, D.L., Silberling, N.J., Coney, P.J., and Plafker, George, 1987, Lithotectonic terrane map of Alaska (west of the 141st meridian): U.S. Geological Survey Miscellaneous Field Studies Map MF-1874-A, scale 1:2,500,000.

Levinson, A.A., 1980, Introduction to exploration geochemistry (2d ed.): Wilmette, Ill., Applied Publishing, 924 p.

Loney, R.A., and Himmelberg, G.R., 1984, Preliminary report on ophiolites in the Yuki River and Mount Hurst areas, west-central Alaska, *in* Coonrad, W.L., and Elliott, R.L., eds., The United States Geological Survey in Alaska—Accomplishments during 1981: U.S. Geological Survey Circular 868, p. 27-30.

—— 1989, The Kanuti ophiolite, Alaska: Journal of Geophysical Research, v. 94, no. B11, p. 15,869-15,900.

Loney, R.A., Himmelberg, G.R., and Coleman, R.G., 1971, Structure and petrology of the alpine-type peridotite at Burro Mountain, California, U.S.A.: Journal of Petrology, v. 12, no. 2, p. 245-309.

Miller, M.L., and Angeloni, L.M., 1985, Ophiolitic rocks of Iditarod quadrangle, west-central Alaska [abs.]: American Association of Petroleum Geologists Bulletin, v. 69, no. 4, p. 669-670.

Miller, M.L., and Bundtzen, T.K., 1987, Geology and mineral resources of the Iditarod quadrangle, west-central Alaska [abs.], *in* Sachs, J.S., ed., USGS Research on Mineral Resources - 1987: U.S. Geological Survey Circular 995, p. 46-47.

Moores, E.M., 1982, Origin and emplacement of ophiolites: Reviews of Geophysics and Space Physics, v. 20, no. 4, p. 735-760.

Patton, W.W., Jr., 1978, Juxtaposed continental and oceanic-island arc terranes in the Medfra quadrangle, west-central Alaska, *in* Johnson, K.M., ed., The United States Geological Survey in Alaska—Accomplishments during 1977: U.S. Geological Survey Circular 772-B, p. B38-39.

Patton, W.W., Jr., and Box, S.E., 1989, Tectonic setting of the Yukon-Koyukuk basin and its borderlands, western Alaska: Journal of Geophysical Research, v. 94, no. B11, p. 15,807-15,820.

Patton, W.W., Jr., Box, S.E., and Grybeck, Donald, 1989a, Ophiolites and other mafic-ultramafic complexes in Alaska: U.S. Geological Survey Open-File Report 89-648, 27 p., scale 1:5,000,000.

Patton, W.W., Jr., Box, S.E., Moll-Stalcup, E.J., and Miller, T.P., 1989b, Geology of west-central Alaska: U.S. Geological Survey Open-File Report 89-554, 41 p.

Patton, W.W., Jr., Tailleur, I.L., Brosgé, W.P., and Lanphere, M.A., 1977, Preliminary report on the ophiolites of northern and western Alaska, *in* Coleman, R.G., and Irwin, W.P., eds., North American ophiolites: Oregon Department of Geology and Mineral Industries Bulletin 95, p. 51-57.

Roberts, W.S., 1984, Economic potential for chromium, platinum, and palladium in the Mount Hurst ultramafics, west-central area, Alaska: U.S. Bureau of Mines Open-File report 84-22, 52 p.

Roeder, Dietrich, and Mull, C.G., 1978, Tectonics of Brooks Range ophiolites (Alaska): American Association of Petroleum Geologists Bulletin, v. 62, no. 9, p. 1696-1702.

Winkler, H.G.P., 1976, Petrogenesis of metamorphic rocks: New York, Springer-Verlag, 334 p.

Reviewers: J.Y. Bradshaw and William W. Patton, Jr.

Shear Sense in Mylonites, and Implications for Transport of the Rampart Assemblage (Tozitna Terrane), Tanana Quadrangle, East-Central Alaska

By Ronny T. Miyaoka *and* James H. Dover

Abstract

Analysis of shear sense in a mylonitic detachment zone beneath the Rampart assemblage of east-central Alaska indicates two distinct episodes of shear. For the segment of the detachment along the northwest boundary of the Rampart assemblage in the eastern Ray Mountains, the first was an episode of mid-Cretaceous or older contractional top-northwest up-dip movement, represented mainly by S-C fabric, asymmetric augen, and asymmetric pressure shadows. The second was an episode of mid-Cretaceous or younger extension having top-southeast normal-slip in the opposite, or down-dip, direction, indicated by rotated plagioclase porphyroblasts and kink bands. For the segment of the detachment along the south side of the Rampart assemblage, in the area between the Yukon and Tozitna Rivers, two equivalent episodes of shear are indicated by a combination of mesoscopic and microfabric data; however, for each episode here, the direction and sense of shear are opposite to those in the eastern Ray Mountains. These variations in shear sense and transport direction are difficult to reconcile with tectonic models involving long-distance, unidirectional transport of the Rampart assemblage. Instead, the data support the alternative concept that the Rampart assemblage originated locally in a rift basin that subsequently underwent (1) contraction involving transport of the Rampart comparatively short distances in opposite directions over its opposing margins, and (2) later extension, or subsidence relative to rising borderlands, when the basin-margin detachments were reactivated as zones of normal slip.

INTRODUCTION

Statement of the Problem

The Rampart assemblage of Dover and Miyaoka (1985a) in east-central Alaska is part of the Tozitna terrane of Jones and others (1987), and comprises predominantly mafic igneous rocks and subordinate intercalations of bedded chert, argillite, graywacke, and carbonate rocks. This assemblage contrasts with structurally underlying rocks of the Ruby geanticline, which are mainly quartz-rich and pelitic metasedimentary rocks.

The origin of the Rampart assemblage is uncertain (fig. 1). Some workers have interpreted present exposures of the Rampart as remnants of regionally extensive obducted sheets of oceanic rocks. Patton and others (1977) proposed southeastward transport across the Ruby geanticline from a

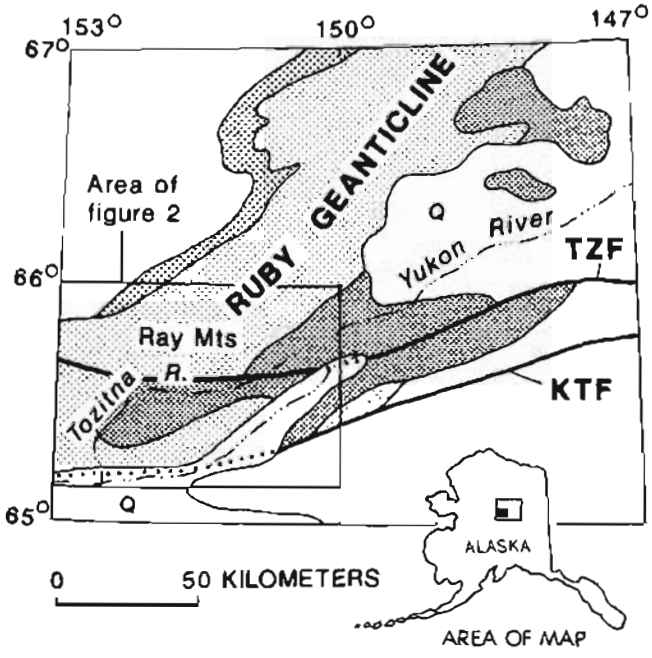

Figure 1. Location map showing regional distribution of major rock sequences in east-central Alaska; modified from Dover (1990). Q, Quaternary surficial deposits; TZF, Tozitna fault; KTF, Kaltag fault; faults dotted where concealed.

root zone in the Koyukuk basin represented by the Kanuti ophiolite (fig. 1). Conversely, Coney (1983) and Coney and Jones (1985) proposed generally northward movement of the Rampart assemblage from an original location south of the Alaska Range. Both models require hundreds of kilometers of semicoherent, unidirectional transport of one or more relatively thin obducted sheets across continental crust. Alternatively, Gemuts and others (1983) interpreted the Rampart as a parautochthonous assemblage originally deposited in an intracontinental rift basin located near the site of present exposures. In this model, structural telescoping during compressional collapse of the basin requires only modest distances of transport of the Rampart onto the rift margins.

The best and most extensive exposures of the contact between the Rampart assemblage and its substrate are in the eastern Ray Mountains (Chapman and others, 1982; Dover and Miyaoka, 1985a,b) and along a displaced segment of the contact in the area between the Yukon and Tozitna Rivers (fig. 1). Mylonitic rocks are common subjacent to the contact. This report expands on an earlier, preliminary study of mylonites in the eastern Ray Mountains (Miyaoka and Dover, 1985). It presents new microfabric data, describes variations in direction and sense of shear in mylonitic rocks at several places subjacent to the basal Rampart contact, and applies these data to the question of the origin of the Rampart assemblage.

GEOLOGIC FRAMEWORK

Recent mapping and geologic relations along the basal contact of the Rampart assemblage (fig. 2) are summarized by Dover (1990). The Rampart assemblage consists mainly of sills and dikes having gabbroic to dioritic composition and diabasic texture; basalt and pillow basalt are present as subordinate flow rocks. Geochemical data on the mafic rocks are sparse and nondiagnostic as to petrologic affinity and geotectonic setting. The rest of the Rampart assemblage consists of incipiently recrystallized sedimentary rocks of the Rampart Group (Brosgé and others, 1969), including bedded chert of Mississippian to Triassic(?) age, argillite, and graywacke, and lesser amounts of chert-pebble conglomerate, volcaniclastic rocks, and Permian limestone.

Rocks of the Ruby geanticline are predominantly those included in the metamorphic suite of the Ray Mountains of Dover and Miyaoka (1985a,b). The main constituents are low- to medium-grade gritty quartzite, pelitic to quartzitic schist, quartzo-feldspathic gneiss, and marble, all thought to be of Late Proterozoic(?) to middle Paleozoic age; Devonian and Mississippian orthogneiss; and metabasite of unknown age. Also present in the Ruby geanticline are continentally derived granitic rocks of the Ray Mountains pluton, which has yielded mid-Cretaceous K-Ar, Rb-Sr, and U-Pb isotopic ages (Patton and others, 1987). The pluton broadly domes metamorphic foliation and contacts; it produced static garnet, andalusite, biotite, muscovite, and albitic plagioclase porphyroblasts in an aureole that overprints preexisting synkinematic mineral assemblages; and it locally cuts the structurally overlying Kanuti ophiolite in the western Ray Mountains (Patton, 1984).

A distinctive unit of interlayered bimodal quartz-wacke, quartz siltite, phyllite or phyllonite, and latest Devonian limestone and dolomite separates the Rampart assemblage and the metamorphic suite of the Ray Mountains in most places (fig. 2). This unit, referred to here as the Devonian metaclastic sequence, has some lithologic similarities with both the Rampart Group and the metamorphic suite of the Ray Mountains, and it generally has a low metamorphic grade that is intermediate between the two. It is characterized by incompletely recrystallized semischistose and mylonitic fabrics, but metamorphic grade and extent of recrystallization appear to increase gradually with structural depth and merge with those of the metamorphic suite of the Ray Mountains. The Devonian metaclastic sequence may correlate with rocks assigned to the Slate Creek thrust panel in the northern part of the Ruby geanticline (Patton and Box, 1989; Moore and Murphy, 1989).

The basal detachment zone of the Rampart assemblage (hereafter referred to as the Rampart detachment zone) is a wide zone of shearing characterized by semibrittle to ductile thrust zones, as well as ductile mylonites and blastomylonites. The shear zone extends from within the lower part of the Rampart assemblage through the Devonian metaclastic sequence and into the metamorphic suite of the Ray Mountains. Sedimentary and basaltic flow rocks of the Rampart assemblage are typically sheared and recrystallized near the basal detachment; intensely sheared basalts locally contain incipient glaucophane. In contrast, diabasic rocks of the Rampart at the basal detachment show little or no evidence of internal shearing or recrystallization. Either the diabase was particularly resistent to these effects, or it represents relatively late intrusions that did not fully participate in deformation and metamorphism related to detachment. Mylonitic rocks are most extensively developed in the Devonian metaclastic sequence, but they are also in restricted zones of intense shear within the metamorphic suite of the Ray Mountains, where they cut earlier schistose fabrics. Most mylonites underwent some metamorphic recrystallization. Some appear to grade with depth into blastomylonitic schists, whereas others define shear zones that seem to merge with semibrittle thrust faults. These variations, along with petrographic variations in crystallization-deformation relations, suggest that the Rampart detachment zone spanned the transition from brittle to ductile deformation in both time and space.

The basal Rampart detachment in the eastern Ray Mountains has been displaced about 50 km relative to its position in the area between the Yukon and Tozitna Rivers by right slip on the Tozitna fault (fig. 2).

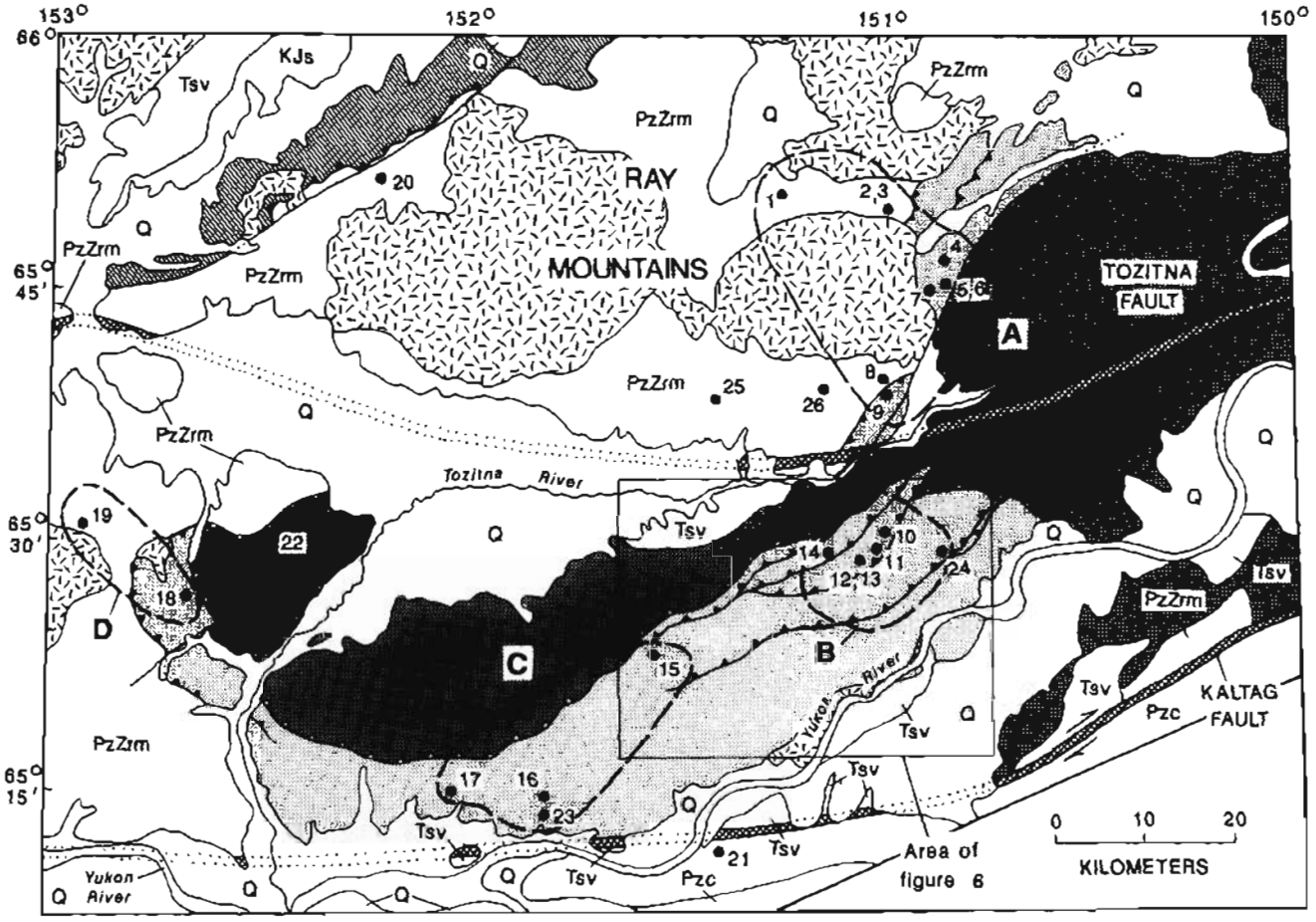

EXPLANATION

- Q — Surficial deposits (Quaternary)
- Tsv — Sedimentary and volcanic rocks (Tertiary)
- KJs — Sedimentary rocks (Cretaceous and Jurassic)
- Granitic rocks (mid-Cretaceous)
- Rampart assemblage of Dover and Miyaoka (1985a) (Jurassic to Mississippian)—Mafic igneous and associated sedimentary rocks
- Kanuti ophiolite (Jurassic to Mississippian)—Ultramafic rocks, chert, and basalt
- Devonian metaclastic sequence (Late Devonian and older?)—Bimodal quartz wacke, siltstone, shale, limestone, and dolomite
- Pzc — Chert, marble, and schist (early Paleozoic)
- PzZrm — Metamorphic suite of the Ray Mountains (Mesozoic to Late Proterozoic)—Quartz-muscovite-biotite schist, quartzitic gneiss, greenschist, diabase, and marble
- Contact
- High-angle normal or oblique-slip fault
- Thrust fault—Dotted where concealed. Sawteeth on upper plate
- Basal detachment zone of Rampart assemblage of Dover and Miyaoka (1985a)—Dotted where concealed
- Strike-slip fault zone—Dotted where concealed. Arrows show relative movement
- 7 — Sample locality
- A — Subarea discussed in text

Figure 2. Simplified geologic map of Tanana quadrangle showing sample locations and subareas discussed in text. Geology generalized from Dover (1990), Chapman and others (1982), and Dover and Miyaoka (1985a).

METHODS

Mesoscopic folds and faults provide some useful information on vergence and sense of fault displacement in the Rampart detachment zone (see Dover and Miyaoka, 1985b), but mesoscopic features are sparse in places. Mylonitic rocks are more abundant and provide microfabric shear-sense data that supplement mesoscopic observations.

Sample collection and preparation

Only oriented samples that exhibit prominent mineral streaking or an intersection lineation, in addition to pervasive mylonitic foliation, were collected for analysis of shear sense. Most samples are from one of four geographically limited subareas, labeled A-D on figure 2 and table 1; two samples (20 and 21) are from other localities. Samples were collected mainly from quartz-rich rocks, such as quartz-wacke, quartz-mica schist, and quartzitic siltite. Shear indicators are best and most consistently developed in coarse-grained, heterogeneous quartz-wacke of the Devonian metaclastic sequence. Samples of metabasite, greenschist, quartz-bearing amphibolite, garnet schist, and marble were also collected; however, these lithologies, along with diabase and other lithologies from the Rampart assemblage, generally do not contain well-developed shear indicators.

For most samples, oversized thin sections were cut perpendicular to mylonitic fabric and parallel to lineation; thin sections of standard size were made from three smaller samples (2, 9, and 11). The unique relation of each thin section to geographic coordinates was determined from its oriented sample.

Petrographic Procedure

Ninteen of the 41 samples collected for analysis were rejected after a preliminary scan of thin sections because they did not exhibit useable microfabric shear indicators. Four samples (5, 6, 8, and 9) from the previous study of Miyaoka and Dover (1985) were reexamined and incorporated into this report (tables 1, 2). Petrographic study of thin sections from these 26 samples included a determination of mineral parageneses and crystallization-deformation history. For each thin section, 25 to 611 nonoverlapping fields of view were examined using a mechanical stage and magnification of either 25x or 63x, depending on grain size (table 2). Within each field, the sense of shear was interpreted for each shear indicator but was counted only once for each type of indicator. For example, three rotated garnet porphyroblasts and two asymmetrical S-C observations observed within one field of view, all indicating dextral (clockwise) shear, would count as only one dextrally rotated garnet reading and one dextral S-C reading.

Interpretive criteria and guidelines

For the ductile or semiductile deformation considered here, mineral streaking and intersection lineation represent the approximate direction of tectonic transport or shear, and thin sections cut parallel to these lineations give the most reliable sense of shear in the transport direction. Mineral streaks are generally thought to form by the smearing out of minerals such as quartz or feldspar in the direction of shearing (Berthé and others, 1979; Simpson and Schmid, 1983). Intersection lineations typically represent the intersection of compositional layering and axial plane foliation, and generally parallel the axes of tight to isoclinal mesoscopic folds. Although initially formed at high angles to directed stress, fold axes and intersection lineations are thought to be rotated under ductile conditions into the direction of tectonic transport and shear (Berthé and Brun, 1980; Bell, 1978; Williams, 1978). Of the two types of lineation, mineral streaks are considered the more reliable because their orientation relative to shearing is constant.

Interpretation of sense of shear is based on five microfabric criteria or shear indicators, described and illustrated in figures 3 and 4: S-C fabric, asymmetric augen (S-type porphyroclast system of Passchier and Simpson, 1986), asymmetric pressure shadows, rotated garnet or plagioclase porphyroblasts, and monoclinic kink folds. The interpretive basis for each of these indicators is referenced in figure 3.

Most samples show some inconsistency in the sense of shear indicated by a particular type of shear indicator, as well as between two or more different types of indicators (table 2). In this study, the shear-sense data for any particular shear indicator were considered acceptible if 70 percent or more of the observations were in agreement. The shear indicators in most of our samples exhibit 75 percent or more consistency. Five samples (22–26) were eliminated from further consideration because their consistency did not meet the 70 percent limit (table 2).

DATA

Mineralogical and deformational characteristics

Three deformational and metamorphic phases are represented in the metamorphic suite of the Ray Mountains (Dover and Miyaoka, 1985b). First-phase isoclinal folds (F_1), axial plane foliation (S_1), and associated synkinematic minerals (M_1) are overprinted by second-generation features (F_2, S_2, M_2). S_2 becomes cataclastic or blastomylonitic along differentially sheared contacts within the metamorphic suite of the Ray Mountains and within the Devonian metaclastic sequence subjacent to the Rampart assemblage. M_3 minerals in aureoles around mid-Cretaceous granitic plutons are late-kinematic to postkinematic with respect to S_2. In the

Table 1. Field number, location, rock type, and dominant mineralogy of samples.

[Subareas shown on figure 2. Minerals listed in order of decreasing abundance. A, andalusite; B, biotite; C, calcite; Cd, chloritoid; Ch, chlorite; E, epidote; G, garnet; H, hornblende; M, muscovite; P, plagioclase; Px, pyroxene; Q, quartz; S, sericite; T, tremolite-actinolite]

Subarea	Sample number	Field number	Latitude	Longitude	Rock type	Mineralogy
A	1	85Do30a	65°51'00"	151°13'48"	Q-M schist	Q,M,B,Ch,Cd
A	2	85Do28b	65°49'48"	150°57'36"	Q-M-B schist	Q,M,B,G,Ch,Cd
A	3	85Do28a	65°49'48"	150°57'36"	Q-M-B schist	Q,B,M,S,G,Ch
A	4	85Do25a	65°46'12"	150°51'00"	Q-phyllonite	Q,S,P(?)
A	5	84Do30a	65°45'36"	150°50'24"	Q-phyllonite	Q,M,B,P,Ch
A	6	84Do30b	65°45'36"	150°57'36"	Q-phyllonite	Q,M,Ch,P
A	7	85Do26a	65°45'36"	150°52'12"	Q-M-B schist	Q,B,P,Ch,A
A	8	84Do28c	65°39'36"	151°00'00"	Q-amphibolite	Q,H,P,S,M,Px
A	9	84Do27c	65°39'00"	150°59'24"	Q-wacke	Q,M,P,Ch
B	10	85Do76b	65°30'00"	151°00'00"	Q-M schist	Q,M,B,Ch
B	11	85Do75	65°29'24"	151°00'00"	Q-wacke	Q,B,M,Ch,A
B	12	85Do77c	65°28'48"	151°00'36"	Greenschist	Ch,Q,P,C
B	13	85Do77e	65°28'48"	151°00'36"	Greenschist	T,Q,P,C,Ch,Cl
B	14	85Do80	65°28'48"	151°06'36"	Q-M semischist	Q,M,B,P,C,Ch
C	15	85Do45b	65°23'24"	151°33'00"	Q-wacke	Q,Ch,S,M
C	16	85Do65a	65°14'24"	151°48'00"	Siltite	Q,M,C,Ch,T
C	17	85Do68a	65°15'00"	152°01'12"	Q-arenite	Q,M,B,Ch,T
D	18	85Do36a	65°27'00"	152°39'36"	Siltite	Q,S,M
D	19	85Do51a	65°30'36"	152°54'00"	Q-M schist	Q,M,B,Ch
—	20	85Do61b	65°52'12"	152°12'36"	Garnet schist	Q,M,B,P,G,E,H
—	21	85Rm2c	65°11'24"	151°24'00"	Siltite	Q,Ch,M,B
—	22	85Do50b	65°28'54"	152°27'30"	Diabase	Ch,Q,Px,P(?)
—	23	85Do70a	65°13'40"	151°48'20"	Siltite	Q,M,B,Ch,T
—	24	85Do144	65°29'12"	150°51'30"	Q-M semischist	Q,M,Ch,Cd
—	25	85Do19b	65°37'22"	151°24'00"	Q-M schist	Q,M,Ch,Cd
—	26	85Do13	65°39'00"	151°07'30"	Q-schist	Q,B,M,Ch

basal Rampart detachment zone, all of these elements may be present, but microfabrics appear to be dominated by second- and third-generation features, including a previously unrecognized S_3 mylonitic foliation that postdates M_3.

S-C tectonites consist of a penetrative (flattening?) foliation (S) and a shear foliation (C) that cuts or merges with S at a low angle. In most of our samples, S- and C-foliation both consist mainly of synkinematic elongate quartz and aligned muscovite (fig. 4*A*, *F*), although C tends to have more muscovite than S. Synkinematic biotite and chlorite are also present in some samples, but are less abundant; some biotite is mimetic. A few samples (2, 18, and 21) have S-foliation consisting almost entirely of dynamically recrystallized elongate quartz grains (fig. 4*C*, *F*). Chlorite and actinolite are common constituents in the foliation of mafic tectonites. In the metamorphic suite of the Ray Mountains, S-foliation typically represents S_1 defined by synkinematic M_1 minerals, and C-foliation is S_2, defined by a second, synkinematic generation (M_2) of the same minerals, enhanced locally by mimetic M_3 recrystallization. In the Devonian metaclastic sequence, C-foliation is either S_2 or S_3, depending on its relation to rotated M_3 porphyroblasts, and S foliation is S_1 and (or) S_2.

In our samples, sigmoidal or lens-shaped asymmetric augen consist mainly of quartz and muscovite intergrowths, or more rarely, intermediate plagioclase (fig. 4*F*). Sparse asymmetric pressure shadows contain directionless aggregates of fine-grained quartz, biotite, muscovite, and chlorite adjacent to megacrysts of quartz, albite, and rarely, pyroxene (fig. 4*E*).

Plagioclase, andalusite, garnet, biotite, and muscovite porphyroblasts (M_3) are common in both the metamorphic suite of the Ray Mountains and the Devonian metaclastic sequence near mid-Cretaceous granitic plutons. Rotated albitic plagioclase porphyroblasts occur in seven samples of the Devonian metaclastic sequence (table 2). The plagioclase encloses foliation that is inferred from its mylonitic

Table 2. Rock fabric data, shear sense indicators, and sense of shear determined for each sample.

[Subareas shown on figure 2; explanation of rock units on figure 2. Lineations: I, intersection lineation; S, mineral streaking lineation. Shear-sense criteria: D, dextral (clockwise); S, sinistral (counterclockwise); SC, S C fabric; AA, asymmetric augen; RP, rotated porphryoblasts; APS, asymmetric pressure shadows; Kinks, monoclinic kink folds; dashes, not present. Shear indicators described in text]

Sub-area	Sample number	Map unit	Fields of view Examined	Magnification	Strike and dip of foliation	Plunge and bearing of lineation	Type of lineation	Occurrence of shear sense criteria										Sense of shear
								SC		AA		RP		APS		Kinks		
								S	D	S	D	S	D	S	D	S	D	
A	1	PzZrm	337	63x	N-S,5°W	1°N55W	I	17	6	3	0	--	--	--	--	--	--	Top-N55W
A	2	PzZrm	270	63x	N65W,5°SW	2°S40E	I	10	2	--	--	--	--	--	--	--	--	Top-S40E
A	3	PzZrm	362	25x	N35E,5°SE	5°S60E	I	6	2	--	--	--	--	--	--	--	--	Top-S60E
A	4	Dms	406	63x	N70W,15°SW	10°S50E	I	0	113	0	4	--	--	--	--	--	--	Top-N50W
							I	--	--	--	--	24	0	--	--	41	0	Top-S50E
A	5	Dms	325	63x	N5E,35°SE	25°S50E	I	1	19	2	4	--	--	--	--	--	--	Top-S50E
A	6	Dms	486	63x	N25E,35°SE	35°S40E	I	0	3	2	19	--	--	--	--	--	--	Top-N40W
							I	--	--	--	--	19	0	--	--	12	3	Top-S40E
A	7	Dms	58	25x	N85E,50°SE	35°S40E	I	0	4	--	--	--	--	--	--	--	--	Top-N40W
							I	--	--	--	--	2	0	--	--	--	--	Top-S40E
A	8	Dms	511	63x	N40E,30°SE	30°S65E	I	4	28	--	--	--	--	1	0	--	--	Top-N67W
A	9	Dms	454	63x	N50E,30°SE	15°S65E	I	108	2	5	3	0	2	3	0	--	--	Top-N65W
A	10	Dms	55	25x	N20E,30°NW	20°N10W	S	12	2	--	--	--	--	--	--	--	--	Top-N10W
							S	--	--	1	12	--	--	--	--	--	--	Top-S10E
							S	--	--	--	--	16	19	1	1	--	--	--
B	11	Dms	36	25x	N5W,20°SW	1°N10W	S	3	12	0	2	--	--	0	1	--	--	Top-S10E
B	12	Dms	213	63x	N45E,15°NW	10°N5E	S	0	1	0	1	0	5	--	--	--	--	Top-N5E
B	13	Dms	611	63x	N80E,10°NW	10°N5E	S	1	62	0	5	--	--	0	2	--	--	Top-N5E
B	14	Dms	563	63x	N25E,20°NW	10°N5E	S	0	17	1	1	0	38	1	1	--	--	Top-N5E
C	15	Dms	355	63x	N60E,35°NW	10°S80W	I	9	27	4	9	--	--	--	--	--	--	Top-S80W
C	16	Dms	340	63x	N55E,60°NW	60°S40E	S	0	52	0	2	--	--	--	--	1	0	Top-N40W
C	17	Dms	44	25x	N55E,40°NW	35°N70W	S	3	12	--	--	--	--	--	--	--	--	Top-N70W
D	18	Dms	345	63x	N60E,10°SE	10°S30E	S	3	32	0	1	--	--	--	--	--	--	Top-N30W
D	19	PzZrm	383	63x	N75E,20°NW	15°N45W	S	3	25	--	--	--	--	--	--	--	--	Top-S45E
—	20	PzZrm	40	63x	N75E,55°NW	50°N5E	S	0	29	1	0	0	4	0	5	--	--	Top-S5W
—	21	Pzc	25	25x	N60E,40°NW	35°N10E	I	8	1	--	--	--	--	--	--	1	0	Top-S10W
—	22	JMra	367	63x	N10E,15°SE	10°S40E	I	0	2	2	3	--	--	2	2	--	--	Inconsistent
—	23	Dms	514	63x	N60E,50°SE	30°N85E	I	18	13	1	2	--	--	--	--	--	--	Inconsistent
—	24	Dms	474	63x	N15E,15°SE	0°N15E	I	14	17	0	1	--	--	--	--	--	--	Inconsistent
—	25	PzZrm	550	63x	N40W,20°SW	12°S85W	I	12	12	3	2	--	--	--	--	--	--	Inconsistent
—	26	PzZrm	342	63x	E-W,20°S	7°N70E	I	12	13	1	2	--	--	--	--	--	--	Inconsistent

character, intensity, and field occurrence to be S_2. This internal foliation (S_i) is generally undeformed, but its continuity with external foliation is disrupted at porphyroblast boundaries, indicating that rotation outlasted or postdated porphyroblast growth (fig. 4*B*, *E*). The shearing that produced rotation therefore represents a phase of S_3 foliation development that commonly parallels and reactivates S_2. Locally within the porphyroblasts, S_i has a weak spiral form that is continuous with external foliation across grain boundaries (fig. 4*B*, *E*). Rotated garnet that is generally free of internal foliation occurs in one sample (20) of the metamorphic suite of the Ray Mountains.

Monoclinic kink bands (fig. 4*D*) occur only in fine-grained, quartz-rich rocks in the Devonian metaclastic sequence, some of which were previously interpreted as phyllonites (Dover and Miyaoka, 1985b). In subarea A, where they are best developed, the kink bands deform and have the same sense of shear as S_3 C-foliation.

Summary of Shear Sense

Shear and other structural data for the 26 samples analyzed are tabulated in table 2. Based on sample orientation, the dextral (clockwise) or sinistral (counterclockwise) sense of rotation or asymmetry of the shear indicators as viewed in thin section is converted to sense of shear relative to geographic coordinates in the last column of table 2.

DISCUSSION

Relation of Shear in Mylonitic Rocks to Movement of the Rampart Assemblage

Whether the Rampart assemblage represents an obducted sheet or a parautochthonous sequence, the regional extent and scale of its basal detachment and the intensity of

Criteria	Reference	Description	Sketch
S-C fabric	Berthe´ and others, 1979; Lister and Snoke, 1984; Ramsey and Huber, 1987, p. 632-633	A flattening (S) foliation and a shear (C) foliation that form obliquely to each other during shearing	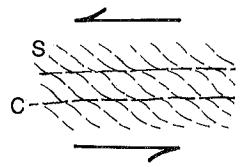
Asymmetric augen	Simpson and Schmid, 1983	Megacrysts, commonly of quartz, feldspar, or muscovite, that are deformed by shearing into a sigmoidal or lensoid shape	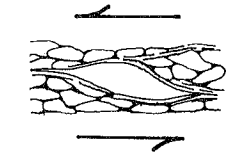
Rotated porphyroblasts	Ramsey and Huber, 1987, p. 632-633	Porphyroblasts, commonly of albite or garnet, that are rotated by shearing	
Asymmetric pressure shadows	Passchier and Simpson, 1986; Ramsey and Huber, 1987, p. 633	"Tails" or "wings" of fine-grained matrix material that form asymmetrically around a megacryst during shearing	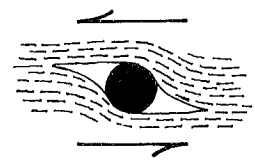
Monoclinal kink folds	Ramsey and Huber, 1987, p. 427-432; Paterson and Weiss, 1966	Asymmetric, angular folds with monoclinal fold axes. Folds combine to form monoclinal kink bands	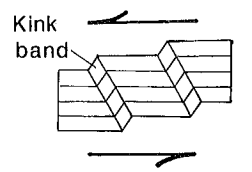

Figure 3. Descriptions of shear-sense criteria. Arrows indicate sense of relative shear; all sketches depict sinistral (counterclockwise) shear. Most sketches modified from Ramsey and Huber (1987).

deformation associated with it make it a feature that should be clearly expressed in the ductile microfabrics of the subjacent rocks. We infer a cause-and-effect relation between movement of the Rampart assemblage and the formation of the mylonites under it, based on (1) the concentrated distribution of mylonitic rocks subjacent to the Rampart contact, (2) the increase in intensity and degree of attenuation of mylonitic shearing toward the Rampart contact (Dover and

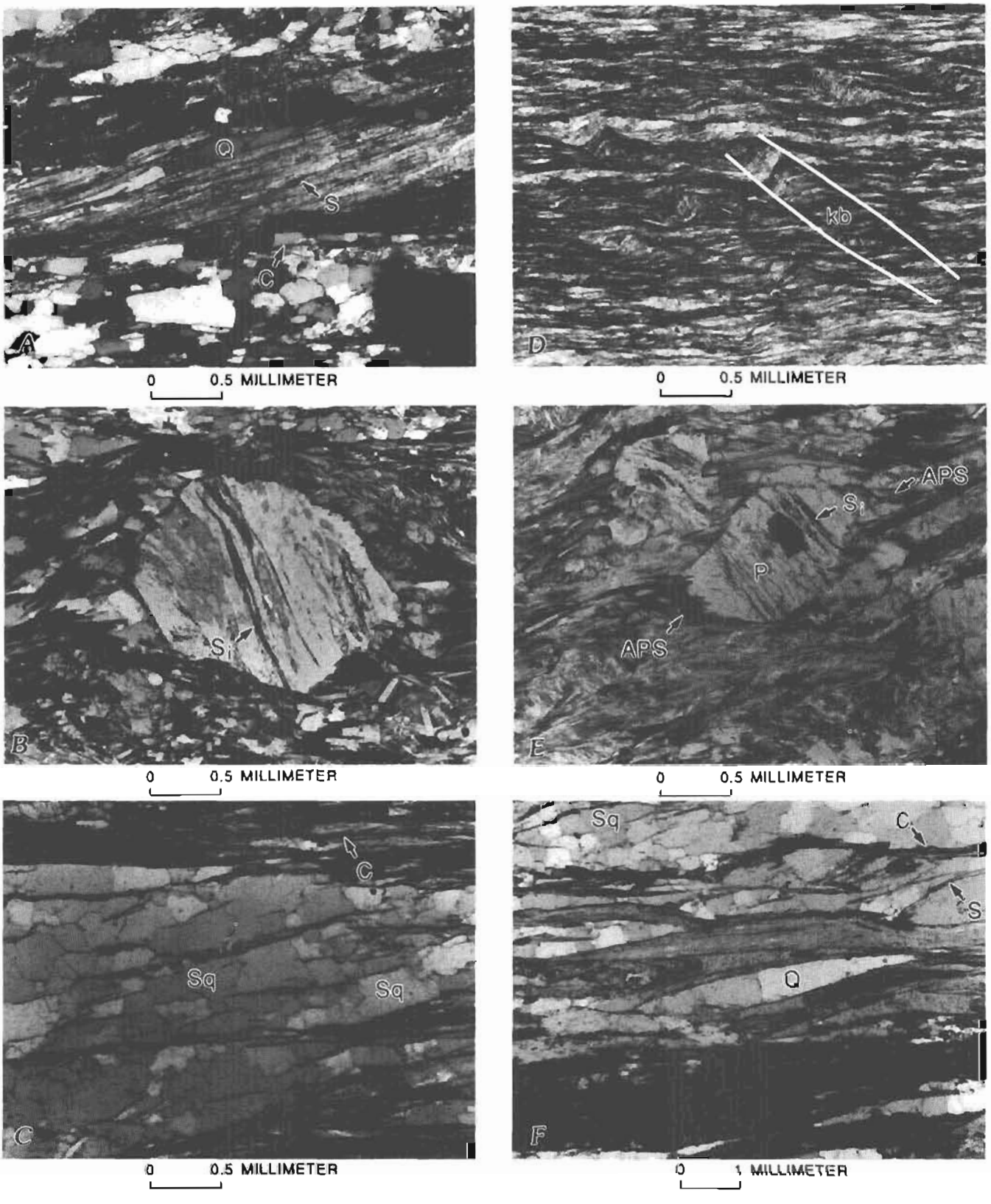

Miyaoka, 1985b; Moore and Murphy, 1989), and (3) the apparently gradational increases in degree of metamorphic recrystallization, metamorphic grade, and ductile deformation with structural depth within the inferred detachment zone. However, some blastomylonites are localized along lithologic contacts within the metamorphic suite of the Ray Mountains that may have been sheared during an earlier phase of its internal deformation.

Eastern Ray Mountains segment of the Rampart detachment zone

When restored to their pre-Tozitna fault positions, subareas A and D represent contiguous parts of the generally southeast-dipping basal Rampart detachment zone in the eastern Ray Mountains (fig. 5). The predominant asymmetry of S-C microfabric in 7 of the 11 samples in both subareas strongly indicates top-to-the-northwest (top-NW) up-dip movement for mylonitic rocks along this 60-km stretch of the detachment; this sense of shear supports mesoscopic S-C evidence for top-NW shear reported in subarea A by Dover and Miyaoka (1985b) and in subarea D by Smith and Puchner (1985). The abundance and consistency of S-C indicators in samples 4, 8, 9, and 18 (table 2) are particularly striking. Asymmetric augen in sample 6 also indicate a top-NW sense of shear. Six of the seven samples indicating top-NW shear are of mylonitic rocks from the Devonian metaclastic sequence. Conversely, four samples in subareas A and D have S-C fabrics indicating top-SE down-dip movement; samples 5 and 19 (table 2) have the most abundant and best developed examples. The reason for the difference in S-C shear sense in these samples compared with that in the other samples is uncertain, but we note that three of the four samples indicating top-SE shear, including samples 5 and 19, are from blastomylonitic rocks of the metamorphic suite of the Ray Mountains. Interpretation of these rocks may be complicated by an earlier generation of mylonitic fabric corresponding to S_1 of Dover and Miyaoka (1985b) or by reversals of asymmetry on the limbs of unrecognized internal folds. Also, these rocks are generally farther from the basal contact of the Rampart assemblage than the Devonian metaclastic sequence. For these reasons, we consider S-C fabric data from samples of the Devonian metaclastic sequence to be the more reliable indicator of Rampart movement, and we interpret that movement to have been up-dip reverse-slip and top-NW along this part of the detachment.

In two samples from the Devonian metaclastic sequence in subarea A (samples 4 and 6, table 2), rotated M_3 plagioclase porphyroblasts (RP) and kinks (K) indicate top-SE down-dip shear, opposite in direction from that indicated by S-C fabric in the same samples. The porphyroblasts occur in the contact aureole of the mid-Cretaceous Ray Mountains pluton. The top-SE down-dip movement that produced the rotated porphyroblasts is therefore attributed to a mid-Cretaceous or younger episode of normal-slip (S_3). This episode postdated the mid-Cretaceous or older reverse-slip event (S_2) represented by top-NW S-C fabric, which is locally incorporated as internal foliation within the porphyroblasts. Reactivation of the earlier mylonitic foliation during porphyroblast rotation might account for some inconsistency in the S-C shear data, but it generally was not of sufficient intensity to destroy the original S–C asymmetry. The change from reverse-slip to normal-slip movement evident in subarea A represents a change from contractional to extensional deformation. The normal-slip event may have been induced by regional extension, or alternatively, by thermal softening and uplift associated with emplacement of the Ray Mountains pluton in mid-Cretaceous time.

Yukon-Tozitna segment of the Rampart detachment zone

The northwest-dipping segment of the Rampart detachment zone in the area between the Yukon and Tozitna Rivers has a contractional tectonic style illustrated by the map distribution of prominent carbonate marker beds within the Devonian metaclastic sequence (fig. 6). Marker beds define major upright to southeast-overturned folds and north- to northwest-dipping ductile to semibrittle imbricate thrust faults. Regional dip, structural vergence, and local older-on-younger thrust displacements indicate top-SE tectonic transport for this segment of the Rampart detachment zone.

All eight samples from subareas B and C are from the Devonian metaclastic sequence, which in this area is of locally higher metamorphic grade and is more completely recrystallized than in subareas A and D. The trend of lineations (slip lines) varies within subarea C and between subareas B and C. We have no compelling explanation for this variation in trend, but dextral drag related to right-slip movement on the Tozitna fault may be involved.

◀ *Figure 4. Photomicrographs showing shear-sense indicators. See figure 2 for sample locations. A, S-C fabric having dextral shear; S, flattening(?) foliation; C, shear foliation. Note asymmetric shape of quartz aggregate (Q), also indicating dextral shear. Sample 11, crossed nicols. B, Albitic plagioclase porphyroblast containing internal foliation (S_i) oblique to subhorizontal external foliation, indicating dextral shear. Sample 14, plane light. C, Dynamically recrystallized quartz grains (Sq) having long axes oblique to shear foliation (C), indicating dextral shear. Sample 11, plane light. D, Monoclinic kink folds defining kink bands (kb), indicating sinistral shear. Sample 4, plane light. E, Albitic plagioclase porphyroblast (P) exhibiting three shear-sense criteria, all indicating dextral shear: asymmetric shape of porphyroblast, asymmetric pressure shadow (APS), and rotation of porphyroblast shown by discordance of internal foliation (S_i) and subhorizontal external foliation. Sample 14, plane light. F, Asymmetric quartz augen (Q), S-C fabric (S,C), and dynamically recrystallized quartz grains (Sq), all indicating dextral shear. Sample 11, plane light.*

The S-C fabric in seven out of the eight samples in subareas B and C indicates predominantly top-N, top-NW, or top-W down-dip movement. The most consistent S-C data are from samples 13, 14, and 16 (table 2). Asymmetric augen, although too sparse to be statistically significant, generally are consistent with the S-C fabric data. Sample 11 (table 2) contains S-C evidence for an opposite sense of top-S up-dip movement. Rotated plagioclase porphyroblasts are common in three samples within subarea B, and in the two samples giving consistent data (samples 12 and 14, table 2; fig. 4*B*, *E*), they indicate the same down-dip sense of shear as the S-C fabric. The plagioclase porphyroblasts are spatially related to a buried granitic pluton, inferred from a variety of contact-metamorphic effects like those produced by the Ray Mountains and Moran Dome plutons. These relations suggest that the rotation of plagioclase porphyroblast in subarea B represents the same episode of normal-slip as in subarea A, but if so, rotation was in an opposite sense along this opposing segment of the Rampart detachment. Based on (1) the close association of intense S-C shear and porphyroblast rotation (fig. 6), (2) the petrographic relation of S-C shear elements with rotated porphyroblasts, and (3) their coincidence in sense of shear, we interpret both the S-C fabric and porphyroblast rotation in subarea B to have developed during the same mid-Cretaceous or younger episode of normal slip.

The absence in subarea B of an S-C fabric equivalent of the mid-Cretaceous or older contractional episode of mylonitization identified in subareas A and D may be a consequence of the greater intensity in subarea B of the later

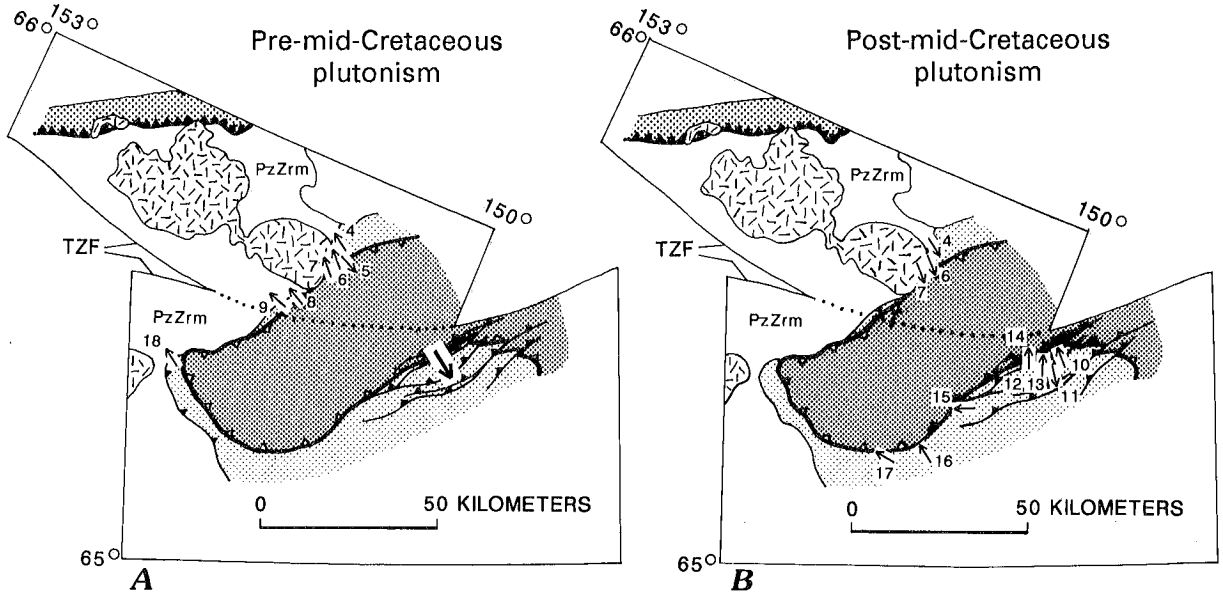

EXPLANATION

- Rampart assemblage of Dover and Miyaoka (1985a) (Tozitna terrane)
- Angayucham terrane
- Devonian metaclastic sequence
- PzZrm — Metamorphic suite of the Ray Mountains
- Granitic pluton (mid-Cretaceous)
- Contact
- Semiductile thrust fault
- Basal detachment of the Rampart assemblage of Dover and Miyaoka (1985a)
- Accretionary boundary
- TZF — Tozitna fault—Restored 50 km; restored position shown by dots
- 6↖ — Shear sense indicated by S-C fabric (in *A*) and by rotated albitic plagioclase porphyroblasts and (or) S-C fabric (in *B*)—Number refers to sample locality
- ↘ — Vergence of semiductile thrusts and folds

Figure 5. Direction of movement of structural top (arrow) determined for metaclastic samples in the basal detachment zone of the Rampart assemblage of Dover and Miyaoka (1985a). Movement arrows approximately located. Rampart assemblage restored to position prior to 50 km of right-slip movement on Tozitna fault (compare with fig. 2).

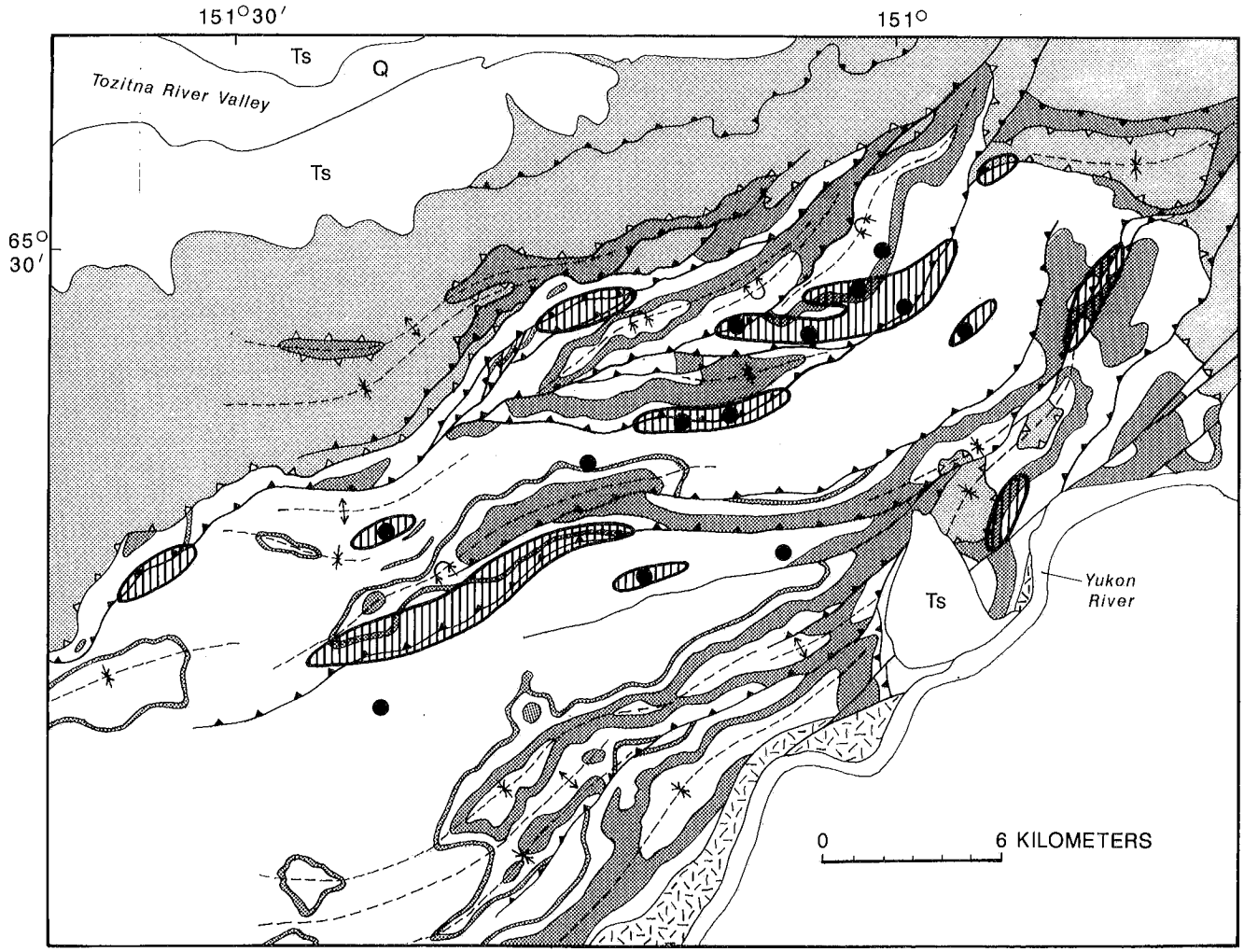

EXPLANATION

Q — Surficial deposits (Quaternary)

Ts — Sedimentary rocks (Tertiary)

Rampart assemblage of Dover and Miyaoka (1985a) (Jurassic to Mississippian)

Devonian metaclastic sequence

Metaclastic rocks

Carbonate beds

Granitic intrusive rocks (Tertiary and (or) Late Cretaceous)

Contact

Fault

Thrust fault—Sawteeth on upper plate

Basal detachment of the Rampart assemblage of Dover and Miyaoka (1985a)

Folds

Anticline

Syncline

Overturned anticline

Overturned syncline

Area of most intense mylonitic shearing

Rotated albitic plagioclase porphyroblast

Figure 6. Geologic map of Tozitna-Yukon segment of basal detachment zone of Rampart assemblage of Dover and Miyaoka (1985a) showing distribution of rotated porphyroblasts and areas of most intense mylonitic shear relative to mapped semiductile thrust faults (from Dover, 1990, and unpub. data).

normal-slip event. A less likely alternative is that some part of the S-C fabric in subarea B corresponds to the first (contractional) episode of mylonitization in subareas A and D, but is indistinguishable here because it has the same top-N or top-NW sense of shear as the normal-slip event. The latter interpretation conflicts with strong mesoscopic and map evidence in subarea B for contractional deformation having a top-SE direction of tectonic transport. There would be no conflict if the mesoscopic features represent a separate and younger deformational event than that which produced the microfabric structures, but there is no evidence to support this. On the contrary, the ductile to semibrittle conditions under which the mesoscopic deformation occurred are consistent with those represented by the microfabrics, and southeast-directed thrust zones, although they are locally crosscutting, appear in places to merge gradationally with mylonitic foliation. Also, the rotated plagioclase porphyroblasts and intense mylonitic shear, which indicate top-N normal-slip and which constitute the latest recognizable microfabrics, are localized along mapped thrust zones (fig. 6). Therefore, we interpret these thrust zones to predate porphyroblast rotation and normal slip and to have an age comparable with contractional deformation in the eastern Ray Mountains, but an up-dip sense of shear in the opposite direction.

On the western flank of the Ray Mountains, lineation and shear indicators in blastomylonitic schist in the metamorphic suite of the Ray Mountains are consistent in indicating a top-SW sense of shear (sample 20, table 2). Although sparse and subject to the same interpretive questions raised by blastomylonite samples from the metamorphic suite of the Ray Mountains in subareas A and D, these data are compatible with the generally south to southeastward transport inferred for the overlying Kanuti ophiolite in this area by Patton and others (1977, 1989). The tectonic significance of the sparse microfabric data of sample 21 (table 2), from an isolated locality south of the Kaltag fault, is unknown.

Interpretive Models

Three possible interpretions relating to previously proposed tectonic models are considered below, based on our shear-sense data and the concept that the bulk of the data reflect movement of the Rampart assemblage.

1. One possibility is that the top-N or top-NW sense of shear indicated by the predominance of S-C, asymmetric augen, and asymmetric pressure shadow data in all subareas represents major north- to northwest-directed transport of the Rampart assemblage. In this case, the up-dip or down-dip sense of shear would merely reflect the local direction of dip of the detachment zone, as determined by synclinal folding of the Rampart allochthon after its emplacement. Rotation of plagioclase porphyroblasts would be attributed to a later, normal-slip event in which either the original mylonitic foliation was reactivated, or a new one was formed by down-dip movement inward toward the synclinal core of the Rampart belt along its two opposing flanks. However, this model is not consistent with observations along the southeast segment of the basal Rampart detachment, where S-C shearing is interpreted to be a normal-slip rather than contractional feature, and where earlier, top-SE contractional shear, as indicated by mesoscopic folds and thrusts, is opposite that of apparently coeval compressional S-C microfabrics in subarea A.

2. The possibility that S-C and related fabrics reflect generally southeastward obduction of the Rampart assemblage from a root zone in the Koyukuk basin now marked by the Kanuti ophiolite seems precluded by mesoscopic and microfabric evidence for top-N and top-NW compressional shear in the eastern Ray Mountains segment of the Rampart detachment zone. Although top-SE down-dip shear is indicated by rotated M_3 plagioclase porphyroblasts and S_3 shear along the same segment, this late-intrusive to postintrusive episode of shear cannot be related to the same deformational event that emplaced the Kanuti, because that emplacement predated mid-Cretaceous intrusion (Patton, 1984; Dover and Miyaoka, 1985a). Also, rotated porphyroblasts give an opposite, top-NW shear sense along the Yukon-Tozitna part of the Rampart detachment. Obduction of the Kanuti ophiolite probably occurred as a result of plate convergence at the present boundary between the Koyukuk basin and Ruby geanticline and was likely accompanied by metamorphism and magmatism within the Ruby geanticline. We speculate that obduction of the Kanuti was limited to the west margin of the Ruby geanticline, was synmetamorphic, and is most likely represented by S_1 (and S_2?) blastomylonites and ductile deformation within the metamorphic suite of the Ray Mountains. In contrast, S_2 and S_3 mylonites in the Devonian metaclastic sequence appear to reflect slightly later (latest metamorphic), two-stage movement of the Rampart assemblage.

3. Our preferred interpretation is that the Devonian metaclastic sequence underwent two distinct episodes of shear, both having opposite senses of shear on the two opposing segments of the basal Rampart detachment zone. The first was a mid-Cretaceous or older contractional episode whereby the Rampart assemblage was thrust up-dip to the northwest, toward the crest of the present Ruby geanticline, along the eastern Ray Mountains segment of the detachment, and up-dip in the opposite (south or southeast) direction along the Yukon-Tozitna segment. Evidence for this event is best expressed by microfabric evidence along the eastern Ray Mountains segment and by mesoscopic and map evidence along the Yukon-Tozitna segment. The second episode of shear, as in possibility 1, was mid-Cretaceous or younger normal slip inward toward the Rampart assemblage along the two opposing segments of the detachment zone. However, in this model, normal slip is interpreted to have been opposite the original up-dip sense of movement along

both flanks, as would occur along the inward-dipping flanks of a basin that was initially compressed and later underwent subsidence or extension.

CONCLUSIONS

1. Mylonitic rocks in the Devonian metaclastic sequence subjacent to the base of the Rampart assemblage of east-central Alaska represent a broad detachment zone that reflects movement of the Rampart relative to its substrate. Blastomylonites in the metamorphic suite of the Ray Mountains appear to have more complex internal fabrics that are regarded as less reliable indicators of movement of the Rampart assemblage.

2. The most consistent and reliable of the microfabric data from the detachment zone indicate two episodes of ductile to semiductile movement, a compressive one of mid-Cretaceous or older age represented mainly by S-C and related fabric elements, and an episode of mid-Cretaceous or younger normal-slip represented mainly by rotated porphyroblasts generated by mid-Cretaceous granitic plutons.

3. Variations in sense of shear indicated by our data are difficult to reconcile with models of major unidirectional transport of the Rampart assemblage. When integrated with mesoscopic and map evidence, the microfabric data seem most compatible with the concept that the Rampart assemblage originated in a rift basin that underwent mid-Cretaceous or older contraction, when the Rampart was thrust relatively short distances in opposite directions over its opposing margins, and mid-Cretaceous or younger extension, when the basin margin detachments were reactivated as zones of normal slip.

REFERENCES CITED

Bell, T.H., 1978, Progressive deformation and reorientation of fold axes in a ductile mylonite zone—The Woodroffe thrust: Tectonophysics, v. 44, p. 285-320.

Berthé, D., and Brun, J.P., 1980, Evolution of folds during progressive shear in the South Amorican Shear Zone, France: Journal of Structural Geology, v. 2, p. 127-133.

Berthé, D., Choukroune, P., and Jegouzo, P., 1979, Orthogneiss, mylonite and non-coaxial deformation of granites: The example of the South Amorican Shear Zone: Journal of Structural Geology, v. 1, p. 31-42.

Brosgé, W.P., Lanphere, M.A., Reiser, H.N., and Chapman, R.M., 1969, Probable Permian age of the Rampart Group, central Alaska: U.S. Geological Survey Bulletin 1294-B, 18 p.

Chapman, R.M., Yeend, Warren, Brosgé, W.P., and Reiser, H.N., 1982, Reconnaissance geologic map of the Tanana quadrangle, Alaska: U.S. Geological Survey Open-File Report 82-734, scale 1:250,000.

Coney, P.J., 1983, Structural and tectonic aspects of accretion in Alaska, *in* Howell, D.G., Jones, D.L., Cox, Allan, and Nur, Amos, eds., Proceedings of the circum-Pacific terrane conference: Stanford, California, Stanford University Publications, p. 68-70.

Coney, P.J., and Jones, D.L., 1985, Accretion tectonics and crustal structure in Alaska: Tectonophysics, v. 119, p. 265-283.

Dover, J.H., 1990, Geology of east-central Alaska: U.S. Geological Survey Open-File Report 90-289, 66 p.

Dover, J.H., and Miyaoka, R.T., 1985a, Major rock packages of the Ray Mountains, Tanana and Bettles quadrangles, *in* Bartsch- Winkler, Susan, and Reed, K.M., eds., The United States Geological Survey in Alaska—Accomplishments during 1983: U.S. Geological Survey Circular 945, p. 32-36.

——— 1985b, Metamorphic rocks of the Ray Mountains—Preliminary structural analysis and regional tectonic implications: U.S. Geological Survey Circular 945, p. 36-38.

Gemuts, I., Steffel, C.I., and Puchner, C.C., 1983, Regional geology and tectonic history of western Alaska: Journal of the Alaska Geological Society, v. 3, p. 67-85.

Jones, D.L., Silberling, N.J., Coney, P.J., and Plafker, George, 1987, Lithotectonic terrane map of Alaska (west of the 141st meridian), *in* Silberling, N.J., and Jones, D.L., eds., Lithotectonic terrane maps of the North American Cordillera: U.S. Geological Survey Miscellaneous Field Studies Map MF-1874A, one sheet, scale 1:2,500,000.

Lister, G.S., and Snoke, A.W., 1984, S-C mylonites: Journal of Structural Geology, v. 6, p. 617-638.

Miyaoka, R.T., and Dover, J.H., 1985, Preliminary study of shear sense in mylonites, eastern Ray Mountains, Tanana quadrangle, *in* Bartsch-Winkler, Susan, ed., The United States Geological Survey in Alaska—Accomplishments during 1984: U.S. Geological Survey Circular 967, p. 29-32.

Moore, T.E., and Murphy, J.M., 1989, Nature of the basal contact of the Tozitna terrane along the Dalton Highway, northeast Tanana quadrangle, Alaska, *in* Dover, J.H., and Galloway, J.P., eds., Geologic studies in Alaska by the U.S. Geological Survey, 1988: U.S. Geological Survey Bulletin 1903, p. 46-53.

Passchier, C.W., and Simpson, Carol, 1986, Porphyroclast systems as kinematic indicators: Journal of Structural Geology, v. 8, p. 831-843.

Paterson, M.S., and Weiss, L.E., 1966, Experimental deformation and folding in phyllite: Geological Society of America Bulletin, v. 77, p. 343-374.

Patton, W.W., Jr., 1984, Timing of arc collision and emplacement of oceanic crustal rocks on the margins of the Yukon-Koyukuk basin, western Alaska: Geological Society of America Abstracts with Programs, v. 16, no. 5, p. 328.

Patton, W.W., Jr.,and Box, S.E., 1989, Tectonic setting of the Yukon-Koyukuk basin and its borderlands, western Alaska: Journal of Geophysical Research, v. 94, no. B11, p. 15,807-15,820.

Patton, W.W., Jr., Box, S.E., and Grybeck, Donald, 1989, Ophiolites and other mafic-ultramafic complexes in Alaska: U.S. Geological Survey Open-File Report 89-648.

Patton, W.W., Jr., Stern, T.W., Arth, J.G., and Carlson, Christine, 1987, New U/Pb ages from granite and granitic gneiss in the Ruby geanticline and southern Brooks Range, Alaska: Journal of Geology, v. 95, p. 118-126.

Patton, W.W., Jr., Tailleur, I.L., Brosgé, W.P., and Lanphere, M.A., 1977, Preliminary report on the ophiolites of northern and western Alaska, *in* Coleman, R.G., ed., North American ophiolites: Oregon Department of Geology and Mineral In-

dustries Bulletin, no. 95, p. 51-57.
Ramsey, J.G., and Huber, M.I., 1987, The techniques of modern structural geology, Volume 2—Folds and fractures: New York, Academic Press, p. 632-633.
Simpson, Carol, and Schmid, S.M., 1983, An evaluation of criteria to deduce the sense of movement in sheared rocks: Geological Society of America Bulletin v. 94, p. 1281-1288.
Smith, G.M., and Puchner, C.M., 1985, Geology of the Ruby geanticline between Ruby and Poorman, Alaska, and the tectonic emplacement of the Ramparts Group: Eos (American Geophysical Union Transactions), v. 66, no. 46, p. 1102.
Williams, G.D., 1978, Rotation of contemporary folds into the x-direction during overthrust processes in Laksefjord, Finland: Tectonophysics, v. 48, p. 29-40.

Reviewers: Dwight C. Bradley and Jack Y. Bradshaw

Petroleum Source Potential and Thermal Maturity of the Tertiary Usibelli Group of Suntrana, Central Alaska

By Richard G. Stanley, Hugh McLean, *and* Mark J. Pawlewicz

Abstract

Results from Rock-Eval pyrolysis and vitrinite reflectance show that nonmarine mudstones and coals in outcrops of the Usibelli Group at Suntrana are potential sources of oil and gas and are thermally immature to marginally mature with respect to the oil window. Calculations based on borehole temperatures and gravity data suggest that the most deeply buried parts of the Usibelli Group in the middle Tanana basin may have reached temperatures high enough to generate petroleum.

INTRODUCTION

The Tertiary Usibelli Group (Wahrhaftig, 1987) is a sequence of coal-bearing nonmarine sedimentary rocks that crops out widely in the Nenana coal field of the northern foothills of the Alaska Range (fig. 1). The Usibelli Group is also present in the subsurface of the middle Tanana basin, where it has been penetrated by two exploratory wells (both dry holes), the Union Nenana No. 1 and the ARCO Totek Hills No. 1 (fig. 1). Coals and mudstones of the Usibelli Group have long been suspected as possible source rocks of petroleum, but published geochemical information is available only for two of the five formations in the Usibelli Group (Stanley, 1987, 1988). The purpose of this paper is to present the results and implications of a detailed study, using Rock-Eval pyrolysis and vitrinite reflectance, of the petroleum source potential of all five formations of the Usibelli Group in its type section at Suntrana (fig. 1). This new information, combined with available borehole and gravity data, raises the possibility that hydrocarbons have been generated in the deepest parts of the middle Tanana basin.

STRATIGRAPHIC AND SEDIMENTOLOGIC SETTING

The Usibelli Group at Suntrana is about 585 m thick and consists of about 64 percent conglomerate and sandstone, 23 percent mudstone, and 13 percent coal. The group is divided into five formations; in ascending stratigraphic order these are the Healy Creek, Sanctuary, Suntrana, Lignite Creek, and Grubstake Formations (table 1). Fossil plant leaves and pollen indicate that the Usibelli Group at Suntrana is entirely of Miocene age, although elsewhere in the Nenana coal field it is as old as Eocene (Wahrhaftig and others, 1969; Csejtey and others, 1986). The Usibelli Group rests nonconformably on Precambrian or Paleozoic metamorphic rocks of the Birch Creek Schist of former usage (Wahrhaftig, 1968, 1970), which are interpreted to be part of the Yukon-Tanana terrane (Silberling and Jones, 1984). The Usibelli Group is unconformably overlain by the Miocene and Pliocene Nenana Gravel, which represents a series of coalescing alluvial fans that developed on the north side of the Alaska Range as it rose during late Miocene and Pliocene time (Wahrhaftig, 1987).

The Healy Creek, Suntrana, and Lignite Creek Formations consist mainly of repeated fining-upward sequences of conglomerate, sandstone, mudstone, and coal that were deposited by a variety of fluvial systems ranging from braided and low-sinuosity bedload streams to high-sinuosity (meandering), mixed bedload and suspended-load streams (Buffler and Triplehorn, 1976; Stanley and others, 1989). During much of Eocene, Oligocene, and Miocene time, these streams flowed south across the site of the Alaska Range (which then did not exist) toward the Gulf of Alaska (Wahrhaftig, 1987).

Of importance to this study are the depositional environments of the coals and mudstones (table 2). Petrologic studies by Merritt (1985) indicate that most of the coals formed from woody tree-vegetation peats that accumulated in poorly drained forest-moor swamps. Some of the coals in the Lignite Creek Formation may have formed under slightly drier conditions than those in the rest of the Usibelli Group (Merritt, 1985).

Mudstones of fluvial origin in the Healy Creek, Suntrana, and Lignite Creek Formations are divided among three environmental categories in table 2. A single mudstone sample was collected from a clast in a conglomerate bed near the base of the Suntrana Formation. Ten mudstone samples were collected from lenticular, channel-form beds with sharp lower contacts and are interpreted as abandoned channel deposits (Stanley and others, 1989). The remaining mudstone samples are lumped into the general category of overbank

deposits and probably represent quiet-water deposition of muddy sediment in ponds, swales, marshes, and swamps on flood plain areas away from major active channels.

The Sanctuary and Grubstake Formations consist mainly of mudstone and fine sandstone that accumulated in large, shallow lakes (Wahrhaftig and others, 1969; Wahrhaftig, 1987). Mudstones of lacustrine origin in the Sanctuary and Grubstake Formations (table 2) are laterally persistent, finely laminated to bioturbated, commonly siderític, and occur interbedded with thin, normally graded beds of fine sandstone that we interpret as turbidity current deposits. In addition, mudstones in the Grubstake Formation contain abundant tests of *Melosira granulata*, a freshwater diatom (Hideyo Haga, Micropaleo Consultants, Inc., written commun., 1985).

METHODS

Eighty-six rock samples (36 coals and 50 mudstones) were collected from a measured stratigraphic section in outcrops of the Usibelli Group in its type section at Suntrana. The section was measured with a Jacob's staff. Generally, one sample was collected from each bed of coal and each unbroken interval of mudstone. The rock samples were taken from about 10 cm to 50 cm back from the outcrop faces in order to obtain the freshest available material and transported to the laboratory in sealed plastic bags to prevent contamination. All 86 samples were analyzed using Rock-Eval pyrolysis, and 49 of these were examined for vitrinite reflectance, in the laboratories of the U.S. Geological Survey, Branch of Petroleum Geology, in Denver, Colorado. The results are shown in table 2 and summarized in table 3.

Rock-Eval pyrolysis is a widely used method of rapidly evaluating the quality and thermal maturity of prospective petroleum source rocks (Tissot and Welte, 1984; Peters, 1986). The procedure mimics the natural hydrocarbon-generation processes which occur at much slower rates within the earth when sediments containing kerogen (sedimentary organic matter) are buried progressively deeper and subjected to higher temperatures (Waples, 1985). Pulverized samples of rock are gradually heated from 300 °C to 550 °C at 25 °C per minute in an oxygen-free atmosphere, causing the release of water, carbon dioxide, and hydrocarbons from the rock. Several parameters are measured automatically by the Rock-Eval apparatus (table 2). The quantity S1 is the

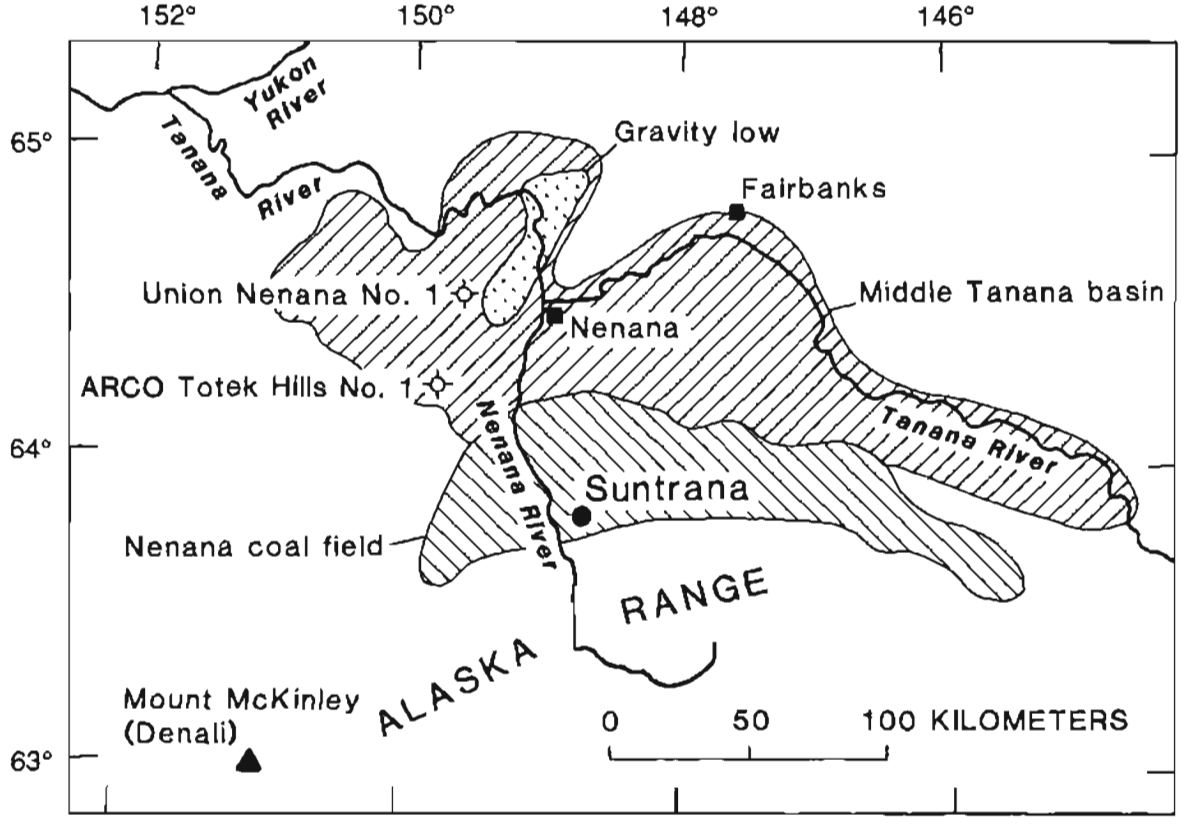

Figure 1. Index map showing location of type section for the Usibelli Group at Suntrana, exploratory oil wells, Nenana coal field (from Merritt and Hawley, 1986), and middle Tanana basin (from Miller and others, 1959). Bouguer gravity low ranges from -35 to -55 mGal and corresponds to deepest part of middle Tanana basin (Barnes, 1961).

Table 1. Generalized stratigraphy at Suntrana

Unit	Age	Thickness (meters)	Major rock types (Approx. relative percent)	Depositional setting
Nenana Gravel	Miocene and Pliocene	1,040	Sandstone and conglomerate (100)	Alluvial fan
Usibelli Group				
Grubstake Formation	Upper Miocene	27	Mudstone (80),sandstone (20)	Lacustrine
Lignite Creek Formation	Upper and middle Miocene	179	Coal (4), mudstone (26), sandstone and conglomerate (70)	Fluvial
Suntrana Formation	Middle Miocene	210	Coal (16), mudstone (11), sandstone and conglomerate (73)	Fluvial
Sanctuary Formation	Middle Miocene	33	Mudstone (85),sandstone (15)	Lacustrine
Healy Creek Formation	Middle and lower Miocene	136	Coal (25), mudstone (12), sandstone and conglomerate (63)	Fluvial
Birch Creek Schist [1]	Precambrian or Paleozoic	Unknown	Quartz-mica schist (100)	(Metamorphic)

[1]of former usage.

amount of hydrocarbons (HC), measured in milligrams HC per gram of rock, that is released upon initial heating to 300 °C; this quantity includes the gas and oil already present in the rock. The quantity S2 (also measured in milligrams HC per gram of rock) is the amount of hydrocarbons generated by pyrolytic degradation of the remaining organic matter in the rock and is an indicator of the potential of the rock to generate additional oil and gas. Tmax is the temperature—generally about 400 °C to 500 °C—at which S2 is at a maximum and is regarded as a rough indicator of thermal maturity. S3 is the amount of carbon dioxide (in milligrams of CO_2 per gram of rock) generated during pyrolysis and is thought to be related to the amount of oxygen in the pyrolyzed organic matter. Additional Rock-Eval parameters include the total organic carbon (TOC) in weight percent; the hydrogen index (HI), defined as the product 100(S2/TOC); and the oxygen index, defined as the product 100(S3/TOC).

Vitrinite reflectance (Ro) is a common method of determining thermal maturity and is obtained by measuring the percentage of light reflected by vitrinite, a type of kerogen formed from woody terrestrial plant material (Tissot and Welte, 1984; Waples, 1985).

QUANTITY OF ORGANIC MATTER

The quantity of organic matter in the samples is indicated by the TOC (total organic carbon, in weight percent) and the quantities S1 and S2. All of the coal samples and all but seven of the mudstone samples have TOC greater than or equal to 0.5 percent (table 1), which generally is regarded as the lower limit for potential source rocks of petroleum (Tissot and Welte, 1984).

Not surprisingly, the values of TOC, S1, and S2 are generally higher for coals than for mudstones (table 3). The TOC of the coals ranges from 2.32 to 66.04 percent, showing that all have very good hydrocarbon generative potential according to the classification of Peters (table 4). The TOC of the mudstones ranges from about 0.05 to 26.45 percent; about half of the mudstones have TOC greater than 1 percent, indicating good to very good generative potential (table 4). TOC in both coals and mudstones can be significantly reduced by outcrop weathering (Leythaeuser, 1973; Clayton and Swetland, 1978; Stanley, 1987); therefore, the TOC results from the outcrops at Suntrana (table 2) should be regarded as minimum values.

Values of S1 are higher than 0.5 for 28 of the 36 coal samples, indicating fair to very good generative potential. However, all but 4 of the 50 mudstone samples exhibit S1 less then 0.5, indicating poor generative potential. Values of S2 greater than 2.5 and indicating fair to very good generative potential are shown by all but two of the coals and about half of the mudstones. The reasons for the generally low values of S1 and S2 may be related to (1) surface weathering of the sampled outcrops, (2) initially poor generative potential due to a large proportion of woody (humic) and oxidized (inertinitic) kerogens, and (3) interference by mineral matrix, including adsorption on clay minerals of the hydrocarbons produced during pyrolysis (Peters, 1986; Stanley, 1987).

Table 2. Rock-Eval and vitrinite reflectance (Ro) data from the Usibelli Group at Suntrana

[Rock-Eval parameters are discussed in the text. mdst = mudstone]

Sample number	Formation	Meters above base[1]	Rock type	Depositional environment	Sample weight (mg)	TOC (wt. pct.)	S1 (mg HC/ g rock)	S2 (mg HC/ g rock)	S3 (mg CO_2/ g rock)	S2/S3	HI	OI	Tmax (°C)	Mean Ro (percent)[2]
86	Grubstake	579.1	mdst	Lake	198.0	0.77	0.02	0.35	3.39	0.10	45	440	422	0.32
85	Grubstake	577.5	mdst	Lake	179.9	.86	.01	.37	3.37	.10	43	391	423	
84	Grubstake	574.6	mdst	Lake	180.6	.84	.01	.39	3.89	.10	46	463	413	.29
83	Grubstake	570.5	mdst	Lake	135.2	.67	0	.23	3.90	.05	34	582	417	
82	Grubstake	569.4	mdst	Lake	58.1	.62	.03	.30	3.58	.08	48	577		.31
81	Grubstake	566.0	mdst	Lake	82.4	.67	0	.23	3.15	.07	34	470	420	.30
80	Grubstake	562.8	mdst	Lake	155.0	.56	0	.16	5.26	.03	28	939		
79	Grubstake	561.1	mdst	Lake	93.4	.47	.01	.11	5.56	.01	23	1,183		
78	Grubstake	559.6	mdst	Lake	100.8	.50	.02	.30	9.04	.03	60	1,808	407	
77	Grubstake	558.1	mdst	Lake	128.4	.74	0	.36	.73	.49	48	98	398	.30
76	Lignite Creek	557.9	coal	Coal swamp	11.7	21.63	4.78	77.94	18.11	4.30	360	83	427	.29
75	Lignite Creek	557.2	coal	Coal swamp	5.9	25.72	9.66	119.32	25.08	4.75	463	97	415	.24
74	Lignite Creek	523.7	coal	Coal swamp	23.2	8.23	.47	11.12	7.41	1.50	135	90	426	.23
73	Lignite Creek	519.1	mdst	Overbank	84.0	.77	.04	1.08	1.14	.94	140	148	429	
72	Lignite Creek	516.5	mdst	Overbank	60.7	4.38	.31	10.41	3.36	3.09	237	76	432	
71	Lignite Creek	515.5	coal	Coal swamp	10.4	35.02	3.75	90.76	25.00	3.63	259	71	407	.25
70	Lignite Creek	515.2	mdst	Overbank	154.3	.84	.04	.61	.94	.64	72	111	420	
69	Lignite Creek	512.1	coal	Coal swamp	6.6	20.24	2.27	42.72	28.48	1.50	211	140	420	.24
68	Lignite Creek	510.8	mdst	Uncertain	163.9	.25	0	.06	6.73	0	24	2,692		
67	Lignite Creek	469.6	coal	Coal swamp	5.4	26.16	3.88	51.85	24.81	2.08	198	94	427	.25
66	Lignite Creek	467.5	mdst	Uncertain	23.4	3.55	.55	9.31	3.24	2.87	262	91	437	
65	Lignite Creek	452.6	coal	Coal swamp	11.9	28.42	3.02	55.12	25.21	2.18	193	88	419	.27
64	Lignite Creek	451.7	mdst	Overbank	135.0	.45	.01	.20	.58	.34	44	128	420	
63	Lignite Creek	450.4	coal	Coal swamp	26.1	15.33	.49	21.30	17.16	1.24	138	111	421	.29
62	Lignite Creek	449.9	mdst	Overbank	121.4	.94	.01	.51	1.15	.44	54	122	424	
61	Lignite Creek	447.7	coal	Coal swamp	7.4	29.20	1.62	78.37	34.59	2.26	268	118	414	.30
60	Lignite Creek	446.9	mdst	Overbank	8.5	9.27	.58	16.35	14.58	1.12	176	157	430	
59	Lignite Creek	423.2	coal	Coal swamp	11.8	28.51	1.77	50.84	31.18	1.63	178	109	423	.27
58	Lignite Creek	422.6	mdst	Aban. channel	91.1	4.95	.32	12.29	4.56	2.69	248	92	426	
57	Lignite Creek	409.5	mdst	Overbank	30.3	3.96	.92	13.99	5.01	2.79	353	126	429	
56	Lignite Creek	408.1	coal	Coal swamp	4.4	45.47	1.59	71.81	46.36	1.54	157	101	409	.27
55	Lignite Creek	406.6	mdst	Overbank	143.0	.38	.02	.19	1.09	.17	50	286		

Table 2. Continued

Sample number	Formation	Meters above base[1]	Rock type	Depositional environment	Sample weight (mg)	TOC (wt. pct.)	S1 (mg HC/ g rock)	S2 (mg HC/ g rock)	S3 (mg CO_2/ g rock)	S2/S3	HI	OI	Tmax (°C)	Mean Ro (percent)[2]
54	Lignite Creek	405.2	coal	Coal swamp	3.6	30.02	.83	56.66	42.22	1.34	188	140	419	.23
53	Lignite Creek	404.8	mdst	Aban. channel	188.4	1.72	.14	2.12	1.74	1.21	123	101	425	
52	Suntrana	377.2	coal	Coal swamp	5.9	52.90	4.57	127.45	45.42	2.80	240	85	407	.30
51	Suntrana	375.5	mdst	Overbank	123.0	1.36	0	.49	1.78	.27	36	130	423	
50	Suntrana	374.9	coal	Coal swamp	5.3	51.37	.56	61.88	43.77	1.41	120	85	385	.32
49	Suntrana	374.4	mdst	Aban. channel	158.4	.56	.01	.31	.79	.39	55	141	416	
48	Suntrana	356.1	coal	Coal swamp	4.6	39.40	1.30	52.6	40.86	1.28	133	103	412	.33
47	Suntrana	355.1	mdst	Overbank	148.5	1.05	.02	.69	1.21	.57	65	115	418	
46	Suntrana	353.1	coal	Coal swamp	2.7	41.38	.74	52.96	49.62	1.06	127	119	411	.29
45	Suntrana	352.5	mdst	Overbank	141	1.95	.11	2.83	1.78	1.58	145	91	420	
44	Suntrana	348.8	coal	Coal swamp	2.7	51.44	1.48	57.03	49.62	1.14	110	96	405	.18
43	Suntrana	297.7	coal	Coal swamp	4.9	48.81	1.22	69.38	41.63	1.66	142	85	409	.24
42	Suntrana	296.9	mdst	Overbank	179.5	1.23	.01	.44	3.69	.11	35	300	421	
41	Suntrana	295.4	coal	Coal swamp	3.8	47.67	.26	38.94	41.57	.93	81	87	418	.24
40	Suntrana	294.6	mdst	Overbank	160.4	2.43	.18	4.23	2.49	1.69	174	102	420	
39	Suntrana	252.1	coal	Coal swamp	4.4	62.48	82.72	123.63	50.00	2.47	197	80	406	.34
38	Suntrana	246.9	mdst	Aban. channel	195.4	.05	.01	.06	.08	.75	120	160		
37	Suntrana	245.2	mdst	Aban. channel	186.0	.15	.01	.06	.19	.31	40	126		
36	Suntrana	214.3	coal	Coal swamp	3.7	61.30	2.16	24.05	43.78	.54	39	71	431	.49
35	Suntrana	212.3	mdst	Aban. channel	141.7	.05	0	.01	.14	.07	20	280		
34	Suntrana	206.2	coal	Coal swamp	4.7	49.51	1.06	93.61	56.17	1.66	189	113	418	.36
33	Suntrana	193.8	coal	Coal swamp	9.3	50.48	2.79	85.16	35.26	2.41	168	69	413	
32	Suntrana	193.6	coal	Coal swamp	4.1	42.29	.97	56.09	44.87	1.25	132	106	415	.33
31	Suntrana	170.4	coal	Clast in cgl.	4.1	59.76	.48	56.09	31.70	1.76	93	53	427	
30	Suntrana	169.4	coal	Clast in cgl.	27.5	15.63	.14	12.07	11.92	1.01	77	76	428	
29	Suntrana	168.5	mdst	Clast in cgl.	8.5	26.45	.58	34.11	19.76	1.72	128	74	427	
28	Sanctuary	164.8	mdst	Lake	106.5	2.19	0	.83	2.62	.31	37	119	439	.32
27	Sanctuary	160.3	mdst	Lake	113.7	1.62	0	.74	2.25	.32	45	138	433	.33
26	Sanctuary	156.8	mdst	Lake	115.1	1.84	0	.91	2.64	.34	49	143	433	.31
25	Sanctuary	149.9	mdst	Lake	163.0	.86	0	.26	1.93	.13	30	224	425	
24	Sanctuary	149.4	mdst	Lake	185.0	.88	0	.26	2.31	.11	29	262	421	
23	Sanctuary	143.4	mdst	Lake	132.3	1.01	0	.47	3.86	.12	46	382	428	.34
22	Sanctuary	139.8	mdst	Lake	144.8	.91	0	.33	3.97	.08	36	436	425	.36

Table 2. Continued

Sample number	Formation	Meters above base[1]	Rock type	Depositional environment	Sample weight (mg)	TOC (wt. pct.)	S1 (mg HC/ g rock)	S2 (mg HC/ g rock)	S3 (mg CO_2/ g rock)	S2/S3	HI	OI	Tmax (°C)	Mean Ro (percent)[2]
21	Sanctuary	136.2	mdst	Lake	95.8	1.40	.02	.83	8.68	.09	59	620	434	.33
20	Healy Creek	133.2	coal	Coal swamp	6.6	59.02	1.06	110.30	32.72	3.37	186	55	413	.37
19	Healy Creek	131.2	mdst	Uncertain	120.9	3.76	.19	15.21	1.42	.71	404	37	427	.32
18	Healy Creek	120.8	coal	Coal swamp	3.3	48.38	.30	85.45	26.66	3.20	176	55	417	.37
17	Healy Creek	119.8	mdst	Overbank	160.3	3.91	.06	5.88	1.84	3.19	150	47	420	.34
16	Healy Creek	116.8	mdst	Uncertain	129.4	1.18	.02	.58	2.96	.19	49	250	429	(.43)
15	Healy Creek	112.5	mdst	Uncertain	116.7	.71	0	.03	.35	.08	4	49		(1.04)
14	Healy Creek	111.7	coal	Coal swamp	3.6	66.04	.55	5.55	15.55	.35	8	23	552	(1.47)
13	Healy Creek	103.7	coal	Coal swamp	97.8	2.32	.01	.06	28.79	0	2	1,240		(1.13)
12	Healy Creek	101.5	coal	Coal swamp	77.6	13.12	.01	.73	24.32	.03	5	185	523	(2.72)
11	Healy Creek	89.5	coal	Coal swamp	3.0	56.97	1.0	112.00	56.66	1.97	196	99	416	.36
10	Healy Creek	82.0	mdst	Uncertain	182.7	1.42	.01	1.06	.44	2.40	74	30	430	.34
9	Healy Creek	77.7	coal	Coal swamp	3.9	24.67	1.02	61.53	24.35	2.52	249	98	422	.37
8	Healy Creek	77.2	mdst	Uncertain	185.9	1.51	.05	3.93	.68	5.77	260	45	419	.33
7	Healy Creek	69.8	coal	Coal swamp	13.6	37.74	1.25	96.47	47.05	2.05	255	124	419	.34
6	Healy Creek	52.6	coal	Coal swamp	14.1	51.58	.56	59.00	48.22	1.22	114	93	417	.39
5	Healy Creek	51.5	coal	Coal swamp	12.9	45.66	.93	94.26	42.79	2.20	206	93	423	.35
4	Healy Creek	50.1	mdst	Aban. channel	122.8	2.89	.06	5.27	1.14	4.62	182	39	425	.36
3	Healy Creek	27.0	mdst	Aban. channel	172.1	2.89	.15	6.36	1.71	3.71	220	59	423	.30
2	Healy Creek	14.1	mdst	Aban. channel	183.5	.65	.01	.41	.43	.95	63	66	418	.32
1	Healy Creek	12.9	mdst	Aban. channel	199.6	.69	.01	.47	.38	1.23	68	55	417	.28

[1] Above base of Healy Creek Formation.

[2] Values in parentheses are from burned zone; see text for discussion.

Table 3. Summary and analysis of Rock-Eval and vitrinite reflectance data from the Suntrana section

Subset	Number of Rock-Eval/ vitrinite samples	TOC (wt. pct.)	S1 (mg HC/ g rock)	S2 (mg HC/ g rock)	S3 (mg HC/ g rock)	S2/S3	HI	OI	Tmax (° C)	Mean Ro (percent)
All samples	86/49									
min		0.05	0	0.01	0.08	0	2	23	385	0.18
max		66.40	82.72	127.45	56.66	5.77	463	2,692	552	.49
mean		17.41	1.70	28.15	16.47	1.34	126	234	424	.31
All coal samples	36/30									
min		2.32	.01	.06	7.41	0	2	23	385	.18
max		66.04	82.72	127.45	56.66	4.75	463	1,240	552	.49
mean		38.72	3.92	62.89	34.97	1.84	166	126	423	.30
All mudstone samples	50/19									
min		.05	0	.01	.08	0	4	30	398	.28
max		26.45	.92	34.11	19.76	5.77	404	2,692	439	.36
mean		2.08	.09	3.14	3.15	.98	96	312	423	.32
Coals										
Lignite Creek Fm.	12/12									
min		8.23	.47	11.12	7.41	1.24	135	71	407	.23
max		45.47	9.66	119.32	46.36	4.75	463	140	427	.30
mean		26.16	2.84	60.65	27.13	2.33	229	104	419	.26
Suntrana Fm.	14/11									
min		15.63	.14	12.07	11.92	.54	39	53	385	.18
max		62.48	82.72	127.45	56.17	2.80	240	119	431	.49
mean		48.17	7.18	65.07	41.87	1.53	132	88	413	.31
Healy Creek Fm.	10/7									
min		2.32	.01	.06	15.55	0	2	23	413	.34
max		66.04	1.25	112.00	56.66	3.37	255	1,240	552	.39
mean		40.55	.67	62.54	34.71	1.69	140	207	445	.36
Mudstones										
Overbank	14/1									
min		.38	0	.19	.58	.11	35	47	418	.34
max		9.27	.92	16.35	14.58	3.19	353	300	432	.34
mean		2.35	.17	4.14	2.90	1.21	124	139	424	.34
Abandoned channel	10/4									
min		.05	0	.01	.08	.07	20	39	416	.28
max		4.95	.32	12.29	4.56	4.62	248	280	426	.36
mean		1.46	.07	2.74	1.12	1.59	114	112	421	.32
Lake	18/11									
min		.47	0	.11	.73	.01	23	98	398	.29
max		2.19	.03	.91	9.04	.49	60	1,808	439	.36
mean		.97	.01	.41	3.90	.14	41	515	423	.32
Grubstake Fm.	10/5									
min		.47	0	.11	.73	.01	23	98	398	.29
max		.86	.03	.39	9.04	.49	60	1,808	423	.32
mean		.67	.01	.28	4.19	.11	41	695	414	.30
Lignite Creek Fm.	12/0									
min		.25	0	.06	.58	0	24	76	420	
max		9.27	.92	16.35	14.58	3.09	353	2,692	437	No data
mean		2.62	.25	5.59	3.68	1.36	149	344	427	
Suntrana Fm.	10/0									
min		.05	0	.01	.08	.07	20	74	416	
max		26.45	.58	34.11	19.76	1.72	174	300	427	No data
mean		3.53	.09	4.32	3.19	.75	82	152	421	
Sanctuary Fm.	8/6									
min		.86	0	.26	1.93	.08	29	119	421	.31
max		2.19	.02	.91	8.68	.34	59	620	439	.36
mean		1.34	0	.58	3.53	.19	41	291	430	.33
Healy Creek Fm.	10/8									
min		.65	0	.03	.35	.08	4	30	417	.28
max		3.91	.19	15.21	2.96	5.77	404	250	430	.36
mean		1.96	.06	3.92	1.14	2.29	147	68	423	.32

Table 4. Geochemical parameters describing source rock generative potential (from Peters, 1986)

Potential	TOC (weight %)	S1 (mg HC/g rock)	S2 (mg HC/g rock)
Poor	0-0.5	0-0.5	0-2.5
Fair	0.5-1.0	0.5-1.0	2.5-5.0
Good	1.0-2.0	1.0-2.0	5.0-10.0
Very good	2.0+	2.0+	10.0+

Table 5. Geochemical parameters describing type of hydrocarbon generated (from Peters, 1986)

Type	Hydrogen Index (HI)[1]	S2/S3
Gas	0-150	0-3
Gas and oil	150-300	3-5
Oil	300+	5+

[1] Assumes a level of thermal maturation equivalent to vitrinite reflectance (Ro) of 0.6 percent, but can be used for rocks with Ro as low as 0.25 percent (K.E. Peters, Chevron Oil Field Research Co., oral commun., 1987).

Coals in the Lignite Creek Formation show generally lower TOC than coals in the Healy Creek and Suntrana Formations (table 3) and also exhibit higher ash contents (Merritt, 1985). Perhaps the organic matter that accumulated in the Lignite Creek coal swamps was diluted by terrigenous sediment; this explanation is consistent with the interpretation that suspended sediment loads generally were higher during deposition of the Lignite Creek than during deposition of the Healy Creek and Suntrana Formations (Stanley and others, 1989).

The quantity of organic matter in the mudstone samples appears to be correlative with depositional environment. Mudstones that were deposited in overbank and abandoned channel environments have higher mean values of TOC, S1, and S2 than mudstones that accumulated in lakes (table 3). The reasons for this may include one or more of the following. (1) Rates of organic productivity may have been higher in overbank and abandoned channel environments, perhaps because they were shallower and better illuminated or more nutrient-rich and therefore more fertile. (2) Rates of consumption of organic matter by bottom-dwelling invertebrates may have been higher in the lakes; this interpretation is supported by our field observation that burrows are abundant in lacustrine mudstones in both the Sanctuary and Grubstake Formations but rare in overbank and abandoned channel mudstones. (3) Preservation of organic matter during diagenesis and weathering may have played a role; perhaps the woody vegetation in the overbank and abandoned channel deposits was more resistant to postdepositional oxidation than the diatomaceous organic matter in some of the lake deposits.

TYPES OF ORGANIC MATTER

Plots of hydrogen index (HI) against oxygen index (OI) on a modified van Krevelen diagram (fig. 2) show that there is a wide range of kerogen compositions in both coals and mudstones in the Usibelli Group. Most kerogens in our samples are intermediate between types II and III, but many are types III and IV. Type II kerogens are generally considered to be oil-prone, while type III kerogens are gas-prone (Tissot and Welte, 1984; Peters, 1986). The source potential of type IV kerogens, however, is controversial. Smyth (1983) argued that type IV kerogens are sources of both oil and gas, but Peters (1986) believed that type IV kerogens have little or no source potential.

Coals and mudstones in the Usibelli Group show considerable overlap in kerogen types (fig. 2). Nevertheless, the mean values of HI and S2/S3 are higher for coals than for mudstones and higher for coals in the Lignite Creek Formation than for coals in the Healy Creek and Suntrana Formations (table 3). In general, higher values of HI and S2/S3 indicate greater potential as source rocks of oil (table 5). However, the conclusion that coals in the Usibelli Group

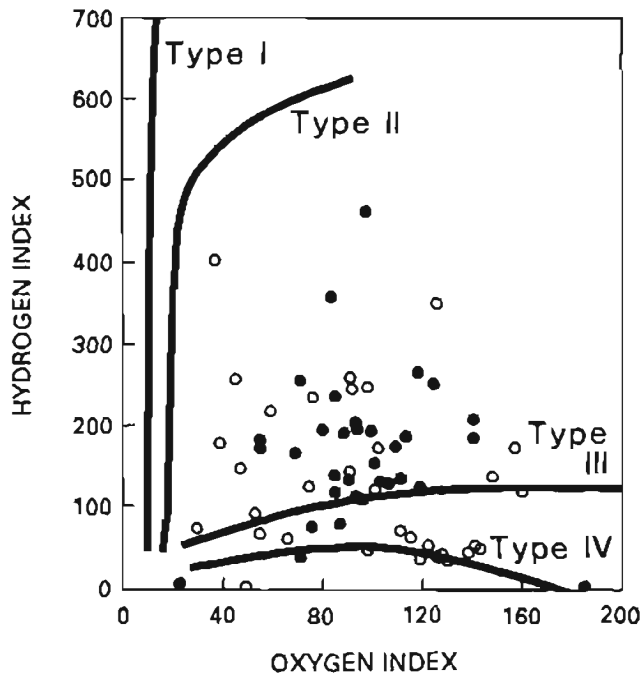

Figure 2. Modified van Krevelen diagram (Peters, 1986) showing idealized kerogen types (solid lines) and results for coal (dots) and mudstone (circles) of the Usibelli Group at Suntrana (table 2). In twenty additional samples not shown in this diagram, oxygen index values exceed 200 and hydrogen index values are less than or equal to 60. Type I and type II kerogens are oil-prone while type III kerogens are gas-prone. Interpretation of type IV kerogens is controversial; they are variously regarded as oil-prone, gas-prone, or inert (Smyth, 1983; Peters, 1986).

are oil-prone should be viewed with caution because the Rock-Eval technique tends to overestimate the oil-generative potential of coals due to poorly understood analytical problems (Peters, 1986).

The petroleum source potential of coals has long been controversial. Recent geochemical and geological investigations, however, indicate that many coals can be sources of gas and that certain coals can be sources of oil (Tissot and Welte, 1984; Waples, 1985). Accumulations of gas derived from coal are commercially produced in Europe, the Soviet Union, Alabama, Colorado, and New Mexico; crude oils thought to be derived from coal occur in Germany, France, the United Kingdom, Indonesia, Australia, and Venezuela (Meissner, 1984; Rightmire, 1984; Tissot and Welte, 1984; Waples, 1985). Given this worldwide experience and the Rock-Eval pyrolysis results noted above, the petroleum source potential of coals in the Usibelli Group should be investigated further by more detailed analysis of kerogen types and geochemistry.

Mudstones of the Usibelli Group that were deposited in overbank and abandoned channel environments exhibit higher mean values of HI and S2/S3 than mudstones that accumulated in lakes (table 3). This may simply reflect differences in the types of vegetation and resulting organic matter that accumulated in the original depositional environments. Alternatively, the HI and S2/S3 in the lake mudstones at Suntrana may have been reduced by oxidation during diagenesis or weathering or by interference from the mineral matrix during pyrolysis (Peters, 1986).

Two coal samples and 21 mudstone samples have oxygen index (OI) values greater than 150 (table 2); such values are unusually high (Katz, 1983). Elevated values of OI can be caused by oxidation of organic matter in the samples during outcrop weathering (Peters, 1986; Stanley, 1987) or by generation of carbon dioxide during pyrolysis by thermal degradation of carbonate minerals such as calcite, dolomite, and siderite (Katz, 1983; Peters, 1986). Either or both of these problems may have affected our data, because the samples were collected from surface exposures susceptible to weathering and because the samples were not treated with acid to remove carbonate before pyrolysis.

THERMAL MATURITY

The thermal maturity of organic matter in our samples is indicated by the vitrinite reflectance (Ro) and the Tmax of Rock-Eval pyrolysis. Nearly all of the samples exhibit vitrinite reflectance less than 0.4 percent and Tmax less than 440 °C; comparison of these values with the thermal maturity range chart (fig. 3) indicates that the coals are lignite and subbituminous and that most of the samples are immature to marginally mature with respect to the oil-generative zone (oil window).

The values of vitrinite reflectance and Tmax show considerable scatter but generally are greater downsection (figs. 4, 5, 6). These results are most easily explained by the generally accepted notion that burial temperatures and thermal maturity increase with burial depth. Furthermore, our results are consistent with a relatively simple burial history in which the Usibelli Group at Suntrana was buried beneath about 1 km of the Nenana Gravel (table 1) and subsequently exposed at the surface by a combination of uplift and erosion.

Anomalously high values of vitrinite reflectance, up to 2.72 percent, are shown by five samples (numbers 12-16) from the Healy Creek Formation (table 2). These five samples were collected from an interval that has recently burned, as shown by the presence in outcrop of red clinker and baked mudstone. Because the high vitrinite reflectances of these five samples were most likely caused by the high temperatures of recent coal fires rather than by temperatures achieved during burial diagenesis, they were not included in the data plotted in table 3 and figures 4 and 6.

IMPLICATIONS FOR PETROLEUM OCCURRENCE IN THE MIDDLE TANANA BASIN

Our Rock-Eval pyrolysis and vitrinite reflectance results show that coals and mudstones of the Usibelli Group at Suntrana are potential source rocks of oil and gas but are thermally immature to marginally mature with respect to

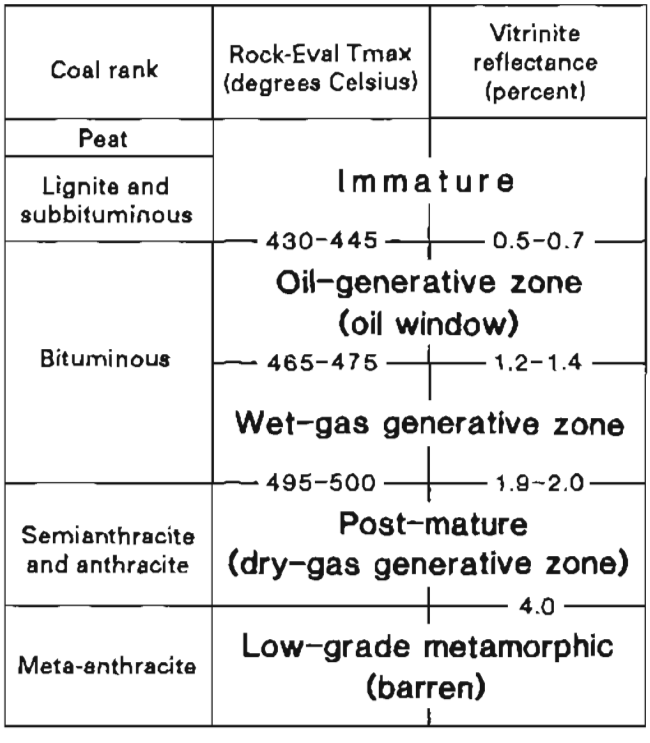

Figure 3. Organic geochemical parameters and levels of thermal maturation, compiled from several sources (Stanley, 1987).

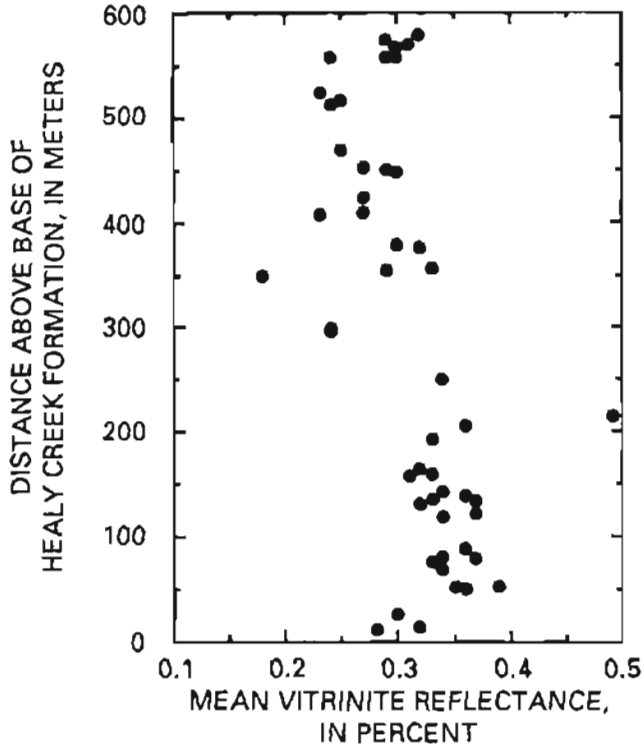

Figure 4. Mean vitrinite reflectance versus stratigraphic position for mudstones and coals of the Usibelli Group at Suntrana.

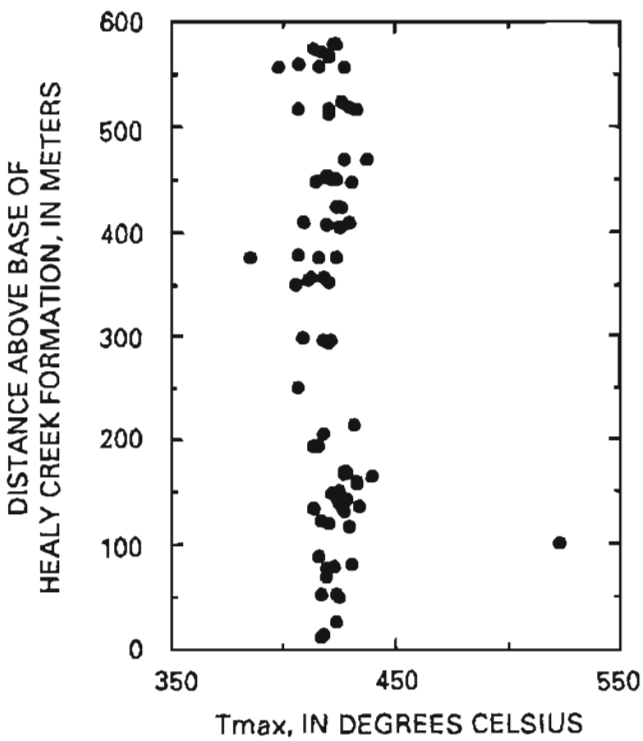

Figure 5. Mean Tmax (°C) versus stratigraphic position for mudstones and coals of the Usibelli Group at Suntrana. See text for explanation of Tmax.

the oil window. In the subsurface middle Tanana basin (fig. 1), the Usibelli Group includes coals and mudstones that are lithologically similar to those at Suntrana, according to mudlogs and other information from exploratory wells (Grether and Morgan, 1988; Kirschner, 1988). If these subsurface strata are also similar to the Suntrana rocks in amount and type of organic matter and have been buried deeply enough to achieve levels of thermal maturity corresponding to the oil window, then they may have generated oil and gas.

Thermal maturity data from wells in the middle Tanana basin have not been published. However, a rough estimate of the depth to the top of the oil window in the basin can be made from information on geothermal gradients and the general relationship between vitrinite reflectance and burial temperature. Reliable data on geothermal gradients are not available for central Alaska, so we made estimates using bottom-hole temperatures from the Union Nenana No. 1 and ARCO Totek Hills No. 1 wells (fig. 1). For both wells we assumed a mean annual surface temperature of 0 °C (T.S. Collett, U.S. Geological Survey, oral commun., 1989). The Union well recorded a bottom-hole temperature of 31 °C at a drilled depth of 930 m for an uncorrected geothermal gradient of 0.033 °C/m. The ARCO well recorded a temperature of 68 °C at 1,079 m for an uncorrected gradient of 0.063 °C/m. For comparison, our calculated geothermal gradients are about the same to slightly higher than those in Cook Inlet and on the North Slope of Alaska (American Association of Petroleum Geologists, Geothermal Survey of North America Subcommittee, 1976). It is possible that our estimates of geothermal gradient are lower than the true gradient, because drilling disrupts the temperature profile in a well by pumping cool drilling fluids down the

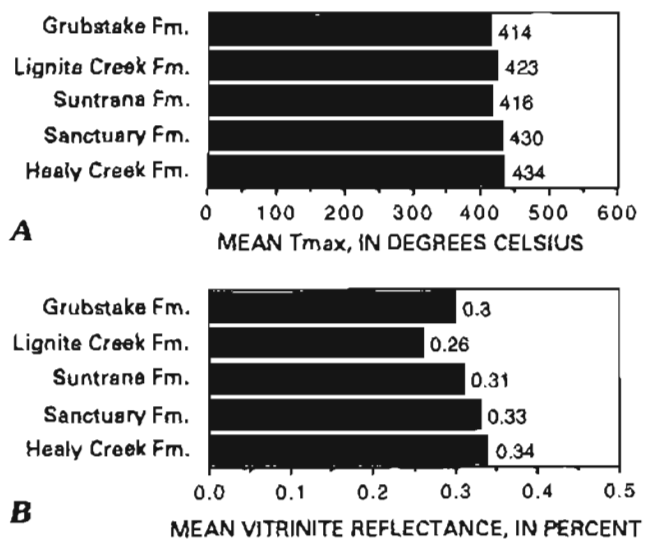

Figure 6. Bar graph of mudstones and coals in all five formations of the Usibelli Group at Suntrana. *A*, Mean Tmax (°C). See text for explanation of Tmax. *B*, Mean vitrinite reflectance.

borehole, resulting in cooling of the rocks at depth and measured bottom-hole temperatures that are too low (Barker and Pawlewicz, 1986).

Experience shows that the top of the oil window occurs at an average vitrinite reflectance (Ro) level of 0.6 percent, which corresponds to a burial temperature of about 88 °C (Barker and Pawlewicz, 1986). Using this temperature and the geothermal gradients calculated above, the estimated top of the oil window in the middle Tanana basin is about 1,400 m to 2,700 m below the ground surface. The top of the oil window may actually be shallower than this, if our assumed bottom-hole temperatures and geothermal gradients are too low as noted above.

Gravity data suggest that the base of the Usibelli Group in the deepest part of the middle Tanana basin is 3,000 m to 3,350 m beneath the surface (Barnes, 1961; Hite and Nakayama, 1980; Kirschner, 1988). If the gravity data have been correctly interpreted, then the base of the Usibelli Group is below the estimated top of the oil window, suggesting that mudstones and coals in at least the lower part of the Usibelli Group have been buried deep enough to generate oil and gas.

This hypothesis can be tested by drilling in the deepest part of the middle Tanana basin, which probably coincides with a gravity low northwest of Nenana (fig. 1). Both the Union Nenana No. 1 and the ARCO Totek Hills No. 1 were drilled away from this gravity low, in areas where the Usibelli Group is thin (Grether and Morgan, 1988; Kirschner, 1988). Mudlogs show that both wells were dry holes that bottomed in schist, with gas shows associated with coal beds but no reported signs of oil. The reason for the lack of oil is unknown but may reflect an absence of appropriate source rocks, failure of the source rocks to reach thermal maturity, or the presence of barriers to migration that prevented oil generated in the deepest parts of the basin from reaching the boreholes.

SUMMARY

Results from Rock-Eval pyrolysis and vitrinite reflectance indicate that coals and mudstones in the type section of the Usibelli Group at Suntrana are potential source rocks of oil and gas and are thermally immature to marginally mature with respect to the oil window. In the samples we studied, coals are more organic-rich and possibly more oil-prone than mudstones; furthermore, mudstones from fluvial overbank and abandoned channel deposits are more organic-rich and possibly more oil-prone than mudstones that accumulated in lakes.

Lithologically similar coals and mudstones were encountered by two wells drilled in the nearby middle Tanana basin. Both wells were drilled in areas where the Usibelli Group is relatively thin and shallowly buried, and both reported shows of gas but no oil. However, calculations based on gravity and uncorrected borehole temperatures suggest that a well drilled in the deepest part of the basin northwest of Nenana will find mudstones and coals buried below the top of the oil window, where they may have generated oil and gas.

REFERENCES CITED

American Association of Petroleum Geologists, Geothermal Survey of North America Subcommittee, 1976, Geothermal gradient map of North America, two sheets, scale 1:5,000,000.

Barker, C.E., and Pawlewicz, M.J., 1986, The correlation of vitrinite reflectance with maximum temperature in humic organic matter, *in* Bunterbarth, G., and Stegena, L., eds., Paleogeothermics: Berlin, Springer-Verlag, Lecture Notes in Earth Sciences, v. 5, p. 79-93.

Barnes, D.F., 1961, Gravity low at Minto Flats, Alaska: U.S. Geological Survey Professional Paper 424-D, p. D254-D257.

Buffler, R.T., and Triplehorn, D.M., 1976, Depositional environments of the Tertiary coal-bearing group, central Alaska, *in* Miller, T.P., ed., Recent and ancient sedimentary environments in Alaska, Proceedings of the Alaska Geological Society Symposium held April 2-4, 1975, Anchorage: Alaska Geological Society, p. H1-H10.

Clayton, J.L., and Swetland, P.J., 1978, Subaerial weathering of sedimentary organic matter: Geochimica et Cosmochimica Acta, v. 42, no. 2, p. 305-312.

Csejtey, Béla, Jr., Mullen, M.W., Cox, D.P., Gilbert, W.G., Yeend, W.E., Smith, T.E., Wahrhaftig, Clyde, Craddock, Campbell, Brewer, W.M., Sherwood, K.W., Hickman, R.G., Stricker, G.D., St. Aubin, D.R., and Goerz, D.J., III, 1986, Geology and geochronology of the Healy quadrangle, Alaska: U.S. Geological Survey Open-File Report 86-396, 92 p., 4 maps, scale 1:250,000.

Grether, W.J., and Morgan, K.A., 1988, Exploration and hydrocarbon potential of interior basins, Alaska [abs.]: American Association of Petroleum Geologists Bulletin, v. 72, no. 2, p. 191-192.

Hite, D.M., and Nakayama, E.N., 1980, Present and potential petroleum basins of Alaska, *in* Landwehr, M.L., ed., Exploration and economics of the petroleum industry: New ideas, new methods, new developments: Dallas, Institute on Petroleum Exploration and Economics, p. 511-554.

Katz, B.J., 1983, Limitations of Rock-Eval pyrolysis for typing organic matter: Organic Geochemistry, v. 4, no. 3/4, p. 195 199.

Kirschner, C.E., 1988, Map showing sedimentary basins of onshore and continental shelf areas, Alaska: U.S. Geological Survey Miscellaneous Investigations Map I-1873, scale 1: 5,000,000.

Leythaeuser, Detlev, 1973, Effects of weathering on organic matter in shales: Geochimica et Cosmochimica Acta, v. 37, no. 1, p. 113-120.

Meissner, F.F., 1984, Cretaceous and lower Tertiary coals as sources for gas accumulations in the Rocky Mountain area, *in* Woodward, Jane, Meissner, F.F., and Clayton, J.L., eds., Hydrocarbon source rocks of the greater Rocky Mountain region: Denver, Rocky Mountain Association of Geologists, p. 401-431.

Merritt, R.D., 1985, Field trip guidebook: Lignite Creek and Healy Creek coal fields, Nenana basin, Alaska: American Association of Petroleum Geologists Annual Meeting, Pacific Section, 60th, Anchorage, Alaska, 1985, Guidebook, 58 p.

Merritt, R.D., and Hawley, C.C., 1986, Map of Alaska's coal resources: Fairbanks, Alaska Division of Mining and Geological and Geophysical Surveys Special Report 37, scale 1:2,500,000.

Miller, D.J., Payne, T.G., and Gryc, George, 1959, Geology of possible petroleum provinces in Alaska: U.S. Geological Survey Bulletin 1094, 131 p.

Peters, K.E., 1986, Guidelines for evaluating petroleum source rock using programmed pyrolysis: American Association of Petroleum Geologists Bulletin, v. 70, no. 3, p. 318-329.

Rightmire, C.T., 1984, Coalbed methane resource, *in* Rightmire, C.T., Eddy, G.E., and Kirr, J.N., eds., Coalbed methane resources of the United States: American Association of Petroleum Geologists Studies in Geology 17, p. 1-13.

Silberling, N.D., and Jones, D.L., eds., 1984, Lithotectonic terrane maps of the North American Cordillera: U.S. Geological Survey Open-File Report 84-523, 106 p., 4 maps, scale 1:2,500,000.

Smyth, Michelle, 1983, Nature of source material for hydrocarbons in Cooper basin, Australia: American Association of Petroleum Geologists Bulletin, v. 67, no. 9, p. 1422-1428.

Stanley, R.G., 1987, Effects of weathering on petroleum-source evaluation of coals from the Suntrana Formation near Healy, Alaska, *in* Hamilton, T.D., and Galloway, J.P., eds., Geologic studies in Alaska by the U.S. Geological Survey during 1986: U.S. Geological Survey Circular 998, p. 99-103.

———1988, Hydrocarbon source potential and thermal maturity of the Sanctuary Formation (middle Miocene), northern foothills of the Alaska Range, *in* Galloway, J.P., and Hamilton, T.D., eds., Geologic studies in Alaska during 1987: U.S. Geological Survey Circular 1016, p 117-120.

Stanley, R.G., Flores, R.M., and Wiley, T.J., 1989, Contrasting depositional environments in Tertiary fluvial deposits of Nenana coal field, Alaska [abs.]: American Association of Petroleum Geologists Bulletin, v. 73, no. 3, p. 415.

Tissot, B.P., and Welte, D.H., 1984, Petroleum formation and occurrence [2d ed.]: Berlin, Springer-Verlag, 699 p.

Wahrhaftig, Clyde, 1968, Schists of the central Alaska Range: U.S. Geological Survey Bulletin 1254-E, 22 p.

———1970, Geologic map of the Healy D-4 quadrangle, Alaska: U.S. Geological Survey Geologic Quadrangle Map GQ-806, scale 1:63,360.

———1987, The Cenozoic section at Suntrana, Alaska, *in* Hill, M.L., ed., Geological Society of America, Cordilleran Section, Centennial Guide, v. 1, p. 445-450.

Wahrhaftig, Clyde, Wolfe, J.A., Leopold, E.B., and Lanphere, M.A., 1969, The coal-bearing group in the Nenana coal field, Alaska: U.S. Geological Survey Bulletin 1274-D, 30 p.

Waples, D.W., 1985, Geochemistry in petroleum exploration: Boston, International Human Resources Development Corporation, 232 p.

Reviewers: Kenneth J. Bird and Timothy S. Collett

K-Ar and $^{40}Ar/^{39}Ar$ Ages of Tuff Beds at Ocean Point on the Colville River, Alaska

By James E. Conrad, Edwin H. McKee, *and* Brent D. Turrin

INTRODUCTION

The age of dinosaur-bone-bearing beds of the Prince Creek Formation along the Colville River has been in debate for the past decade. Early paleontological studies suggest that at least part of the section near Ocean Point and near the site of the dinosaur bones be assigned a Paleocene to early Eocene (Thanetian to Ypresian) age on the basis of mollusks and ostracodes (Marincovich and others, 1985). This age seemed to confirm a fission-track age on zircon of 50.9±7.7 Ma reported by Carter and others (1977). Other studies of benthic foraminifers, vertebrates, and ostracodes suggest that the marine strata are late Campanian to early Maastrichtian (McDougall, 1987; Brouwers and others, 1987). The need to resolve this conflict by accurately dating these strata is of greater than normal interest to the geologic community because a Paleocene age for dinosaurs would cast doubt on the bolide impact theory for the extinction of dinosaurs (and many other taxa) at the end of the Cretaceous Period (Alvarez and others, 1980).

A number of tuff beds in the bluffs on the south side of the Colville River about 7 km west of Ocean Point (fig.1) contain glass shards suitable for dating by the K-Ar and the $^{40}Ar/^{39}Ar$ methods. Four samples of glass were dated by K-Ar and eight were dated by the $^{40}Ar/^{39}Ar$ incremental heating technique.

GEOLOGIC SETTING

The Prince Creek Formation 7 km west of Ocean Point consists of a series of thin- to medium-bedded sandstones and siltstones with interbeds of tuff and coal. Stratigraphically higher parts of the section that are several kilometers to the east consist entirely of mudstone and siltstone. The lower part of the section, which contains tuff

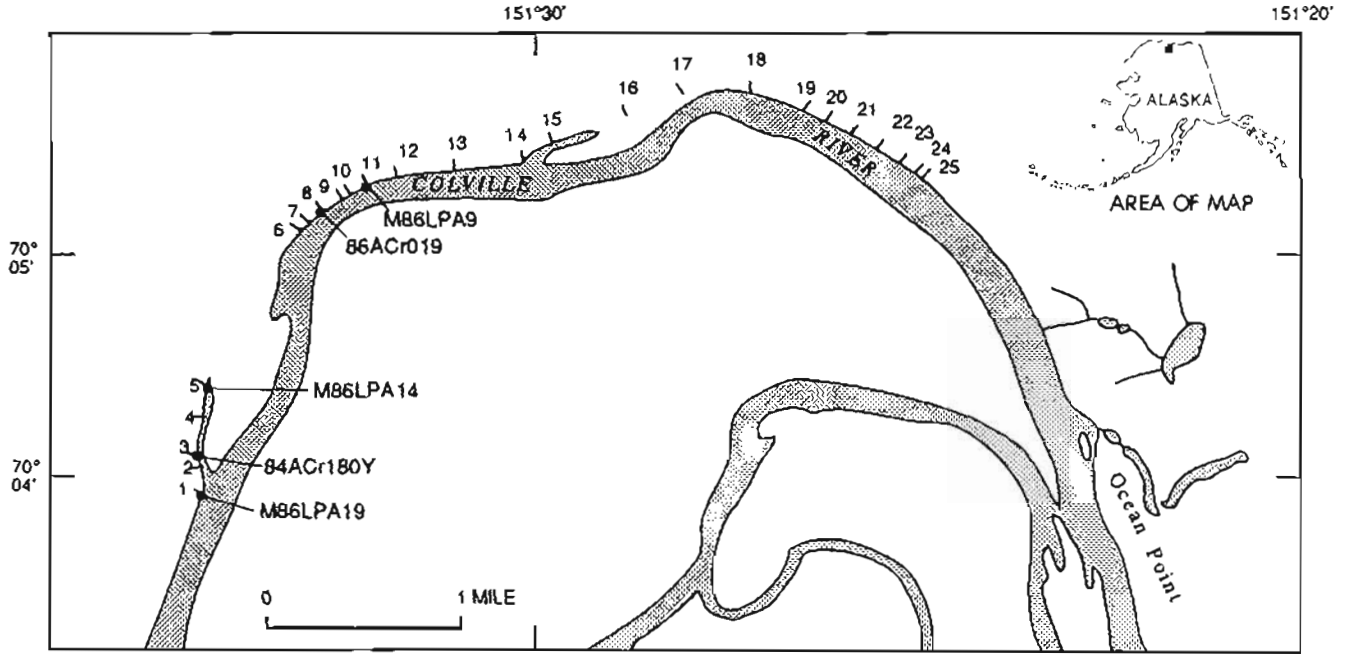

Figure 1. Index map showing location of samples dated by K-Ar and $^{40}Ar/^{39}Ar$ methods. See tables 1 and 2 for detailed information. Numbers 1-25 correspond to sections measured by Phillips (this volume).

Table 1. Results of conventional K-Ar analyses of the Colville River tuff beds

Sample No.	Experiment number	Material	K_2O (wt. percent)	^{40}Ar rad mole/g ($\times 10^{-10}$)	^{40}Ar rad	Age±1σ (Ma)
M86LPA9	871589	Glass	5.74	5.811	88.8	69.5±2.1
86ACr019	871535	Glass	3.87	3.732	77.0	65.8±2.0
M86LPA19	871452	Glass	5.46	5.647	76.7	70.4±2.1

Constants: $\lambda_\varepsilon + \lambda'_\varepsilon = 0.581 \times 10^{-10}\ yr^{-1}$, $\lambda_\beta = 4.962 \times 10^{-10}\ yr^{-1}$, $^{40}K/K_{total} = 1.167 \times 10^{-4}$ mol/mol

beds, also contains abundant dinosaur bones in organic-rich beds. Measured sections from along the Colville River showing the tuff beds sampled for this report and relations to the dinosaur-bone-bearing horizons are shown in Phillips (this volume, figs. 2 and 3). The tuff beds form resistant white to buff markers 1 cm to 2 m thick that pinch out along strike over distances of hundreds of meters. As many as 10 tuff beds occur in the 20- to 30-m-thick section 7 km west of Ocean Point. The tuff-bearing strata represent flood-plain deposits (Phillips, 1988), whereas overlying siltstones and mudstones were deposited in a marine environment. The extent of the flood-plain deposits, including tuff beds and dinosaur-bone-bearing beds, is unknown; overlying marine strata crop out about 2 km to the east.

Glass shards from some of the tuff beds are remarkably fresh and well preserved. The unabraded character of the delicate shards indicates that they are airfall deposits that have not been transported by water for any distance. Microscopic examination in normal and polarized light and in refractive oils reveals no trace of devitrification or alteration of the glass. The potassium (K_2O) content of the glass is between 3.5 and 5.7 weight percent, indicating a rhyolitic composition.

METHODS

Conventional K-Ar analyses were performed using standard isotope-dilution techniques similar to those described by Dalrymple and Lanphere (1969). A 60°-sector, 15.2-cm-radius, Nier-type mass spectrometer was used for argon analysis. Potassium analyses were performed by a lithium metaborate flux fusion-flame photometry technique, using lithium as an internal standard (Ingamells, 1970).

Samples used in the $^{40}Ar/^{39}Ar$ age spectrum experiments were heated by two different techniques—induction coil (Dalrymple and Lanphere, 1969) and continuous laser (Dalrymple, 1989).

RESULTS

Conventional K-Ar ages on the Colville River tuff beds range from 65.8±2.0 to 70.4±2.1 Ma (table 1). The four samples listed in table 1 are in probable stratigraphic order (see Phillips, this volume). Faults and covered intervals in the section prohibit a direct correlation between some of the dated tuff units. Within the limits of analytical uncertainty, the ages are indistinguishable from one another. The age of sample 86ACr019 is concordant with the other ages, but $^{40}Ar/^{39}Ar$ data (described later) suggest that this sample may have undergone some argon loss. The K-Ar data indicate that the age of these beds ranges from about 70–71 Ma to about 66–68 Ma.

The $^{40}Ar/^{39}Ar$ analyses were performed to evaluate the degree of argon loss by diffusion or alteration of the glass, which would lead to anomalously young conventional K-Ar ages. The assumption used for interpreting incremental heatings of glass is that the low-temperature steps (about 300 to 500 °C) release loosely held argon from the outside edges of the glass shards and from alteration products, most likely clays. Higher temperature steps (about 550 °C and higher) release argon (by volume diffusion) from inner portions of the shards that have been less affected by alteration and diffusion over geologic time. Alteration and diffusion of argon will be most pronounced along the edges of the shards; low-temperature steps will reveal these effects of argon loss by yielding anomalously young apparent ages.

All samples were analyzed by the incremental or age spectrum $^{40}Ar/^{39}Ar$ technique (table 2), using induction-heating or laser-heating methods. Analysis of age spectra and isochron plots using the criteria of Lanphere and Dalrymple (1978) readily distinguishes between samples that have undergone some degree of argon redistribution and those that are essentially undisturbed and therefore give reliable cooling ages. The $^{40}Ar/^{39}Ar$ age spectra for three of the glass samples (M86LPA19, 84ACr180Y, M86LPA9) have concordant, well-defined plateaus and show only minor evidence of argon loss caused by alteration or diffusion. Samples M86LPA14 and 86ACr019 gave disturbed age spectra and appear to have some degree of argon redistribution, but only one of these (86ACr019) shows evidence of significant argon loss.

The argon release patterns show minor argon loss in all samples, which is reflected by slightly younger ages in the low-temperature steps of the incremental-heating experiments. The total radiogenic ^{40}Ar loss in all samples is

Table 2. Results of $^{40}Ar/^{39}Ar$ analyses of the Colville River tuff beds

[Bold entries indicate data used in calculation of plateau ages. In the third column, temperatures (°C) reported for samples heated by induction coil, lettered steps for samples heated by continuous laser]

Sample No.	Exp. No.	Temp (°C) or step	$^{40}Ar/^{39}Ar$	$^{37}Ar/^{39}Ar$	$^{36}Ar/^{39}Ar$	Percent ^{39}Ar released	^{40}Ar rad	Apparent age (Ma)
M86LPA9	L121-2	A	22.28	0.08604	0.06051	1.28	19.7	22.1±25.8
		B	**16.41**	**0.003099**	**0.008048**	**3.90**	**85.5**	**69.8±6.5**
		C	**14.73**	**0.01691**	**0.003862**	**16.24**	**92.2**	**67.6±1.7**
		D	**14.26**	**0.01690**	**0.001943**	**27.32**	**95.9**	**68.1±0.8**
		E	**14.18**	**0.01330**	**0.001050**	**20.67**	**97.7**	**68.9±1.0**
		F	**14.07**	**0.01413**	**0.0004771**	**10.11**	**98.9**	**69.2±1.0**
		G	**14.14**	**0.01139**	**0.0004163**	**5.80**	**99.0**	**69.7±1.0**
		H	**14.08**	**0.01649**	**0.0008217**	**14.68**	**98.2**	**68.8±1.3**
J=0.00281								
Reactor corrections: $^{36}Ar/^{37}Ar$ (Ca)=0.0003; $^{39}Ar/^{37}Ar$(Ca)=0.0003; $^{40}Ar/^{39}Ar$(K)=0.0086								
	87A076	350	222.2694	0.05515	0.7520	0.17	0.03	0.6±26.7
		400	27.77	0.0111	0.07389	1.97	21.4	50.0±1.8
		475	11.27	0.01715	0.01176	13.36	69.1	65.5±0.4
		600	**8.803**	**0.01659**	**0.002101**	**62.55**	**92.9**	**68.7±0.2**
		750	**9.160**	**0.01430**	**0.003466**	**19.41**	**88.8**	**68.3±0.3**
		865	**17.38**	**0.003415**	**0.03180**	**2.46**	**45.9**	**67.0±1.3**
		FUSE	338.2	0.1253	1.153	0.08	-0.7	-20.9±78.8
J=0.004745								
Reactor corrections: $^{36}Ar/^{37}Ar$ (Ca)=0.000234; $^{39}Ar/^{37}Ar$(Ca)=0.000654; $^{40}Ar/^{39}Ar$(K)=0.0057								
86ACr019	88A003	450	16.67	0.1756	0.003098	9.35	45.0	63.0±1.8
		550	9.126	0.1562	0.004647	42.38	84.7	65.0±0.5
		625	8.788	0.1621	0.004158	29.18	85.8	63.4±0.7
		700	10.01	0.1809	0.008652	11.89	74.3	62.6±1.4
		800	13.49	0.2357	0.01977	5.67	56.6	64.2±2.8
		FUSE	41.95	1.256	0.1153	1.52	18.9	66.7±2.8
J=0.004745								
Reactor corrections: $^{36}Ar/^{37}Ar$ (Ca)=0.000278; $^{39}Ar/^{37}Ar$(Ca)=0.0007; $^{40}Ar/^{39}Ar$(K)=0.0332								
M86LPA14	88A004	450	17.30	0.1889	0.03943	4.59	32.5	47.4±2.9
		525	13.01	0.1510	0.01474	23.36	66.3	72.1±0.8
		600	10.07	0.1439	0.004354	32.74	87.0	73.2±0.6
		700	9.355	0.1463	0.002891	26.64	90.6	70.9±0.7
		775	9.517	0.1630	0.004225	9.73	86.7	69.0±1.4
		FUSE	64.77	0.3460	0.1842	2.94	16.0	86.0±5.1
J=0.004725								
Reactor corrections: $^{36}Ar/^{37}Ar$ (Ca)=0.000278; $^{39}Ar/^{37}Ar$(Ca)=0.0007; $^{40}Ar/^{39}Ar$(K)=0.0332								
84ACr180Y	87A075	350	35.37	0.05557	0.1041	0.58	13.0	39.0±8.9
		450	16.69	0.05418	0.03560	6.26	36.9	52.0±0.9
		525	10.31	0.04298	0.007529	34.06	78.4	68.0±0.3
		600	**8.773**	**0.03772**	**0.001751**	**24.51**	**94.1**	**69.3±0.3**
		700	**8.497**	**0.04671**	**0.008265**	**25.86**	**97.1**	**69.3±0.3**
		850	**13.02**	**0.2258**	**0.01610**	**7.38**	**63.6**	**69.5±0.8**
		FUSE	14.75	1.956	0.02166	1.34	57.5	71.3±3.90
J=0.004745								
Reactor corrections: $^{36}Ar/^{37}Ar$ (Ca)=0.000234; $^{39}Ar/^{37}Ar$(Ca)=0.000654; $^{40}Ar/^{39}Ar$(K)=0.0057								

Table 2. Results of $^{40}Ar/^{39}Ar$ analyses of the Colville River tuff beds—continued

[Bold entries indicate data used in calculation of plateau ages. In the third column, temperatures (°C) reported for samples heated by induction coil, lettered steps for samples heated by continuous laser]

Sample No.	Exp. No.	Temp (°C) or step	$^{40}Ar/^{39}Ar$	$^{37}Ar/^{39}Ar$	$^{36}Ar/^{39}Ar$	Percent ^{39}Ar released	^{40}Ar rad	Apparent age (Ma)
86LPA19	L115-1	TFU	15.29	0.02571	0.005813	100	88.7	67.5±1.5
	L115-2	A	18.15	0.07131	0.02405	6.29	60.8	55.1±7.4
		B	**15.36**	**0.03294**	**0.004176**	**20.85**	**91.9**	**70.2±2.4**
		C	**14.88**	**0.02771**	**0.002610**	**17.40**	**94.8**	**70.1±2.1**
		D	**14.85**	**0.02393**	**0.003381**	**20.15**	**93.2**	**68.8±2.0**
		E	**14.87**	**0.03198**	**0.003107**	**11.37**	**93.8**	**69.3±2.9**
		F	**14.45**	**0.03979**	**0.001380**	**1.83**	**97.1**	**69.8±3.0**
		G	**14.77**	**0.02632**	**0.001768**	**22.12**	**96.4**	**70.8±1.4**
	L115-3	A	17.34	0.007356	0.01290	2.80	78.0	67.3±4.2
		B	15.01	0.02244	0.003973	28.68	92.1	68.8±0.6
		C	**14.77**	**0.02248**	**0.001475**	**47.44**	**97.0**	**71.2±0.8**
		D	**14.65**	**0.01742**	**0.0007919**	**15.67**	**98.4**	**71.6±0.7**
		E	**14.92**	**0.01306**	**0.001839**	**2.76**	**96.3**	**71.4±3.3**
		F	**15.03**	**0.01364**	**0.002773**	**2.64**	**94.5**	**70.6±3.4**

J=0.00281

Reactor corrections: $^{36}Ar/^{37}Ar$ (Ca)=0.0003; $^{39}Ar/^{37}Ar$(Ca)=0.0003; $^{40}Ar/^{39}Ar$(K)=0.0086

Decay constants: $\lambda_\varepsilon+\lambda'_\varepsilon = 0.581\times10^{-10}$ yr^{-1}, $\lambda_\beta = 4.962\times10^{-10}$ yr^{-1}, $^{40}K/K_{total} = 1.167\times10^{-4}$ mol/mol

Table 3. Summary of K-Ar and $^{40}Ar/^{39}Ar$ ages of the Colville River tuff beds

Sample no.	Experiment no.	K-Ar age (Ma)	$^{40}Ar/^{39}Ar$ plateau age (Ma)	$^{40}Ar/^{39}Ar$ isochron age (Ma)	$^{40}Ar/^{39}Ar$ total-gas age (Ma)
M86LPA9	L121-2		68.8±0.5	69.0±0.8	68.0±0.7*
	87A076		68.5±0.4	68.7±0.4	67.6±0.4*
	87I589	69.5±2.1			
86ACr019	88A003		No plateau		64.1±0.5*
	87I535	65.8±2.0			
M86LPA14	88A004		No plateau		71.1±0.5*
	87I590	68.5±2.0			
84ACr180Y	87A075		69.3±0.4	69.3±0.4	67.6±0.4*
M86LPA19	L115-1				67.5±1.5
	L115-2		70.0±0.9	69.5±3.1	69.0±1.0*
	L115-3		71.4±0.6	72.0±1.1	70.4±0.6*
	87I452	70.4±2.1			

*Recombined age.

less than about 2 percent, estimated by comparison of plateau and total-gas ages (table 3). The minor ^{40}Ar loss observed in the low-temperature heating steps is attributed to loss of ^{40}Ar due to surface alteration and (or) diffusion near shard boundaries. Nonetheless, $^{40}Ar/^{39}Ar$ plateau ages are indistinguishable from conventional K-Ar ages within the limits of analytical uncertainty. Of the two samples giving apparently disturbed $^{40}Ar/^{39}Ar$ age spectra, one (M86LPA14) gave a reasonable K-Ar age of 68.5±2.0 Ma on the basis of the other radiometric ages, suggesting that some argon redistribution occurred without significant argon loss. The slightly old total-gas age of 71.1±0.5 Ma obtained on this sample by $^{40}Ar/^{39}Ar$ may be an artifact of the irradiation process (recoil of ^{39}Ar). Sample 86ACr019 appears to have suffered significant ^{40}Ar loss due to alteration or diffusion on the basis of the incremental heating data. The K-Ar age

of 65.8±2.0 Ma for this sample is therefore considered a minimum age.

The "best" or preferred age for each of the tuff beds is shown in figure 2. For samples M86LPA9 and M86LPA19, preferred ages are 68.8±0.4 and 70.4±0.8 Ma respectively, and are calculated from weighted means of $^{40}Ar/^{39}Ar$ isochron ages, $^{40}Ar/^{39}Ar$ total fusion ages, and K-Ar ages for each tuff. The preferred age for sample 84ACr180Y is the $^{40}Ar/^{39}Ar$ isochron age of 69.3±0.4 Ma. The best age estimate for sample M86LPA14 is the K-Ar age of 68.5±2.0 Ma, because of possible irradiation-induced disturbance in the $^{40}Ar/^{39}Ar$ analysis. The K-Ar age of 65.8±2.0 Ma for sample 86ACr019 is considered a minimum age because of significant argon redistribution and loss apparent in the $^{40}Ar/^{39}Ar$ analysis. Although there appears to be a slight decrease in age upward through the section, none of the tuffs are demonstrably different in age at a 95-percent confidence level. Since the ages are concordant, a best age estimate of 69.1±0.3 Ma for the dinosaur-bone-bearing beds was calculated using the weighted mean of all the analyses. Assuming that offsets across the faults and covered intervals are small, the location of the Cretaceous-Tertiary boundary, considered to be at about 66 Ma, appears to be at least 100 m above the youngest dated tephra bed (M86LPA9), provided depositional and environmental conditions remained constant. This new dating, by establishing a Late Cretaceous age for the dinosaur-bone-bearing beds, is therefore compatible with the impact theory for the extinction of the dinosaurs. Unfortunately, no tuff beds have been identified near the probable location of the Cretaceous-Tertiary boundary to allow for K-Ar or $^{40}Ar/^{39}Ar$ dating. About 40–60 m above the youngest tephra bed, the section passes into a marine depositional environment (Phillips, 1988). Thus, any tuff beds deposited at this time would likely be reworked and altered by diagenetic interaction with sea water.

REFERENCES CITED

Alvarez, L.W., Alvarez, W., Asaro, F., and Michel, H.V., 1980, Extraterrestrial cause for the Cretaceous-Tertiary extinction: Science, v. 208, p. 1095-1108.

Brouwers, E.M., Clemens, W.A., Spicer, R.A., Ager, T.A., Carter, L.D., and Sliter, W.V., 1987, Dinosaurs on the North Slope, Alaska: High latitude, latest Cretaceous environments: Science, v. 237, p. 1608-1610.

Carter, L.D., Repenning, C.A., Marincovich, L.N., Hazel, J.E., Hopkins, D.M., McDougall, Kristen, and Naeser, C.W., 1977, Gubik and pre-Gubik Cenozoic deposits along the Colville River near Ocean Point, North Slope, Alaska, *in* Blean, K.M., ed., The United States Geological Survey in Alaska: Accomplishments during 1976: U.S. Geological Survey Circular 751-B, p. B12-B14.

Dalrymple, G.B., 1989, The GLM continuous laser system for $^{40}Ar/^{39}Ar$ dating: Description and performance characteristics: U.S. Geological Survey Bulletin 1890, p. 89-96.

Dalrymple, G.B., and Lanphere, M.A., 1969, Potassium-argon dating: San Francisco, W. H. Freeman, 258 p.

Ingamells, C.O., 1970, Lithium metaborate flux in silicate analysis: Analytica Chimica Acta, v. 52, p. 323-334.

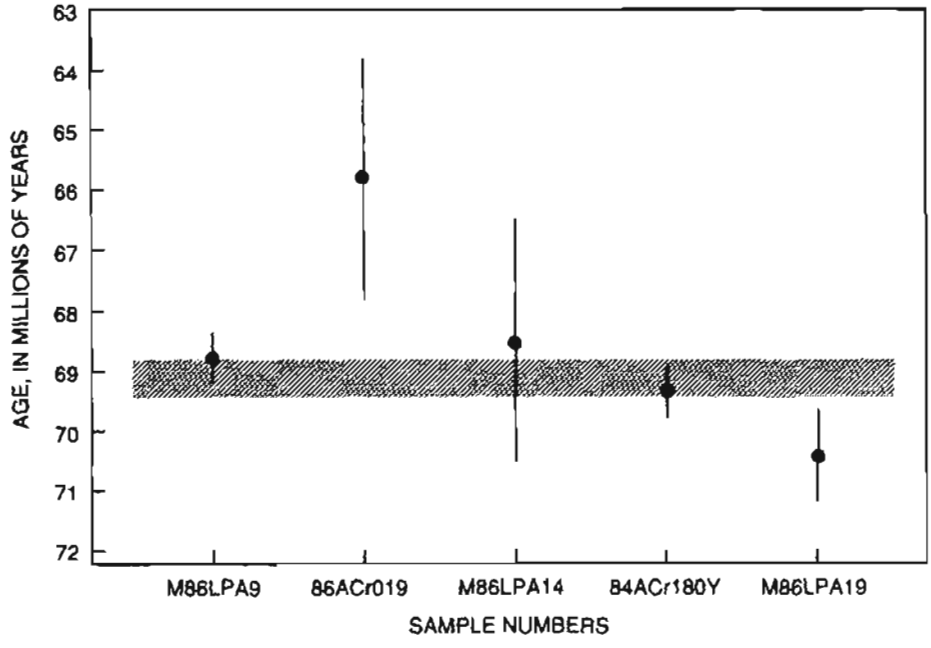

Figure 2. Best age estimates for Colville River tuff beds (dots) and associated 1-sigma errors (bars). Shaded area shows best estimate of age of bone-bearing beds on basis of all analyses. See text for discussion.

Lanphere, M.A., and Dalrymple, G.B., 1978, The use of $^{40}Ar/^{39}Ar$ data in evaluation of disturbed K-Ar systems, *in* Zartman, R.E., ed., Short papers of the Fourth International Conference, geochronology, cosmochronology, isotope geology: U.S. Geological Survey Open-File Report 78-701, p. 241-243.

Marincovich, Louie, Jr., Brouwers, E.M., and Carter, L.D., 1985, Early Tertiary marine fossils from northern Alaska: Implications for Arctic Ocean paleogeography and faunal evolution: Geology, v. 13, p. 770-773.

McDougall, Kristen, 1987, Maestrichtian benthic foraminifers from Ocean Point, North Slope, Alaska: Journal of Foraminiferal Research, v. 17, no. 4, p. 344-366.

Phillips, R.L., 1988, Measured sections, paleoenvironments, and sample locations near Ocean Point, Alaska: U.S. Geological Survey Open-File Report 88-40.

Reviewers: Michael F. Diggles and John P. Galloway

Development of an Alaskan Radiocarbon Data Base as a Subset of the International Radiocarbon Data Base (IRDB)

By John P. Galloway *and* Renee Kra

INTRODUCTION

The purpose of this paper is to give a brief review of the historical availability of radiocarbon age determinations for Alaska and introduce the Alaska radiocarbon data base as part of the larger International Radiocarbon Data Base (IRDB). Since 1951 more than 2,900 radiocarbon ages have been reported in the literature for geological and archaeological samples from Alaska. Thirty-five U.S. laboratories (Federal, State, commercial, and academic institutions) and 14 foreign laboratories have reported radiocarbon ages on Alaskan samples in *Radiocarbon* or other scientific journals (table 1). Within the last 15 years (1975 to 1990), the number of radiocarbon ages obtained from Alaska has doubled. As of 1984, there were more than 375 geological and archaeological papers that contain one or more radiocarbon age for Alaska, excluding the 80 lists of ages published in *Radiocarbon* and 14 in *Science* (Galloway, 1984). This growth reflects not only an increase in geological and archaeological field investigations in Alaska, but also greater confidence among researchers in the radiocarbon dating technique. There has also been a shift toward research that requires more precise dating of geological and archaeological sites (Gal, 1982; Nelson and others, 1988).

With an increasing interest both at the national and international levels in geological and biological processes in arctic environments and the reconstruction of paleoenvironments, the development of a digital data base for radiocarbon data for Alaska greatly facilitates the availability and dissemination of radiocarbon data for this part of the Arctic. Although developed independently, the Alaska data base is now an integral subset of the larger International Radiocarbon Data Base (IRDB). The implementaion of the IRDB and regional data bases is timely and will provide multiple resources for interpretative and dynamic research (Kra, 1986).

HISTORICAL AVAILABILITY OF RADIOCARBON DATA IN ALASKA

Between 1951 and 1959, 14 radiocarbon age lists were published in *Science*. In 1959, *Radiocarbon* (originally, *American Journal of Science Radiocarbon Supplement*) was introduced as a primary archive for all radiocarbon laboratory age lists. Galloway (1984) indexed the citations in *Radiocarbon* that referred to ages from Alaska.

Publication of radiocarbon age determination lists was not limited to *Radiocarbon*, although the first volume included radiocarbon ages from Alaska (Heusser, 1959). Rainey and Ralph (1959) published a list of archaeological ages determined at the University of Pennsylvania. The purpose of the radiometric age list was to present a tentative framework for Arctic dating. Thus, by the early 1960's, archaeologists were using the radiocarbon dating technique to establish a tentative cultural chronology for the Arctic.

It was not until the mid-1960's that geologists started using radiocarbon ages in the discussion of regional chronologies. Karlstrom (1964) was the first to develop a regional glacial chronology using radiocarbon ages. Karlstrom integrated the partly dated morainal sequences with the more detailed and continuous depositional record of the radiocarbon-dated coastal-bog stratigraphy. He based his study, which included more than 25 radiocarbon ages, on the internal consistency of the ages and their stratigraphic positions (Karlstrom, 1964, p. 58-59).

Since the middle 1970's and early 1980's, several papers have included published radiocarbon ages for specific geographic regions. Péwé (1975) published a detailed discussion of 15 long-recognized stratigraphic units of Quaternary age in unglaciated central Alaska. More than 150 radiocarbon ages were discussed and arranged by geological formation and locality. Gal (1982) published an annotated and indexed roster of archaeological radiocarbon ages from Alaska north of 68° latitude. Hamilton published several U.S. Geological Survey Open-File Reports that list radiocarbon ages and Quaternary stratigraphic sections for 1:250,000 quadrangles in the central Brooks Range, (fig. 1, northern region) the latest being the Survey Pass quadrangle (Hamilton and Brubaker, 1983). Williams and Galloway (1986) published a summary of stratigraphic sections and 61 radiocarbon age determinations from the Copper River Basin (fig. 1, southern region)

DEVELOPMENT OF THE ALASKA DATA BASE

The Radiocarbon Dating Laboratory of the Institute of Marine Science, University of Alaska, compiled the first

Table 1. Laboratories that have reported radiocarbon age determinations on Alaskan samples

[*, inactive laboratory]

Laboratory abbreviation	Number of age determinations	Laboratory
		Domestic
A	18	University of Arizona, Tucson
AA	14	NSF-Arizona Accelerator Facility, Tucson
AU	76	University of Alaska, Fairbanks
Beta	172	Beta Analytic, Inc., Miami, Florida
BGS	10	Brock University, St. Catharines, Ontario, Canada
C*	19	University of Chicago, Chicago
DIC	88	Dicarb Radioisotope Company, Gainesville, Florida
Gx	251	Geochron Laboratories, Cambridge, Massachusetts
I	641	Teledyne Isotopes, Westwood, New Jersey
ISGS	3	Illinois State Geological Survey, Urbana
L	92	Lamont-Doherty Geological Observatory, Columbia University, Palisades, New York
LJ*	13	University of California, San Diego, La Jolla
M*	27	University of Michigan, Ann Arbor
ML	2	Rosensteil School of Marine and Atmospheric Sciences, University of Miami, Florida
OWU*	1	Ohio Wesleyan University, Delaware, Ohio
P*	176	University of Pennsylvania, Philadelphia
PIC*	9	Packard, Downers Grove, Illinois
PIT	10	University of Pittsburgh, Pennsylvania
QL	43	Quaternary Isotope Laboratory, University of Washington, Seattle
RL*	2	Radiocarbon, Ltd., Lampasas, Texas
Sh*	1	Shell, Houston, Texas
SI*	198	Smithsonian Institution, Rockville, Maryland
SM*	13	Mobil Oil Corporation, Dallas, Texas
SMU	5	Southern Methodist University, Dallas, Texas
TAM	1	Texas A & M University, College Station
Tx	8	University of Texas, Austin
UCLA	3	University of California, Los Angeles
UCR	3	University of California, Riverside
UGa	27	University of Georgia, Athens
USGS	279	U.S. Geological Survey, Menlo Park, California
UW*	19	University of Washington, Seattle
W	402	U.S. Geological Survey, Reston, Virginia
WIS	22	University of Wisconsin, Madison
WSU	46	Washington State University, Pullman
Y*	68	Yale University, New Haven, Connecticut
	2,762	Total domestic
		Foreign
B	20	Bern, Switzerland
Birm	1	Birmingham, England
GaK	19	Gakushuin University, Tokyo
Gif	11	Gif-Sur-Yvette, France
GrN	10	Groningen, The Netherlands
GSC	12	Geological Survey of Canada, Ottawa
Hv	2	Hannover, West Germany
IVIC*	1	Caracas, Venezuela
K	27	Copenhagen, Denmark
N	12	Nishina Memorial, Tokyo, Japan
S	21	University of Saskatchewan, Saskatoon, Canada
St	4	Stockholm, Sweden
T	1	Trondheim, Norway
TK	2	University of Tokyo, Japan
	143	Total foreign
Total	2,905	

comprehensive data base of radiocarbon ages for Alaska and adjacent portions of the Yukon Territory and British Columbia (Wilson and Young, 1976). Although the development of the data base was a major contribution, the reporting of radiocarbon ages was limited to citations in *Radiocarbon* and selected USGS Professional Papers. To address this limitation, a literature search of both geological and archaeological publications was undertaken which resulted in the publication of a bibliography of Alaskan radiocarbon ages (Galloway, 1984). Galloway (1987a, b) then used his bibliography and a modified form of Wilson and Young's age list to produce a radiocarbon data base for the State of Alaska.

ALASKA DATA BASE FILE FORMAT

For the Alaska data base the record for each age consists of a minimum of eight fields: (1) radiocarbon age determination, in years B.P., (2) the standard deviation, or one-sigma error, (3) the laboratory code number, (4) latitude, (5) longitude, (6) 1:250,000 quadrangle abbreviation, (7) geographic region abbreviation, and (8) author citation index. Table 2 is an example of the Alaska data base file format.

Most age lists appearing in *Radiocarbon* contain geographic coordinates in the sample descriptions. Articles in journals and other reports, however, often report only a general geographic location. If a geographic location is included in the *Dictionary of Alaska Place Names* (Orth, 1967), the geographic coordinates listed are incorporated into the Alaska data base (Galloway, 1987a). Geographic region (fig. 1) and 1:250,000 quadrangle abbreviations are those used by the U.S. Geological Survey, Branch of Alaskan Geology, and are listed in Galloway (1984, 1987a).

It is not uncommon for researchers to disagree on the interpretation of an age or series of ages. Thus, unpublished ages and ages lacking a laboratory and reference number are excluded from the Alaskan radiocarbon data base (Galloway, 1987a). The author citation index field contains at least one published reference and may include nine additional citations. Future goals for increasing the completeness of the file include a thorough search of all doctoral and masters' theses related to the Quaternary geology and archaeology of Alaska.

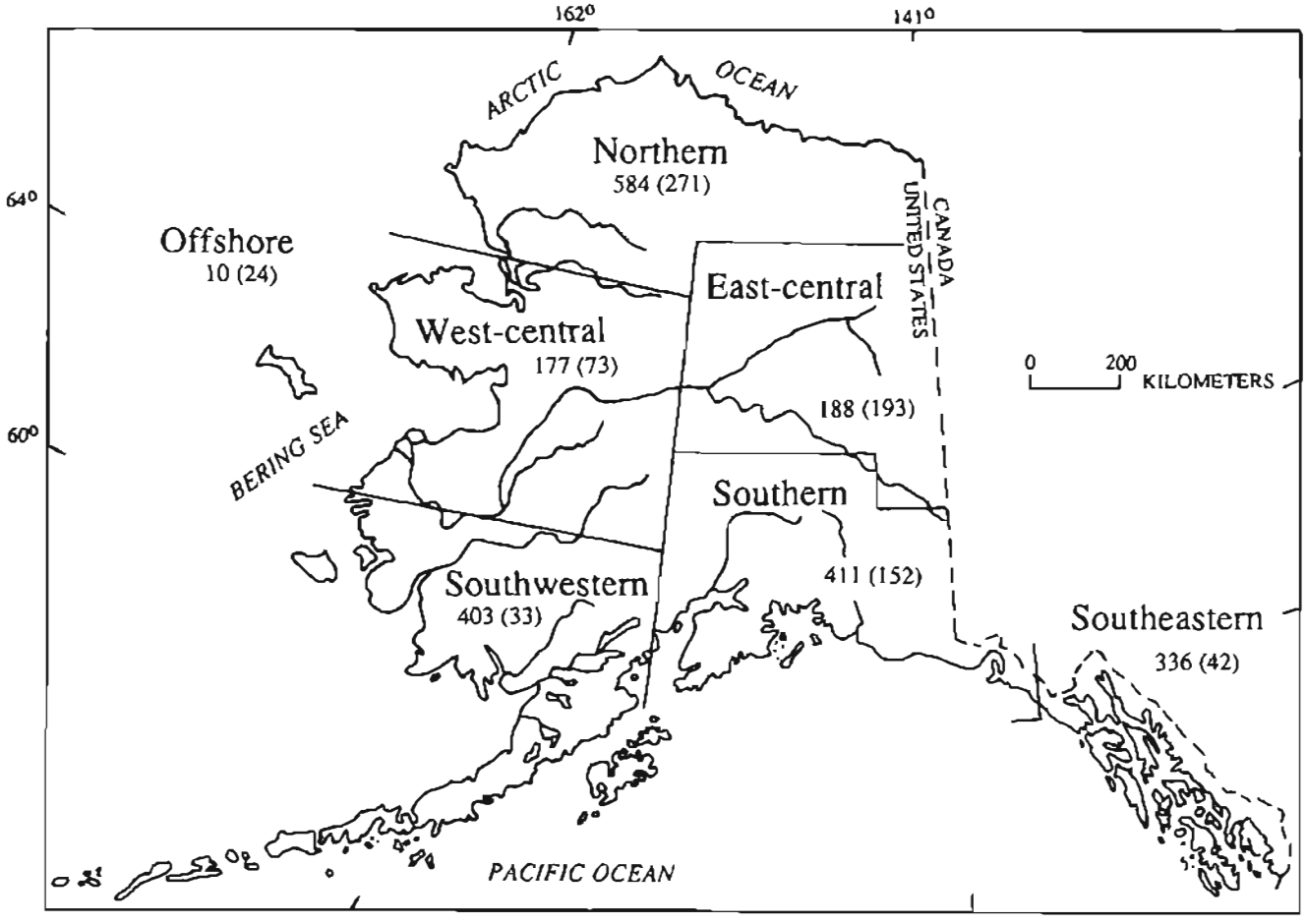

Figure 1. Map of Alaska showing number of Holocene and Pleistocene radiocarbon age determinations by geographic region (number of Pleistocene ages in parentheses).

Table 2. Alaska data base file format

[Quadrangle and region abbreviations are those used by the U.S. Geological Survey, Branch of Alaskan Geology]

Field	Data	Comments
Age	17730	^{14}C determination (yrs B.P.)
Standard deviation	320	One-sigma error
Laboratory	I-4777	Laboratory code and number
Latitude	67:05n	Degrees and minutes north
Longitude	158:10w	Degrees and minutes east or west
Quadrangle	ar	1:250,000 quadrangle (in this case, Ambler River)
Region	nor	Geographic region (in this case, Northern)
Reference 1	Schweger, 1982	Published reference
Reference 2	Hamilton, 1982	Published reference
Reference 3	Hamilton, 1986	Published reference

The Alaska data base is available as ASCII character files on IBM-compatible 360 K diskettes (Galloway, 1987b). The Alaska data base contains 2,905 radiocarbon age determinations (2,113 Holocene and 792 Pleistocene). Figure 1 shows the number of Holocene and Pleistocene radiocarbon age determinations by geographic region. Additional information regarding the Alaska data base can be obtained by writing Galloway.

INTERNATIONAL RADIOCARBON DATA BASE (IRDB)

As stated by Austin Long (1989), editor of *Radiocarbon*, "this journal will respond to the changing manner of accessing ^{14}C dates by co-evolving with the digital data bases containing ^{14}C dates and site information. As centralized digital data bases take over an increasing share of the responsibility of providing this service to the scientific community, *Radiocarbon* will decrease its commitment to publication of date lists." "Decrease" is indeed the overriding trend in the publication and dissemination of radiocarbon data for a variety of reasons (Kra, 1988a). The IRDB was implemented to manage the abundant data that have resulted from technological advances in the field and to provide a research tool for investigators in many disciplines.

The Alaska radiocarbon data base is a subset of the larger International Radiocarbon Data Base. Other data bases are maintained by the Geological Survey of Canada (Roger McNeely, personal commun., 1989); for California (Breschini and others, 1990); Oxford, United Kingdom (R.E.M. Hedges, personal commun., 1989); Harwell, United Kingdom (Walker and others, 1990) and Groningen, The Netherlands (Engelsman and others, in press), to name but a few of the regional data bases that are interrelated with the IRDB.

Table 3. International Radiocarbon Data Base (IRDB) file format

[I, index (search capabilities); I-K, index to keyword; VL, variable length]

Field	Characters	Type
1. Laboratory code (for example, A)	10	I
2. Laboratory number (for example, 4755)	10	--
3. Sample name (or ID number)	--	VL
4. ^{14}C determination (yrs B.P.)	10	I
5. ^{13}C value	10	--
6. Sample material	25	I-K
7. Country	20	I-K
8. Latitude	15	I
9. Longitude	15	I
10. Site name (also state, provinces)	25	I-K
11. Submitter (last name, initial, date)	25	I
12. Discipline (archaeology, geology)	15	I-K
13. Association (period, context)	25	I-K
14. References	--	VL
15. Comments (includes calibration data)	--	VL

In addition to the Alaska data base, Galloway has also compiled an unpublished file of 190 published ages from the USSR, a data set that will become an integral element in the emerging cooperative projects between the U.S. and USSR.

IRDB FILE FORMAT

The data entry format of the IRDB consists of 15 fields in ASCII character files (table 3). The criteria for these fields evolved from the cooperative efforts of the Radiocarbon Data Base Commission over a period of several years (Kra, 1986, 1988a, b, 1989, in press; Walker and Kra, 1988). The present structure is considered a workable minimum, or catalogue-type directory, which has been set up to integrate regional data bases.

The first two fields of the file format (table 3) contain the sample number, divided into letters and numerals. Fields 8 and 9, latitude and longitude, have also been divided into two separate units. There are three variable length (VL) fields: (3) sample name, (14) references, and (15) comments, which constitute the relational part of the data base. The data base is brief, but adaptable and versatile, and can be used for interpretational information. Where only essential data are supplied, as in the case of the Alaska data base, the investigator is directed to primary sources.

ACCESS TO THE DATA BASES

Retrieval of data from either the Alaska data base or IRDB may be sorted according to individual needs. For example, an investigator who is interested in Pleistocene fossils from west-central Alaska (WCE) can request a printout or a file on a diskette listing first, WCE site locations, and second, ages older than 10,000 yrs B.P.

Information regarding access to the Alaska Data Base and the IRDB can be obtained by contacting:

John P. Galloway
Branch of Alaskan Geology
U.S. Geological Survey Mail Stop 904
345 Middlefield Road
Menlo Park, Calif. 94025
415-329-5688

Renee Kra
International Radiocarbon Data Base
Department of Geosciences
The University of Arizona
4717 E. Ft. Lowell Road
Tucson, Arizona 85712
602-881-0857
Bitnet: C14@ARIZRVAX
Fax: 602-881-0554

REFERENCES CITED

Breschini, G.S., Haversat, T., and Erlandson, J., 1990, California radiocarbon dates, 6th ed.: Salinas, Calif., Coyote Press.

Engelsman, F.M.R., Mook, W.G., and Taaijke, E., in press, Operations of the Groningen ^{14}C data base, *in* International Symposium, Archaeology and ^{14}C, 2d. PACT.

Gal, R., 1982, Appendix I: An annotated and indexed roster of archaeological radiocarbon dates from north of 68° latitude: Fairbanks, Anthropological Papers of the University of Alaska, v. 20, nos. 1-2, p. 159-180.

Galloway, J.P., 1984, Bibliography of published radiocarbon dates for Alaska: U.S. Geological Survey Open-File Report 84-21, 42 p.

——— 1987a, A list and index of published radiocarbon dates for Alaska with a bibliography: U.S. Geological Survey Open-File Report 87-517-A, 117 p.

——— 1987b, Radiocarbon date list for Alaska to accompany USGS Open-File Report 87-517-A: U.S. Geological Survey Open-File Report 87-517-B (5 1/4 inch diskette formatted for IBM-PCs using DOS 2.0 in a standard ASCII format).

Hamilton, T.D., and Brubaker, L.B., 1983, Quaternary stratigraphic sections, with radiocarbon dates, Survey Pass quadrangle: U.S. Geological Survey Open-File Report 83-72, 47 p.

Heusser, C.J., 1959, Radiocarbon dates of peat from North Pacific North America: American Journal of Science Radiocarbon Supplement, v. 1, p. 29-34.

Karlstrom, T.N.V., 1964, Quaternary geology of the Kenai lowland and glacial history of the Cook Inlet region, Alaska: U.S. Geological Survey Professional Paper 443, 69 p.

Kra, Renee, 1986, Report of the ^{14}C data base workshop, *in* Stuiver, Minze, and Kra, R.S., eds., International ^{14}C Conference, 12th, Proceedings: Radiocarbon, v. 28, no. 2A, p. 800-802.

——— 1988a, Updating the past: The establishment of the International Radiocarbon Data Base: American Antiquity, v. 53, no. 1, p. 118-125.

——— 1988b, The first American Workshop on the International Radiocarbon Data Base: Radiocarbon, v. 30, no. 2, p. 259-260.

——— 1989, Report of the International Radiocarbon Data Base Workshop, *in* Long, Austin, and Kra, R.S., eds., International ^{14}C Conference, 13th, Proceedings: Radiocarbon, v. 31, no. 3., p. 1076-1078.

——— in press, Establishing the International Radiocarbon Data Base, *in* International Symposium, Archaeology and ^{14}C, 2d: PACT.

Long, Austin, 1989, From the editor: Radiocarbon, v. 31, no. 1, p. ii.

Nelson, R.E., Carter, L.D., and Robinson, S.W., 1988, Anomalous radiocarbon ages from a Holocene detrital organic lens in Alaska and their implications for radiocarbon dating and paleoenvironmental reconstructions in the Arctic: Quaternary Research, v. 29, no. 1, p. 66-71.

Orth, D.J., 1967, Dictionary of Alaska place names: U.S. Geological Survey Professional Paper 567, 1084 p.

Péwé, T.L., 1975, Quaternary stratigraphy nomenclature in unglaciated central Alaska: U.S. Geological Survey Professional Paper 862, 32 p.

Rainey, F. and Ralph, E.K., 1959, Radiocarbon dating in the Arctic: American Antiquity, v. 24, no. 4, pt. 1, p. 365-374.

Walker, A.J., and Kra, R., 1988, Report on the International Radiocarbon Data Base (IRDB) Workshop, Archaeology and ^{14}C Conference, Groningen, The Netherlands: Radiocarbon, v. 30, no. 2, p. 255-258.

Walker, A.J., Otlet, R.L., Housley, R.A., and van der Plicht, J., 1990, Operation of the Harwell UK ^{14}C data base and its expansion through data exchange with other laboratories: Radiocarbon, v. 32, no. 1, p. 31-35.

Williams, J.R., and Galloway, J.P., 1986, Map of western Copper River Basin, Alaska, showing lake sediments and shorelines, glacial moraines, and location of stratigraphic sections and radiocarbon-dated samples: U.S. Geological Survey Open-File Report 86-390, 30 p., 1 sheet.

Wilson, F.H. and Young, M.S., 1976, Radiocarbon dates for Alaska, Yukon Territory and British Columbia: Fairbanks, University of Alaska, Institute of Marine Science, IMS Report R76-6, 64 p.

Reviewers: Richard Koch and Warren Yeend

The Nature and Significance of Post-Thermal-Peak Shear Zones West of the Great Tonalite Sill Near Juneau, Southeastern Alaska

By Robert J. Hooper, David A. Brew, Glen R. Himmelberg, Harold H. Stowell, Robert L. Bauer, *and* Arthur B. Ford

INTRODUCTION

The Coast Mountains of the northern Cordillera are underlain by a linear belt of plutonic and metamorphic rocks, the Coast plutonic-metamorphic complex (CPMC) as defined by Brew and Ford (1984), that extends over 1,700 km along the Pacific coast of Alaska and Canada, from the Yukon Territory to southern British Columbia. The belt has been divided into three segments in southeastern Alaska and adjacent British Columbia: a western metamorphic belt; a central belt of dominantly granitic rocks, variously called the Coast plutonic complex, central gneiss complex, or central granitic belt; and an eastern metamorphic belt (fig. 1).

The western metamorphic belt of the CPMC is an extremely long (≥900 km) and narrow (7–25 km) belt of dynamothermally metamorphosed rocks. In the time period 120 to 50 Ma, multiple episodes of deformation and regional and contact metamorphism affected the belt, resulting in a complex overprinting of mineral assemblages and tectonite fabrics (Brew and others, 1989).

The metamorphic grade and amount of deformation within the western metamorphic belt increases from southwest to northeast, culminating adjacent to the "great tonalite sill" of the CPMC. Isograds of a Barrovian metamorphic sequence (the M5 metamorphic belt of Brew and others, 1989) parallel the trend of the great tonalite sill to the west of the sill near Juneau. Mineral isograds in pelitic rocks were first identified by Forbes (1959) and have subsequently been confirmed and refined over a 150-km segment of the western metamorphic belt in the northern Coast Mountains (Ford and Brew, 1973, 1977; Brew and Ford, 1977; Stowell, 1986, 1989). Bauer and others (1988) described the relative timing of porphyroblast growth, foliation development, and early high-temperature ductile shearing in the rocks near Juneau and noted, but did not discuss in detail, local late-stage shear zones that postdate the emplacement of the sill. These late-stage shear zones developed during one of the latest and most poorly documented and understood deformational events recognized in the western metamorphic belt. This preliminary note describes the available data about these important features.

The late-stage shear zones near Juneau developed within a complexly deformed sequence of metasedimentary and metavolcanic rocks. The most common rock types in the sequence are greenstone, slate, impure quartzite, impure limestone, amphibolite, amphibole mica schist, and mica schist. The late-stage shear zones contrast with the surrounding foliated metamorphic rocks in three ways: they are finer grained, they contain lower grade mineral assemblages, and they are marked by abundant microscopic shear-sense indicators. Their distribution is currently poorly understood; they are clearly recognizable in thin section, but they have not yet been mapped as laterally continuous zones in the field. The distribution of thin sections that lack the late-stage microscopic features demonstrates that the zones are discrete and are probably concentrated in meter- to several-meter-thick packages within the higher grade metamorphic rocks. The shear zones apparently parallel the dominant local northwest-striking and moderately to steeply northeast-dipping foliation and compositional layering.

The heterogeneous nature of the country rocks exerts considerable control over shear-zone location. The shear zones are preferentially located in mica-rich or pelitic rocks; they are less common in greenstones and carbonate-rich rocks and seldom found in quartz-rich or psammitic rocks. We therefore interpret our available data to indicate that shear-zone location within the metamorphic rock sequence is controlled in part by lithology and that shear-zone orientation is controlled in part by preexisting structure. More intensive study of shear-zone orientation and location and more extensive sampling are needed to fully explore the controls of shear-zone distribution and development.

We collected 19 oriented samples in two traverses, about 7 km apart, across an 8-km width of the western metamorphic belt. Metamorphic mineral assemblages represented indicate that the samples range from the biotite to the sillimanite zones. At least two oriented thin sections were cut from each oriented sample. Of the 19 samples, 5

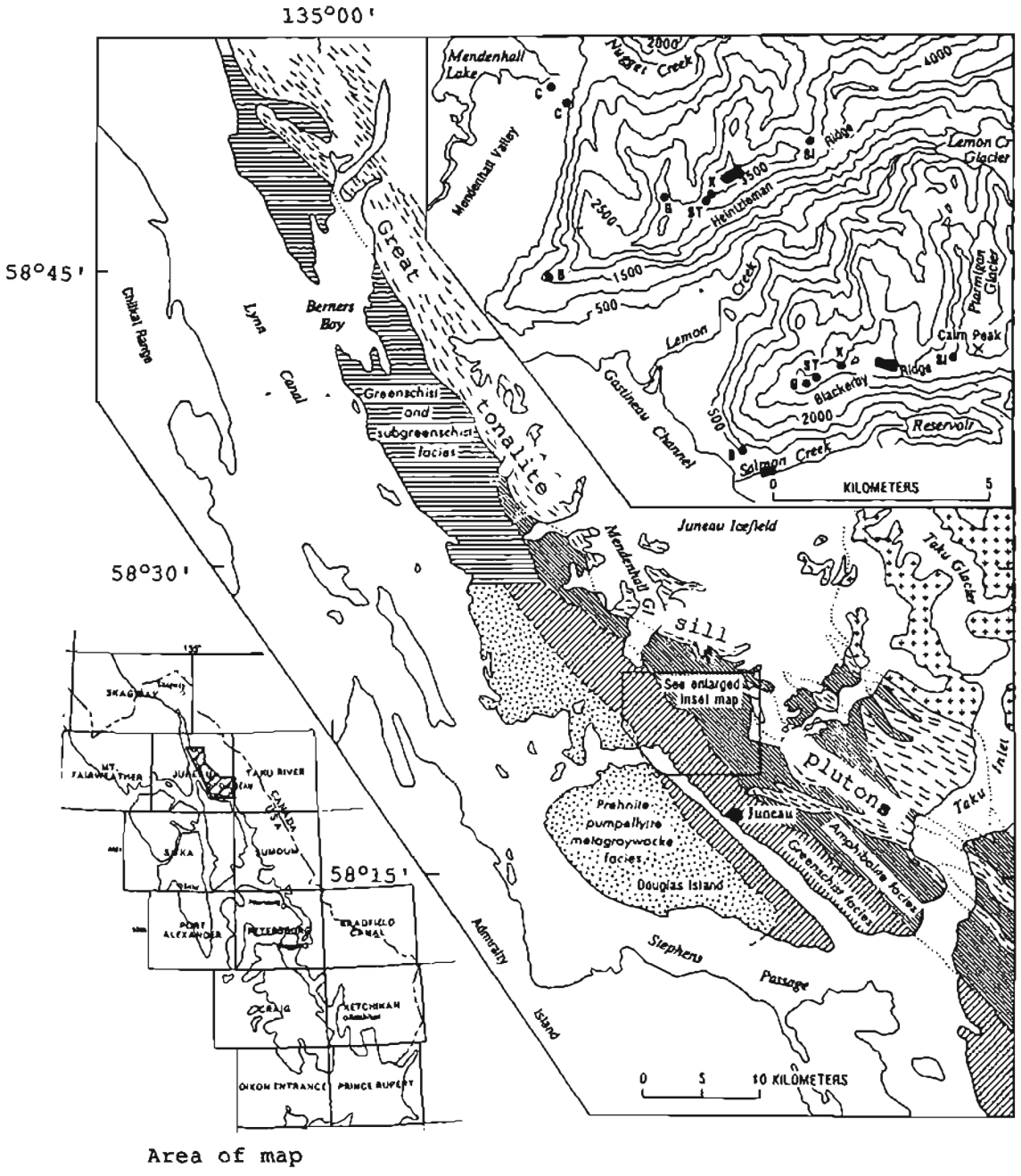

Figure 1. Sketch map of Juneau area, southeastern Alaska, showing regional distribution of metamorphic facies in western metamorphic belt and their relation to plutonic units of Coast plutonic-metamorphic complex as defined by Brew and Ford (1984). Dashed-line pattern shows approximate foliation trends in orthogneiss plutons of great tonalite sill. Crosses denote weakly foliated post-tectonic granodiorite pluton. Geologic contacts dashed where approximately located; dotted where concealed. Inset topographic map (500-ft contours) shows first occurrences in northeastward transects on Heintzleman and Blackerby Ridges of biotite (B), garnet (G), staurolite (ST), kyanite (K), and sillimanite (SI), and occurrences of chloritoid. Solid rectangular boxes enclose locations of five samples studied. After Himmelberg and others (1984b).

are described in detail below; several others contained similar, but not as well developed, features. The five samples described here are all from a 4.8-km-wide part of the 8-km-wide sampled area; their locations are shown in figure 1. Other samples within this 4.8-km-wide area do not contain the late-stage shear zones. The distribution of samples unaffected by late-stage shearing suggests that the late-stage shear zones may not be as common within about 2.5 km of the southwest margin of the great tonalite sill as they are farther west in our two traverses. Although the numbers of traverses, of samples within the traverses, and of samples studied in detail at this time are not large, we believe they are representative of the western metamorphic belt in this general area.

MICROSCOPIC CHARACTERISTICS OF THE SHEAR-ZONE ROCKS

Metamorphic textures in these rocks were recently described by Himmelberg and others (1984a, b) and Bauer and others (1988). Chlorite and muscovite in low-grade pelitic rocks generally occur as small laths parallel to and defining the schistosity. Biotite in the garnet zone, the staurolite zone, and part of the kyanite zone occurs both as porphyroblasts and as small plates that parallel the schistosity. These porphyroblasts commonly contain an internal schistosity, defined by strings of quartz inclusions and opaque dust, that is at a high angle to the external schistosity. In the upper kyanite zone and higher grade zones, biotite occurs only as small plates that, together with muscovite (where present), define the schistosity. Garnets range in size from small idioblastic grains to large porphyroblasts. Some garnet porphyroblasts contain well-preserved rotated internal foliation; others contain nonrotated internal foliation. Staurolite and kyanite porphyroblasts commonly contain helicitic inclusion trails. Sillimanite occurs primarily as fibrolite parallel to schistosity, although small prismatic grains are also present. Sillimanite locally replaces kyanite and is commonly found in biotite. Quartz and plagioclase form polygonal granoblastic aggregates.

In addition to the above information, we note that many quartz-rich samples have distinctive granoblastic textures with abundant grain boundary triple points (fig. 2*A*). Foliations within these samples are generally weak in thin section, defined by aligned individual crystals and crystal aggregates of biotite. Individual crystals within elongate grain aggregates of biotite are locally oriented with cleavage at a high angle to foliation (fig. 2*A*).

The late-stage shear zones in all rock types in the metamorphic sequence are identifiable as zones of considerable grain-size reduction that have a closer spaced and more uniform foliation than in the surrounding rocks (for example, compare fig. 2*A*, *B*). Lineation defined by elongate biotite clots and by aligned staurolite and kyanite crystals is common. Schistosity and lineations that developed during earlier orogenesis have been completely transposed into the new foliation in the shear zones. The only recognizable fabrics that predate this late shearing are the inclusion trails of quartz and opaque minerals sometimes preserved in garnet and biotite porphyroclasts (fig. 2*C*).

Porphyroclasts of biotite, garnet, and calcite-quartz are clearly definable in rocks of appropriate composition (fig. 2*B*, *C*, *D*, *E*, *F*). The porphyroclasts are isolated in a fine-grained foliated matrix that locally contains quartz ribbons aligned parallel with the foliation (fig. 2*B*, *F*, *G*). Weak shear-band foliation is locally developed in fine-grained mica-rich rocks in regions of homogeneous foliation (fig. 2*E*). Aluminum silicate minerals do not occur in the shear zones, even where they are abundant in adjacent parent rocks.

Foliation in quartzofeldspathic rocks is defined by a strong dimensional preferred orientation of biotite, white mica, chlorite, and quartz ribbons (fig. 2*B*, *G*, *H*). Quartz ribbons in regions of homogeneous foliation display a strong dimensional preferred orientation parallel to the mylonitic foliation (fig. 2*G*). Matrix phyllosilicates display strong lattice preferred orientations with c-axes aligned normal to the mylonitic foliation. Locally, chlorite crystals are oriented with their cleavage traces at a high angle to the dominant foliation. Perturbed zones occur in the shear-zone foliation where ribbons and matrix flow around porphyroclasts (fig. 2*C*, *D*, *E*).

Quartz ribbons are polycrystalline aggregates composed predominantly of equant grains with high-angle, planar grain boundaries that define a granoblastic polygonal texture (fig. 2*G*). Grain boundary triple-points are common. Individual grains display weak nonuniform extinction and minor subgrain development; they are for the most part free of unrecovered strain (fig. 2*G*). Pronounced quartz lattice preferred orientations within ribbons (as determined using a gypsum plate) and preferred quartz subgrain fabric orientations have not been observed.

Some garnet porphyroclasts have a sievelike appearance (fig. 2*C*, *E*). Quartz inclusion trails are present in some garnets but they rarely bear a systematic relationship to the shear-zone foliation (fig. 2*C*, *E*). Curved inclusion trails often have a sense of vorticity that is opposite to that in the matrix (fig. 2*C*) indicating that the trails record a pre-shear-zone deformation.

Biotite porphyroclasts occur as augen- or fish-shaped crystal fragments or crystal aggregates (fig. 2*B*, *D*) in shear zones with in biotite-bearing parent rocks. They are commonly asymmetric with tails of biotite, white-mica, and chlorite that extend into, and are parallel with, the dominant foliation in the rock (fig. 2B, *D*). The porphyroclasts are commonly poikiloblastic, containing abundant quartz blebs and vermicules (fig. 2*D*). Some porphyroclasts are partially replaced by chlorite (fig. 2*D*) that may or may not be parallel with the foliation in the matrix.

Foliation in shear zones within amphibolites is defined by a strong dimensional preferred orientation of phyllosilicates, calcite-quartz ribbons, and aggregates of both epidote and fine-grained opaque minerals (fig. 2*F*).

SHEAR-SENSE INDICATORS

The late-stage shear zones strike west of north (320°–350°) and dip moderately to steeply to the northeast (60°–75°); mineral lineations within the shear zones plunge moderately to the northeast. The zones are invariably developed parallel to compositional layering in the surrounding rocks. Offset layering cannot, therefore, be used to determine the sense and magnitude of displacement across the shear zones; the sense of displacement can only be deduced using microstructures. Identifiable microstructural criteria potentially useful in determining shear-sense in the late-stage shear zones include asymmetrical porphyroclast systems (as described by Simpson and Schmid, 1983, and Passchier and Simpson, 1986) and shear-band foliations (as described by White and others, 1980) or extensional crenulation cleavages (as described by Platt and Vissers, 1980, and Dennis and Secor, 1987). As is typical in deformed metamorphic rocks, only a small percentage of tailed and nontailed porphyroclast systems yield an unequivocal sense of shear due to local clast interference and perturbations of the flow field in the matrix.

Biotite fish commonly display an asymmetric habit, with tails that stretch out into and merge with the shear-zone foliation. The tails step-up in the shear direction; for example, the sense of shear of the porphyroclast in figure 2*D* is top-to-the-left. Calcite-quartz porphyroclasts in sheared amphibolitic rocks also have asymmetrical tails of recrystallized material that step-up in the shear direction; the sense of shear of porphyroclasts in figure 2*F* is top-to-the-left. Distinctive asymmetrical perturbed zones occur in the matrix immediately adjacent to some garnet and calcite-quartz porphyroclasts. The foliation in perturbed zones is inclined in the shear direction; the sense of shear from the garnet porphyroclasts in figure 2*C* and 2*E* is thus top-to-the-left. Microscopic-scale shear-bands are developed in fine grained rocks with high matrix phyllosilicate content. The shear-bands have a normal fault geometry and step down in the shear direction. The shear-bands at the bottom of figure 2*E* cut down to the right, hence the sense of shear is top-to-the-left; this is in accordance with the sense of shear determined from the matrix perturbations around the garnet porphyroclast.

Microstructural criteria within the late-stage shear zones, irrespective of type, produce a consistent sense of shear both within (fig. 2*E*) and between samples. Thin sections were cut parallel with the mineral lineation. All sections display clockwise shear sense when viewed in the plane of the foliation down the plunge of the normal to the lineation, here, to the southeast. Mineral lineations within the shear zones plunge moderately to the north-northeast on northwest-striking (320°–350°) foliation that dips moderately to the east-northeast (60°–75°). The shear zones are, therefore, zones of contractional oblique-slip. The dip-slip motion component is northeast-side-up or northeast over southwest; the strike-slip motion component is right-lateral.

The Barrovian sequence mineral assemblages in the protolithic rocks developed in response to the initial intrusion/emplacement of the great tonalite sill during the M5 metamorphic event (Brew and others, 1989). The granoblastic textures evident in many protolith samples are similar to those that develop as a result of thermally driven static annealing; these textures overprint earlier high-temperature fabrics. This relationship was recognized by Brew and others (1989), and both the contrasting textural and mineral assemblage data are discussed by Himmelberg and others (1990). The granoblastic textures and lower temperature and pressure mineral assemblages are now referred to by those workers as the M5' metamorphic event. The details of the timing of mineral growth and fabric development in relation to pluton emplacement and thermal events are not easy to resolve, however, and their relations need further careful evaluation. The late-stage shear zones described here modify the Barrovian mineral assemblages and contain lower temperature mineral assemblages than their parent rocks. The stable assemblages in the shear zones (chlorite-white mica; calcite-epidote) indicate that the zones developed under hydrous conditions at lower greenschist facies pressures and temperatures. The shear zones must, therefore, have developed after the thermal peak of the M5 event of Brew and others (1989), but probably still within the same thermal event. We presently consider them likely to be part of the M5' event.

DISCUSSION

The currently available microscopic shear-sense data suggest dominant east-side-up motion with a right-lateral component across the late-stage shear zones. This movement is compatible with displacement sense determined for low-temperature shear zones west of the Coast Range megalineament about 25 km southeast of Juneau (Hooper and Stowell, 1989) and in the Holkham Bay area about 90 km southeast (Stowell and Hooper, 1990). Late shear zones in the Holkham Bay area are all zones of oblique slip with a right-lateral motion component. More importantly, the shear-zone lineations there plunge in both a northerly and a southerly direction (Stowell, 1986), indicating both east-side-up and east-side-down displacement. It is possible, therefore, that though individual shear zones may have had simple oblique-slip histories, the late-stage shear-zone system along the west side of the CPMC as a whole did not develop during a simple oblique-slip event. The difference between the east-side-up and east-side-down displacement vectors

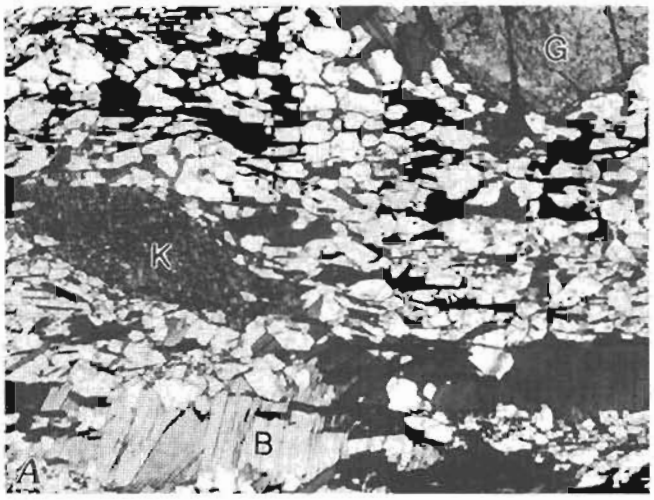

0 1 MILLIMETER

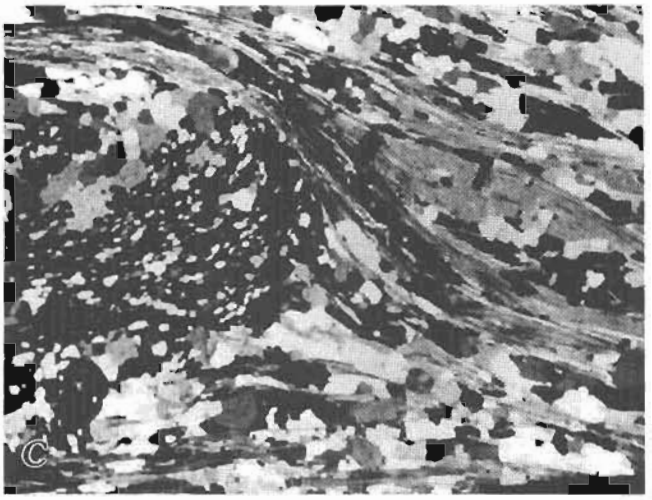

0 1 MILLIMETER

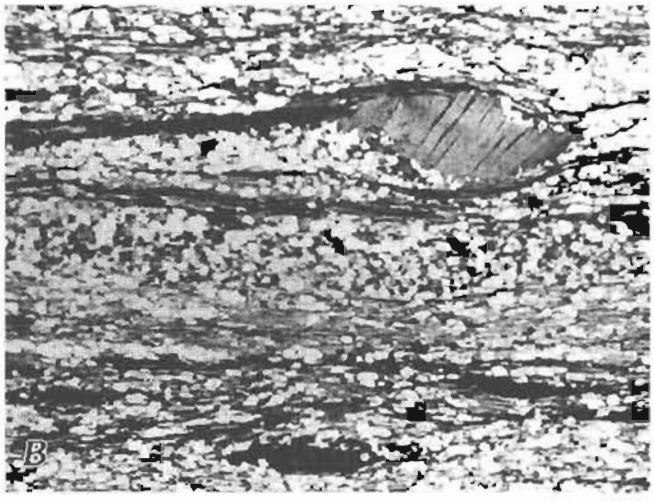

0 1 MILLIMETER

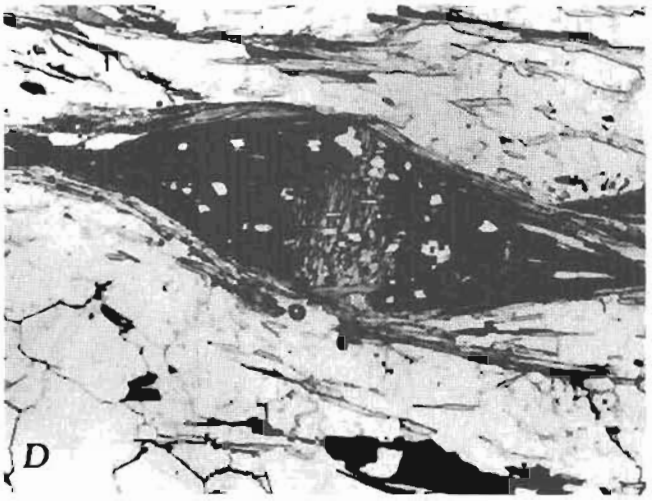

0 1 MILLIMETER

Figure 2. Photomicrographs of late-stage shear zone and related samples from western metamorphic-belt of the Coast plutonic-metamorphic complex near Juneau, Alaska. All views [are looking] north-northwest. *A*, Inferred protolith of sample 51AP2 (see *H*). Porphyroblasts of garnet (G) and kyanite (K) occur in a dominantly quartz matrix that has a distinctly granoblastic texture. Weak subhorizontal foliation is defined by aligned individual crystals and crystal aggregates of biotite. Individual crystals within elongate aggregates of biotite (B) are oriented at a high angle to subhorizontal layering. Sample 50AP2; plane-polarized light. *B*, Shear-zone foliation defined by strong dimensional preferred orientation of white mica and biotite. Quartz ribbons parallel with foliation display granoblastic texture. Shear sense determined from asymmetrical biotite fish is anticlockwise or top-to-left. Sample 41BP2; plane-polarized light. *C*, Poikilitic garnet porphyroclast with asymmetrical tails of quartz and white mica that extend into shear-zone foliation. Dominant foliation is defined by strong dimensional preferred orientation of white mica, biotite, quartz ribbons, and minor chlorite. Quartz inclusion trails within garnet indicate clockwise sense of vorticity. Shear sense determined from symmetrical quartz tails in shadow of garnet porphyroclast and asymmetry of matrix perturbation around the porphyroclast is anticlockwise or top-to-left. Sample 42AP1; cross-polarized light. *D*, Poikilitic biotite fish with rim of white mica and chlorite. Center of fish is replaced by chlorite. Dominant subhorizontal foliation is defined by aligned white mica and biotite. Shear sense is anticlockwise or top-to-left.

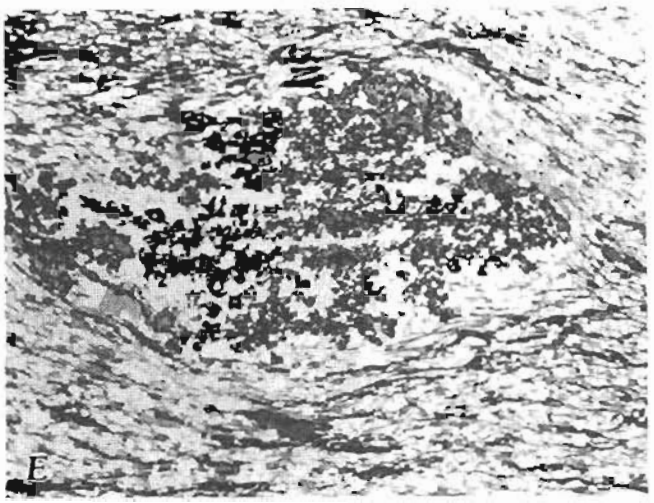

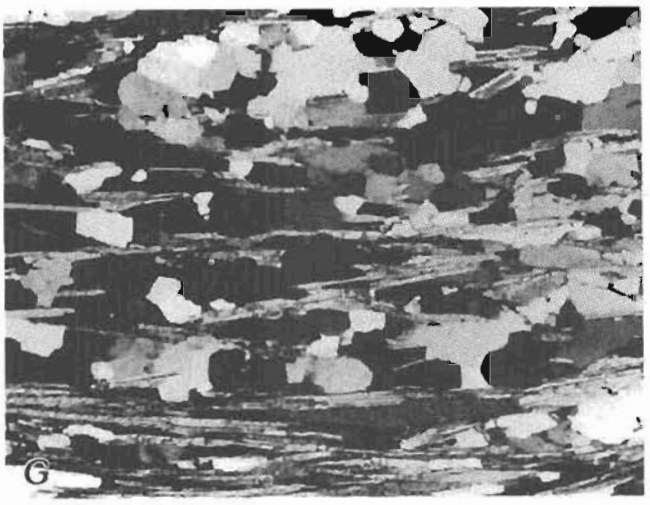

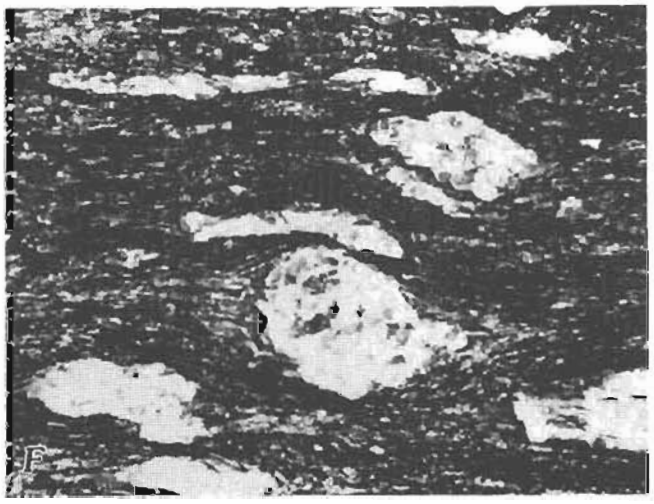

Sample 42AP1; plane-polarized light. *E*, Asymmetrical skeletal garnet porphyroclast in matrix composed of fine-grained quartz, white mica, and biotite. A shear-band foliation with normal fault geometry is visible in lower half of picture. Foliation steps down to the left—sense of shear is therefore anticlockwise or top-to-left. This is consistent with top-to-left shear sense determined from asymmetrical step-up of foliation around garnet porphyroclast. Sample 52AP1; plane-polarized light. *F*, Porphyroclasts of calcite, quartz, and epidote in a fine-grained matrix of epidote, biotite, quartz, minor calcite, and opaque minerals. Foliation in matrix is defined by aligned biotite, epidote aggregates, opaque blebs, and calcite-quartz ribbons. Porphyroclast asymmetry indicates anticlockwise shear sense or top-to-left. Sample 48AP1; plane-polarized light. *G*, Homogeneous shear-zone foliation in region away from influence of porphyroclasts. Foliation is defined by a strong dimensional preferred orientation of white mica, biotite, and quartz ribbons. Ribbons are composed predominantly of equant grains with high-angle, planar grain boundaries. Grain boundary triple-points are common. Individual grains display weak nonuniform extinction and with minor subgrain development; they are for the most part free of unrecovered strain. Sample 42AP1; cross-polarized light. *H*, Late-stage shear zone in same material as sample 50AP2 (see *A*). Note considerable grain size reduction and closer spaced foliation (as compared with protolith) defined by preferred orientation of white mica and biotite. Garnet porphyroclast (G) has partial shell of chlorite. Sample 51AP2; plane-polarized light.

could be related to different motion increments that were kinematically necessary components of an overall right-lateral strike-slip system oriented generally north-south. The dip-slip motion components could reflect adjustments for local compression (possibly related to local compressional bridges) or a broader transpressional environment for the system as a whole.

REFERENCES CITED

Bauer, R.L., Himmelberg, G.R., Brew, D.A., and Ford, A.B., 1988, Relative timing of porphyroblast growth, foliation development, and ductile shear in pelitic metamorphic rocks from the Juneau area, southeastern Alaska, *in* Galloway, J.P., and Hamilton, T.D., eds., Geologic studies in Alaska by the U.S. Geological Survey during 1987: U.S. Geological Survey Circular 1016, p. 138-142.

Brew, D.A., and Ford, A.B., 1977, Preliminary geologic and metamorphic-isograd map of the Juneau B-1 quadrangle, Alaska: U.S. Geological Survey Miscellaneous Field Studies Map MF-846, scale 1:31,680.

———1984, The northern Coast plutonic complex, southeastern Alaska and northwestern British Columbia, *in* Coonrad, W.L., and Elliott, R.L., eds., The United States Geological Survey in Alaska: Accomplishments during 1981: U.S. Geological Survey Circular 868, p. 120-124.

Brew, D.A., Ford, A.B., and Himmelberg, G.R., 1989, Evolution of the western part of the Coast plutonic-metamorphic complex, south-eastern Alaska, USA: A summary, *in* Daly, J.S., Cliff, R.A., and Yardley, B.W.D., eds., Evolution of metamorphic belts: Geological Society of London Special Publication 43, p. 447-452.

Dennis, A., and Secor, D., 1987, A model for the development of crenulations in shear zones with applications from the Southern Appalachian Piedmont: Journal of Structural Geology, vol. 9, p. 809-817.

Forbes, R.B., 1959, The bedrock geology and petrology of the Juneau Ice Field area, southeastern Alaska: Seattle, University of Washington, Ph.D. dissertation, 260 p.

Ford, A.B., and Brew, D.A., 1973, Preliminary geologic and metamorphic-isograd map, Juneau B-2 quadrangle, Alaska: U.S. Geological Survey Miscellaneous Field Studies Map MF-527, scale 1:31,680.

———1977, Preliminary geologic and metamorphic-isograd map of the northern parts of the Juneau A-1 and A-2 quadrangles, Alaska: U.S. Geological Survey Miscellaneous Field Studies Map MF-847, scale 1:31,680.

Himmelberg, G.R., Ford, A.B., and Brew, D.A., 1984a, Progressive metamorphism of pelitic rocks in the Juneau area, southeastern Alaska, *in* Coonrad, W.L., and Elliott, R.L., eds., The United States Geological Survey in Alaska: Accomplishments during 1982: U.S. Geological Survey Circular 939, p. 105-108.

———1984b, Progressive metamorphism of pelitic rocks in the Juneau area, southeastern Alaska, *in* Coonrad, W.L., and Elliott, R.L., eds., The United States Geological Survey in Alaska: Accomplishments during 1981: U.S. Geological Survey Circular 868, p. 131-134.

Hooper, R.J., and Stowell, H.H., 1989, Kinematics of faulting within the western metamorphic belt, south of Juneau, Alaska: Geological Society of America Abstracts with Programs, v. 21, no. 5, p. 94.

Passchier, C.W., and Simpson, C., 1986, Porphyroclast systems as kinematic indicators: Journal of Structural Geology, vol. 8, p. 831-843.

Platt, J., and Vissers, R., 1980, Extensional structures in anisotropic rocks: Journal of Structural Geology, vol. 2, p. 397-410.

Simpson, C., and Schmid, S.M., 1983, An evaluation of criteria to deduce the sense of movement in sheared rocks: Geological Society of America Bulletin, vol. 94, p. 1281-1288.

Stowell, H.H., 1986, Sphalerite geobarometry in metamorphic rocks and the tectonic history of the Coast Ranges near Holkham Bay, southeastern Alaska: Princeton N.J., Princeton University, Ph.D. dissertation, 276 p.

———1989, Silicate and sulphide thermobarometry of low- to medium-grade metamorphic rocks from Holkham Bay, southeast Alaska, Journal of Metamorphic Geology, vol. 7, p. 343-358.

Stowell, H.H., and Hooper, R.J., 1990, Constraints on the structural development of the western metamorphic belt, Holkham Bay, SE Alaska: Tectonics (in press).

White, S., Burrows, S., Carreras, J., Shaw, N., and Humphreys, F., 1980, On mylonites in ductile shear zones: Journal of Structural Geology, vol. 2, p. 175-187.

Reviewers: Mary M. Donato and Richard M. Tosdal

Proterozoic U-Pb Zircon Age of Granite in the Kallarichuk Hills, Western Brooks Range Alaska: Evidence for Precambrian Basement in the Schist Belt

By Susan M. Karl *and* John N. Aleinikoff

INTRODUCTION

The southwestern Brooks Range consists dominantly of metasedimentary rocks, with subordinate metavolcanic and meta-intrusive rocks. Age information for these metamorphosed rocks is very limited. Earlier studies have yielded Paleozoic fossils, and a few K-Ar ages suggest Late Proterozoic metamorphism of some rocks structurally underlying the schist belt of the southern Brooks Range (Turner and others, 1979; Mayfield and others, 1982). U-Pb analyses of zircons from various metamorphosed granitic rocks in the southern Brooks Range have yielded Proterozoic to Devonian ages (Dillon and others, 1980). Because the metasedimentary rocks are metamorphosed to greenschist, blueschist, and locally amphibolite facies, sedimentary structures and fossils are typically rare and poorly preserved, and it is difficult to distinguish the age of constituent marble, quartzite, and pelite protoliths. For this reason, protolith ages of meta-intrusive rocks provide especially important constraints on the ages of the metasedimentary and metavolcanic rocks.

A new U-Pb age of 705±35 Ma has been determined for zircons from granite intruding rocks, previously considered to be Paleozoic in age (Brosgé and others, 1967; Mull and others, 1987), that structurally underlie extensive thrust sheets of quartz mica-schist of the schist belt in the southwestern Brooks Range (fig. 1). This age is similar to a U-Pb age of 750±6 Ma (Karl and others, 1989a) determined for zircons from granite north of and structurally underlying the schist belt at Mount Angayukaqsraq (fig. 1). The granites also show some similarities in composition and chemistry. Both granites intrude mixed metasedimentary and metavolcanic rocks structurally underlying the schist belt in the Baird Mountains quadrangle, but until now there has been no means of correlating the two rock sequences, and geologic mapping has not confirmed structural connections between them.

REGIONAL GEOLOGY

The southwestern Brooks Range is composed of marble, quartzite, metapelitic rocks, and mafic metavolcanic rocks that range from Proterozoic to Cretaceous in age. The rocks record a long history of continental margin and carbonate platform sedimentation interrupted by minor episodes of volcanic activity. Shallow-water facies are indicated by the abundance of marble and the rapid stratigraphic alternation of marble, quartzite, metaconglomerate, and pelite throughout the section. The Proterozoic rocks locally retain evidence of a Proterozoic amphibolite-facies metamorphic event (Turner and others, 1979; Armstrong and others, 1986; Till and others, 1988; Karl and others, 1989a). This metamorphism is one of the few distinguishing characteristics of the Proterozoic rocks, but it is commonly masked by pervasive mid-Cretaceous greenschist- to blueschist-facies metamorphism and deformation that resulted in development of a fold and thrust belt that extends for the length of the Brooks Range (summarized in Mayfield and others, 1983).

The Proterozoic rocks are interpreted to be stratigraphic basement (Mayfield and others, 1982) that is exposed both in structural windows and lateral ramps (Karl and others, 1989b) and in out-of-sequence thrusts. In the western Brooks Range, they are structurally the lowest component observed in the fold and thrust belt. They are overlain by extensive thrust sheets of quartz-mica and mica-quartz schist, which collectively form the schist belt, a major component of the hinterland of the fold and thrust belt in the southern Brooks Range.

SAMPLE DESCRIPTION

The dated sample (85SK175B) was collected from a granite body of irregular shape, 1/2 to 1 km across, occurring within massive light-gray marble. Contacts are very poorly exposed, but an intrusive relation is inferred based on (1) the irregular shape of the granite and (2) the presence of smaller lenses or layers of granite that resemble dikes in the marble. The marble is hundreds of meters thick and occurs as a thick lens in a sequence of metasedimentary rocks in the Kallarichuk Hills (fig. 2). No fossils have been recovered from this marble, and no sedimentary textures are preserved. The marble, granite, and metasedimentary

rocks have greenschist-facies mineral assemblages. They are exposed structurally below, and west of, quartz-mica schist of the schist belt (fig. 1).

The granite sampled is light gray, medium to fine grained, with pink potassium feldspar and white centimeter-sized albite porphyroblasts and is locally well foliated to gneissic. It is an alkali-feldspar granite by the classification of Streckeisen (1976) and contains 7 percent mafic minerals, which consist of biotite partly being replaced by chlorite. Accessory minerals include sphene and zircon. Secondary minerals include chlorite, sericite, magnetite, and calcite. Quartz grains are locally granulated parallel to the foliation, indicating high strain. Major- and trace-element chemistry of the dated sample is presented in table 1.

The sample is texturally and mineralogically similar to alkali-feldspar granites that are a minor phase of the Proterozoic intrusive rocks in the vicinity of Mount Angayukaqsraq (Karl and others, 1989a), 75 km to the northeast of the Kallarichuk Hills, on the north side of the schist belt (fig. 1). However, although some trace-element abundances are similar, the chemistry shows some differences between the granites, such as CaO percent, K_2O/Na_2O, FeO/MgO, and Rb/Sr, which suggest that the rocks from Mount Angayukaqsraq are more highly fractionated (table 1).

GEOCHRONOLOGY

The dated sample, 85SK175B, contains zircons that are blocky, with length-to-width ratios of 1 to 4, subhedral to euhedral, and medium to dark brown. All grains have pitted faces, and most have only one pyramidal termination. Five zircon fractions, based on size and magnetic susceptibility, were analyzed for U-Pb isotopes. The least discordant fractions are the ones that were abraded (prior to dissolution), and they also have the highest common lead. Uranium con-

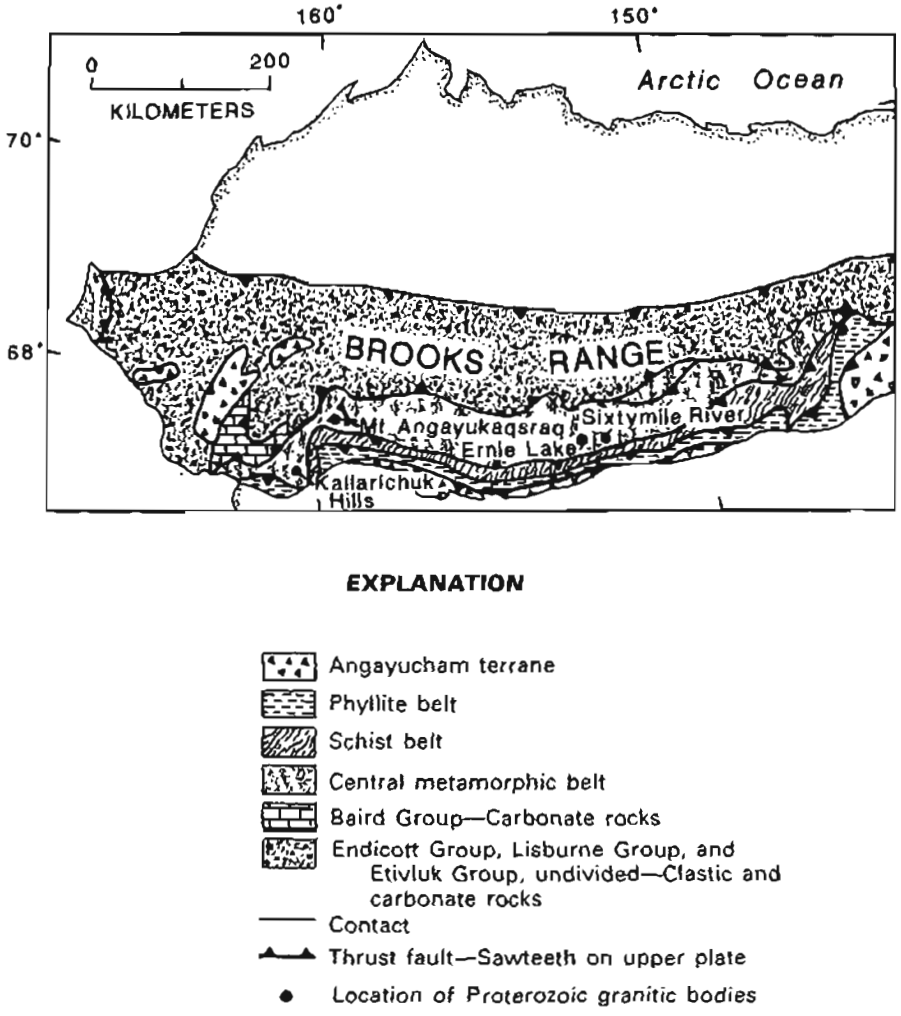

Figure 1. Map of northern Alaska showing location of intrusive rocks at Kallarichuk Hills, Mt. Angayukaqsraq, Ernie Lake, and Sixtymile River within central metamorphic belt of Brooks Range.

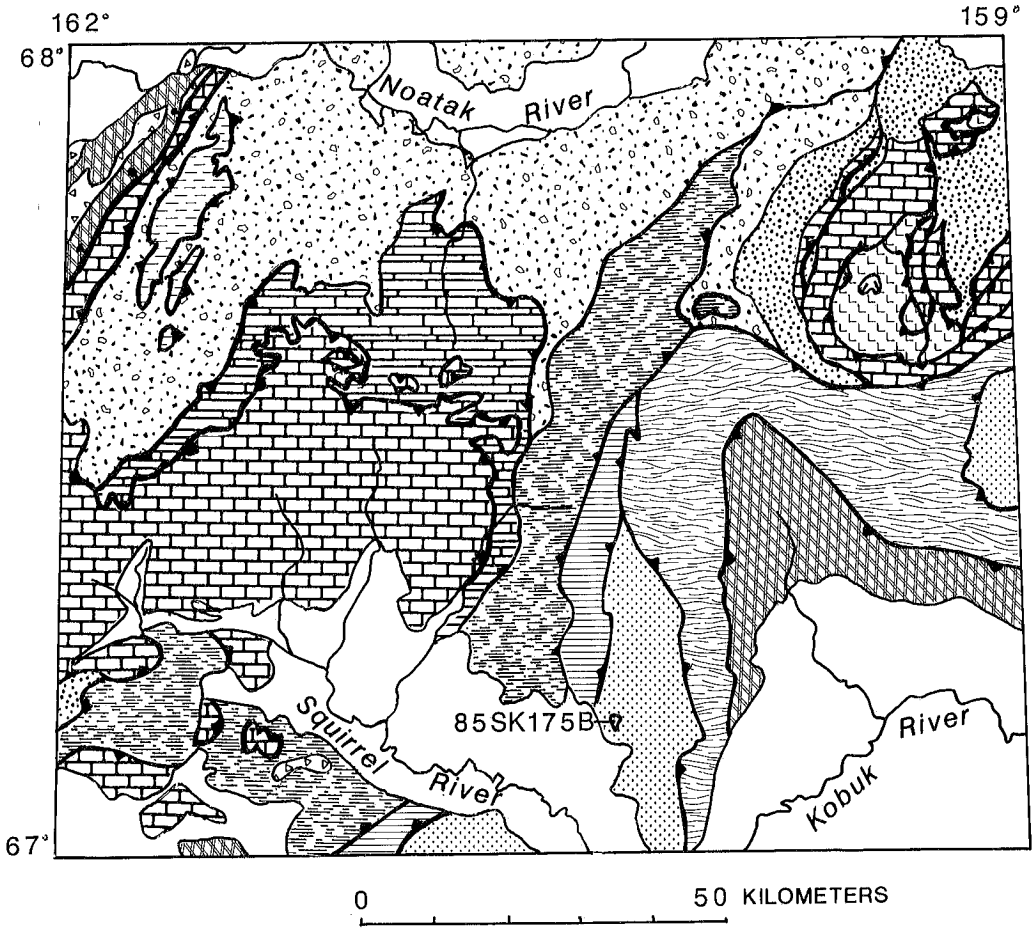

EXPLANATION

- Surficial deposits (Quaternary)
- Mafic to intermediate intrusive, extrusive, and volcaniclastic rocks (Mesozoic to Paleozoic)
- Melange with blocks of greenstone, chert, marble, and greenschist in a phyllitic matrix (Mesozoic or Paleozoic)
- Etivluk Group, Lisburne Group, and Kayak Shale, undivided (Triassic to Mississippian)
- Endicott Group (Mississippian and Devonian)
- Limestone and clastic rocks of Nakolik River (Devonian)
- Baird Group and carbonate rocks, undivided (Paleozoic)
- Quartz-mica schist (Paleozoic)
- Marble, siliceous schist, and calc schist (Paleozoic)
- Carbonaceous quartzite, micaceous marble, and phyllite (Paleozoic)
- Metasedimentary rocks (Paleozoic)
- Quartzose and pelitic schists (Paleozoic and Proterozoic)
- Intrusive rocks (Proterozoic)
- Metasedimentary and metavolcanic rocks (Proterozoic)
- Contact
- Fault
- Thrust fault—Sawteeth on upper plate
- Normal fault—Ball and bar on hanging wall

Figure 2. Generalized geologic map of the Baird Mountains quadrangle and location of sample 85SK175B.

Table 1. Major- and trace-element chemistry for a Proterozoic granite sample from the Kallarichuk Hills and average of four Proterozoic granite samples (Karl and others, 1989a) from Mount Angayukaqsraq, western Brooks Range

[Samples analyzed by the U.S. Geological Survey, Menlo Park, Calif. LOI, volatiles lost in the analytical process]

Map locality	(1) Kallarichuk Hills	(2) Mount Angayukaqsraq
Sample numbers	85SK175B	Average (78MD119, 84SK214A, 85SK163A, 85SK165C)
Rock type	Alkali-feldspar granite	Alkali-feldspar granite
SiO_2	71.37%	76.33%
Al_2O_3	12.60	12.64
Fe_2O_3	3.04	94
FeO	1.18	52
MgO	39	30
CaO	2.10	41
Na_2O	3.10	2.43
K_2O	5.49	6.13
TiO_2	.57	.22
P_2O_5	.13	.05
MnO	.03	.03
Total	100.00	100.00
(LOI)	(1.55)	(.74)
Nb	34 ppm	39 ppm
Rb	120	181
Sr	170	20
Zr	365	381
Y	62	70

centrations range from about 168 to 296 ppm (table 2). The isotopic data are discordant, with intercept ages of 705±35 and 63±140 Ma (fig. 3). The scatter in the data may be due to the large component of common lead, ranging from 2 to 15 ppm, in the zircons (table 2), combined with lead loss during more than one heating event. The upper intercept provides a crystallization age; the lower intercept is permissible for the mid-Cretaceous metamorphic event which affected the rocks of the Brookian sequence, but it does not preclude earlier or later events.

CONCLUSION

A new U-Pb zircon age of 705±35 Ma obtained for a granite body in the Kallarichuk Hills in the southwestern Brooks Range is significant because (1) the granite intrudes rocks that were previously thought to be Paleozoic in age (Brosgé and others, 1967; Mull and others, 1987) and (2) the age and composition of this rock are similar to those of the granite at Mount Angayukaqsraq (Karl and others, 1989a), suggesting that the two sequences may be correlative. The important implication is that there may be considerably more Precambrian rocks in the southern Brooks Range than are presently recognized.

The composition and chemistry of the granites from the Kallarichuk Hills and Mount Angayukaqsraq, and the U-Pb systematics of their zircons, differ from those of zircons of the Ernie Lake and Sixtymile River orthogneissic granitic bodies of older Proterozoic age (800–1000 Ma) in the central Brooks Range (fig. 1). The zircons from those orthogneisses show evidence of inheritance of an older crustal component (Dillon and others, 1980, 1987) not observed in zircons from the western Brooks Range (Karl and others, 1989a). However, Sm-Nd isotopic signatures of the granites from Mount Angayukaqsraq yield depleted-mantle crust formation ages of 1.3 to 1.5 Ga (Nelson and others, 1989), indicating the presence of an inherited crustal component in the western Brooks Range granites as well.

REFERENCES CITED

Armstrong, R.L., Harakal, J.E., Forbes, R.B., Evans, B.W., and Thurston, S.P., 1986, Rb-Sr and K-Ar study of metamorphic rocks of the Seward Peninsula and southern Brooks Range, Alaska: Geological Society of America Memoir 164, p. 185-203.

Brosgé, W.P., Reiser, H.M., and Tailleur, I.L., 1967, Copper analyses of selected samples, southwestern Brooks Range, Alaska: U.S. Geological Survey Open-File Report 274, 1 sheet, scale 1:1,000,000.

Dillon, J.T., Pessel, G.H., Chen, J.H., and Veach, N.C., 1980, Middle Paleozoic magmatism and orogenesis in the Brooks Range, Alaska: Geology, v. 8, p. 338-343.

Dillon, J.T., Tilton, G.R., Decker, J., and Kelly, M.J., 1987, Resource implications of magmatic and metamorphic ages for Devonian igneous rocks in the Brooks Range, *in* Tailleur, I.L., and Weimer, Paul, eds., Alaskan North Slope Geology: Bakersfield, Calif., Pacific Section Society of Economic Paleontologists and Mineralogists and Alaska Geological Society, Book 50, p. 713-723.

Karl, S.M., Aleinikoff, J.N., Dickey, C.F., and Dillon, J.T., 1989a, Age and chemical composition of the Proterozoic intrusive complex at Mount Angayukaqsraq, western Brooks Range, Alaska, *in* Dover, J.H., and Galloway, J.P., eds., Geological Studies in Alaska 1988: U.S. Geological Survey Bulletin 1903, p. 10-19.

Karl, S.M., Dumoulin, J.D., Ellersieck, Inyo, Harris, A.G., and Schmidt, J.M., 1989b, Preliminary geologic map of the Baird Mountains and part of the Selawik quadrangles, Alaska: U.S. Geological Survey Open-File Report 89-551, 65 p., scale 1:250,000.

Mayfield, C.F., Silberman, M.L., and Tailleur, I.L., 1982, Precambrian metamorphic rocks from the Hub Mountain terrane,

Table 2. U-Pb isotopic data from zircon from granite in the Killarichuk Hills, western Brooks Range (sample 85SK175B)

Fraction[1]	Wt (mg)	Concentration (ppm)		Pb composition[2]			Ratios (percent error)[3]			Ages (Ma)[4]		
				$^{206}Pb/^{204}Pb$	$^{206}Pb/^{207}Pb$	$^{206}Pb/^{208}Pb$	$^{206}Pb/^{238}U$	$^{207}Pb/^{235}U$	$^{207}Pb/^{206}U$	$^{206}Pb/^{238}U$	$^{207}Pb/^{235}U$	$^{207}Pb/^{206}Pb$
		U	Pb									
(+100)DA	0.55	194.2	37.29	95.514	4.6752	1.8870	0.1036(.16)	0.8929(.67)	0.0625(.62)	635	648	692
(-100+150)D	2.39	203.4	28.35	130.54	5.7831	2.3167	.0868(.18)	.7433(.36)	.0621(.29)	537	564	678
(-100+150)M	.23	168.5	17.92	447.27	10.536	4.1405	.0887(.21)	.7655(.58)	.0626(.49)	547	577	694
(100+150)DA	1.53	172.8	25.48	180.49	6.9907	2.797	.1026(.15)	.8909(.30)	.0630(.25)	630	647	708
(-250)NM	1.15	295.7	29.32	364.74	9.7995	3.7627	.0800(.17)	.6882(.27)	.0624(.19)	496	532	688

[1]Abbreviations: D, diamagnetic; A, abraded; NM, nonmagnetic; M, magnetic.
[2]Blank and fractionation corrected. Blank lead composition is 1:18.7:15.6:37.2.
[3]2σ errors.
[4]Common lead correction uses appropriate values from Stacey and Kramers (1975).

Constants: $^{235}\lambda = 9.8485$ E-10/yr; $^{238}\lambda = 1.55125$ E-10/yr; $^{234}U/^{235}U = 137.88$ (Steiger and Jäger, 1977)

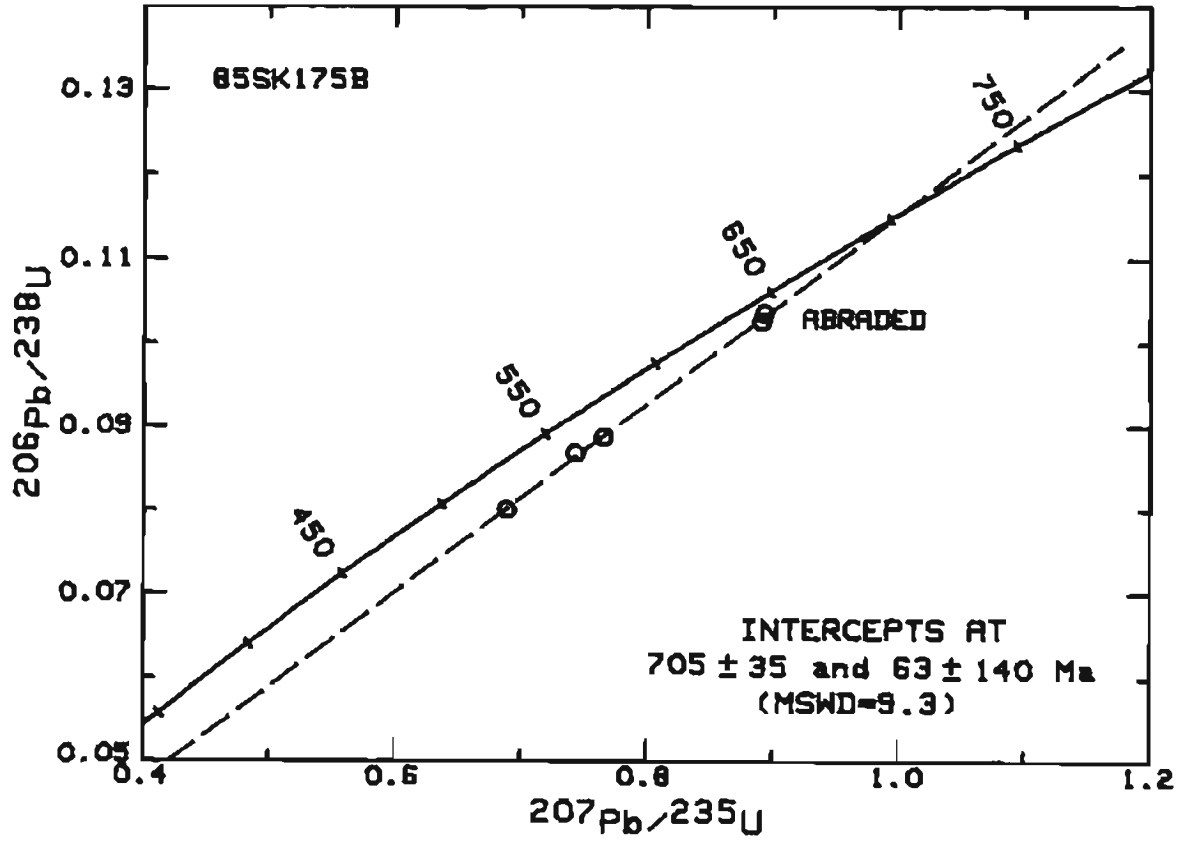

Figure 3. Concordia plot of zircon analyses (open circles) from granite of Killarichuk Hills (sample 85SK175B). Sample data are presented in table 2. MSWD, mean student weighted deviate.

Baird Mountains quadrangle, Alaska, *in* Coonrad, W.L., ed., The U.S. Geological Survey in Alaska: Accomplishments during 1980: U.S. Geological Survey Circular 844, p. 18-24.

Mayfield, C.F., Tailleur, I.L., and Ellersieck, Inyo, 1983, Stratigraphy, structure, and palinspastic synthesis of the western Brooks Range, northwestern Alaska: U.S. Geological Survey Open-File Report 83-779, 58 p.

Mull, C.G., Roeder, D.H., Tailleur, I.L., Pessel, G.H., Grantz, Arthur, and May, S.D., 1987, Geologic sections and maps across Brooks Range and Arctic Slope to Beaufort Sea: Geological Society of America Map and Chart series, MC-28S, scale 1:500,000.

Nelson, B.K., Nelson, S.W., and Till, A.B., 1989, Isotopic evidence of an Early-Proterozoic crustal source for granites of the Brooks Range, northern Alaska: Geological Society of America Abstracts with Programs, v. 21, no. 6, p. A105.

Stacey, J.S., and Kramers, J.D., 1975, Approximation of terrestrial lead isotope evolution by a two-stage model: Earth and Planetary Science Letters, v. 26, p. 207-221.

Steiger, R.H., and Jäger, E., 1977, Subcommission on geochronology: Convention on the use of decay constants in geo- and cosmochronology: Earth and Planetary Science Letters, v. 36, p. 359-362.

Streckeisen, A., 1976, To each plutonic rock its proper name: Earth Science Reviews, v. 12, p. 1-33.

Till, A.B., Schmidt, J.S., and Nelson, S.W., 1988, Thrust involvement of metamorphic rocks, southwestern Brooks Range, Alaska: Geology, v. 16, p. 930-933.

Turner, D.L., Forbes, R.B., and Dillon, J.T., 1979, K-Ar geochronology of the southwestern Brooks Range, Alaska: Canadian Journal of Earth Sciences, v. 16, p. 1789-1804.

Reviewers: Jack Y. Bradshaw and Jeanine M. Schmidt

Summary of Late Cretaceous Environments near Ocean Point, North Slope, Alaska

By R. Lawrence Phillips

INTRODUCTION

Nearly flat lying strata exposed in low bluffs along the big bend of the lower Colville River, near Ocean Point, Alaska, contain North America's northernmost dinosaur remains, record a range of environments including nonmarine, bay, and marine, and are near or may even span the Cretaceous-Tertiary boundary. Identification of depositional features allows reconstruction of paleoenvironments in these high-latitude northern regions where deltaic progradation into the Arctic Ocean dominated the sedimentological history. This report summarizes the stratigraphic setting and depositional environments that existed during the latest Cretaceous and possibly earliest Tertiary in these northern latitudes.

The study area is located on the Arctic Coastal Plain physiographic province along the lower Colville River, approximately 45 km south of the Beaufort Sea at about 70° north latitude (fig. 1).

METHODS

The field investigations, conducted in August 1986, consisted of measuring, describing, and collecting samples from 25 stratigraphic sections along a 10-km stretch of the Colville River. The stratigraphically lowest section begins about 5 m below the lowest dinosaur remains; the highest section is about 70 m above the highest dinosaur remains found to date. The lithology, sedimentary structures, paleocurrent trends, fossils, and texture are identified within each depositional sequence.

SETTING

In the lower Colville River region an angular unconformity separates the Upper Cretaceous (and possibly lower Tertiary) sands and silts of the Prince Creek and Schrader Bluff Formations from the overlying Pliocene and Pleistocene sands and gravels of the Gubik Formation. The strata underlying the Gubik Formation dip gently at 3° or less to the northeast. The beds studied are part of a 178-m-thick stratigraphic section, of which approximately 150 m is exposed (Phillips, 1988).

In the study area along the western and northern sides of the Colville River, 30-m-high bluffs contain excellent and laterally extensive exposures. The strata, in ascending order, represent nonmarine, marginal marine, and marine depositional environments and are all part of the Colville Group (fig. 2). The nonmarine beds are assigned to the Kogosukruk Tongue of the Prince Creek Formation (Brosgé and Whittington, 1966). The bay sediments and the marine beds constitute part of the Sentinel Hill Member of the Schrader Bluff Formation (MacBeth and Schmidt, 1973; Marincovich and others, 1985; McDougall, 1987).

The nonmarine strata are Late Cretaceous in age, but the overlying marine beds may be either Late Cretaceous or early Tertiary in age based on various fossil types found

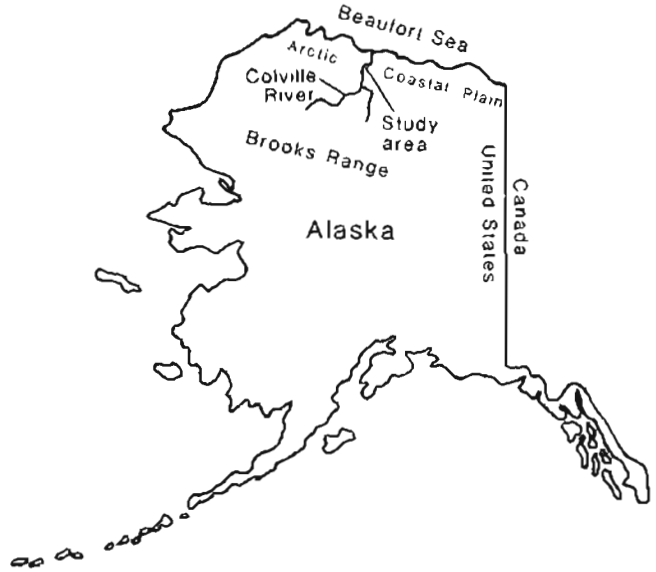

Figure 1. Index map showing location of study area along Colville River in northern Alaska.

within them. The age of the nonmarine strata, based on vertebrate remains, has been called Late Cretaceous (Clemens and Allison, 1985), Maastrichtian or possibly Campanian (Davies, 1987), or Campanian-Maastrichtian (Nelms, 1989), and based on vertebrates and ostracodes Late Campanian to Early Maastrichtian (Brouwers and others, 1987). K-Ar dating of tephra beds bracketing the dinosaur-bone-bearing strata yielded ages between 68 and 71 Ma (Maastrichtian) (McKee and others, 1989; Conrad and others, this volume). The age of the overlying marine beds is in question; on the basis of mollusks and ostracodes the strata have been assigned a Paleocene to early Eocene (Thanetian to Ypresian) age by Marincovich and others (1985). On the basis of benthic foraminifers, the age of the marine strata is considered Campanian (MacBeth and Schmidt, 1973) or early Maastrichtian (McDougall, 1987). On the basis of palynomorphs, the beds are Maastrichtian (Frederiksen and others, 1985, 1986, Frederiksen and Schindler, 1987) or Maastrichtian to Danian (Nelson, 1981).

The exposed sediments consist of well-bedded, unlithified sand, silt, clay, tephra, and organic-rich silt (fig. 3). Silt and clay dominate the flood-plain deposits, whereas, sand dominates the major fluvial, bay, and marine strata.

Nonmarine strata, which make up the lower part of the section, contain major and minor fluvial distributaries, extensive overbank strata, and tephra beds. The nonmarine sediments interfinger toward the top of the stratigraphic interval with interdistributary-bay deposits. A shallow-marine transgressive deposit overlies the nonmarine and bay sediments.

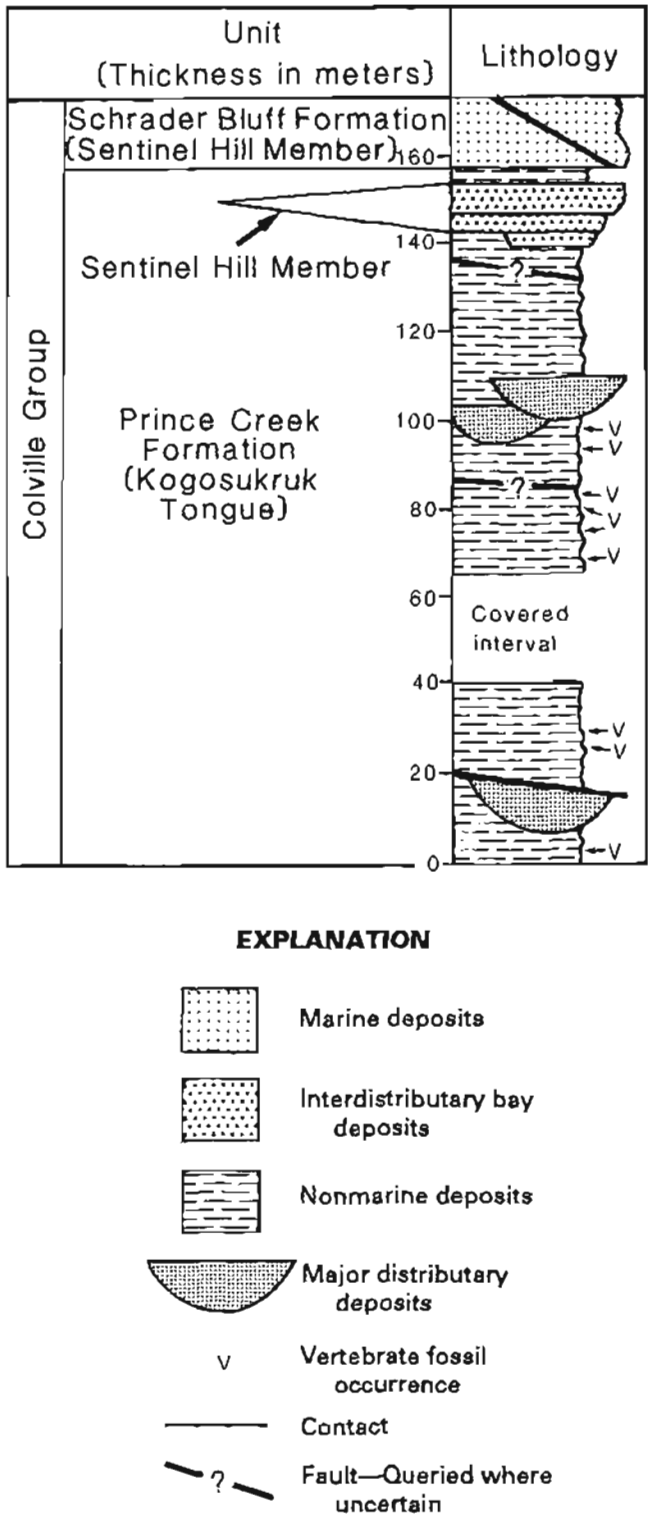

Figure 2. Stratigraphic section and major lithologic features of the Prince Creek and Schrader Bluff Formations along Colville River near Ocean Point, North Slope, Alaska.

NONMARINE DEPOSITS

Major Distributary Deposits

Three sand-filled channels and one mud-filled channel form the major fluvial distributaries identified in the nonmarine section (fig. 3). These strata represent major rivers crossing a flood plain. A thin, discontinuous lag deposit consisting of mud rip-up clasts, carbonized wood fragments, comminuted plant debris, and rare vertebrate fossils set in a matrix of sand forms the basal stratum in the river-channel deposits. Strata overlying the lag deposits exhibit large- and small-scale trough and tabular crossbedding developed in fine to medium sand. The upper beds of the channel deposits, which contain abundant root structures, are composed of sandy mud and are gradational with overlying flood-plain strata.

The fluvial channels represent a meandering river system, one that meandered eastward across the coastal plain transporting the coarsest sediment fraction (medium sand); the rivers were at least 10 m deep and 500 to 600 m wide (width determined from method of Leeder, 1973), approximately the same dimensions as the present-day Colville River in this area. The sediment was transported as suspended load with the sand fraction in lower-flow-regime bedforms; fluctuating velocities produced different bedform types.

Minor-Distributary Deposits

Minor-distributary-stream deposits consist of tabular channel-fill strata having a sharp erosional base and a lower coarse member of gently inclined sandy mud beds grading upward to a fine member of silt and clay. These deposits range in thickness from 2.7 to 5.5 m, averaging 3.4 m. The basal lag deposit consists of fine comminuted plant material, carbonized wood, fresh water invertebrate fossils, mud rip-up clasts, and vertebrate skeletal remains set in a matrix of muddy sand. Small-scale crossbeds interbedded with parallel laminations in fine sand to silt form the basal structures overlying the lag deposits. Sets of epsilon crossbeds dipping at angles of as much as 7°, composed of sets of small-scale crossbeds, grade updip into structureless silt and clay or organic-rich black mud. Vertical, carbonized root traces of ferns and horsetails are common throughout the stream deposits.

The fining-upward beds, as indicated by the abundant epsilon cross-strata, represent fluvial point-bar and accretionary-bank deposits. These grade upward into vertical-accretionary deposits of the flood plain. Shallow (2 to 5 m deep) streams are indicated by the thickness of the epsilon strata. The channel width varied from 25 to 70 m. Current velocities were low, as indicated by the small-scale crossbeds formed by lower-flow-regime current ripples. The deposits containing epsilon crossbeds are interpreted as deposits of streams meandering on a low-gradient coastal plain.

Overbank Deposits

Overbank flood-plain deposits, which are interbedded with the river and stream-channel strata, are the most abundant deposits of the nonmarine sediments. The overbank deposits contain fine sediment (silt and clay) forming laterally continuous fining-upward tabular beds ranging from 17 to 330 cm in thickness. Interbedded fining-upward beds, rare coarsening-upward beds, laminated silt and sand, structureless silt and clay, organic-rich silt, and tephra make up the deposits (fig. 3).

Small-scale crossbeds, planar- and undulatory-laminated sand and silt, thin organic laminations, abundant root structures (ferns and horsetails), load casts, and flame structures composed of organic debris are the typical sedimentary structures in the flood-plain deposits.

Black to dark-brown organic-rich beds, which are laterally continuous and up to 89 cm thick, are found at the top of 69 percent of the fining-upward beds. The strata contain jarosite, pyrite, variable concentrations of comminuted plant debris (including conifer needles), and vertebrate remains.

Crevasse splays and overbank sheetfloods are the most abundant depositional environments recognized in the overbank deposits. The organic-rich strata interbedded with the overbank deposits may have multiple origins, but many are interpreted or inferred to represent immature paleosols.

Interbedded with the organic-rich strata and flood-plain deposits are 16 tephra beds. The tephra deposits, which range up to 60 cm in thickness, are laterally continuous, pinch out, or are interbedded with the organic-rich paleosols. Small-scale crossbeds, horizontal laminations, and abundant root structures are common in the tephra deposits.

The tephra deposits are interpreted as resulting from air-fall of ash onto the flood plain, where, in some beds, the ash may have been reworked either by wind or water.

Vertebrate Occurrences

Associated with some organic-rich sediments and fluvial deposits are abundant hadrosaurian remains (Clemens and Allison, 1985; Davies, 1987; Brouwers and others, 1987; and Nelms, 1989), which record histories of multiple deposition and transport. Four organic-rich vertebrate-bearing flood-plain deposits and five channel-lag occurrences were identified (fig. 3). The vertebrate remains are found in abundance within the four thickest organic-rich beds. The bones are disarticulated and vertically size-graded, with the largest bones usually at the base of the bed. The vertebrate remains are inferred to have initially accumulated on the flood plain but were later transported, probably short distances, by currents during overbank flooding, swept along with organic debris and deposited in local depressions (ponds or marshes). Scattered bones are also found within the basal lag deposits in both the major and minor distributary fluvial deposits.

INTERDISTRIBUTARY BAY DEPOSITS

The bay deposits are recognized in two stratigraphic sequences separated by rooted nonmarine mud beds. Where the basal contact of the upper-bay deposit is exposed, these strata rest on organic-rich coastal-plain beds. The bay strata grade upward into prograding coastal-plain beds (fig. 3). Very fine sandy silt to silty sand forms the bay sediment. Sedimentary structures consist of sets of trough and tabular small- and large-scale crossbeds, flaser beds, parallel laminations, hummocky crossbeds (in upper part of upper bay sequence), deformed beds, abundant bioturbation, and abundant root structures (some truncated). Fossils, found only within the hummocky cross-strata, consist of mussels, ostracodes, and foraminifers.

The assemblages of sedimentary structures define specific depositional environments within the bay deposits. Depositional environments identified include intertidal sand flats (tidal range >20 cm based on truncated roots), small

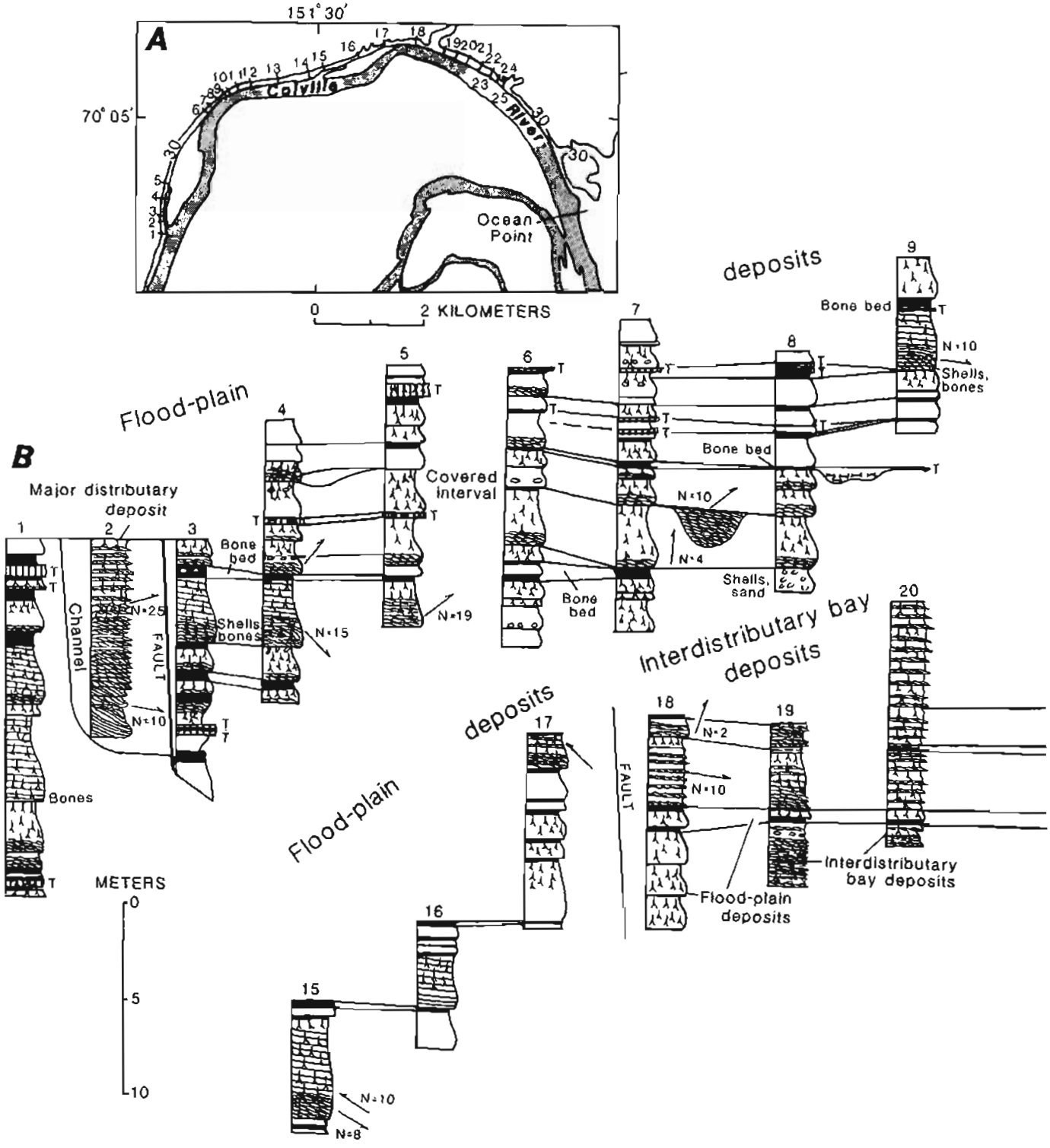

Figure 3. Measured sections of the Prince Creek and Schrader Bluff Formations along Colville River near Ocean Point, North Slope, Alaska. *A*, Location of measured sections. Contour in meters. *B*, Measured sections, depositional features, and environmental interpretation of part of the Prince Creek and Schrader Bluff Formations.

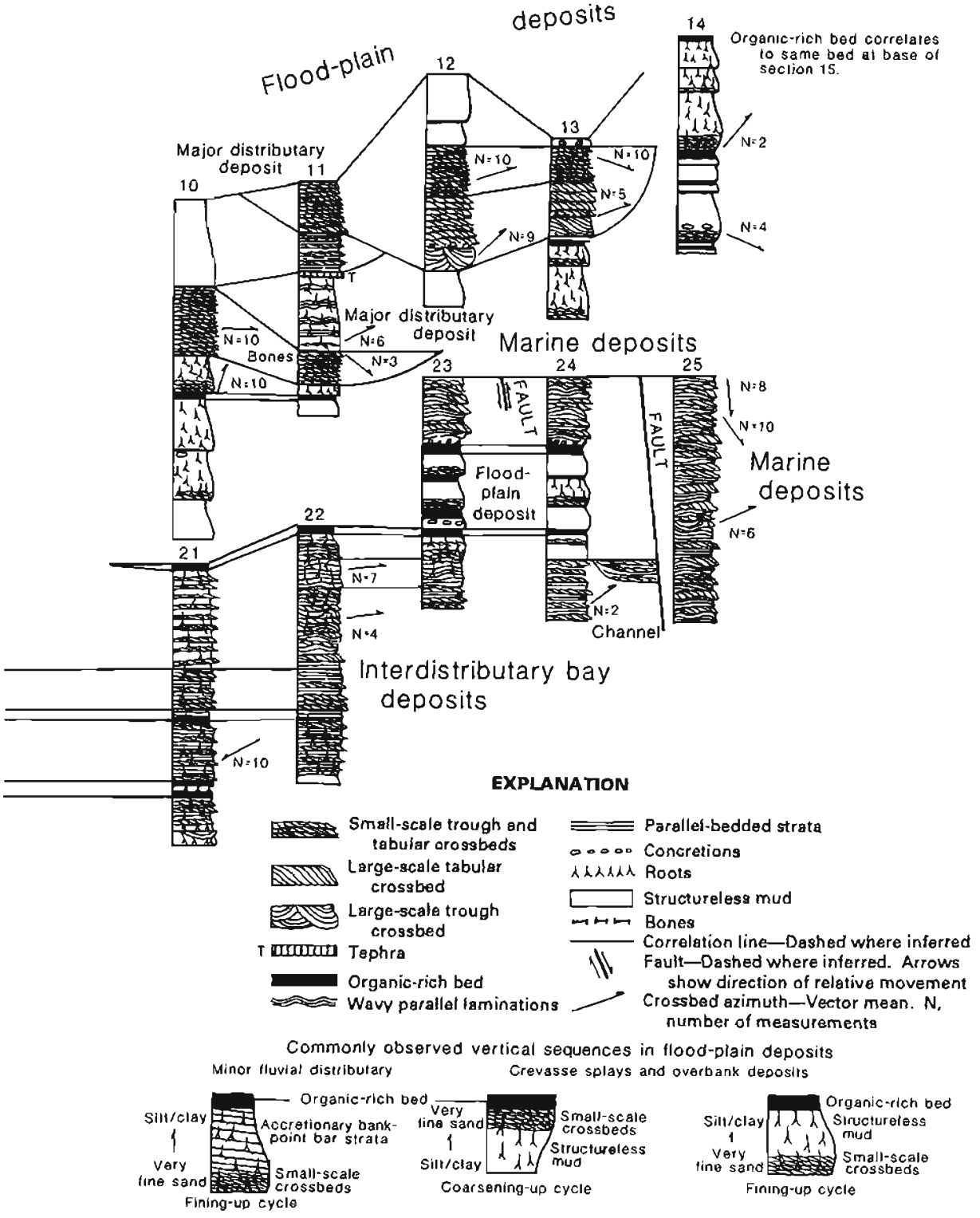
deposits
Flood-plain
12
14
Organic-rich bed correlates to same bed at base of section 15.
13
Major distributary deposit
11
10
N=10
N=10
N=5
N=9
N=2
N=4
T
Major distributary deposit
N=6
N=3
Marine deposits
N=10
Bones
N=10
23
24
25
FAULT
FAULT
N=8
N=10
Marine deposits
Flood-plain deposit
N=6
22
21
N=7
N=4
N=2
Channel
Interdistributary bay deposits
N=10
EXPLANATION
Small-scale trough and tabular crossbeds
Large-scale tabular crossbed
Large-scale trough crossbed
T Tephra
Organic-rich bed
Wavy parallel laminations
Parallel-bedded strata
Concretions
Roots
Structureless mud
Bones
Correlation line—Dashed where inferred
Fault—Dashed where inferred. Arrows show direction of relative movement
Crossbed azimuth—Vector mean. N, number of measurements
Commonly observed vertical sequences in flood-plain deposits
Minor fluvial distributary
Organic-rich bed
Silt/clay
Accretionary bank-point bar strata
Very fine sand
Small-scale crossbeds
Fining-up cycle
Crevasse splays and overbank deposits
Very fine sand
Small-scale crossbeds
Silt/clay
Structureless mud
Coarsening-up cycle
Organic-rich bed
Silt/clay
Structureless mud
Very fine sand
Small-scale crossbeds
Fining-up cycle

channel deposits, and storm deposits. The maximum water depth during deposition of the upper bay deposit would be less than 7 m. The shallow bays were open to the ocean, allowing storm waves direct access to the bay. Filling of the bay by coastal progradation resulted in deposition of nonmarine strata over the bay-fill strata.

MARINE DEPOSITS

Marine strata overlying the nonmarine beds represent a transgressive, shallow, storm-dominated depositional sequence (fig. 3). The sediment texture ranges from sand to silty sand in storm-generated beds to sandy silt in nonstorm intervals. Sedimentary structures consist of interbedded planar to gently dipping laminations, sets of climbing small-scale crossbeds, trough crossbeds, hummocky cross-stratification, and abundant bioturbation. Shell lag deposits and pelecypods in growth position are common. Megafossils reported from the marine beds include pectens and other pelecypods, gastropods, brachiopods, echinoids, and a cephalopod; microfossils include both ostracodes and foraminifers (MacBeth and Schmidt, 1973; Marincovich and others, 1985; McDougall, 1987).

The depositional environment of this marine sequence is interpreted to be a shallow storm-dominated shelf environment. As storm-generated hummocky cross stratification is believed to be preserved between fair-weather wavebase and storm wavebase, water depths were probably between a few meters to several tens of meters (Dott and Bourgeois, 1982).

SUMMARY OF ENVIRONMENTS

Most of the 178 m of strata studied at the Ocean Point area was deposited on a low-gradient, low-relief coastal lowland that toward the top of the section was periodically inundated with marginal-marine and marine waters. The coastal plain was extensively vegetated by wetland plants (ferns and horsetails). Major rivers and streams meandered across the flood plain carrying a suspended sediment load. Overbank sheet-flow, the result of river flooding, was the primary mechanism of sediment aggradation along the coastal plain. The coastal-plain environment graded into a marginal-marine shallow bay environment. Shallow channels, extensively vegetated tidal flats, and storm-wave reworking of the bay sediments are the dominant features of the bay deposits. The transgressive shallow-marine sediments record repetitive storm events within a shelf environment. The overall paleogeographic setting during deposition of these strata was probably very similar to that of the present-day North Slope coastal plain shoreline and shelf. Regional relations suggest that the coastline at this time had a northwest-southeast trend.

REFERENCES CITED

Brosgé, W.P., and Whittington, C.L., 1966, Geology of the Umiat-Maybe Creek region, Alaska: U.S. Geological Survey Professional Paper 303-H, p. 501-638.

Brouwers, E.M., Clemens, W.A., Spicer, R.A., Ager, T.A., Carter, L.D., and Sliter, W.V., 1987, Dinosaurs on the North Slope, Alaska: Reconstruction of high latitude latest Cretaceous environments: Science, v. 237, p. 1608-1610.

Clemens, W.A., and Allison, C.W., 1985, Late Cretaceous terrestrial vertebrate fauna, North Slope, Alaska: Geological Society America, Abstracts with Programs, v. 17, p. 548.

Davies, K.L., 1987, Duck-billed dinosaurs (Hadrosauridae; Ornithischia) from the North Slope of Alaska: Journal of Paleontology, v. 61, p. 198-200.

Dott, R.H., Jr., and Bourgeois, J., 1982, Hummocky stratification: Significance of its variable bedding sequences: Geological Society America Bulletin, v. 93, p. 663-680.

Frederiksen, N.O., Ager, T.A., Oftendahl, O.G., and Edwards, L.E., 1985, Palynological samples near the Cretaceous/Tertiary boundary, North Slope of Alaska: Society Economic Paleontologists and Mineralogists, Annual Meeting, 2d, Golden, Colorado, Abstract vol., p. 31.

Frederiksen, N.O., Ager, T.A., and Edwards, L.E., 1986, Comment and reply on "Early Tertiary marine fossils from northern Alaska: implications for Arctic Ocean paleogeography and faunal evolution": Geology, p. 802-803.

Frederiksen, N.O., and Schindler, K.S., 1987, Campanian to Maastrichtian pollen biostratigraphy and floral turnover rates, Colville River region, North Slope of Alaska: American Association of Petroleum Geologists Bulletin, v. 71, p. 558.

Leeder, M.R., 1973, Fluviatile fining-upwards cycles and the magnitude of paleochannels: Geology Magazine, v. 110, p 265.

MacBeth, J., and Schmidt, R.A.M., 1973, Upper Cretaceous foraminifera from Ocean Point, northern Alaska: Journal of Paleontology, v. 47, p. 1047-1061.

Marincovich, L., Jr., Brouwers, E.M., and Carter, D.L., 1985, Early Tertiary marine fossils from northern Alaska: Implication for Arctic Ocean paleogeography and faunal evolution: Geology, v. 13, p. 770-773.

McDougall, K., 1987, Maestrichtian benthic foraminifers from Ocean Point, North Slope, Alaska: Journal of Foraminiferal Research, v. 17, p. 344- 366.

McKee, E.H., Conrad, J.E., and Turin, B.D., 1989, Dinosaurs from northern Alaska are of Latest Cretaceous age: Eos (Transactions American Geophysical Union), v. 70, no. 4, p. 74.

Nelms, L.G., 1989, Late Cretaceous dinosaurs from the north slope of Alaska: Journal of Vertebrate Paleontology, v. 9, p. 34A.

Nelson, R.E., 1981, Paleoenvironments during deposition of a section of the Gubik Formation exposed along the lower Colville River, North Slope, *in* Albert, N.R.D., and Hudson, Travis, eds., The United States Geological Survey in Alaska: Accomplishments during 1979: U.S. Geological Survey Circular 823-B, p. 9-11.

Phillips, R.L., 1988, Measured sections, paleoenvironments, and sample locations in the Prince Creek Formation near Ocean Point, Alaska: U.S. Geological Survey Open-File Report 88–40.

Reviewers: Kenneth J. Bird and William V. Sliter

Gold Placers, Geomorphology, and Paleo-Drainage of Eureka Creek and Tofty Areas, Alaska

By Warren Yeend

Gold-bearing gravels are present on benches as high as 80 m above Eureka and Pioneer Creeks in central Alaska (figs. 1 and 2). The occurrence of as many as four levels of gold-bearing, gravel-covered benches differs from many placers in central Alaska, which yield gold primarily from gravel in the present stream flood plain. Based on a visit during the summer of 1989, gold-bearing bench gravel, the asymmetric creek valleys, and recent placer mining are described, and reconstruction of the earlier drainage pattern that produced the present gravel distribution is proposed.

Eureka Creek is near the geographic center of Alaska approximately 130 km north-northeast from Fairbanks (fig. 1).

Gold was discovered in the Eureka Creek area in 1898 by a group of prospectors called the "Boston Boys." A stampede from the nearby, previously discovered Rampart area resulted in the development of Eureka Creek as a viable mining community. A hotel was built by Frank Manley at a nearby hot springs, and the town of Manley Hot Springs became the supply point for the Eureka Creek placer mines (Mertie, 1934). Mining has been carried on more or less continuously since the discovery, and in 1989, eight different mining operations were active at various locations in the Eureka Creek area.

Eureka Creek is approximately 20 km in length; only the upper one-third of its course includes bench gravels.

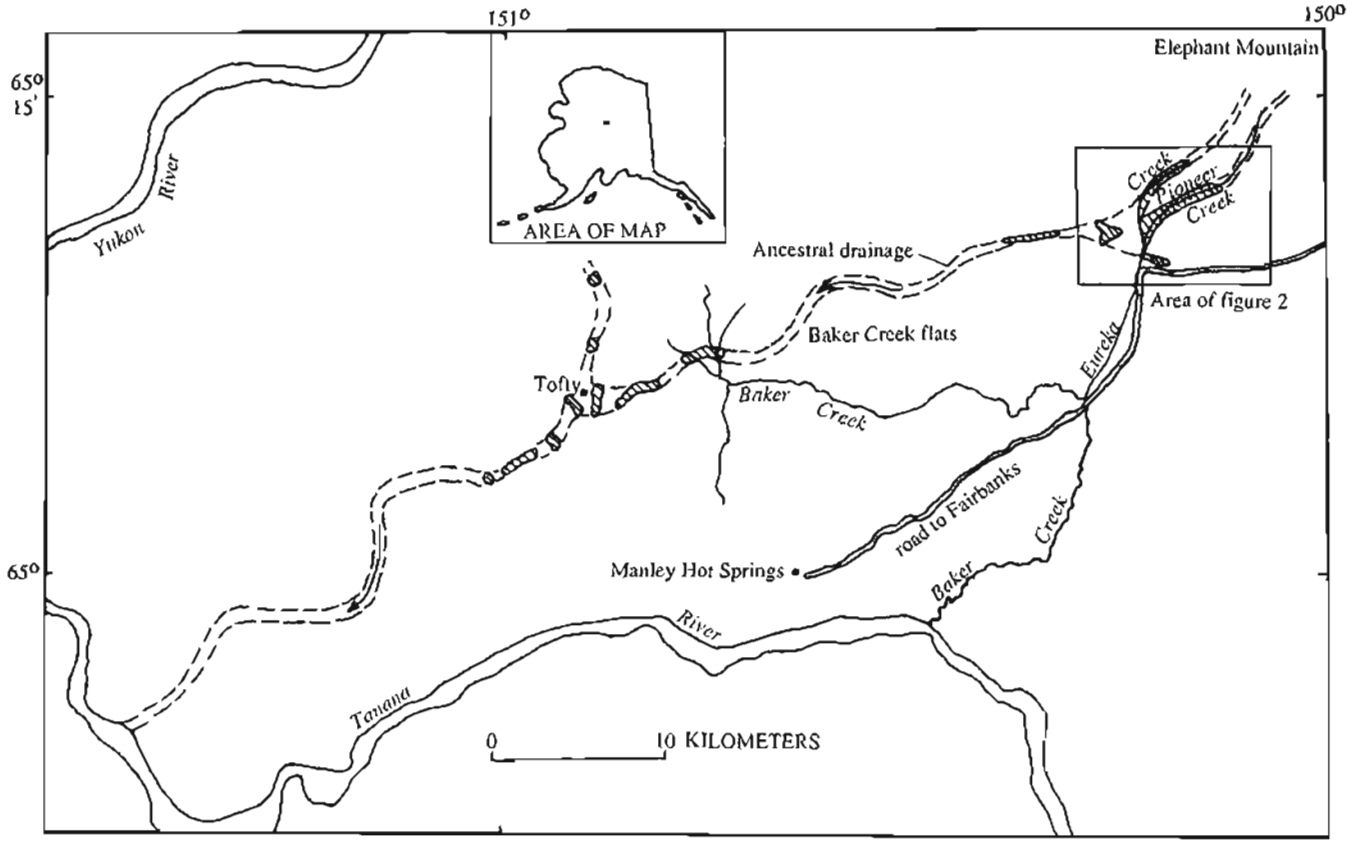

Figure 1. Index map showing location of study area, Eureka Creek placers, and postulated ancestral drainage. Arrow, direction of flow; lined area, mined placer.

Pioneer Creek, a prominent tributary, is parallel to the upper part of Eureka Creek. Both Eureka and Pioneer Creeks have asymmetric cross sections (figs. 3 and 4) characterized by steep southeast sides with no tributaries or preserved gold-bearing bench gravels and gentle northwest slopes with numerous tributaries. Mertie (1934) stated that the upper portions of both Eureka Creek and Pioneer Creek occupy strike valleys and are therefore structurally controlled. He thought that the asymmetry of the valleys was due to differential erosion as a result of differing resistance of rock types and increased solar exposure with "soil flow" on southeast-facing slopes. Other drainages in the area have similar asymmetry even where rock type is uniform, thus solar exposure would seem to be the controlling factor. Bedrock dips steeply to the northwest, thus the gentle southeast-facing slopes aren't "dip slopes." Hopkins and Taber (1961) believed that both structural control and the different insolation received by different slope exposures could be ruled out as a cause of valley asymmetry here. They attributed the asymmetry to "persistent southward and westward lateral migration of streams during a prolonged period of slow downcutting." They claimed that the cause of the lateral southward and westward migration by the streams was unknown.

Bedrock in the area is dominated by Jurassic to Cretaceous quartzite, argillite, and conglomerate (Chapman and others, 1982). Rare granitic boulders are present, most likely derived from the pluton in the vicinity of Elephant Mountain.

The most prominent and extensively mined gravel-covered surface is about 80 m above creek level (fig. 3). It is well developed on the northwest side of Pioneer Creek (What Cheer Bar) and on the west (Shirley Bar) and east (McCaskey Bar) sides of Eureka Creek near the mouth of Pioneer Creek (fig. 2). The tributaries of Pioneer and Eureka Creeks have dissected this old surface, and it remains

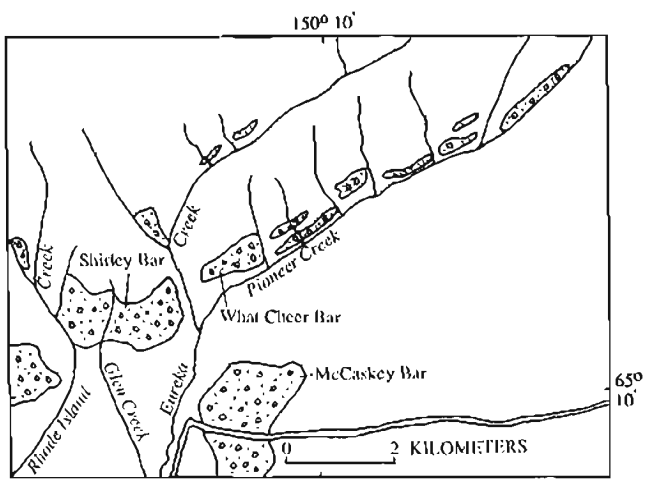

Figure 2. Eureka Creek-Pioneer Creek area showing terrace deposits (patterned).

only on the high interfluves between these tributaries. At least three other less well developed terraces are present at successively lower levels. All the surfaces have been modified by colluvial action, and much of the unconsolidated covering material present is a mixture of colluvium and alluvium.

The bench gravels are composed of locally derived oblate pebbles and cobbles of Mesozoic sedimentary and rare granitic rocks. A few boulders are as much as 0.5 m across; boulders up to 2 m in diameter are rare. The gravel is generally 2 to 4 m thick but is thinner on parts of the high terrace where soil and colluvium contain a few rounded clasts less than 1 m in thickness. Miners describe the presence of "gold in the dirt" in these thin upper deposits.

Gold is rarely coarser than 5 mm, but nuggets up to 26 oz have been recovered. Values are commonly $2 to $10 per cubic yard ($350/oz), although richer pockets are found. The highest values are near the back of the benches (away from the creek) where the gravel is thickest. The local miners report that the higher the bench the coarser the gold. The coarser gold almost always has attached quartz. Gold content in the gravels is generally greatest at and near the gravel-bedrock contact. The upper 0.5 m of eroded and fractured bedrock also is generally scraped off and mined to recover the trapped gold. The benches are easier to mine than the stream flood plain, according to the local miners, because the active creek does not have to be diverted. Gold recovered from the Eureka Creek area ranges in fineness from 780 to 800 as reported by Mertie (1934) and by local miners in the area in 1989. There are no known lode gold sources in the area. Mertie (1934) thought the gold was probably derived from "quartz stringers," which occur in the local bedrock.

The present stream flow in the area is generally east and south into the Tanana River via Baker Creek. During the Pleistocene, ancestral Pioneer and Eureka Creeks flowed southwest and, most likely, joined the ancestral Tanana River farther west than does the drainage today. Alluvial gravels in the vicinity of Tofty (fig. 1), many of which are buried by 10 to 50 m of silt, probably were deposited by this earlier drainage system.

A connection between the buried gravels at Tofty and the bench gravels in the Eureka Creek area is suggested by several lines of evidence: (1) Imbrication of gravel pebbles in the vicinity of Tofty indicate a water flow direction to the southwest and would be a logical continuation of the ancestral drainages coming from the Eureka-Pioneer Creeks area. The 80-m-high remnants of gold-bearing bench gravel in the Pioneer-Eureka Creeks area (shown on fig. 1 as mined placer) were deposited by a southwest-flowing river, based on the linear gravel occurrence and the underlying bedrock slope. (2) Bedrock elevations at the base of the bench gravels in the Eureka Creek area (260 m) as compared to those at Tofty (180 m), if part of the same drainage, indicate a 2 to 4 m/km gradient, depending on how

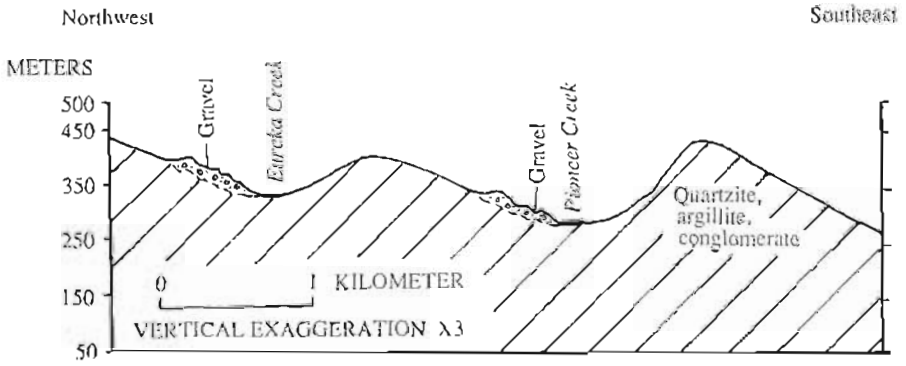

Figure 3. Diagrammatic cross section showing asymmetrical valleys of Pioneer and Eureka Creeks and gold-bearing terrace gravels.

circuitous the ancestral drainage was between these areas. This is less than that of creeks in the vicinity of Tofty today, but it is reasonable for this older and larger drainage which would have had a lower gradient due to its heading much farther east than do local drainages today. (3) Gravels in both the Eureka and Tofty areas are gold-bearing. Gold at Tofty varies from 807 to 839 fineness (Mertie, 1934), somewhat higher than at Eureka Creek. This would be expected in a more downstream location as silver is progressively leached from the gold particles during longer transport. (4) Rock types and heavy minerals at Tofty and Eureka Creek are similar except for the presence of considerable tin minerals at Tofty. It is speculated that a lode tin source near the Tofty area either has been eroded or is concealed by surficial deposits (Wayland, 1961).

Subsequent to its development, this inferred ancestral drainage was largely buried by windblown silt derived from the nearby Yukon and Tanana River flood plains. Much of this old drainage valley remains buried in the Tofty area where hydraulic methods must be used to melt and strip the overlying frozen silt and muck from the gold-bearing gravel. The low-gradient, poorly drained, silt- and vegetation-covered Baker Creek flats between Tofty and Eureka Creek may conceal this old drainage (fig. 1), which could contain gold-bearing gravel.

Figure 4. Asymmetric valley of Pioneer Creek. Foreground is mined area on Shirley Bar. Mined gravels on What Cheer Bar are evident in the middle distance on left. Elephant Mountain is skyline on left. View northeast.

REFERENCES CITED

Chapman, R.M., Yeend, Warren, Brosgé, W.P., and Reiser, H.N., 1982, Reconnaissance geologic map of the Tanana quadrangle, Alaska: U.S. Geological Survey Open-File Report 82-734, 20 p., 1 sheet, scale 1:250,000.

Hopkins, D.M., and Tabor, Bond, 1961, Asymmetrical valleys in central Alaska [abs.]: Geological Society of America Special Paper 68, p. 116.

Mertie, J.B., Jr., 1934, Mineral deposits of the Rampart and Hot Springs districts, Alaska: U.S. Geological Survey Bulletin 844-D, p. 163-226.

Wayland, R.G., 1961, Tofty tin belt, Manley Hot Springs District, Alaska: U.S. Geological Survey Bulletin 1058-I, p. 363-414.

Reviewers: Robert Chapman and William Brosgé

U.S. Geological Survey Reports on Alaska Released in 1989

Compiled by Ellen R. White

[Some reports dated 1988 did not become available until 1989; they are included in this listing]

ABBREVIATIONS

B1903 Dover, J.H., and Galloway, J.P., eds., 1989, Geologic studies in Alaska by the U.S. Geological Survey, 1988: U.S. Geological Survey Bulletin 1903.

C1026 Carter, L.D., Hamilton, T.D., and Galloway, J.P., eds., 1989, Late Cenozoic history of the interior basins of Alaska and the Yukon: U.S. Geological Survey Circular 1026.

C1035 Schindler, K.S., ed., 1988, USGS research on mineral resources-1989; Program and abstracts: U.S. Geological Survey Circular 1035.

OF88-673 Jacobson, M.L., ed., National Earthquake Hazards Reduction Program; Summaries of technical reports, v. XXVII: U.S. Geological Survey Open-File Report 88-673.

P1399 Gryc, George, ed., Geology and exploration of the National Petroleum Reserve in Alaska, 1974 to 1982: U.S. Geological Survey Professional Paper 1399.

Ager, T.A., 1989, History of late Pleistocene and Holocene vegetation in the Copper River basin, south-central Alaska: C1026, p. 89-92.

Albers, J.P., Fraticelli, L.A., and Dawson, K.M., 1989, Metallogenic maps of the northeast quadrant of the Circum-Pacific region, showing inferred mineral belts in accreted terranes and cratons: U.S. Geological Survey Mineral Investigations Resource Map MR-95, scale 1:20,000,000, 1 sheet.

Aleinikoff, J.N., and Nokleberg, W.J., 1989, Age of deposition and provenance of the Cleary sequence of the Fairbanks schist unit, Yukon-Tanana terrane, east-central Alaska: B1903, p. 75-83.

Aleinikoff, J.N., and Plafker, George, 1989, In search of the provenance and paleogeographic location of the White Mountains terrane: Evidence from U-Pb data of granite boulders in the Fossil Creek Volcanics: B1903, p. 68-74.

Allison, C.W., 1988, Paleontology of Late Proterozoic and Early Cambrian rocks of east-central Alaska: U.S. Geological Survey Professional Paper 1449, 50 p., 18 pls.

Armbrustmacher, T.J., 1989, Minor element content, including radioactive elements and rare-earth elements, in rocks from the syenite complex at Roy Creek, Mount Prindle area, Alaska: U.S. Geological Survey Open-File Report 89-146, 11 p.

Barnes, D.F., Brew, D.A., and Morin, R.L., 1989, Bouguer gravity map of the Petersburg quadrangle and parts of the Port Alexander, Sitka, and Sumdum quadrangles: U.S. Geological Survey Miscellaneous Field Studies Map MF-1970-A, scale 1:250,000, 1 sheet.

Barnes, D.F., and Morin, R.L., 1988, Results of a gravity survey of McCarthy's Marsh, Seward Peninsula, Alaska: U.S. Geological Survey Open-File Report 88-546, 14 p., scale 1:63,360, 2 sheets.

Bartsch-Winkler, Susan, and Huffman, A.C., Jr., 1988, Sandstone petrography of the Nanushuk Group and Torok Formation: P1399, p. 801-831.

Bartsch-Winkler, Susan, and Lynch, D.K., 1988, Catalog of worldwide tidal bore occurrences and characteristics: U.S. Geological Survey Circular 1020, 17 p. [Includes information on Knik Arm and Turnagain Arm tidal bores.]

Bayliss, G.S., and Magoon, L.B., 1988, Organic facies and thermal maturity of sedimentary rocks in the National Petroleum Reserve in Alaska: P1399, p. 489-518.

Beaudoin, B.C., Perkins, Gregory, Fuis, G.S., and Luetgert, J.H., 1989, Data report for the 1987 seismic refraction survey: Alaska Range and Fairbanks south deployments: U.S. Geological Survey Open-File Report 89-321, 114 p.

Beavan, John, 1988, Crustal deformation measurements in the Shumagin seismic gap, Alaska: OF88-673, p. 183-188.

———1989, Crustal deformation measurements in the Shumagin seismic gap, Alaska: U.S. Geological Survey Open-File Report 89-453, p. 181-184.

Beyer, L.A., and Clutsom, F.G., 1989, Basic data and preliminary density and porosity profiles from three borehole gravity surveys made in the Kuparuk River and Prudhoe Bay oil fields, Alaska: U.S. Geological Survey Open-File Report 89-369, 26 p.

Bigelow, B.B., 1988, Hydrologic data collection activities in the Solomon Gulch basin near Valdez, Alaska: U.S. Geological Survey Open-File Report 88-719, 15 p.

Bird, K.J., 1988, Alaskan North Slope stratigraphic nomenclature and data summary for government-drilled wells: P1399, p. 317-353.

———1988, The geologic basis for appraising undiscovered hydrocarbon resources in the National Petroleum Reserve of Alaska by the play-appraisal method: P1399, p. 81-116.

———1988, Structure-contour and isopach maps of the National Petroleum Reserve in Alaska: P1399, p. 355-377.

Bird, K.J., and Powers, R.B., 1988, Comparison of six assessments of the hydrogen resources of the National Petroleum Reserve in Alaska: P1399, p. 77-80.

Bliss, J.D., 1989, Quantitative mineral resource assessment of undiscovered mineral deposits for selected mineral deposit types in the Chugach National Forest, Alaska: U.S. Geological Survey Open-File Report 89-345, 25 p.

Bliss, J.D., Brosgé, W.P., Dillon, J.T., Dutro, J.T., Jr., Cathrall, J.D., and Cady, J.W., 1988, Mineral resource assessment of the Wiseman 1° x 3° quadrangle, Alaska: U.S. Geological Survey Open-File Report 88-533, 84 p., scale 1:250,000, 3 sheets.

Blome, C.D., Reed, K.M., and Tailleur, I.L., 1988, Radiolarian biostratigraphy of the Otuk Formation in and near the National Petroleum Reserve in Alaska: P1399, p. 725-776.

Bohn, Diedra, ed., 1988, 1988 annual report on Alaska's mineral resources: U.S. Geological Survey Circular 1023, 57 p.

Brew, D.A., Grybeck, D.J., Cathrall, J.B., Karl, S.M., Koch, R.D., Barnes, D.F., Newberry, R.J., Griscom, Andrew, and Berg, H.C., 1989, Mineral-resource map of the Petersburg quadrangle and parts of the Port Alexander, Sitka, and Sumdum quadrangles, southeastern Alaska: U.S. Geological Survey Miscellaneous Field Studies Map MF-1970-B, 47 p., scale 1:250,000, 1 sheet.

Brosgé, W.P., Nilsen, T.H., Moore, T.E., and Dutro, T.J., Jr., 1988, Geology of the Upper Devonian and Lower Mississippian(?) Kanayut Conglomerate in the central and eastern Brooks Range: P1399, p. 299-316, 1 sheet.

Brosgé, W.P., and Tailleur, I.L., 1988, Inorganic chemical analyses of black shale from wells in the National Petroleum Reserve in Alaska: P1399, p. 563-582.

Bugg, Paul, Miller, Stanley, and White, L.P., 1988, Policy analysis of the National Petroleum Reserve in Alaska—Methods and applications: P1399, p. 129-138.

Carey, M.A., Roberts, S.B., and Clark, A.C., 1988, Chemical analyses for nine coal samples from the Sagwon Member (Tertiary) of the Sagavanirktok Formation, North Slope, Alaska: U.S. Geological Survey Open-File Report 88-678, 17 p.

Carter, L.D., 1989, Canadian-American collaborative research, *in* Summaries of discussion sessions: C1026, p. 113-114.

Carter, L.D., and Ager, T.A., 1989, Late Pleistocene spruce (*Picea*) in northern interior basins of Alaska and the Yukon: Evidence from marine deposits in northern Alaska: C1026, p. 11-14.

Carter, L.D., and Hamilton, T.D., 1989, Introduction: C1026, p. 1-2.

Carter, L.D., Hamilton, T.D., and Galloway, J.P., eds., Late Cenozoic history of the interior basins of Alaska and the Yukon: C1026, 114 p.

Cathrall, J.B., Albanese, Mary, VanTrump, George, Mosier, E.L., and Lueck, Larry, 1989, Geochemical signatures, analytical results, mineralogical data, and sample locality map of placer and lode gold, and heavy-mineral concentrates from the Fortymile mining district, Eagle quadrangle, Alaska: U.S. Geological Survey Open-File Report 89-451, 32 p.

Cathrall, J.B., Antweiler, J.C., VanTrump, George, and Mosier, E.L., 1989, Gold analytical results and gold signatures from the Fairbanks mining district, Fairbanks and Livengood quadrangles, Alaska: U.S. Geological Survey Open-File Report 89-490, 32 p.

———1989, Gold, platinum, and silver analytical results and gold signatures from the Bonnifield mining district, Fairbanks and Healy quadrangles, Alaska: U.S. Geological Survey Open-File Report 89-461, 23 p.

Cathrall, J.B., Tripp, R.B., McDanal, S.K., Mosier, E.L., and VanTrump, George, 1988, Analytical results, geochemical signatures, mineralogical data, and sample locality map of placer gold, and heavy-mineral concentrates from the Circle mining district, Circle quadrangle, Alaska: U.S. Geological Survey Open-File Report 88-676, 48 p., scale 1:250,000, 1 sheet.

Church, S.E., Detterman, R.L., and Wilson, F.H., 1989, Mineral and energy resource assessment maps of the Ugashik, Bristol Bay, and western Karluk quadrangles, Alaska: U.S. Geological Survey Miscellaneous Field Studies Map MF-1539-I, scale 1:250,000, 2 sheets.

Cieutat, B.A., Goldfarb, R.J., and Speckman, W.S., 1988, Analytical results and sample locality map of stream-sediment, heavy-mineral concentrate, and organic material samples from the Goodnews, Hagemeister Island, and Nushagak Bay quadrangles, southwest Alaska: U.S. Geological Survey Open-File Report 88-591, 188 p., scale 1:250,000, 1 sheet.

Claypool, G.E., and Magoon, L.B., 1988, Oil and gas source rocks in the National Petroleum Reserve in Alaska: P1399, p. 451-481.

Collett, T.S., Bird, K.J., Kvenvolden, K.A., and Magoon, L.B., 1989, The origin of natural gas hydrates on the North Slope of Alaska: B1903, p. 3-9.

Combellick, R.A., and Reger, R.D., 1989, Evaluation of Holocene subsidence events of Cook Inlet estuarine flats near Anchorage, Alaska, as a basis for assessing seismic hazards in southcentral Alaska: U.S. Geological Survey Open-File Report 89-453, p. 445-446.

Cox, Dennis, Light, T.D., Csejtey, Béla, Jr., and Campbell, D.L., 1989, Mineral resource assessment map of the Healy quadrangle, Alaska: U.S. Geological Survey Miscellaneous Field Studies Map MF-2058-A, scale 1:250,000, 1 sheet.

Curtin, G.C., Tripp, R.B., and Nokleberg, W.J., 1989, Summary and interpretation of geochemical maps for stream sediment and heavy-mineral concentrate samples, Mount Hayes quadrangle, eastern Alaska Range, Alaska: U.S. Geological Survey Miscellaneous Field Studies Map MF-1996-B, 11 p., scale 1:250,000, 3 sheets.

Dean, W.E., Gardner, J.V., Briggs, P.H., and Riddle, G.O., 1989, Data on the geochemistry of pelagic clay of the subarctic North Pacific Ocean: U.S. Geological Survey Open-File Report 89-371, 28 p.

Detterman, R.L., 1988, Mesozoic biogeography of southern Alaska, with implications for the paleogeography: U.S. Geological Survey Open-File Report 88-662, 27 p.

Donovan, T.J., Hendricks, J.D., Roberts, A.A., and Eliason, P.T., 1988, Low-level aeromagnetic surveying for petroleum in arctic Alaska: P1399, p. 623-632.

Douglass, S.L., Webster, J.H., Burrell, P.D., Lanphere, M.L., and Brew, D.A., 1989, Major-element chemistry, radiometric ages,

and locations of samples from the Petersburg and parts of the Port Alexander and Sumdum quadrangles, southeastern Alaska: U.S. Geological Survey Open-File Report 89-527, 66 p., scale 1:250,000, 1 sheet.

Dover, J.H., and Galloway, J.P., eds., 1989, Geologic studies in Alaska by the U.S. Geological Survey, 1988: B1903, 134 p.

Dover, J.H., and Galloway, J.P.,1989, Introduction: B1903, p. 1.

Drinkwater, J.L., Brew, D.A., and Ford, A.B., 1989, Petrographic and chemical description of the variably deformed Speel River pluton, south of Juneau, southeastern Alaska: B1903, p. 104-112.

DuBois, G.D., Wilson, F.H., Detterman, R.L., and Hopkins, R.T., Jr., 1989, Reconnaissance geology and exploration geochemistry of King Cove, Alaska Peninsula: U.S. Geological Survey Open-File Report 89-350, 23 p.

Dusel-Bacon, Cynthia, Brosgé, W.P., Till, A.B., Doyle, E.O., Mayfield, C.F., Reiser, H.N., and Miller, T.P., 1989, Distribution, facies, ages, and proposed tectonic associations of regionally metamorphosed rocks in northern Alaska: U.S. Geological Survey Professional Paper 1497-A, 44 p., scale 1:1,000,000, 2 sheets.

Dutro, J.T., and Silberling, N.J., 1988, Megafossil biostratigraphy of some deep test wells, National Petroleum Reserve in Alaska: P1399, p. 667-675, 5 pls.

Edwards, M.E., and McDowell, P.F., 1989, Quaternary deposits at Birch Creek, northeastern interior Alaska: The possibility of climatic reconstruction: C1026, p. 48-50.

Espinosa, A.F., 1988, Seismic hazard studies, Anchorage, Alaska: OF88-673, p. 462-464.

———1989, Seismic hazard studies, Anchorage, Alaska: U.S. Geological Survey Open-File Report 89-453, p. 453-455.

Ferrians, O.J., Jr., 1989, Glacial Lake Atna, Copper River basin, Alaska: C1026, p. 85-88.

Fitzpatrick-Lins, Katherine, Doughty, E.F., Shasby, Mark, and Benjamin, Susan, 1989, Alaska interim land cover mapping program—final report: U.S. Geological Survey Open-File Report 89-128, 10 p.

Gamble, B.M., 1988, Mineral resource assessment, Bendeleben and Solomon quadrangles, western Alaska [abs.]: C1035, p. 22-23.

Gehrels, G.E., and Berg, H.C., 1988, A review of the regional geology and tectonics of southeastern Alaska: U.S. Geological Survey Open-File Report 88-659, 23 p., 3 pls.

Grantz, Arthur, and May, S.D., 1988, Regional geology and petroleum potential of the United States Chukchi shelf north of Point Hope: P1399, p. 209-229.

Grantz, Arthur, May, S.D., and Dinter, D.A., 1988, Geologic framework, petroleum potential, and environmental geology of the United States Beaufort and northeasternmost Chukchi Seas: P1399, p. 231-255.

Gryc, George, 1988, Introduction and role of the U.S. Geological Survey: P1399, p. 1-12.

Gryc, George, ed., 1988, Geology and exploration of the National Petroleum Reserve in Alaska, 1974 to 1982: U.S. Geological Survey Professional Paper 1399, 940 p., 58 pls.

Hall, E.S., Jr., and Gal, Robert, 1988, The U.S. Geological Survey-Bureau of Land Management cultural resources program in the National Petroleum Reserve in Alaska, 1977-1981: P1399, p. 859-897.

Hamilton, T.D., 1989, Early and middle Pleistocene events, *in* Summaries of discussion sessions: C1026, p. 110-111.

———1989, Upper Cenozoic deposits, Kanuti Flats and upper Kobuk trench, northern Alaska: C1026, p. 45-47.

Hillhouse, J.W., and Grommé, Sherman, 1988, Cretaceous remagnetization of Paleozoic sedimentary rocks in the Brooks Range, Alaska: P1399, p. 633-644.

Holdsworth, B.K., and Murchey, B.L., 1988, Paleozoic radiolarian biostratigraphy of the northern Brooks Range, Alaska: P1399, p. 777-792, 2 pls.

Huffman, A.C., Jr., Ahlbrandt, T.S., and Bartsch-Winkler, Susan, 1988, Sedimentology of the Nanushuk Group, North Slope: P1399, p. 281-298.

Kachadoorian, Reuben, and Crory, F.E., 1988, Engineering geology studies in the National Petroleum Reserve in Alaska: P1399, p. 899-922.

Karl, S.M., Aleinikoff, J.N., Dickey, C.F., and Dillon, J.T., 1989, Age and chemical composition of Proterozoic intrusive rocks at Mount Angayukaqsraq, western Brooks Range, Alaska: B1903, p. 10-19.

Kaufman, D.S., Calkin, P.E., Whitford, W.B., Przybyl, B.J., Hopkins, D.M., Peck, B.J., and Nelson, R.E., 1989, Surficial geologic map of the Kigluaik Mountains area, Seward Peninsula, Alaska: U.S. Geological Survey Miscellaneous Field Studies Map MF-2074, scale 1:63,360, 1 sheet.

Kaufman, D.S., and Hopkins, D.M., 1989, Late Cenozoic geologic controls on placer-gold distribution in the Nome nearshore area: B1903, p. 26-45.

Kelley, J.S., 1989, Draft generalized geologic map of the Chandler Lake quadrangle, north-central Alaska: U.S. Geological Survey Open-File Report 89-495, 33 p., scale 1:250,000, 1 sheet.

Kelley, J.S., and Molenaar, C.M., 1988, Geologic map of the north flank of the Sadlerochit Mountains, Mount Michelson C-1, C-2, and C-3 quadrangles, northeastern Alaska: U.S. Geological Survey Open-File Report 89-11, scale 1:63,360, 1 sheet.

Kharaka, Y.K., and Carothers, W.W., 1988, Geochemistry of oilfield water from the North Slope: P1399, p. 551-561.

King, H.D., Light, T.D., and O'Leary, R.M., 1989, Maps showing distribution and abundance of selected elements in stream-sediment samples from a reconnaissance geochemical survey of the Healy quadrangle, Alaska: U.S. Geological Survey Miscellaneous Field Studies Map MF-2058-B, scale 1:250,000, 2 sheets.

King, H.D., Smith, S.C., Sutley, S.J., and Greene, K.R., 1989, Geochemical maps showing the distribution and abundance of selected elements in nonmagnetic heavy-mineral-concentrate samples from stream sediment, Solomon and Bendeleben 1° x 3° quadrangles, Seward Peninsula, Alaska: U.S. Geological Survey Miscellaneous Field Studies Map MF-2071-B, 13 p., scale 1:250,000, 1 sheet.

King, H.D., Smith, S.C., and Werschky, Scott, 1989, Mineralogical maps showing the distribution and abundance of selected minerals in nonmagnetic heavy-mineral-concentrate samples from stream sediment, Solomon and Bendeleben 1° x 3° quadrangles, Seward Peninsula, Alaska: U.S. Geological Survey Miscellaneous Field Studies Map MF-2071-C, 4 p., scale 1:250,000, 1 sheet.

Kirschner, C.E., 1988, Map showing sedimentary basins of onshore and continental shelf areas, Alaska: U.S. Geological

Survey Miscellaneous Investigations Series Map I-1873, scale 1:2,500,000, 1 sheet.

Kirschner, C.E., and Rycerski, B.A., 1988, Petroleum potential of respresentative stratigraphic and structural elements in the National Petroleum Reserve in Alaska: P1399, p. 191-208, 7 pls.

Kisslinger, Carl, 1988, Central Aleutian Islands seismic network: OF88-673, p. 15-16.

Kisslinger, Carl, and Kubicheck, Sharon, 1989, Central Aleutian Islands seismic network: U.S. Geological Survey Open-File Report 89-453, p. 17-25.

Lachenbruch, A.H., Sass, J.H., Lawver, L.A., Brewer, M.C., Marshall, B.V., Munroe, R.J., Kennelly, J.P., Jr., Galanis, S.P., Jr., and Moses, T.H., Jr., 1988, Temperature and depth of permafrost of the Arctic Slope of Alaska: P1399, p. 645-656.

Lahr, J.C., Stephens, C.D., Page, R.A., and Fogleman, K.A., 1988, Alaska seismic studies: OF88-673, p. 17-22.

———1989, Alaska seismic studies: U.S. Geological Survey Open-File Report 89-453, p. 26-32.

Light, T.D., King, H.D., and Sutley, S.J., 1989, Maps showing distribution and abundance of selected elements in heavy-mineral-concentrate samples from a reconnaissance geochemical survey of the Healy quadrangle, Alaska: U.S. Geological Survey Miscellaneous Field Studies Map MF-2058-C, scale 1:250,000, 2 sheets.

Light, T.D., and Rinehart, C.D., 1989, Molybdenite in the Huron Creek pluton, western Livengood quadrangle, Alaska: B1903, p. 54-61.

Lipscomb, S.W., 1989, Flow and hydraulic characteristics of the Knik-Matanuska River estuary, Cook Inlet, southcentral Alaska: U.S. Geological Survey Water Resources Investigations Report 89-4064, 52 p.

Luepke, Gretchen, and Escowitz, E.C., 1989, Grain-size, heavy-mineral, and geochemical analyses of sediments from the Chukchi Sea, Alaska: U.S. Geological Survey Bulletin 1896, 12 p.

Magoon, L.B., and Bird, K.J., 1988, Evaluation of petroleum source rocks in the National Petroleum Reserve in Alaska, using organic-carbon content, hydrocarbon content, visual kerogen, and vitrinite reflectance: P1399, p. 381-450.

Magoon, L.B., Bird, K.J., Claypool, G.E., Weitzman, D.E., and Thompson, R.H., 1988, Organic geochemistry, hydrocarbon occurrence, and stratigraphy of government-drilled wells, North Slope, Alaska: P1399, p. 483-487, 39 pls.

Magoon, L.B., and Claypool, G.E., 1988, Geochemistry of oil occurrences, National Petroleum Reserve in Alaska: P1399, p. 519-549.

Mann, D.M., Scholl, D.W., and Sliter, R.W., 1989, Multichannel seismic-reflection data collected in 1980 across the Aleutian arc and trench, Alaska: U.S. Geological Survey Open-File Report 89-202, 5 p., scale 1:500,000, 1 sheet.

Mayfield, C.F., Tailleur, I.L., and Ellersieck, Inyo, 1988, Stratigraphy, structure, and palinspastic synthesis of the western Brooks Range, northwestern Alaska: P1399, p. 143-186, 4 pls.

Mayfield, C.F., Tailleur, I.L., and Kirschner, C.E., 1989, Bedrock geologic map of the National Petroleum Reserve in Alaska: P1399, p. 187-190, 2 pls.

Mickey, M.B., and Haga, Hideyo, 1988, Distribution of large-scale depositionally related biostratigraphic units, National Petroleum Reserve in Alaska: P1399, p. 657-665, 1 pl.

Miller, B.M., 1988, Methods for assessing the petroleum resources in the National Petroleum Reserve in Alaska: P1399, p. 117-128.

Miller, M.L., Belkin, H.E., Blodgett, R.B., Bundtzen, T.K., Cady, J.W., Goldfarb, R.J., Gray, J.E., McGimsey, R.G., and Simpson, S.L., 1989, Pre-field study and mineral resource assessment of the Sleetmute quadrangle, southwestern Alaska: U.S. Geological Survey Open-File Report 89-363, 115 p., scale 1:250,000, 3 sheets.

Molenaar, C.M., 1988, Depositional history and seismic stratigraphy of Lower Cretaceous rocks in the National Petroleum Reserve in Alaska and adjacent areas: P1399, p. 593-621.

Molenaar, C.M., Egbert, R.M., and Krystinik, L.F., 1988, Depositional facies, petrography, and reservoir potential of the Fortress Mountain Formation (Lower Cretaceous), central North Slope, Alaska: P1399, p. 257-280.

Moore, T.E., and Murphy, J.M., 1989, Nature of the basal contact of the Tozitna terrane along the Dalton Highway, northeast Tanana quadrangle, Alaska: B1903, p. 46-53.

Motooka, J.M., Adrian, B.M., Church, S.E., McDougal, C.M., and Fife, J.B., 1989, Analytical data and sample locality map for aqua-regia leachates of stream sediments analyzed by ICP, and emission spectrographic and ICP results for many NURE stream sediments from the Killik River quadrangle, Alaska: U.S. Geological Survey Open-File Report 89-12, 77 p., scale 1:250,000, 2 sheets.

Murchey, B.L., Jones, D.L., Holdsworth, B.K., and Wardlaw, B.R., 1988, Distribution patterns of facies, radiolarians, and conodonts in the Mississippian to Jurassic siliceous rocks of the northern Brooks Range, Alaska: P1399, p. 697-724.

Newberry, R.J., and Brew, D.A., 1988, Multiple sources for gold in the Juneau gold belt, Alaska [abs.]: C1035, p. 48-49.

———1989, Epigenetic hydrothermal origin of the Groundhog Basin-Glacier Basin silver-tin-lead-zinc deposits, southeastern Alaska: B1903, p. 113-121.

Nichols, D.R., 1989, Pleistocene glacial events, southeastern Copper River basin, Alaska: C1026, p. 78-80.

Nokleberg, W.J., Bundtzen, T.K., Berg, H.C., Brew, D.A., Grybeck, Donald, Robinson, M.S., and Smith, T.E., 1989, Metallogenic map of significant volcanogenic massive-sulfide and related lode deposits in Alaska: U.S. Geological Survey Miscellaneous Field Studies Map MF-1853-C, scale 1:5,000,000, 1 sheet. [Volcanogenic massive-sulfide map series, edited by R.L. Earhart.]

Nokleberg, W.J., Bundtzen, T.K., Grybeck, D.J., and Smith, T.E., 1988, Metallogenesis of lode mineral deposits of "mainland" Alaska [abs.]: C1035, p. 50-51.

Patrick, L.D., Brabets, T.P., and Glass, R.L., 1989, Simulation of ground-water flow at Anchorage, Alaska, 1955-83: U.S. Geological Survey Water-Resources Investigations Report 88-4139, 41 p.

Patton, W.W., Jr., Box, S.E., Moll-Stalcup, E.J., and Miller, T.P., 1989, Geology of west-central Alaska: U.S. Geological Survey Open-File Report 89-554, 56 p.

Péwé, T.L., 1989, Quaternary stratigraphy of the Fairbanks area, Alaska: C1026, p. 72-77.

Phillips, R.L., Barnes, P.W., Hunter, R.E., Reiss, T.E., and Rearic, D.M., 1988, Geologic investigations in the Chukchi Sea, 1984,

NOAA ship *Surveyor* cruise: U.S. Geological Survey Open-File Report 88-25, 82 p.

Plafker, George, Lull, J.S., Nokleberg, W.J., Pessel, G.H., Wallace, W.K., and Winkler, G.R., 1989, Geologic map of the Valdez A-4, B-3, B-4, C-3, C-4 and D-4 quadrangles, northern Chugach Mountains and southern Copper River basin, Alaska: U.S. Geological Survey Open-File Report 89-569, scale 1:125,000, 1 sheet.

Preuss, Jane, 1988, Utilization of tsunami hazard maps in Alaska: U.S. Geological Survey Open-File Report 88-13-A, p. 377-387.

Rasmussen, L.A., 1989, Surface velocity variations of the lower part of Columbia Glacier, Alaska, 1977-1981: U.S. Geological Survey Professional Paper 1258-H, 52 p. ["An internally consistent, two-dimensional data set of surface topography, surface velocity, bed topography, and mass balance distribution—obtained entirely from vertical aerial photography and photogrammetry."]

Rearic, D.M., Williams, S.R., Carlson, P.R., and Hall, R.K., 1988, Acoustic evidence for gas-charged sediment in the abyssal Aleutian basin, Bering Sea, Alaska: U.S. Geological Survey Open-File Report 88-677, 41 p.

Repenning, C.A., 1989, Arctic microtine biochronology—Current status: C1026, p. 99-102.

Richter, D.H., Ratté, J.C., Schmoll, H.R., Leeman, W.P., Smith, J.G., and Yehle, L.A., 1989, Geologic map of the Gulkana B-1 quadrangle, south-central Alaska: U.S. Geological Survey Geologic Quadrangle Map GQ-1655, scale 1:63,360, 1 sheet [color].

Riehle, J.R., Bailey, E.A., Church, S.E., and Yount, M.E., 1989, Sample locality maps, analytical data, and statistical summary of analyses of rock samples from the Mount Katmai quadrangle and adjacent portions of the Naknek and Afognak quadrangles, Alaska: U.S. Geological Survey Open-File Report 89-570, variously paged, scale 1:250,000, 2 sheets.

Riehle, J.R., Brew, D.A., and Lanphere, M.A., 1989, Geologic map of the Mount Edgecumbe volcanic field, Kruzof Island, southeastern Alaska: U.S. Geological Survey Miscellaneous Investigations Series Map I-1983, scale 1:63,360, 1 sheet [color].

Roberts, A.A., and Cunningham, K.I., 1988, Helium surveying, a geochemical exploration technique for petroleum on the North Slope: P1399, p. 583-589.

Schindler, J.F., 1988, History of exploration in the National Petroleum Reserve in Alaska, with emphasis on the period from 1975 to 1982: P1399, p. 13-72, 1 pl.

Schmidt, J.M., and Zierenberg, R.A., 1988, Reconstruction of primary features and isotopic evidence for multiple sulfur sources at the Red Dog zinc-lead-silver deposit, Noatak district, Alaska [abs.]: C1035, p. 62-63.

Schmitt, L.J., 1989, Map showing the areal distribution of oil shales with associated mineral resources and metal anomalies in the western United States and Alaska: U.S. Geological Survey Miscellaneous Field Studies Map MF-2091, scale 1:7,500,000 [for Alaska section], 2 sheets.

Scholl, D.W., Mann, D.M., Vallier, T.L., and Sliter, R.W., 1988, Multichannel seismic-reflection data collected in 1981 across the Aleutian arc and trench, Alaska: U.S. Geological Survey Open-File Report 88-592, 5 p., scale 1:500,000, 2 sheets.

Selkregg, L.L., 1988, Research and its application; the case of NSF-sponsored planning and policy research in Alaska: U.S. Geological Survey Open-File Report 88-13-A, p. 542-545. [Proceedings of Conference XLI; a review of earthquake research applications in the National Earthquake Hazards Reduction Program, 1977-1987.]

Smith, S.C., King, H.D., O'Leary, R.M., 1989, Geochemical maps showing the distribution and abundance of selected elements in stream-sediment samples, Solomon and Bendeleben 1° x 3° quadrangles, Seward Peninsula, Alaska: U.S. Geological Survey Miscellaneous Field Studies Map MF-2071-A, 13 p., scale 1:250,000, 1 sheet.

Sohn, I.G., 1988, Early Mississippian (Tournaisian) ostracodes from the Lisburne test well, northern Alaska: P1399, p. 687-690, 2 pls.

Still, P.J., and Cosby, J.M., 1989, Alaska index: Streamflow, lake levels, and water-quality records to September 30, 1988: U.S. Geological Survey Open-File Report 89-269, 189 p.

Taber, John, 1988, Seismic monitoring of the Shumagin seismic gap, Alaska: OF88-673, p. 38-40.

———1989, Analysis of seismic data from the Shumagin seismic gap, Alaska: U.S. Geological Survey Open-File Report 89-453, p. 264-265.

———1989, Seismic monitoring of the Shumagin seismic gap, Alaska: U.S. Geological Survey Open-File Report 89-453, p. 47-49.

Taber, John, and Huang, Paul, 1988, Analysis of seismic data from the Shumagin seismic gap, Alaska: OF88-673, p. 268-270.

Thorson, R.M., 1989, Late Quaternary paleofloods along the Porcupine River, Alaska: Implications for regional correlation: C1026, p. 51-54.

———1989, Neotectonics in Alaska and northwestern Canada, *in* Summaries of discussion sessions: C1026, p. 108-109.

Till, A.B., 1989, Proterozoic rocks of the western Brooks Range: B1903, p. 20-25.

Tooker, E.W., 1989, Geographic distribution of gold mining regions and types of deposits in the United States, *in* Shawe, D.R., and Ashley, R.P., eds., U.S. gold terranes: U.S.Geological Survey Bulletin 1857B, p. B1-B10.

Townshend, J.B., and others, 1989, Preliminary geomagnetic data, College Observatory, Fairbanks, Alaska: U.S. Geological Survey Open-File Report 89-300-A-L. [Each monthly report has its own letter designation; authorship and number of pages vary.]

Underwood, M.B., Laughland, M.M., Wiley, T.J., and Howell, D.G., 1989, Thermal maturity and organic geochemistry of the Kandik basin region, east-central Alaska: U.S. Geological Survey Open-File Report 89-353, 41 p.

U.S. Geological Survey, 1979 [revised 1987], Valdez, Alaska 1:250,000-scale vegetation and land cover, 1977-1979: U.S. Geological Survey Map L-209, scale 1:250,000, 1 sheet [color]. [Date on map is 1979, date on envelope is 1987, map does contain updated information.]

———1989, National Earthquake Hazards Reduction Program, summaries of technical reports, v. 28: U.S. Geological Survey Open-File Report 89-453, 638 p.

———1989, North American datum of 1983, map data conversion tables, Alaska: U.S. Geological Survey Bulletin 1875-C, 355 p.

Updike, R.G., Olsen, H.W., Schmoll, H.R., Kharaka, Y.K., and

Stokoe, K.H., II, 1988, Geologic and geotechnical conditions adjacent to the Turnagain Heights landslide, Anchorage, Alaska: U.S. Geological Survey Bulletin 1817, 40 p., 5 pls.

Updike, R.G., and Ulery, C.A., 1988, Bedrock geology of the Anchorage (B-7SE) quadrangle, Alaska: U.S. Geological Survey Open-File Report 88-418, scale 1:25,000, 1 sheet.

Vaill, J.E., and others, 1988, Water resources data, Alaska, water year 1987: U.S. Geological Survey Water-Data Report AK-87-1, 284 p.

van de Kamp, P.C., 1988, Stratigraphy and diagenetic alteration of Ellesmerian sequence siliclastic rocks, North Slope, Alaska: P1399, p. 833-854.

Vincent, J.-S., Carter, L.D., Matthews, J.V., Jr., and Hopkins, D.M., 1989, Joint Canadian-American investigation of the Cenozoic geology of the lowlands bordering the Beaufort Sea: C1026, p. 7-9.

Weber, F.R., Light, T.D., McCammon, R.B., and Rinehart, C.D., 1988, Mineral resource assessment of the White Mountains National Recreation Area, east-central Alaska [abs.]: C1035, p. 78.

Weber, W.S., Barnes, P.W., and Reimnitz, Erk, 1989, Data on the characteristics of dated gouges on the inner shelf of the Beaufort Sea, Alaska; 1977-1985: U.S. Geological Survey Open-File Report 89-151, not paginated.

White, E.R., compiler, 1989, Reports about Alaska in non-USGS publications released in 1988 that include USGS authors: B1903, p. 130-134.

———1989, U.S. Geological Survey reports on Alaska released in 1988: B1903, p. 122-129.

White, W.M., and Queen, L.D., 1989, Preliminary geologic and rock-chip geochemical data from drill core and trenches at the Shumagin gold deposit, Unga Island, Alaska: U.S. Geological Survey Open-File Report 89-361, variously paginated.

Whitesides, Jonathan, and Schmidt, J.M., 1988, Map showing land status by section, western Brooks Range, Alaska: U.S. Geological Survey Open-File Report 89-316, scale 1:500,000, 1 sheet. [Basemaps used: Ambler River, Baird Mtns., De Long Mtns., Howard Pass, Hughes, Killik River, Misheguk Mtn., Noatak, Pt. Hope, Selawik, Shungnak, Survey Pass.]

Wilcox, L.A., Coit, T.A., and Magoon, L.B., 1988, The National Petroleum Reserve in Alaska computer data and graphic system—An aid to geologic interpretation: P1399, p. 923-940.

Williams, J.R., 1989, A working glacial chronology for the western Copper River basin, Alaska: C1026, p. 81-84.

Wilson, F.H., 1989, Creation of a full color geologic map by computer: A case history from the Port Moller Project resource assessment, Alaska Peninsula: B1903, p. 96-103.

———1989, Geologic setting, petrology, and age of Pliocene to Holocene volcanoes of the Stepovak Bay area, western Alaska Peninsula: B1903, p. 84-95.

Wilson, F.H., White, W.H., and Detterman, R.L., 1988, Geology and mineral resources of the Port Moller region, western Alaska Peninsula, Aleutian Arc [abs.]: C1035, p. 80-81.

Wilson, F.H., White, W.H., and DuBois, G.D., 1988, Brief descriptions of mines, prospects, and mineral occurrences in the Port Moller and Stepovak Bay quadrangles, Alaska Peninsula: U.S. Geological Survey Open-File Report 88-666, 128 p., scale 1;250,000, 1 sheet.

Woo, C.C., 1989, Mineralogical determination of heavy minerals in beach sands, Cape Mountain district, Seward Peninsula, Alaska: U.S. Geological Survey Open-File Report 89-155, 24 p., 6 p. oversize tables.

Wrucke, C.T., Kelley, J.S., and Armstrong, A.K., 1989, Preliminary geologic map and structural setting of the Katakuruk [=Katakturuk] Dolomite in the Sadlerochit Mountains, northeastern Alaska: U.S. Geological Survey Open-File Report 89-123, 11 p., scale 1:63,360, 1 sheet.

Yeend, Warren, 1989, Late Cenozoic sedimentary history along major fault zones, Alaska: C1026, p. 55-59.

Yeend, Warren, Ager, T.A., and Kline, J.T., 1989, Stratigraphy and palynology of an Upper Tertiary terrace deposit of the ancestral Yukon River near Circle, Alaska: B1903, p. 62-67.

Yehle, L.A., and Schmoll, H.R., 1989, Surficial geologic map of the Anchorage B-7 SW quadrangle, Alaska: U.S. Geological Survey Open-File Report 89-318, 33 p., scale 1:25,000, 2 sheets.

Reports About Alaska in Non-USGS Publications Released in 1989 That Include USGS Authors

Compiled by Ellen R. White

[Some reports dated 1987 and 1988 did not become available until 1989; they are included in this listing. USGS authors are marked with asterisks (*)]

ABBREVIATIONS

ADGGS Mull, C.G., and Adams, K.E., eds., 1989, Dalton Highway, Yukon River to Prudhoe Bay, Alaska: Alaska Division of Geological and Geophysical Surveys Guidebook 7. [2 vols.]

AAPG American Association of Petroleum Geologists Bulletin, v. 73, no. 3

BB *Scholl, D.W., *Grantz, Arthur, and *Vedder, J.G., eds., 1987, Geology and resource potential of the continental margin of western North America and adjacent ocean basins—Beaufort Sea to Baja California: Houston, Tex., Circum-Pacific Council for Energy and Mineral Resources, Earth Science Series, v. 6.

Eos Eos (Transactions American Geophysical Union), v. 70, no. 43.

GSA Geological Society of America, Abstracts with Programs, v. 21, no. 5.

JGR Journal of Geophysical Research, v. 94, no. B4.

T104 Schmidt, R.A.M., *Nokleberg, W.J., and *Page, R.A., 1989, Alaska geological and geophysical transect, Valdez to Coldfoot, Alaska: American Geophysical Union, Field Trip Guidebook T104.

*Affolter, R.H., and *Stricker, G.D., 1987, Offshore Alaska coal, in BB, p. 639-647.

*Aleinikoff, J.N., *Stanley, W.D., and *Nokleberg, W.J., 1989, Pb isotopic evidence for underthrusted Mesozoic flysch beneath the Yukon-Tanana terrane, east-central Alaska [abs.]: Eos, p. 1337.

*Armstrong, A.K., and Mamet, B.L., 1989, Stratigraphy of the Lisburne Group in the central Brooks Range, in ADGGS, v. 2, p. 253-265.

*Arth, J.G., Criss, R.E., Zmuda, C.C., *Foley, N.K., *Patton, W.W., Jr., and *Miller, T.P., 1989, Remarkable isotopic and trace element trends in potassic through sodic Cretaceous plutons of the Yukon-Koyukuk basin Alaska, and the nature of the lithosphere beneath the Koyukuk terrane: Journal of Geophysical Research, v. 94, no. B11, p. 15957-15968.

*Arth, J.G., Zmuda, C.C., *Foley, N.K., Criss, R.E., *Patton, W.W., Jr., and *Miller, T.P., 1989, Isotopic and trace element variation in the Ruby batholith, Alaska, and the nature of the deep crust beneath the Ruby and Angayucham terranes: Journal of Geophysical Research, v. 94, no. B11, p. 15,941-15,955.

*Bartsch-Winkler, Susan, and Schmoll, H.R., 1989, Late Holocene peat and silt stratigraphy, Upper Cook Inlet, Alaska, and Isla Chiloé, Chile [abs.]: GSA, p. 55.

*Bird, K.J., 1989, Fossil fuel and mineral resources in northern Alaska [abs.]: American Association for the Advancement of Science, Annual meeting, San Francisco, Calif., 1989, Abstracts, p. 28.

*Box, S.E., 1989, Togiak terrane, SW Alaska: Jura-Cretaceous arc built on Triassic oceanic crust [abs.]: GSA, p. 59.

*Box, S.E., and *Patton, W.W., Jr., 1989, Igneous history of the Koyukuk terrane, western Alaska: Constraints on the origin, evolution and ultimate collision of an accreted island arc terrane: Journal of Geophysical Research, v. 94, no. B11, p. 15,843-15,867.

*Brew, D.A., *Ford, A.B., and Himmelberg, G.R., 1989, Relative timing of pluton emplacement and regional deformation, northern southeastern Alaska [abs.]: GSA, p. 59.

*Brocher, T.M., *Fisher, M.A., *Geist, E.L., and Christensen, N.I., 1989, A high-resolution seismic reflection/refraction study of the Chugach-peninsular terrane boundary, southern Alaska: JGR, p. 4441-4455.

*Brocher, T.M., *Hart, P.E., and *Fisher, M.A., 1989, Wide-angle recordings of the 1988 TACT MCS survey in Prince William Sound, Alaska [abs.]: Eos, p. 1339.

*Brouwers, E.M., 1988, Paleobathymetry on the continental shelf based on examples using ostracods from the Gulf of Alaska, *in* De Deckker, Patrick, Colin, J.-P., and Peypouquet, J.-P., eds., Ostracoda in the earth sciences: New York, Elsevier, p. 55-76.

———1988, Sediment transport detected from the analysis of ostracod population structure: An example from the Alaska continental shelf, *in* De Deckker, Patrick, Colin, J.-P., and Peypouquet, J.-P., eds., Ostracoda in the earth sciences: New York, Elsevier, p. 231-244.

*Bruns, T.R., and *Carlson, P.R., 1987, Geology and petroleum potential of the southeast Alaska continental margin, *in* BB, p. 269-282.

*Bruns, T.R., *Carlson, P.R., *Stevenson, A.J., *Fisher, M.A.,

*Ryan, H.F., *Mann, D.M., Dobson, M., Huggett, Q., Parson, L., Fannin, N.G.T., 1989, GLORIA images from the Gulf of Alaska and British Columbia: Subduction zones, transforms, and channels [abs.]: Eos, p. 1338.

*Bruns, T.R., *von Huene, Roland, *Culotta, R.C., Lewis, S.D., and Ladd, J.W., 1987, Geology and petroleum potential of the Shumagin margin, Alaska, *in* BB, p. 157-189.

Bundtzen, T.K., and *Miller, M.L., 1989, Geology and metallogeny of Cretaceous-Early Tertiary volcanic and plutonic rocks of western Alaska [abs.], *in* Tectonics, Energy and Mineral Resources of the North-West Pacific, International Symposium, Khabarovsk, USSR, 1989, Abstracts, v. 2, p. 80.

*Cady, J.W., 1989, Geologic implications of topographic, gravity, and aeromagnetic data in the northern Yukon-Koyukuk province and its borderlands, Alaska: Journal of Geophysical Research, v. 94, no. B11, p. 15,821-15,841.

*Campbell, D.L., 1989, Gravity and magnetic models of profiles near Richardson Highway, southern Alaska, *in* T104, p. 69-74.

*Carlson, P.R., 1989, Seismic reflection chracteristics of glacial and glacimarine sediment in the Gulf of Alaska and adjacent fjords: Marine Geology, v. 85, no. 2-4, p. 391-416.

*Carlson, P.R., and EEZ-Scan Team, 1989, GLORIA side-scan imagery of the deep Bering Sea [abs.], *in* Tectonics, Energy and Mineral Resources of the North-West Pacific, International Symposium, Khabarovsk, USSR, 1989, Abstracts, v. 2, p. 62.

*Carlson, P.R., Powell, R.D., and *Rearic, D.M., 1989, Turbidity-current channels in Queen Inlet, Glacier Bay, Alaska: Canadian Journal of Earth Sciences, v. 26, no. 4, p. 807-820.

*Carter, Claire, and Churkin, Michael, Jr., Biostratigraphy and graptolite faunas of the Terra Cotta Mountains, Alaska Range, Alaska [abs.]: GSA, p. 63.

Churkin, Michael, Jr., and *Carter, Claire, 1989, Tectonostratigraphy of Ordovician through Devonian strata in the Terra Cotta Mountains, Alaska Range [abs.]: GSA, p. 65-66.

*Clifton, H.E., and *Luepke, Gretchen, 1987, Heavy-mineral placer deposits of the continental margin of Alaska and the Pacific Coast states, *in* BB, p. 691-738.

*Collett, T.S., *Bird, K.J., *Kvenvolden, K.A., and *Magoon, L.B., 1989, Gas hydrates of Arctic Alaska [abs.] : AAPG, p. 345-346.

*Collett, T.S., and *Kvenvolden, K.A., 1989, Distribution and origin of permafrost-associated gas hydrates in northern Alaska [abs.]: Eos, p. 1151.

*Cooper, A.K., *Marlow, M.S. and *Scholl, D.W., 1987, Geologic framework of the Bering Sea crust, *in* BB, p. 73-102.

*Cooper, A.K., and *Scholl, D.W., 1989, Structure and tectonics of the Bering Sea and Aleutian Ridge [abs.], *in* Tectonics, Energy and Mineral Resources of the North-West Pacific, International Symposium, Khabarovsk, USSR, 1989, Abstracts, v. 2, p. 63-64.

*Cooper, A.K., *Scholl, D.W., and *Marlow, M.S., 1987, Structural framework, sedimentary sequences, and hydrocarbon potential of the Aleutian and Bowers basins, Bering Sea, *in* BB, p. 473-502.

*Cooper, A.K., *Scholl, D.W., *Marlow, M.S., *Stevenson, A.J., and *Dadisman, S.V., 1989, Cenozoic crustal extension in the Aleutian basin, Bering Sea [abs.]: Eos, p. 1366.

*Davis, A.S., *Pickthorn, L.-B.G., *Vallier, T.L., and *Marlow, M.S., 1989, Petrology and age of volcanic-arc rocks from the continental margin of the Bering Sea: Implications for early Eocene relocation of plate boundaries: Canadian Journal of Earth Sciences, v. 26, no. 7, p. 1474-1490.

Diebold, J., Moore, J.C., *Brocher, T., *Fisher, M., *Page, B., Davies, J., Stone, D., Ewing, J.I., Talwani, M., Sample, J., Sawyer, D., and von Huene, R., 1989, Marine seismic reflection transect of the Aleutian trench/arc system at Cook Inlet [abs.]: Eos, p. 1338.

Dillon, J.T., Solie, D.N., Decker, J.E., *Murphy, J.M., Bakke, A.A., and Huber, J.A., 1989, Road log from south fork Koyukuk River (mile 156.2) to Chandalar shelf (mile 237.1), *in* ADGGS, v. 1, p. 74-99.

*Dutro, J.T., Jr., 1989, A brief history of eighty years of geological exploration in the central Brooks Range, northern Alaska, *in* ADGGS, v. 1, p. 17-21.

Eichelberger, J.C., *Yount, M.E., Papike, J.J., and *Hildreth, W., 1989, Geophysical expedition to Novarupta: A progress report [abs.]: Eos, p. 1412.

Ekström, Göran, and *Engdahl, E.R., 1989, Earthquake source parameters and stress distribution in the Adak Island region of the central Aleutian Islands, Alaska: Journal of Geophysical Research, v. 94, no. B11, p. 15499-15519.

*Emmett, W.W., *Burrows, R.L., and Chacho, E.F., Jr., 1989, Gravel transport in a gravel-bed river, Alaska [abs.]: Eos (American Geophysical Union Transactions), v. 70, no. 15, p. 320. [Toklat River at highway crossing in Denali National Park.]

*Engdahl, E.R., Billington, S., and Kisslinger, C., 1989, Teleseismically recorded seismicity before and after the May 7, 1986, Andreanof Islands, Alaska, earthquake: Journal of Geophysical Research, v. 94, no. B11, p. 15,481-15,498.

*Espinosa, A.F., *Rukstales, K.S., and Udias, A., 1989, Focal mechanism solutions and their distribution in Alaska and the Aleutian Islands [abs.]: Eos, p. 1226.

Farmer, G.L., *Barker, Fred, *Plafker, George, and *Nokleberg, W.J., 1989, Isotopic evidence on the provenance of Tertiary metasedimentary rocks and on the origin of Eocene granites in the Prince William terrane, south-central Alaska [abs.]: Eos, p. 1336-1337.

*Fierstein, Judy, and *Hildreth, Wes, 1989, Ejecta dispersal and dynamics of the 1912 eruptions at Novarupta and the plinian-ignimbrite transition, Katmai, Alaska [abs.], *in* Continental Magmatism, International Association of Volcanology and Chemistry of the Earth's Interior, General Assembly, Santa Fe, N.M., 1989, Abstracts: New Mexico Bureau of Mines and Mineral Resources Bulletin 131, p. 90.

*Fisher, M.A., and *Brocher, T.M., 1989, Seismic reflection data reveal the crustal structure of the Chugach Mountains and eastern Alaska Range, southern Alaska, *in* T104, p. 26-33.

*Fisher, M.A., *Brocher, T.M., *Bruns, T.R., and *Geist, Eric, 1989, Deep crustal structure and hydrocarbon potential of the convergent margin near the eastern Aleutian trench [abs.], *in* Tectonics, Energy and Mineral Resources of the North-West Pacific, International Symposium, Khabarovsk, USSR, 1989, Abstracts, v. 2, p. 106-107.

———1989, Seismic reflections from a possible brittle/ductile transition within the accretionary wedge near the eastern Aleutian trench [abs.]: Eos, p. 1339.

*Fisher, M.A., *Brocher, T.M., *Nokleberg, W.J., *Plafker, George, and *Smith, G.L., 1989, Seismic reflection images of the

crust of the northern part of the Chugach terrane, Alaska: Results of a survey for the Trans-Alaska Crustal Transect (TACT): JGR, p. 4424-4440.

*Fischer, M.A., *Detterman, R.L., and *Magoon, L.B., 1987, Tectonics and petroleum geology of the Cook-Shelikof basin, southern Alaska, *in* BB, p. 213-228.

Flueh, E.R., *Mooney, W.D., *Fuis, G.S., and *Ambos, E.L., 1989, Crustal structure of the Chugach Mountains, southern Alaska: A study of peg-leg multiples from a low-velocity zone: Journal of Geophysical Research, v. 94, no. B11, p. 16,023-16,035.

*Foxworthy, B.L., Hanneman, D.L., *Coffin, D.L., and Halstead, E.C., 1988, Region 1, western mountain ranges, *in* Back, William, Rosenshein, J.S., and Seaber, P.R., eds., Hydrogeology: Geological Society of America, Geology of North America, v. O-2, chap. 4, p. 25-35.

*Fuis, G.S., *Ambos, E.L., *Mooney, W.D., and Christensen, N.I., 1989, Summary of deep structure of accreted terranes in the Chugach Mountains and Copper River basin, southern Alaska, from seismic refraction results, in T104, p. 23-26.

*Geist, E.L., and *Scholl, D.W., 1989, Deformation of the Aleutian arc using thin viscous sheet models [abs.]: Eos, p. 1314.

Goodwin, E.B., *Fuis, G.S., *Nokleberg, W.J., and *Ambos, E.L., 1989, The crustal structure of the Wrangellia terrane along the east Glenn Highway, eastern-southern Alaska: Journal of Geophysical Research, v. 94, no. B11, p. 16,037-16,057.

*Grantz, Arthur, 1989, Geology and resources of the Arctic Ocean basin [abs.]: American Association for the Advancement of Science, Annual meeting, San Francisco, Calif., 1989, Abstracts, p. 28.

———1989, Geology and tectonic significance of southern Northwind Ridge, Arctic Ocean [abs.]: International Geological Congress, 28th, Washington, D.C., 1989, Abstracts, v. 1, p. 580.

———1989, Seismic reflection character, distribution, estimated volume and stability of gas hydrate deposits beneath the Arctic Ocean north of Alaska [abs.]: Eos, p. 1152.

*Grantz, Arthur, and *May, S.D., 1987, Regional geology and petroleum potential of the United States Chukchi shelf north of Point Hope, *in* BB, p. 37-58.

*Grantz, Arthur, *May, S.D., and Dinter, D.A., 1987, Regional geology and petroleum potential of the United States Beaufort and northeasternmost Chukchi Seas, *in* BB, p. 17-35.

*Grantz, A., *Moore, T.E., and *Roeske, S.M., 1989, Transect of Alaska from the Gulf of Alaska to the Arctic Ocean [abs.]: International Geological Congress, 28th, Washington, D.C., 1989, Abstracts, v. 1, p. 579-580.

*Gross, W.K., *Lisowski, M., and *Savage, J.C., 1989, Deformation in the Shumagin seismic gap, Alaska [abs.]: Eos, p. 1063.

*Hamilton, T.D., 1989, Glacial geology of the Brooks Range, *in* ADGGS, v. 1, p. 23-26.

*Hampton, M.A., 1989, Geotechnical properties of sediment on the Kodiak continental shelf and upper slope, Gulf of Alaska: Marine Geotechnology, v. 8, no. 2, p. 159-180.

Hemming, Sidney, Sharp, W.D., and *Moore, T.E., 1989, Pb/U dating of detrital zircons from the carboniferous Nuka Formation, Brooks Range, Alaska: Evidence for a 2.07 Ga provenance [abs.]: Geological Society of America, Abstracts with Programs, v. 21, no. 6, p. A190.

*Hildreth, Wes, 1989, Caldera collapse at Mount Katmai, Alaska [abs.]: Eos, p. 1412.

*Howell, D.G., and Desegaulx, P., 1989, A comparison between decollement levels and thin- and thick-skinned thrusting in the central Brooks Range, Alaska and the western Alps, Europe [abs.]: Eos, p. 1338.

*Huffman, A.C., Jr., 1989, The Nanushuk Group, *in* ADGGS, v. 2, p. 303-309.

*Jones, J.E., *Molnia, B.F., *Schoonmaker, J.W., Jr., Taylor, T.E., and *Krimmel, R.M., 1989, Radar mapping of glaciers for global change investigations [abs.], *in* Global change, Arctic Science Conference, 40th, Fairbanks, Alaska, University of Alaska, 1989, Proceedings: American Association for the Advancement of Science, Arctic Division, p. 23.

*Kamata, Hiroki, and *Waitt, R.B., 1989, Stratigraphy, chronology, and style of the 1976 pyroclastic eruption of Augustine Volcano, Alaska [abs.], *in* Continental Magmatism, International Association of Volcanology and Chemistry of the Earth's Interior, General Assembly, Santa Fe, N.M., 1989, Abstracts: New Mexico Bureau of Mines and Mineral Resources Bulletin 131, p. 146.

*Karl, H.A., Huggett, Q., Kenyon, N.H., Masson, D., Parson, L.M., Dobson, M.R., and Underwood, M.B., 1989, GLORIA view of sedimentation styles and patterns across Aleutian Island Arc: Outer oceanic plate to back-arc basin of Bering Sea [abs.]: International Geological Congress, 28th, Washington, D.C., 1989, Abstracts, v. 2, p. 157.

*Karl, S.M., 1989, Paleoenvironmental implications of Alaskan siliceous deposits, *in* *Hein, J.R., and Obradovic, Jelena, eds., Siliceous deposits of the Tethys and Pacific regions: New York, Springer, p. 169-200.

*Karl, S.M., and *Dickey, C.F., 1989, Geology and geochemistry indicate belts of both ocean floor and arc basalt and gabbro in the Maiyumerak Mountains, northwestern Brooks Range, Alaska [abs.]: GSA, p. 100.

*Kayen, R.E., and *Lee, H.J., 1989, Effect of sea-level fall induced gas-hydrate decomposition on stability of continental slope, Beaufort Sea [abs.]: Eos, p. 1152.

*Kelley, J.S., and *Brosgé, W. P., 1989, Endicott Mountains allochthon, its relation to framework and structural development of central Brooks Range, Alaska [abs.]: American Association of Petroleum Geologists Bulletin, v. 73, no. 4, p. 543.

*Kelley, J.S., and *Detterman, R.L., 1989, Distribution of Mesozoic strata under Lower Cretaceous unconformity in Sadlerochit Mountains and adjacent coastal plain, northeastern Alaska [abs.]: American Association of Petroleum Geologists Bulletin, v. 73, no. 4, p. 543.

*Kempema, E.W., *Reimnitz, Erk, and *Barnes, P.W., 1989, Sea ice sediment entrainment and rafting in the Arctic: Journal of Sedimentary Petrology, v. 59, no. 2, p. 308-317.

Kienle, Juergen, Davies, John, and *Miller, T.P., 1988, Mitigation of the 1986 eruption of Mt. St. Augustine, Alaska [abs.]: International Conference on Volcanoes, Kagoshima, Japan, 1988, Abstracts, p. 484.

Kienle, Juergen, Davies, J.N., *Miller, T.P., and *Yount, M.E., 1988, Mitigation of the effects of the 1986 eruption of Mt. St. Augustine, Alaska, *in* International Conference on Volcanoes, Kagoshima, Japan, 1988, Proceedings, p. 565-568.

*Kvenvolden, K.A., 1987, Gas hydrates offshore Alaska and western continental United States, *in* BB, p. 581-593.

*Kvenvolden, K.A., and *Collett, T.S., 1989, Arctic gas hydrates

and global climate [abs.]: Eos, p. 1151.

*Labson, V.F., *Cady, J.W., *Long, C.L., *Sampson, J.A., and *McNair, D.W., 1989, Thin-skinned tectonics of Yukon-Tanana upland from interpretation of magnetotelluric and aeromagnetic data [abs.]: Eos, p. 1339.

*Labson, V.F., and Stanley, W.D., 1989, Electrical resistivity structure beneath southern Alaska, *in* T104, p. 75-78.

*Lahr, J.C., *Page, R.A., and *Stephens, C.D., 1988, Unusual earthquakes in the Gulf of Alaska and fragmentation of the Pacific plate: Geophysical Research Letters, v. 15, no. 13, p. 1438-1486.

*Lisowski, M., *Savage, J.C., *Prescott, W.H., and *Gross, W.K., 1988, Absence of strain accumulation in the Shumagin seismic gap, Alaska, 1980-1987: Journal of Geophysical Research, v. 93, no. B7, p. 7909-7922. .

Little, T.A., and *Naeser, C.W., 1989, Tertiary tectonics of the Border Ranges fault system, Chugach Mountains, Alaska: Deformation and uplift in the forearc setting: JGR, p. 4333-4359.

*Loney, R.A., and *Himmelberg, G.R., 1989, The Kanuti ophiolite, Alaska: Journal of Geophysical Research, v. 94, no. B11, p. 15,869-15,900.

*Luzitano, R., *Fuis, G., and *Brocher, T., 1989, Regional crustal thinning across the Alaska Range from seismic refraction/wide-angle reflection data, TACT 1987 [abs.]: Eos, p. 1339.

*Magoon, L.B., *Bird, K.J., and *Molenaar, C.M., 1989, Petroleum systems of the Arctic National Wildlife Refuge, northeastern Alaska—One of the remaining frontiers in U.S. petroleum exploration [abs.]: International Geological Congress, 28th, Washington, D.C., 1989, Abstracts, v. 2, p. 346.

*Marincovich, Louie, Jr., 1989, Tectonically-induced early middle Miocene marine glaciation and molluscan fauna in the Gulf of Alaska [abs.]: Geological Society of America, Abstracts with Programs, v. 21, no. 6, p. A115.

*Marlow, M.S., *Cooper, A.K., and *Fisher, M.A., 1987, Petroleum geology of the Beringian continental shelf, *in* BB, p. 103-122.

*McLean, Hugh, and *Wiley, T.J., 1987, Geologic potential for hydrocarbons in unexplored offshore basins of western North America, *in* BB, p. 595-619.

*Miller, T.P., 1989, Contrasting plutonic rock suites of the Yukon-Koyukuk basin and the Ruby geanticline, Alaska: Journal of Geophysical Research, v. 94, no. B11, p. 15969-15987.

*Moll-Stalcup, E.J., and *Arth, J.G., 1989, The nature of the crust in the Yukon-Koyukuk province as inferred from the chemical and isotopic composition of five Late Cretaceous to early Tertiary volcanic fields in western Alaska: Journal of Geophysical Research, v. 94, no. B11, p. 15989-16020.

*Moll-Stalcup, E.J., *Wooden, J.L., *Box, S.E., and *Frost, T.P., 1989, Preliminary Sr, Nd, and Pb isotopic evidence for magma sources in southwestern Alaska [abs.], *in* Continental Magmatism, International Association of Volcanology and Chemistry of the Earth's Interior, General Assembly, Santa Fe, N.M., 1989, Abstracts: New Mexico Bureau of Mines and Mineral Resources Bulletin 131, p. 192.

*Molnia, B.F., 1989, Advance induced retreat of the Mendenhall Glacier, Alaska [abs.]: Geological Society of America, Abstracts with Programs, v. 21, no. 6, p. A54.

*Molnia, B.F., and *Jones, J.E., 1989, Use of side-looking airborne radar for delineating surface and subglacial features of Malaspina Glacier, Alaska [abs.]: International Geological Congress, 28th, Washington, D.C., 1989, Abstracts, v. 2, p. 451.

———1989, View through ice: Are unusual airborne radar backscatter features from the surface of the Malaspina Glacier, Alaska, expressions of subglacial morphology?: Eos (American Geophysical Union Transactions), v. 70, no. 28, p. 701.

*Molnia, B.F., *Jones, J.E., *Schoonmaker, J.W., Jr., *Krimmel, R.M., *Trabant, D.C., and *Taylor, T.E., 1989, Ice-penetrating radar investigations of the Malaspina Glacier, Alaska [abs.]: Eos, p. 1085.

*Mooney, W.D., Beaudoin, B.C., and *Cotton, J.A., 1989, Crustal structure across the northwestern boundary of the Yukon-Tanana terrane, central Alaska: Results from TACT 1987: Eos, p. 1339.

Moore, J.C., Diebold, J., *Fisher, M., *Brocher, T., *Page, B., Stone, D., Talwani, M., and Ewing, J., 1989, Geological and geophysical context of the EDGE deep seismic reflection line: Gulf of Alaska [abs.]: Eos, p. 1338.

Moore, J.C., Diebold, J., *Fisher, M., Sample, J., and Bol, A., 1989, Accretionary history of the Kodiak-Kenai region: Insights from edge deep reflection data, geology, and paleomagnetism [abs.]: Eos, p. 1336.

*Moore, T.E., and Mull, Gil, 1989, Geology of the Brooks Range and North Slope, *in* T104, p. 107-131.

*Moore, T.E., Nilsen, T.H., and *Brosgé, W.P., 1989, Sedimentology of the Kanayut conglomerate, *in* ADGGS, v. 2, p. 220-252.

*Moses, M.J., *Brocher, T.M., *Fisher, M.A., Talwani, M., and Ewing, J.I., 1989, Wide-angle recordings of the 1989 EDGE MCS survey along the eastern Aleutian arc-trench transect, Alaska [abs.]: Eos, p. 1339.

*Mosier, E.L., *Cathrall, J.B., *Antweiler, J.C., and *Tripp, R.B., 1989, Geochemistry of placer gold, Koyukuk-Chandalar mining district, Alaska: Journal of Geochemical Exploration, v. 31, no. 3, p. 97-115.

Mozley, P.S., and *Carothers, W.W., 1989, Elemental and isotopic compositions of diagenetic siderite in the Kuparuk River Formation, Alaska [abs.]: Geological Society of America, Abstracts with Programs, v. 21, no. 6, p. A273.

*Murphy, J.M., *Moore, T.E., *Patton, W.W., Jr., and Saward, S.E., 1989, Stratigraphy of Cretaceous conglomerates, NE Koyukuk basin, Alaska: Unroofing of southeastern Brooks Range [abs.]: GSA, p. 120.

Nelson, B.K., *Nelson, S.W., and *Till, A.B., 1989, Isotopic evidence of an early-Proterozoic crustal source for granites of the Brooks Range, northern Alaska [abs.]: Geological Society of America, Abstracts with Programs, v. 21, no. 6, p. A105.

*Nokleberg, W.J., *Dusel-Bacon, Cynthia, *Foster, H.L., *Lanphere, M.A., *Plafker, George, and *Aleinikoff, J.N., 1989, Structure and tectonics of the Yukon-Tanana southern Wickersham, and Seventymile terranes along the Trans-Alaska Crustal Transect (TACT), Alaska [abs.]: Eos, p. 1337.

*Nokleberg, W.J., and *Fisher, M.A., 1989, IGC Field Trip T104: Alaskan geological and geophysical transect; summary of guidebook, *in* T104, p. 1-3.

*Nokleberg, W.J., *Foster, H.L., and *Aleinikoff, J.N., 1989, Geology of the northern Copper River basin, eastern Alaska

Range, and southern Yukon-Tanana Upland, *in* T104, p. 34-63.

*Nokleberg, W.J., *Plafker, George, *Lull, J.S., Wallace, W.K., and *Winkler, G.R., 1989, Structural analysis of the southern peninsular, southern Wrangellia, and northern Chugach terranes along the Trans-Alaska Crustal Transect, northern Chugach Mountains, Alaska: JGR, p. 4297-4320.

*Nokleberg, W.J., *Zierenberg, R.A., Lange, L.M., and *Schmidt, J.M., 1989, Metallogenesis of sedimentary-exhalative zinc-lead-silver deposits, northwestern Brooks Range, Alaska [abs.], *in* Tectonics, Energy and Mineral Resources of the North-West Pacific, International Symposium, Khabarovsk, USSR, 1989, Abstracts, v. 2, p. 95-97.

*Page, R.A., 1989, Introduction to special section on the northern Chugach Mountains-southern Copper River basin segment of the Alaskan transect, Part 1: JGR, p. 4253-4254.

———1989, Introduction to special section on the northern Chugach Mountains-southern Copper River basin segment of the Alaskan transect, Part 2: Journal of Geophysical Research, v. 94, no. B11, p. 16021.

———1989, Seismicity along the southern end of the Alaska transect, *in* T104, p. 20-23.

*Page, R.A., *Plafker, G., Davies, J.N., and Pulpan, H., 1989, Block rotation and seismicity in east-central Alaska [abs.]: Eos, p. 1337.

*Page, R.A., *Stephens, C.D., and *Lahr, J.C., 1989, Seismicity of the Wrangell and Aleutian Wadati-Benioff zones and the North American plate along the trans-Alaska crustal transect, Chugach Mountains and Copper River basin, southern Alaska: Journal of Geophysical Research, v. 94, no. B11, p. 16,059-16,082.

*Pallister, J.S., *Budahn, J.R., and *Murchey, B.L., 1989, Pillow basalts of the Angayucham terrane: Oceanic plateau and island crust accreted to the Brooks Range: Journal of Geophysical Research, v. 94, no. B11, p. 15,901-15,923.

Papike, J.J., Spilde, M.N., Galbreath, K.C., Shearer, C.K., *Keith, T.E.C., and Laul, J.C., 1989, Geochemistry and mineralogy of fumarole deposits, Valley of Ten Thousand Smokes, Alaska: Reference intensity method (RIM)XRD modal analyses [abs.]: Eos, p. 1412-1413.

*Patton, W.W., Jr., 1989, Framework geology: Yukon to Brooks Range, *in* ADGGS, v. 1, p. 27-30.

*Patton, W.W., Jr., and *Box, S.E., 1989, Introduction to special section on the Yukon-Koyukuk basin and its borderlands, western Alaska: Journal of Geophysical Research, v. 94, no. B11, p. 15805-15806.

———1989, Tectonic setting of the Yukon-Koyukuk basin and its borderlands, western Alaska: Journal of Geophysical Research, v. 94, no. B11, p. 15807-15820.

*Patton, W.W., Jr., *Miller, T.P., and *Box, S.E., 1989, Road log from Yukon crossing (mile 56) to south fork Koyukuk River (mile 156.2), *in* ADGGS, v. 1, p. 59-73.

*Patton, W.W., Jr., and *Murphy, J.M., 1989, Geology between the Yukon River and Coldfoot, east-central Alaska, *in* T104, p. 96-107.

*Phillips, R.L., and Colgan, M.W., 1989, Gravel fields, bedforms, and episodic storm events on shallow epi-continental Chukchi Sea [abs.]: International Geological Congress, 28th, Washington, D.C., 1989, Abstracts, v. 2, p. 604.

*Plafker, George, 1987, Regional geology and petroleum potential of the northern Gulf of Alaska continental margin, *in* BB, p. 229-268.

———1989, Geology of the Chugach Mountains and southern Copper River basin, southern Alaska, *in* T104, p. 3-20.

———1989, Neotectonic deformation in Alaska [abs.]: Eos, p. 1062-1063.

———1989, Phanerozoic tectonic evolution of Alaska [abs.], *in* Tectonics, Energy and Mineral Resources of the North-West Pacific, International Symposium, Khabarovsk, USSR, 1989, Abstracts, v.2, p. 44.

*Plafker, George, *Blome, C.D., and *Silberling, N.J., 1989, Reinterpretation of lower Mesozoic rocks on the Chilkat Peninsula, Alaska, as displaced fragment of Wrangellia: Geology, v. 17, no. 1, p. 3-6.

*Plafker, George, *Grantz, A., *Moore, T.E., *Nokleberg, W.J., *Patton, W.W., Jr., and *Tailleur, I.L., 1989, Tectonic framework of Alaska [abs.]: International Geological Congress, 28th, Washington, D.C., 1989, Abstracts, v. 2., p. 614.

*Plafker, George, *Nokleberg, W.J., and *Lull, J.S., 1989, Bedrock geology and tectonic evolution of the Wrangellia, peninsular, and Chugach terranes along the Trans-Alaska Crustal Transect in the Chugach Mountains and southern Copper River basin, Alaska: JGR, p. 4255-4295.

*Powell, R.D., and *Molnia, B.F., 1989, Glacimarine sedimentary processes, facies and morphology of the south-southeast Alaska shelf and fjords: Marine Geology, v. 85, no. 2-4, p. 359-390.

*Ryan, H.F., and *Scholl, D.W., 1989, Golat earthquakes beneath the Aleutian Ridge—a geologic perspective [abs.]: Eos, p. 1063.

*Schmidt, J.M., 1988, Mineral and whole-rock compositions of seawater-dominated hydrothermal alteration at the Arctic volcanogenic massive sulfide prospect, Alaska: Economic Geology, v. 83, no. 4, p. 822-842.

Schmidt, R.A.M., *Nokleberg, W.J., and *Page, R.A., 1989, Alaska geological and geophysical transect, Valdez to Coldfoot, Alaska, *in* T104, 131 p.

*Scholl, D.W., and *Stevenson, A.J., 1989, The Aleutian-Bowers-Shirshov Arc system, response to deformation of Alaska ("orocline") by subduction-driven impact and escape of crustal masses—Exploration of an idea [abs.]: Eos, p. 1307.

*Scholl, D.W., *Stevenson, A.J., *Vallier, T.L., *Ryan, H.F., and *Geist, E.L., 1989, Aleutian arc-trench system: Perspective of ocean margin evolution controlled by regional changes in plate-boundary conditions [abs.]: International Geological Congress, 28th, Washington, D.C., 1989, Abstracts, v. 3, p. 52-53.

*Scholl, D.W., *Vallier, T.L., and *Stevenson, A.J., 1987, Geologic evolution and petroleum geology of the Aleutian Ridge, *in* BB, p. 123-155.

*Sloan, C.E., and van Everdingen, R.O., 1988, Region 28, permafrost, *in* Back, William, Rosenshein, J.S., and Seaber, P.R., eds., Hydrogeology: Geological Society of America, Geology of North America, v. O-2, chap. 31, p. 263-270.

*Stanley, R.G., *Flores, R.M., and *Wiley, T.J., 1989, Contrasting depositional styles in Tertiary fluvial deposits of Nenana coal field, central Alaska: AAPG, p. 415..

*Stauffer, P.H., 1987, Quaternary depositional history and potential sand and gravel resources of the Alaskan continental margins, *in* BB, p. 649-690.

*Stevenson, A.J., and Embley, Robert, 1987, Deep-sea fan bodies, terrigenous turbidite sedimentation, and petroleum geology, Gulf of Alaska, *in* BB, p. 503-522.

Sweeney, J.F., Kristoffersen, Y., Weber, J.R., Sobczak, L., and *Grantz, A., 1989, Arctic Ocean crustal profile [abs.]: International Geological Congress, 28th, Washington, D.C., 1989, Abstracts, v. 3, p. 205.

Taber, J.J., McNutt, S.R., and *Miller, T.P., 1989, Seismological and geological activity of Pavlof Volcano, Alaska, 1986-1989 [abs.]: Eos, p. 1190.

Underwood, M.B., Laughland, M.M., and *Wiley, T.J., 1989, Thermal maturity, tectonostratigraphic terranes, and regional history: Examples from Kandik basin, Alaska [abs.]: American Association of Petroleum Geologists Bulletin, v. 73, no. 9, p. 1176.

*von Huene, Roland, 1989, Continental margins around the Gulf of Alaska, *in* Winterer, E.L., Hussong, D.M., and Decker, R.W., eds., The eastern Pacific Ocean and Hawaii: Geological Society of America, The Geology of North America, v. N, p. 383-401.

*von Huene, Roland, *Fischer, M.A., and *Bruns, T.R., 1987, Geology and evolution of the Kodiak margin, Gulf of Alaska, *in* BB, p. 191-212.

von Huene, R., Vosberg, H., *Hart, P., and *Fisher, M.A., 1989, Tectonic structure across the northeast end of the Aleutian trench [abs.]: Eos, p. 1338.

*Waitt, R.B., *Kamata, Hiroki, and *Denlinger, R.P., 1989, Rapid mobilization of winter-spring snowpack during eruptions at Mount St. Helens volcano in 1980-1986 and at Augustine volcano in 1986 [abs.], *in* Continental Magmatism, International Association of Volcanology and Chemistry of the Earth's Interior, General Assembly, Santa Fe, N.M., 1989, Abstracts: New Mexico Bureau of Mines and Mineral Resources Bulletin 131, p. 285.

Watts, K.F., Imm, T.A., and *Harris, A.G., 1989, Stratigraphy and paleogeographic significance of the Carboniferous Wahoo Limestone—reexamination of the type section, northeastern Brooks Range, Alaska [abs.]: GSA, p. 157.

*Weber, F.R., 1989, Geology between Fairbanks and the Yukon River, east-central Alaska, *in* T104, p. 84-95.

*Stevenson, A.J., and Embley, Robert, 1987, Deep-sea fan bodies, terrigenous turbidite sedimentation, and petroleum geology, Gulf of Alaska, *in* BB, p. 503-522.

Sweeney, J.F., Kristoffersen, Y., Weber, J.R., Sobczak, L., and *Grantz, A., 1989, Arctic Ocean crustal profile [abs.]: International Geological Congress, 28th, Washington, D.C., 1989, Abstracts, v. 3, p. 205.

Taber, J.J., McNutt, S.R., and *Miller, T.P., 1989, Seismological and geological activity of Pavlof Volcano, Alaska, 1986-1989 [abs.]: Eos, p. 1190.

Underwood, M.B., Laughland, M.M., and *Wiley, T.J., 1989, Thermal maturity, tectonostratigraphic terranes, and regional history: Examples from Kandik basin, Alaska [abs.]: American Association of Petroleum Geologists Bulletin, v. 73, no. 9, p. 1176.

*von Huene, Roland, 1989, Continental margins around the Gulf of Alaska, *in* Winterer, E.L., Hussong, D.M., and Decker, R.W., eds., The eastern Pacific Ocean and Hawaii: Geological Society of America, The Geology of North America, v. N, p. 383-401.

*von Huene, Roland, *Fischer, M.A., and *Bruns, T.R., 1987, Geology and evolution of the Kodiak margin, Gulf of Alaska, *in* BB, p. 191-212.

von Huene, R., Vosberg, H., *Hart, P., and *Fisher, M.A., 1989, Tectonic structure across the northeast end of the Aleutian trench [abs.]: Eos, p. 1338.

*Waitt, R.B., *Kamata, Hiroki, and *Denlinger, R.P., 1989, Rapid mobilization of winter-spring snowpack during eruptions at Mount St. Helens volcano in 1980-1986 and at Augustine volcano in 1986 [abs.], *in* Continental Magmatism, International Association of Volcanology and Chemistry of the Earth's Interior, General Assembly, Santa Fe, N.M., 1989, Abstracts: New Mexico Bureau of Mines and Mineral Resources Bulletin 131, p. 285.

Watts, K.F., Imm, T.A., and *Harris, A.G., 1989, Stratigraphy and paleogeographic significance of the Carboniferous Wahoo Limestone—reexamination of the type section, northeastern Brooks Range, Alaska [abs.]: GSA, p. 157.

*Weber, F.R., 1989, Geology between Fairbanks and the Yukon River, east-central Alaska, *in* T104, p. 84-95.